Silicon biogeochemical cycle along the land to ocean continuum : Focus on Indian monsoonal estuaries

Mangalaa Kameswari Rajasekaran

Université Pierre et Marie Curie

Ecole doctorale ED 129 Sciences De l'environnent, Ile de France

Laboratoire d'océanographie et du climat: expérimentations et approches numériques

Silicon biogeochemical cycle along the land to ocean continuum: Focus on Indian monsoonal estuaries

Presented by

Mangalaa Kameswari Rajasekaran

Thèse de doctorat de Biogeochemistry

Directeur de these: **Prof. Damien CARDINAL**

Co-supervisor: **Dr. V.V.S.S. SARMA**

Présentée et soutenue publiquement le 16/12/2016

Devant un jury composé de :

Me. Isabelle BASILE-DOELSCH	Directrice de Recherche INRA	Rapporteure
M. Damien CARDINAL	Professeur UPMC	Directeur de thèse
Me. Josette GARNIER	Directrice de Recherche CNRS	Examinatrice
M. Alain SALIOT	Professeur UPMC	Examinateur
M. Vedula V.S.S. SARMA	Directeur de Recherche CSIR	Co-directeur de thèse
M. Nicolas SAVOYE	Physicien-Adjoint INSU	Rapporteur

Dedicated to my parents

and my best friend

தந்தை மகற்காற்று நன்றி அவையத்து
முந்தி இருப்பச் செயல்.

Le Bien que fait le père à son enfant, c'est de le rendre habile à tenir le premier rang dans l'assemblée.

மகன்தந்தைக்கு ஆற்றும் உதவி இவன்தந்தை
என்நோற்றான் கொல்எனும் சொல்.

La reconnaissance de l'enfant envers son père consiste à faire dire:
''Par quelles ascèses, ce père a-t-il pu obtenir un tel fils ''

உடுக்கை இழந்தவன் கைபோல ஆங்கே
இடுக்கண் களைவதாம் நட்பு.

De même que la main sert instantanément à celui dont le vêtement est dérangé, pour couvrir sa nudité, l'ami sert à délivrer sur-le-champ celui qui souffre, de sa douleur

ACKNOWLEDGEMENTS

Completion of this doctoral dissertation was possible with the support of several people. I take this opportunity to extend my sincere gratitude and appreciation to all those who made this Ph.D thesis possible and success. I would like to express my sincere gratitude to all of them.

First of all, I am extremely grateful to my research supervisor ***Prof. Damien CARDINAL****, professor and researcher, LOCEAN-UPMC for introducing me to this exciting research topic and for his dedicated help, advice, inspiration, encouragement, and integral view on research, high quality work and constant support throughout my Ph.D. I am really delighted to be associated with a person like him in my life and I owe a bundle of thankfulness to him.*

My special words of gratitude to my research co-supervisor ***Dr. V.V.S.S Sarma****, Principal Scientist, NIO, Visakhapatnam, India for his continuous support, cooperation, encouragement and for facilitating all the requirements kept me going ahead. I owe a lot of gratitude to him and I feel privileged to be associated with a person like him.*

Besides my advisors, I would like to thank the rest of my thesis committee: ***Dr. Ioanna BOULOUBASSI*** *CR CNRS, LOCEAN,* ***Dr. Josette Garnier*** *DR CNRS, METIS and* ***Dr. Alexis Groleau*** *MCF Paris Diderot, IPGP for their insightful comments and encouragement, but also for the hard question which incented me to widen my research from various perspectives. I would also like to thank and obliged my gratitude to the reviewers,* ***Dr. Isabelle Basile-Doelsch*** *(CEREGE) and* ***Dr. Nicolas Savoye*** *(EPOC) for their insightful comments and suggestions to improve the thesis manuscript. I would also like to express my special gratitude to the president/chairman of the PhD Jury* ***Prof. Alain Saliot*** *(LOCEAN-UPMC) for his kind suggestions and extraordinary coordination. He always encourages me with smiling face.*

Several people helped with: the field trips, sample collection, analysis in the laboratories and all of them are thanked for their great support and contributions. Special mention goes to MR. ***M. Benrahmoune*** *(LOCEAN, CNRS), Technician, for managing the clean lab and helping me with spectrophotometric measurements and Mrs.* ***I.Djouraev****, engineer (IRD, Bondy) and MR.* ***A.Dapoigny****, engineer (LCSE, Gif-Sur-Yvette) for their analytical support in ICPMS and MC-ICPMS respectively. I am extending my thanks also to* ***Mrs. Sandrine*** *for her excellent support in XRD measurements. My special thanks also to* ***Dr. Julien Brajard*** *(Scientist, LOCEAN) for his perceptive support in statistical knowledge and interpretation.*

To my many friends and family, you should know that your support, encouragement and love were worth more than I can express on paper. My sincere and lovable thanks extending to my

best friends ***Dr. Ivia, Ms. Violaine, Dr. Celine, Mrs. Fanny, Dr. Julie, Mrs. Catherine, Dr. Tila, Mr. Vincent, Dr. Nicolas, Mr. Renaud*** *and other colleagues from LOCEAN for their incredible moral support. To my friends scattered around the country, thank you for your thoughts, well-wishes/prayers, phone calls, e-mails, texts, visits, editing advice, and being there whenever I needed a friend.*

I would like to specially thank my very best and close friend ***Mr.C. Muthukumar****, Project Scientist, whose constant support throughout my research career and personal life made me successful at this level. I also thank* ***Dr. M. Venkatesh*** *and his family for their moral support during my downs in family.*

Ultimately, I would like to acknowledge the people, who mean world to me, my parents for supporting me spiritually throughout writing this thesis and my life in general. I extend my respect to my parents, my paternal brothers and sisters and all elders to me in the family. I don't imagine a life without their love and blessings. Thank you ***mom Mrs. R. Kameswari*** *and* ***dad Mr. M.Rajasekaran*** *for showing faith in me and giving me liberty to choose what I desired. I consider myself the luckiest in the world to have such a supportive family, standing behind me with their love and support.*

Lastly, I would like to acknowledge all the ***funding bodies*** *for their financial support and* ***research laboratories*** *for their full pledged analytical support. I would like to highlight the funding bodies and research laboratories:*

Thank you one and all. ☺

Kameswari Rajasekaran ***Mangalaa***

Abstract

Silicon is the second most abundant element in Earth's crust and one of the key nutrient in aquatic ecosystems. There are strong interactions of Si with carbon cycle and biogeochemical processes. The present thesis focused on variability of silicon (amorphous-ASi, lithogenic-LSi and dissolved-DSi) and Si isotopes along the land to ocean continuum.

We investigated the seasonal and spatial variability of ASi, LSi & DSi and Si isotopes in ~20 Indian estuaries. We categorize the estuaries using statistical analysis (PCA and cluster analysis). Diatom uptake seems to be the main process controlling ASi during dry period, especially in the South. Weathering and erosion control the variability of LSi in the remaining estuaries. Similarly lithogenic supply controls Si during wet period in all estuaries and no impact of diatoms was seen because of high suspended load. Si isotopic compositions trace the Si sources and biogeochemical pathways. The isotopic results exhibit clear seasonal difference with high impact of type of weathering during both seasons. They show that southwest watersheds are very special in terms of weathering regime compared to the other watersheds because of topography and climate. The impact of agriculture and forest cover on Si cycle is also clearly evidenced in all the basins during wet period. We show that groundwater Si isotopic variability results from a combination of dissolution and production of minerals. Overall, this study shows the preponderant influence of weathering and type of secondary clays on Si isotopes irrespective to the seasons, rather than the biological uptake or mixing as reported elsewhere.

Résumé

Le silicium est le second élément le plus abondant de la croûte terrestre et un nutriment clefs des écosystèmes aquatiques. Il existe de fortes interactions entre Si, le cycle du carbone et les processus biogéochimiques. Cette étude porte sur la variabilité de Si (amorphe-ASi, lithogène-LSi et dissous-DSi) et les isotopes de Si le long du continuum continent-océan.

Nous avons étudié la variabilité saisonnière et spatiale de ASi, LSi, DSi et des isotopes dans ~20 estuaires indiens. Nous avons catégorisé les estuaires selon une analyse statistique (PCA et regroupement). Le prélèvement par les diatomées semble être le principal processus contrôlant ASi en saison sèche, surtout au Sud. L'altération et l'érosion contrôlent LSi dans les autres estuaires. En saison humide, l'impact des diatomées n'est pas observé à cause d'une trop forte charge sédimentaire et tous les estuaires sont dominés par les apports lithogéniques.

Les compositions isotopiques de Si peuvent tracer les sources de Si et les interactions biogéochimiques. Les résultats isotopiques montrent une différence saisonnière claire avec un impact fort de l'altération aux deux saisons. Les bassins versants du sud-ouest sont très différents des autres bassins du fait de leur topographie et climat. L'impact de l'agriculture et de la couverture forestière est aussi clairement présent dans tous les bassins tandis que la composition isotopique de Si des eaux souterraines résulte d'une combinaison de production et dissolution de minéraux. Ainsi, cette étude montre le rôle prépondérant de l'altération et du type d'argiles formées sur les isotopes de Si, indépendamment des saisons, plutôt que des processus biologiques ou de mélange tels que rapportés précédemment.

Table of contents

Chapter 1: Introduction

1. Silicon biogeochemical cycle (2)

1. 1. Continental Si cycle (2)

1.2. Adsorption of Silicon (5)

1.3. Silicon in the biosphere (6)

1.3.1. Vegetation and silicon (6)

1.3.2. Diatoms and silica (7)

1.4. Transport of silica in the land-ocean continuum (7)

1.4.1. Conservative vs. non-conservative behavior of DSi (9)

1.5. Anthropogenic perturbations over Si cycle in the land-ocean continuum (11)

2. Silicon isotopes (13)

2.1 Basic principles

2.2 Variability of Si isotopes in Earth surface (15)

2.3 Estuaries and Si isotopes (16)

3. Indian estuaries (18)

3.1. Lithology of river basins (20)

3.2. Why Si cycle in Indian estuaries? (22)

4. Objectives of the study and thesis outline (23)

4.1 Framework (23)

4.2 Objectives (24)

4.3 Thesis outline (24)

5. References (25)

Chapter 2: Methodological procedures and quality of measurements

1. Amorphous silica (38)

1.1. Analytical measurements of amorphous silica (ASi) (38)

1.2. GEOTRACES Intercalibration exercise (40)

2. Silicon Isotopes (41)

2.1. Preconditioning (42)

2.1.1 Pre-concentration (42)

2.1.2 Purification of Si (42)

2.2. Potential dissolved organic carbon (DOC) matrix effect on Si isotopes measurements (43)

2.3. Si isotope measurements (45)

3. Sampling strategy (50)

3.1. Estuarine sampling (50)

3.2. River sampling (51)

4. References (52)

Chapter 3: Seasonal, anthropogenic and biogeochemical processes on silicon cycle in Indian estuaries

Abstract (56)

1. Introduction (58)

2. Materials and Methods (61)

2.1 Sampling and ancillary biogeochemical parameters (62)

2.2 Water Discharge (63)

2.3 Measurement of Amorphous (ASi) and Lithogenic silica (LSi) (64)

2.4 Statistical Analysis (66)

3. Results (66)

3.1 Seasonal variability of Dissolved Silicon (DSi) (66)

3.2 Seasonal variability of ASi (68)

3.3 Seasonal variability of LSi (Lithogenic silicon) and Total Suspended Material (TSM) (69)

3.4 Inter estuaries biogeochemical and seasonal variability (70)

4. Discussion (73)

4.1 Main processes controlling the Si pools in the Indian estuaries (73)

4.2 Biogeochemical processes in the dry period (75)

4.2.1 Upper estuaries (75)

4.2.2 Middle estuaries- dry period (79)

4.2.3 Lower estuaries- dry period (83)

4.3 Biogeochemical processes in Wet period (85)

4.3.1 Upper estuary- Wet period (85)

4.3.2 Middle estuary- Wet period (88)

4.4 Fluxes of ASi, LSi and DSi from Indian estuaries to North Indian Ocean (91)

4.4.1 Bulk fluxes (91)

4.4.2 Net fluxes (92)

4.5 Impact of land use on Si cycle (94)

5. Conclusions (96)

6. References (98)

Chapter 4: Seasonal silicon isotope compositions of surface and ground waters in the Indian estuaries

1. Introduction (106)

2. Materials and methods (107)

3. Results (111)

3.1 General trends on DSi (111)

3.2 General trends on δ^{30}Si-DSi (111)

3.3 Major Cations (112)

3.4 Clay Mineralogy (112)

4. Discussion (116)

4.1 Wet season (116)

4.1.1 Geochemical processes in all estuaries: An overview (116)

4.1.2 Upper estuaries (119)

4.1.3 Land use (126)

4.2 Variability within estuaries (wet) (128)

4.3 Ground water (130)

4.3.1 Groundwater and upper estuaries (130)

Saturation indexes (132)

4.4 Dry period (136)

4.4.1 Upper dry and comparison with upper wet (136)

4.4.2 Conservativity vs. non-conservativity within all estuaries (139)

Biological uptake (141)

Dissolution or DSi supply (143)

4.5 Common estuaries (143)

5. Conclusion (144)

6. References (145)

Chapter 5: Seasonal, biological and weathering processes controlling silicon cycle along the land-ocean continuum in two contrasted rivers of India (Cauvery and Netravathi)

1. Introduction (154)

2. Study area and materials (156)

2.1. River Settings, climate and hydrology (156)

2.2. Geology of Cauvery and Netravathi Basin (158)

2.3. Materials (160)

3. Results (161)

3.1. Dissolved load concentrations (161)

3.1.1. Dissolved Silicon (DSi) (161)

3.1.2. Dissolved cations load (165)

3.2. Seasonal variability of δ^{30}Si in Cauvery and Netravathi basins (167)

4. Discussion (170)

4.1. General overview (170)

4.1.1 Cauvery (170)

4.1.2 Netravathi (171)

4.2. Weathering processes (171)

4.3. Biological processes (181)

5. Conclusions (183)

6. References (184)

Chapter 6: Conclusions and perspectives

1. Conclusions (190)

1.1 Controlling of biotic and abiotic factors (191)

1.1.1 Dry period (base flow season) (191)

1.1.2 Wet season (192)

1.2 Impact of Land use on Si cycle (196)

1.3 Groundwater (196)

2. Weathering: a first order control over biological uptake (196)

3. Perspectives (199)

4. References (200)

Appendix of Chapter 3

Appendix A: Agreement with Ganges ASi data (202)

Appendix B: Individual samples data (204)

Appendix C: Additional PCA and clustering figure and tables (208)

Appendix D: Details of flux calculation (216)

Appendix E: SEM pictures (218)

Appendix F: Lithogenic contribution (219)

Appendix G: Influence of Nitrogen in land use (220)

Appendix of Chapter 4

Annex A (222)

Annex B (226)

Annex C (229)

Sampling pictures (231)

CHAPTER 1

Introduction

1. Silicon biogeochemical cycle

Silicon (Si) is the second most abundant element in the Earth's crust (28.8%) next to oxygen (Wedephol, 1995) and exists in the form of silica (silicon dioxide, SiO_2) as well as of different types of silicate minerals. There are different forms of silicon existing in the terrestrial and aquatic systems. They are (i) the dissolved silicon (DSi) originated from weathering of (ii) silicate minerals (referred to as Lithogenic silicon, LSi) that is cycled through vegetation as (iii) phytoliths (terrestrial) and (iv) diatoms (aquatic). Both (iii) and (iv) are made of opal and found in sediments and suspended particles. This biologic Si is referred as biogenic silica (BSi) is amorphous in nature (and therefore sometimes referred to as ASi). Below, the general pathway of different forms of silicon and their role in Si cycle is briefed under separate sections from land to ocean.

1. 1 Continental Si cycle

The Si contained in the crust is broken down by physical, chemical and biological processes resulting from different weathering processes. This leads to congruent dissolution of primary minerals and/or formation of secondary minerals (e.g. clays). Chemical weathering links the continental Si cycle with C cycle via removal of CO_2 from the atmosphere with the net effect of HCO_3^- formation in solution and thereby regulating the climate on geological timescales (Berner, 1995, 1997). There are many types of weathering reactions and equation (1) provides an example of potassium feldspar weathered to form kaolinite:

$$KAlSi_3O_{8(s)} + CO_{2\,(g)} + 11/2H_2O = 1/2\ Al_2Si_2O_5\,(OH)_{4(s)} + K^+ + HCO_3^- + 2H_4SiO_4 \qquad \text{Eq. (1)}$$

Hence, the products of chemical weathering include both particulate (kaolinite in Eq. 1) and dissolved forms (cation, bicarbonate anion and silicic acid in Eq. 1). In the particulate Si there is also some residual primary mineral fraction (quartz, feldspar) resulting from physical weathering (Fig. 1). The formation of new particulate forms i.e., neoformed minerals or secondary minerals (clays, Fe-Al oxy-hydroxides) is very slow and depends on lithology, climate, vegetation and erosion. It thereby controls the continental particulate and dissolved fluxes to the ocean (Gaillardet et al., 1999; White 2011; Dessert et al., 2003; Moulton et al., 2000). For example, climatic agents like heavy rainfall and high temperature enhance chemical weathering (White and Blum 1995) and ultimately increase the dissolved and particulate elements' fluxes to rivers. Steep slope and rainfall also increase the physical weathering leading to high

erosion of primary and secondary minerals. The composition of clay minerals and their crystalline structure is based on the local physicochemical conditions where they formed (Dove, 1995). Phyllosilicates represent the majority of clay minerals (<2 μm in diameter) in the soils (Velde and Meunier 2008). Under the tropical climate with intense rainfall, most of the cations are leached from the surface soils and kaolinite is the major type of clay mineral formed and accompanied by gibbsite, iron oxides and oxyhydroxides for the most intense chemical weathering. A schematic representation of weathering process with subsequent clay mineral formation and the intensity of silicate weathering is shown in the figure 2.

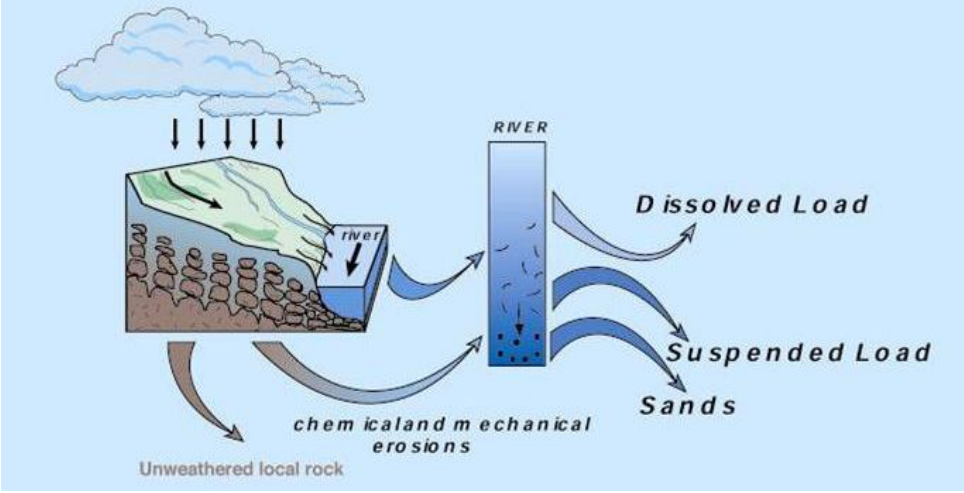

Fig. 1 *Scheme of weathering and erosion processes connecting bedrock to materials transported by rivers (from J. Gaillardet).*

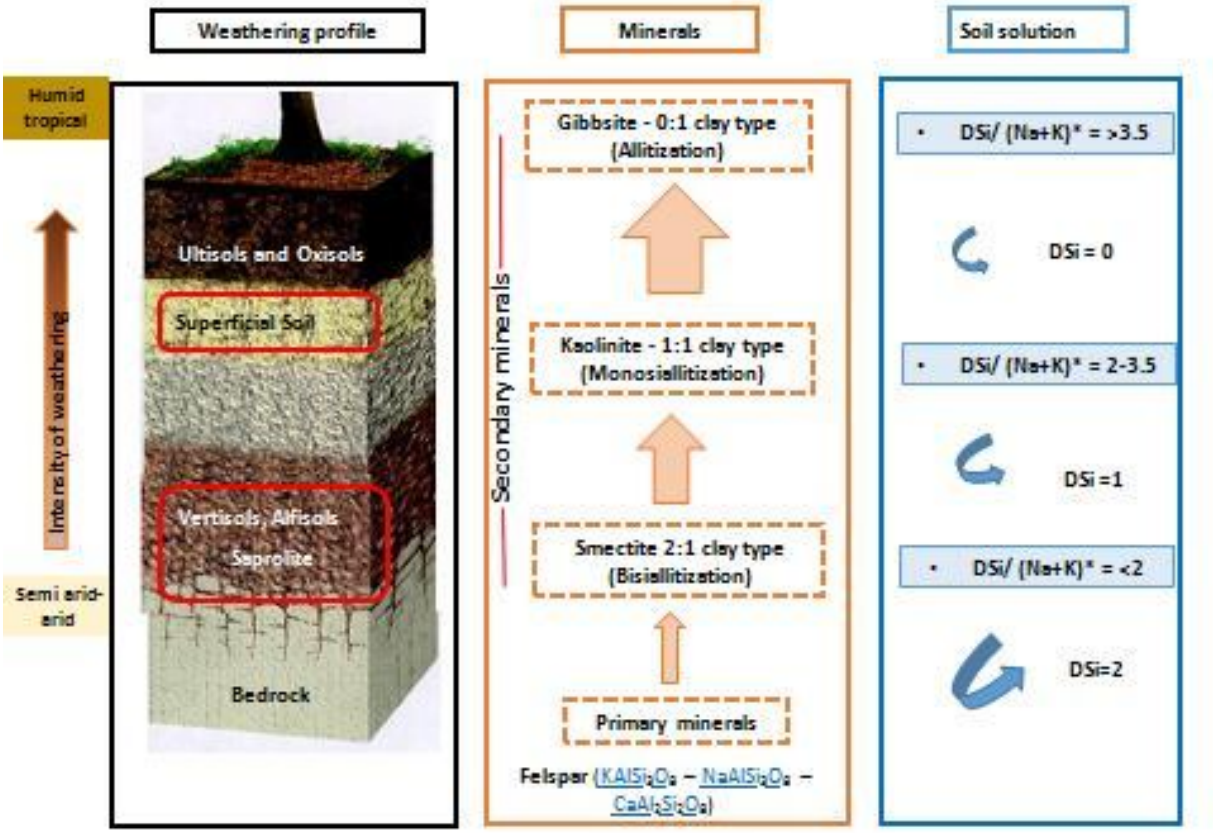

Fig. 2 *General scheme of weathering depth (black rectangular box) and subsequent clay mineral formation (orange rectangular box) associated with the proxy to determine the intensity of silicate weathering in soil solution (blue rectangular box). The size of the arrows (orange) indicating the intensity of weathering with respect to climate (greater the size indicates higher weathering intensity) and the blue arrows indicate the proportion of dissolved silicon (DSi) remaining in the soil solution after clay mineral formation.*

It is well known that the part of the DSi produced during weathering is then involved in further geochemical processes and biological uptake. The DSi is mainly present in the form of monomeric silicic acid ($H_4SiO_4^0$) at natural pH value (pH <8.5; Iler 1979; Drees et al., 1989). It is transported from soils to rivers and eventually to the ocean. DSi serves as a major nutrient for terrestrial plants and aquatic organisms and indirectly plays a major role in oceanic CO_2 control (Smetacek 1999). At present, 6.2 ± 1.8 $Tmol.yr^{-1}$ of DSi is supplied to the ocean via rivers, corresponding to 85% of external Si input to the ocean (Tréguer and de la Rocha 2013). Before entering into the ocean, DSi will travel among several

pools (Fig. 3). These pools are mainly incorporation into neoformed clays, biological uptake, DSi of rivers, soil solutions, ground waters and adsorption on iron oxides, a potentially important process that remains to be better quantified.

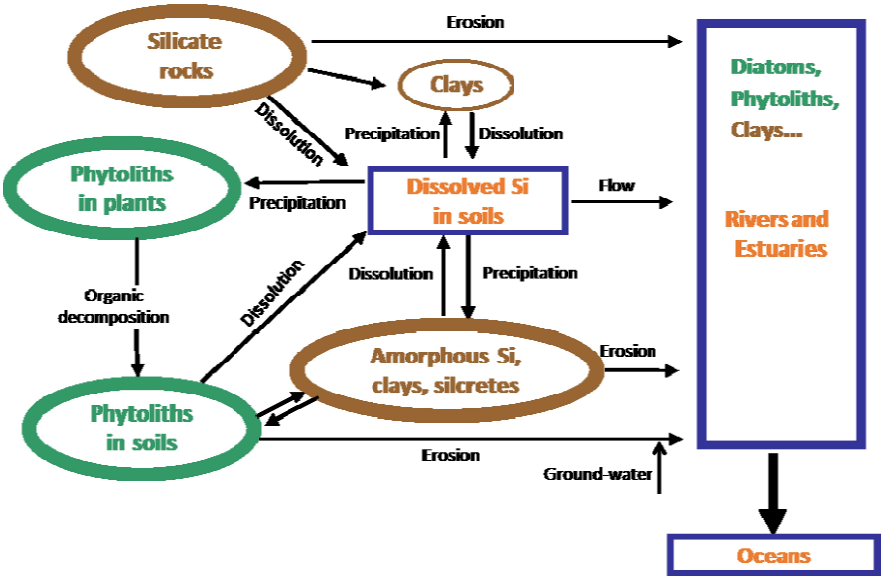

Fig. 3 *A schematic representation of Si biogeochemical cycle in the continental environment (Adapted from Meunier et al., 2001).*

1.2 Adsorption of silicon

Apart from weathering, Si can be adsorbed onto the soil minerals (McKeague and Cline, 1963). Aluminium and iron oxides are ubiquitous in soil and have the greater capacity to absorb $H_4SiO_4^0$ (Beckwith and Reeve, 1963; Jones and Handreck, 1963; McKeague and Cline, 1963). Si interacts with OH groups of Fe oxide surface via bond exchange by forming silicate bi-dendate inner sphere complex (Parfitt, 1978; Pokrovski et al., 2003; Hiemstra et al., 2007). This Si adsorption is highly pH dependent and increases with increasing pH from 4 to 9 (McKeague and Cline, 1963). In addition, Si polymerisation also occurs on the oxide surfaces and gets interacted with mineral structures (Swedlund and Webster, 1999). Such Si sequestration in soil Fe-Al oxi-hydroxides may affect the Si terrestrial cycle and the Si supply to the rivers.

1.3 Silicon in the biosphere

1.3.1 Vegetation and silicon

Unlike lithosphere, the average Si concentration is only 0.03 wt. % in the global biosphere and Si ranks after H, O, C, N, S, Ca and K (Exley 1998). Before reaching the aquatic system, higher terrestrial plants can take up DSi through their roots and deposit in their shoot system Biogenic silica (BSi) particles of few micrometers size called phytoliths (Conley 2002). Even though Si is not an essential nutrient for terrestrial plants, it is beneficial for many of them since the lack of DSi may affect the development of plants and resistance to their external stress (Epstein 1999). Indeed, after evaporation of water from the plants, Si precipitates in the form of hydrated amorphous silica ($SiO_2.nH_2O$ phytoliths). The Si content of plant varies from 1% up to 10% of dry weight (Epstein 1994; Conley 2002).The best examples of Si accumulated plants are grass (rice, wheat...), bamboo, and banana (Alxandre et al., 1997; Derry et al., 2005), all being extremely important food source in the world. Phytoliths exhibit different shapes and structures based on their taxonomic units (Piperno et al., 1988). Generally, the size varied from 100 nm (Watteau and Villemin, 2001) to 200 μm (Piperno et al., 1988). The smaller sizes (<5 μm) of phytoliths are relatively more reactive and play important role in the export flux of Si from the land to aquatic system (Sommer et al., 2006). After the plant dies, phytoliths return to the upper soil and enter into the amorphous silica (ASi) pool. This ASi is generally dominated by the BSi from phytoliths, but include also volcanic ashes or allophane. In general, BSi stock in the soils can be larger than observed in the live plants (Conley 2002).

Several studies indicated that phytoliths are one of the most soluble forms of particulate silicon and are considered as important DSi source (Fraysse et al., 2006; 2009; 2010). Phytolith dissolution can release twice more than that of Si released during silicate mineral weathering (Alexandre et al., 1997). The high solubility of phytoliths may even control the DSi concentration in rivers as seen for Hawaiian streams (Derry et al., 2005). Conley, 2002 emphasized that the annual production of BSi accumulated in plants as phytoliths ranges from 60-200 Tmol Si yr^{-1} and seems to be an order of magnitude higher than the annual supply of DSi to the ocean (5 $Tmol.yr^{-1}$, [Treguer et al., 1995]) demonstrating the important phytoliths contribution in Si pool . Based on temperature and pH, the dissolution of phytoliths again resupplies the DSi in to the system. For instance, decreasing pH may decrease the dissolution of phytoliths (~8% in tropical forests), but their release into the saline environment swiftly increases their

dissolution (~90% in tidal wetlands) and hence favours Si bioavailability (Fraysse et al., 2006; Loucaides et al., 2008; Alexandre et al., 1997; Struyf et al., 2007). Note however that the factors controlling the BSi dissolution are not well constrained. For instance the proportion lithogenic can influence BSi dissolution (Struyf and Conley 2011).

1.3.2 Diatoms and Silica

Silicic acid or dissolved silicon (DSi), is a key nutrient for diatoms (Bacillariophyceae), unicellular photosynthetic algae whose size ranges from 20 to 200 μm and can sometimes be up to 2mm. Diatoms require DSi to build up their opal frustules, a rigid cell wall made up of hydrated BSi that may account for 15-75% of total mass of the cell (Martin-Jézéquel et al., 2000; Sabater 2009). Diatoms play a dominant role amongst phytoplankton communities in carbon uptake (75% of coastal primary production, Nelson et al., 1995) and sediment burial because of their larger size and harder structure (Ducklow et al., 2001). Carbon and silicon cycles are thus inter-related since diatoms play currently a dominant role in carbon sequestration while weathering connects C and Si cycles at long-term geological cycles (Berner 1992). Apart from diatoms, Si is also utilized by other aquatic organisms like sponges and radiolarians to form their skeletal structures.

Role of diatoms on the biological pump

The primary production occurring via different siliceous or non-siliceous phytoplankton groups (e.g., Coccolithophorids) results in the net flux of atmospheric CO_2 to the deep ocean and is generally referred to as "biological carbon pump" (Raven and Falkowski, 1999). However, there exists crucial difference between diatoms and coccolithophorids primary production. The coccolithophorids are made up of calcite shells called "coccoliths", where CO_2 is indeed produced when calcium reacts with bicarbonate (Rost and Riebesell, 2004). Therefore, the increased preeminence of non-siliceous phytoplankton decreases the net CO_2 sequestration. On contrary, the diatoms primary production is more efficient to increase the net CO_2 sequestration (Ragueneau et al., 2006).

1.4 Transport of silicon in the land-ocean continuum

Estuaries

An estuary can be defined as "*a semi-enclosed coastal body of water which has a free connection with the sea water and within which sea water is measurably diluted with freshwater derived from land drainage*" (Pritchard, 1967). Estuaries are more valuable environments in terms of ecological diversity and are also of economical concerns. From a biogeochemical point of view, estuaries serve as the transformation of nutrients, cycling of biogeochemical substances and consequently influence the health of the coastal ecosystems. Moreover, estuaries serve as an interface through which some of the biogenic and clay minerals will be transferred to the coastal ocean from rivers. They also act as filters due to several chemical and biological processes such as colloid formations, scavenging, reverse weathering, production, and sedimentation of biogenic materials that generally reduce supply to the ocean (Bianchi, 2007). In contrast, dissolution (e.g. regeneration of biogenic materials) may serve as an additional source to the ocean (Carbonnel et al., 2009). The tidal influence in the estuaries leading to longer residence time of water compared to adjacent rivers induces higher turbulence and turbidity via resuspension of sediments and/or particle aggregation (Schuchardt et al., 1993; McLusky 1993). This results in low light conditions and limit phytoplankton growth. It may favor diatoms due to their lower light requirements relatively to other algae (Reynolds 1988; Lionard 2006). Therefore a longer residence time is likely to result in higher diatom production and DSi consumption in the estuaries (Carbonnel 2009).

The interactions of Si along the land-ocean continuum and in the aquatic ecosystems are of growing concern since 1970's. The coastal waters are rapidly approaching Si limitation showing the importance of Si for coastal ecosystems and it is necessary to quantify the input fluxes of DSi and ASi to the coastal zone (Laruelle et al., 2009). Rivers represent the key link between the land and the ocean and are the dominant source of external DSi supply in the modern ocean (85%, Tréguer and De La Rocha, 2013). They also supply 1.1 ± 0.2 Tmol.yr^{-1} of BSi (Fig. 4) to the estuaries (Tréguer and De La Rocha, 2013). Amorphous silica (ASi) is mostly of biogenic origin (phytoliths, diatoms, sponge spicules) and relatively dissolvable in the aquatic ecosystems. ASi or BSi transport through rivers has often been neglected compared to DSi, but some studies showed a substantial contribution of ASi flux to the ocean (Conley 1997). For instance, ASi flux in some rivers can be >50% of DSi flux and thus may significantly contribute to the global Si cycle (Frings et al., 2014). Overall, the continental Si fluxes are not well constrained with ± 30% uncertainties in the estimates (Fig. 4). From the total Si riverine supply, 1.5 ± 0.5 Tmol Si year^{-1} (~21%) is trapped in the estuaries via several processes such as diatom uptake (De La Rocha et al., 1997; Sun et al., 2013), BSi settling, reverse weathering that incorporate Si during clay mineral formation from

BSi in sediment (Michalopoulos and Aller 2004; Presti and Michalopoulos, 2008; Sun et al., 2014). Though the tropical regions contribute ~ 75% of global DSi supply to the ocean, they are the least studied so far (Tréguer et al., 1995). Similarly, even though ~21% of Si is trapped in the estuaries (Treguer and De La Rocha. 2013), the fate of Si cycle within estuaries and their influence on the Si isotopes are not well studied. Moreover, studies on groundwater flux to the land-ocean continuum remain particularly scarce despite that groundwater is a major source of fresh water and Si enriched (Ziegler et al., 2005; Georg et al., 2009; Opfergelt et al., 2011; Pogge von Standmann et al., 2014). Si supply to the ocean by submarine groundwater discharge has indeed ± 100% uncertainty (Tréguer and De La Rocha 2013 and Fig. 4).

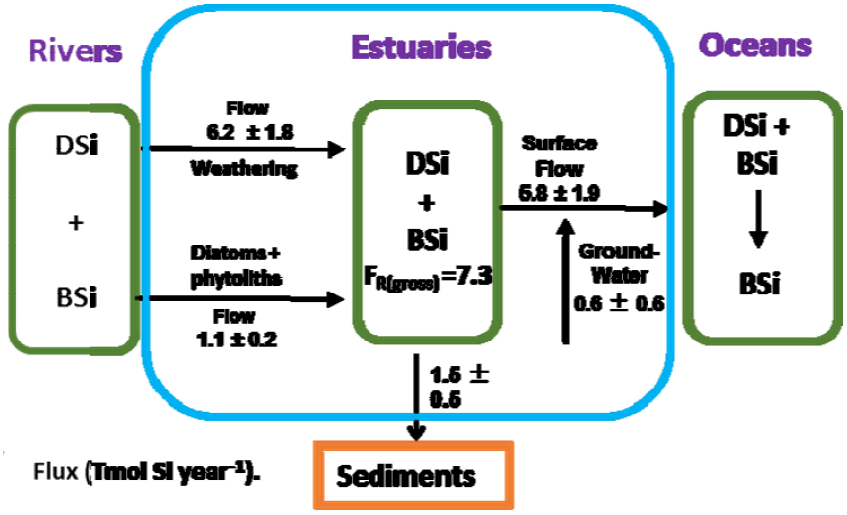

Fig. 4 *The biogeochemical cycle of Si in the land-ocean continuum at steady state with a close up on estuaries. (Adapted from Treguer and De La Rocha,,2013).*

1.4.1 Conservative vs. non-conservative behavior of DSi

From the biogeochemical point of view, the tidal effect is the most important to determine the type of estuary and the associated processes via the mixing of fresh water and salt water. For instance, when the seawater is mixed with freshwater in the estuary, there is a dramatic change in the concentration as well as the properties of riverine components. It is possible to determine the conservative or non conservative mechanism of DSi concentration by defining the mixing line. This is achieved by plotting the

concentration of DSi as a function of the concentration of a conservative property such as salinity (Fig. 5). If the estuary is in steady state, then the material fluxes between both the end-members are constant and the mixing line is the straight line joining the two end members (fresh and seawater) which is indicative of conservative behavior. If the points fall above the mixing line, it indicates that the component (DSi) is added in to the system (e.g. dissolution of BSi), and the points falling below the straight line, represents that the component is consumed (e.g., biological uptake). This simple two-end member mixing approach has been used widely to examine the conservative and non-conservative behavior of DSi in the tide dominated estuaries.

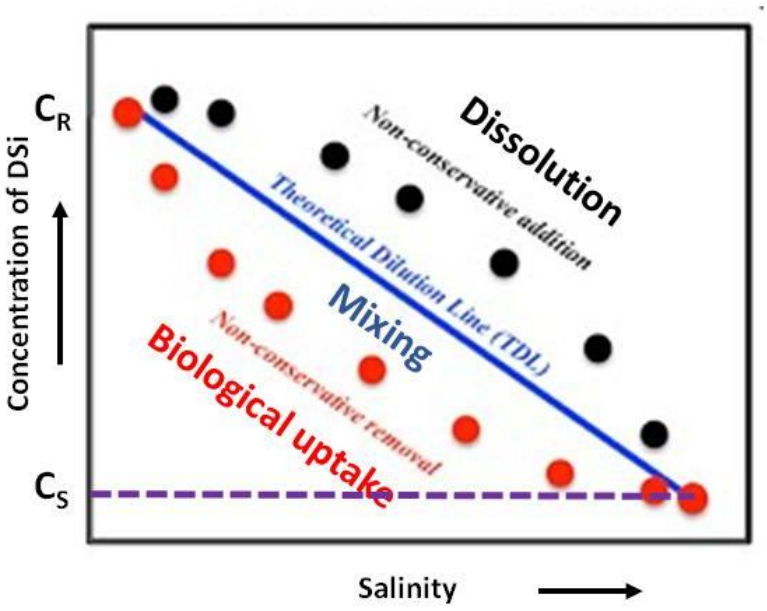

Fig. 5 *Idealized plot of the concentration of DSi and salinity during mixing process. C_R and C_S are the concentrations of DSi in river water and sea water end member respectively. The points above the mixing line indicating addition of DSi in the system (e.g., dissolution process) and the points below the mixing line represents the removal from the system (e.g., diatom uptake).The solid blue straight line indicating the theoretical mixing line and remains linear when the system is controlled by simple mixing of two end members (conservative behavior).*

Estuarine turbidity maxima (ETM)

In addition to simple mixing, the turbulence generated by the strong tidal force creates the resuspension of sediment and other particulate material from the river bed. Concurrently, the flocculation (adsorption or desorption) of dissolved materials (exchange of ions) occurs in the salt wedge region (Fig. 6). Consequently, the concentration of suspended material remains elevated within the estuary (~5 salinity). This zone is referred as Estuarine Turbidity Maximum (ETM) and its strength varies based on the tidal force and water flow in the system. During mixing of sea water and fresh water, the DSi may get adsorbed on the suspended matter (Fe and Al oxides, Ding et al., 2011) when in contact with electrolytes of sea water which may result in reduced supply of DSi to the downstream.

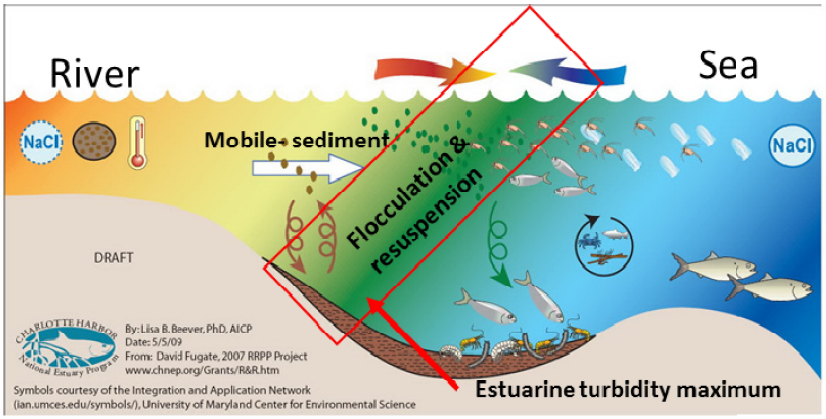

Fig. 6 *Schematic picture of estuarine turbidity maxima (ETM) and the red box indicating the ETM zone with high suspended material concentration, where flocculation (adsorption and desorption) and resuspension occur resulting in non-conservative behavior. (Source: www.chnep.org/Grants/R&R.htm).*

1.5 Anthropogenic perturbations over Si cycle in the land-ocean continuum

Increasing human activities in the river catchments are greatly influencing the nutrients and sediment load in the system (Milliman 1997; Turner et al., 2003). Even if the direct human inputs of DSi are limited, the indirect impacts can be important such as deforestation, damming and agriculture might alter the supply of DSi fluxes to the aquatic systems (Humborg et al., 2006; Conley et al., 2008; Struyf et al., 2010; Hughes et al., 2012). For example, river damming increases the water residence time and thereby creates favorable conditions for diatom growth. This consumes DSi to produce BSi followed by sedimentation (Conley et al., 2000; Laruelle et al., 2009; Hughes et al., 2012). At the end, this results in reduced DSi supply downstream. Likewise, increasing agricultural practice can also be responsible for the depletion of Si supply (Clymans et al., 2011; Keller et al., 2012; Guntzer et al., 2012 and Vandevenne

et al., 2015). On the other hand, deforestation might enhance the erosion and favor the weathering, leading to higher DSi supply (Conley et al., 2008; Alexandre et al., 2011; Ran et al., 2015). Finally, increased fertilizer usage for the agricultural activities (Li et al., 2007) results in the excess supply of N and P over Si causing a nutrient imbalance with the development of non-siliceous phytoplankton growth in the coastal ecosystem (Garnier et al., 2010; Howarth et al., 2011). This could result in Harmful Algal Bloom (HAB) and create eutrophication, a major threat to the basic food chain (Fig. 7). Agriculture is the most common land use in the tropical regions. More particularly in Asia, agriculture is dominated by 70% rice cultivation (a Si-accumulated plant, Ma et al., 2007) and produces 91% of global rice harvest (FAO, 2003). For example, it has been shown that heavy vegetation (inter tropical & low elevation forest) significantly supply phytoliths via physical erosion and represented 90% of total BSi in Nyong river in Cameroon (Cary et al., 2005). Likewise, phytoliths contributes 50 % of total ASi pool in river Cauvery through erosion of soils from thick agriculture land (Meunier et al., 2015). Then, the burial of phytoliths in the sediments accumulated in the dams decreases their active biogeochemical role in the Si cycle and thus may reduce the supply of DSi in rivers when dams are present.

Increasing agricultural activities associated with deforestation are more noticeable in tropical regions. Drastic environmental changes in the catchments are well reported, especially in Asia (Elvidge et al., 1997; Dudgeon 2000; Vorosmarty et al., 2003). A study on Indonesian Brantas River, which is heavily dammed did not notice Si retention whereas high load of N fertilizer altered the DSi: N ratio (Jennerjahn et al., 2004). This shows that tropical rivers might not have the same processes altering Si fluxes (Conley 1993). It has also been suggested that natural factors like climate and lithology play a dominant role compared to anthropogenic factors on the control of DSi in tropical rivers (Subramanian et al., 2006). This has been attributed to the existence of intense weathering resulting from young geology, high precipitation, runoff and widespread silicate rocks (including basalt) in the tropical regions compared to the temperate regions (Jennerjahn et al., 2006). However, increasing human-induced changes gain importance in the control of Si in the aquatic system. Indeed the coastal eutrophication potential is increasing since 4 decades for the rivers draining into the Indian ocean due to an decrease in Si:N and Si:P ratios in rivers (Garnier et al., 2010). Therefore, the knowledge of the DSi fluxes to the coastal zones is primarily important to understand the biogeochemical processes and health of the ecosystem.

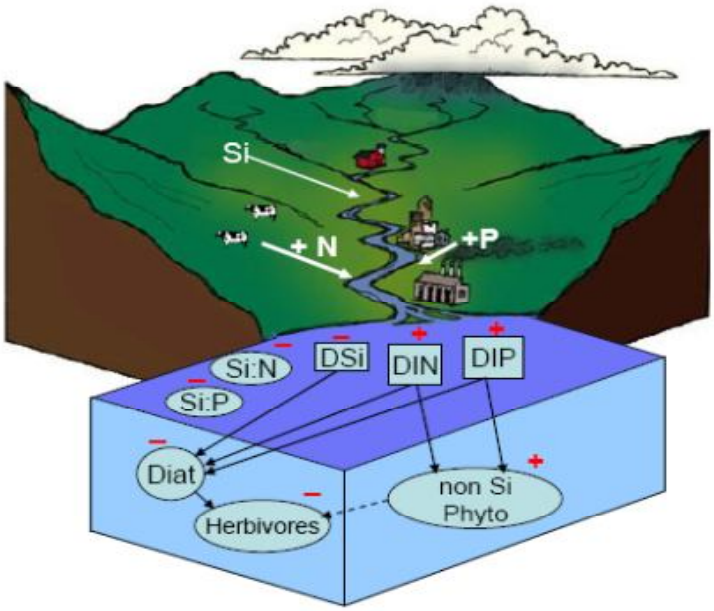

Fig. 7 *Schematic impacts of reduced supply of Si and increased supply of N and P in the land-ocean continuum due to the anthropogenic activities. The nutrient imbalance reduces Si:N and Si:P and results in the development of non-siliceous phytoplankton bloom that could ultimately lead to eutrophication and development of HAB's (harmful algal blooms) in the coastal ecosystems.*

2. Silicon isotopes

2.1 Basic principles

Isotopes are atoms of the same chemical element (i.e. with same number of protons and electrons) but differ in the number of neutrons. Therefore they have same chemical properties. However, due to their mass difference, the rate of the chemical reactions or processes differs amongst different isotopes, either kinetic (unidirectional / irreversible reactions) or equilibrium (bidirectional / reversible reactions in equilibrium). Silicon has three stable isotopes, ^{28}Si (92.23%), ^{29}Si (4.67 %) and ^{30}Si (3.10%) with their respective percentage of terrestrial abundance (Faure and Mensing 2005). The variations of stable Si isotopes are expressed in delta notation (δ) and represent the isotopic ratio of the sample relative to a standard reference material in ‰. Generally, the reference material of Si is NBS28 (quartz). It can be written as Eq. (2),

$$\delta^{30}Si\ (‰) = \left[\frac{(^{30}Si/^{28}Si)_{sample}}{(^{30}Si/^{28}Si)_{standard}} - 1 \right] \times 1000 \qquad \text{Eq. (2)}$$

The terrestrial processes are described by mass dependent fractionation between $\delta^{29}Si$ and $\delta^{30}Si$. The mass-dependent fractionation falls on a straight line and any deviation from this line indicates mass independent fractionation process, normally occurring only in extraterrestrial materials like meteorites (Zinner et al., 1989; Stone et al., 1991). Analytically, a deviation from mass-dependent line is indicative of an artifact due to isobaric interference unresolved by the mass spectrometer during the analysis (e.g. $^{14}N^{16}O$ signal superimposed on ^{30}Si peak). The precise value of the slope between $\delta^{29}Si$ and $\delta^{30}Si$ indicates the kinetic or equilibrium process. Yet the slope values of the reactions are similar with small variation i.e. 1.96 in the case of kinetic and 1.93 for equilibrium reactions which is close to the analytical error.

The degree of the isotopic fractionation between two materials A and B for given process is denoted by the isotope fractionation factor α (Coplen et al. 2011) and defined at equilibrium as:

$$\alpha_{A\text{-}B} = R_A / R_B \qquad \text{Eq. (3)}$$

Where R= $^{30}Si/\ ^{28}Si$ and when α =1, there is no fractionation. The ε represents the isotopic fractionation and is expressed in ‰ ; it is related to α via:

$$^{30}\varepsilon_{\ A-B} = 1000\ (\alpha_{\ A/B} - 1). \qquad \text{Eq. (4)}$$

Usually, the terrestrial processes exhibit limited isotopic fractionations and therefore the Si fractionation between the substances A and B can also be estimated by the isotopic difference Δ ($\Delta^{30}Si_{\ A\text{-}B} = \delta^{30}Si_A - \delta^{30}Si_B$) when equilibrium is reached. Generally, two models are used to describe the evolution of Si isotopic composition. They are Rayleigh model (closed system) assuming a limited Si reservoir without substitute by any external sources (De La Rocha et al., 1997) and steady state model (open system), where continuous supply of Si (Varela et al., 2004) and then the δ^{30}Si-DSi and $\delta^{30}Si$ of product can be described as,

Steady state model: $\delta^{30}Si_{DSi} = \delta^{30}Si_{initial} + {}^{30}\varepsilon\ (\ln f)$ Eq. (5)

$\delta^{30}Si_{Solid} = \delta^{30}Si_{DSi} + {}^{30}\varepsilon$ Eq. (6)

The Rayleigh model can be described as,

Rayleigh model: $\delta^{30}Si_{DSi} = \delta^{30}Si_{initial} - {}^{30}\varepsilon\ (1-f)$ Eq. (7)

$\delta^{30}Si_{Solid} = \delta^{30}Si_{initial} + {}^{30}\varepsilon\ f$ Eq. (8)

$\delta^{30}Si_{bSiO2\ acc} = \delta^{30}Si_{Si\ (OH)4\ initial} - {}^{30}\varepsilon.\ (f.\ \ln(f)\ /1-f)$ Eq. (9)

Where $\delta^{30}Si_{initial}$ is the Si isotopic composition in the initial reservoir, *f* is the fraction of DSi remaining in the solution and ${}^{30}\varepsilon$ is the isotopic fractionation between dissolved and the product phase.

With the advent of Multi-Collectors – Inductively Coupled Plasma Mass Spectrometers (MC-ICP-MS), the Si stable isotopes are measured with very good precision in dry plasma mode at medium resolution with negligible isobaric interference (more details in Chapter 2).

Si isotopes studies became a useful tool to investigate the complex biotic and abiotic processes that control the Si biogeochemical cycle. This is possible because of the occurrence of significant fractionation of Si isotopes during e.g. clay mineral formation and biological uptake by terrestrial and aquatic organisms (Ding et al., 2005; Georg et al., 2007; Opfergelt et al., 2006; Ziegler et al., 2005).

2.2 Variability of Si isotopes in Earth surface

The range of Si isotopic compositions on the Earth surface has been compiled by several studies and used to trace back the source of DSi from various reservoirs. So far, the lightest and heaviest Si isotopic compositions were found in silcretes (δ^{30}Si =-5.7 ‰, Basile-Doelsch et al., 2005) and in rice grains (δ^{30}Si =6.1 ‰, Ding et al., 2005), respectively. The variability of δ^{30}Si values found in natural samples is shown in the Fig. 8 ascribing various processes like weathering, dissolution/precipitation reactions, and biological processes. So far, there is no study existing on δ^{30}Si variability of Indian rivers except Ganges basin whose δ^{30}Si variability of DSi ranges from 0.8 to 3.04 ‰ (Frings et al., 2015). Near congruent (upper river-near Himalayas) to incongruent dissolution of primary minerals (middle and lower river-

peninsular and alluvial plains) with subsequent clay mineral formation and biological uptake are the major controlling mechanisms of Si isotopes. The heavier δ^{30}Si of Ganges basin is concurrent with other tropical Yangtze river (Ding et al., 2002) and semi arid Nile basin (Cockerton et al., 2013) with δ^{30}Si up to 3.4 ‰ and 4.7‰ respectively. Noteworthy, the δ^{30}Si of other tropical rivers like Tana (1.6 ± 0.4 ‰), Amazon (1.0 ± 0.6 ‰), Congo (0.9 ± 0.1‰) are less variable than the Ganges and Chinese rivers [Hughes et al., 2011, 2012 and 2013].

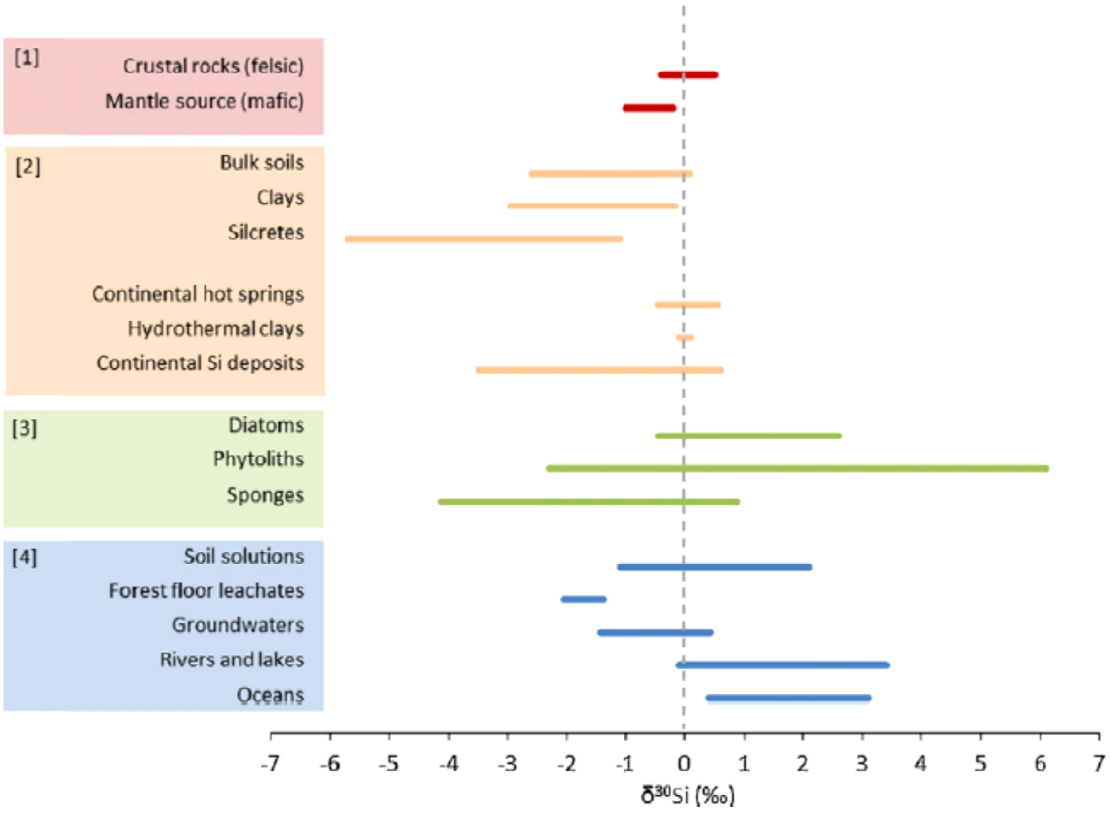

Fig. 8 *Variability of Si isotopic compositions of various natural samples of Earth's surface grouped under major reservoirs or processes [1] rock formation, [2] water-rock interaction, [3] biological processes and [4] water reservoirs (from Opfergelt and Delmelle, 2012).*

2.3 Estuaries and Si isotopes

The Si isotopic composition of estuaries could be altered via several processes such as diatoms uptake (De la Rocha et al., 1997; Sun et al., 2013), dissolution of BSi from phytoliths and dead diatoms (Demarest et al., 2009; Loucaides et al., 2008), reverse weathering process that utilize Si from biogenic

materials to form clay minerals (Michalopoulos and Aller 2004; Sun et al., 2014; Wetzel et al., 2014) and finally the lateral transport via tidal marsh areas (Struyf et al., 2006; Weiss et al., 2013, 2015). Other processes such as groundwater supply or adsorption – desorption have never been studied for Si isotopes in estuaries but are potentially impacting the δ^{30}Si signatures with larger isotope fractionation (Georg et al., 2009; Delstanche et al., 2009; Oelze et al., 2014). The Si isotopic composition of seawater greatly depends on the balance between continental weathering supplied via rivers and oceanic crust weathering (Treguer and De La Rocha 2013). So far, only few estuarine δ^{30}Si values are available, this includes tropical Tana estuary in Kenya (Hughes et al., 2012) suggesting simple mixing governing the δ^{30}Si variability. Another study on Scheldt freshwater estuary (Belgium) suggests dominant diatom uptake – dissolution in spring-summer and mixing of different tributaries bearing different δ^{30}Si due to different lithology and land-use in winter (Delvaux et al., 2013). In Elbe estuary (Germany) seasonal changes was explained by diatom uptake and lateral transport from adjacent tributaries (Weiss et al., 2015). Finally, in Yellow river the δ^{30}Si varied from 0.4 to 2.5 ‰ and is getting heavier downstream before entering in to the sea (Ding et al., 2011). Combination of several biotic (biological uptake and phytolith formation) and abiotic processes (increased weathering intensity, adsorption of Si on iron oxides and dissolution of phytoliths) are responsible for the heavier and variable isotopic signature in the Yellow river. However, the δ^{30}Si signatures of the Yellow river are less variable than in the Yangtze river (0.7 to 3.4 ‰, Ding et al., 2004). This has been mainly ascribed to the higher rate of weathering intensity and agricultural activities in the later basin.

Si isotopes and mixing

The isotopic composition due to mixing only is the intermediate composition of two end members i.e., river water and sea water without any fractionation, weighted by the concentration of DSi in the two end-members. Therefore unlike the mixing straight line on concentrations (Fig. 5), isotopic mixing exhibit hyperbolic curve (Fig. 9a). When the difference between the two elemental concentrations of end members is close to zero, then the hyperbola will flatten in to line. Therefore, δ^{30}Si vs. inverse of DSi concentration yields to a straight line controlled by mixing only. Hence, fractionation processes can be delineated from mixing process by checking whether a straight line is obtained on a δ^{30}Si vs. 1/DSi plot (Fig. 9b).

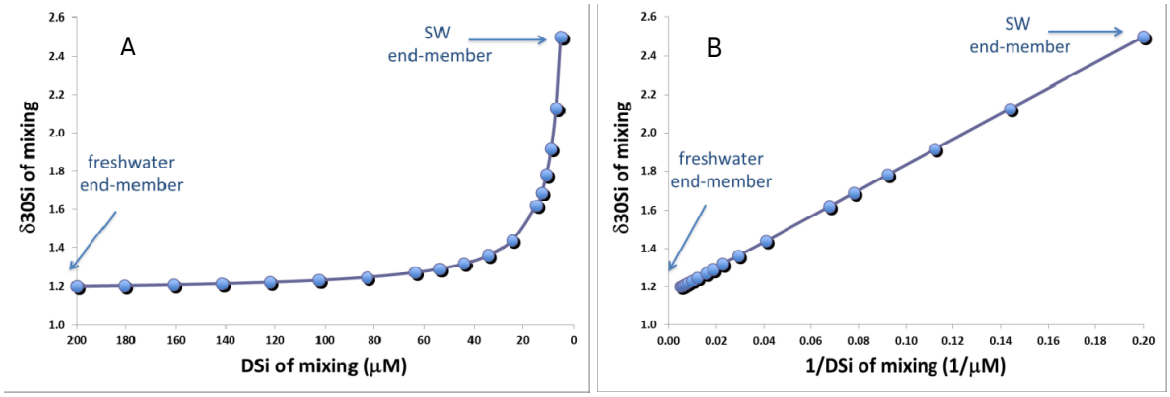

***Fig. 9 A and B**, Simple isotopic mixing model of two end member river water and sea water respectively. Simple mixing of isotopes exhibits hyperbolic curve (A) and mixing process is delineated from other fractionating processes by obtaining straight line between $\delta^{30}Si$ & 1/DSi (B): used as a tracer for explaining mixing process.*

3. Indian estuaries

India has ~220 major and minor estuaries with varying size and shape across the ~7500 km Indian coastline (Rao et al., 2013; Sarma et al., 2012). India has a typical monsoonal climate. The reversal of surface winds from January to July causes two types of monsoon. The winter, dry and cold air from land in the northern latitudes flows southwest (northeast monsoon) and in summer, the warm and humid air initiates over the ocean and flows in opposite direction (southwest monsoon). In general, 70-95% of annual rainfall is brought by the monsoon and in which maximum part of India receives rainfall from southwest monsoon (i.e. between June and September). Indeed, the south-eastern part of India (Tamil Nadu and adjoining areas) receives rainfall only during the northeast monsoon (October and November, Attri and Tyagi, 2010). India has an average annual precipitation of 1170 mm and 80% of the total area of the country is fed by the annual rainfall of 750 mm (source: www.fao.org). India has a high variety of climates from semi-arid in North-West and South-East to tropical wet in South-West (Fig. 10)

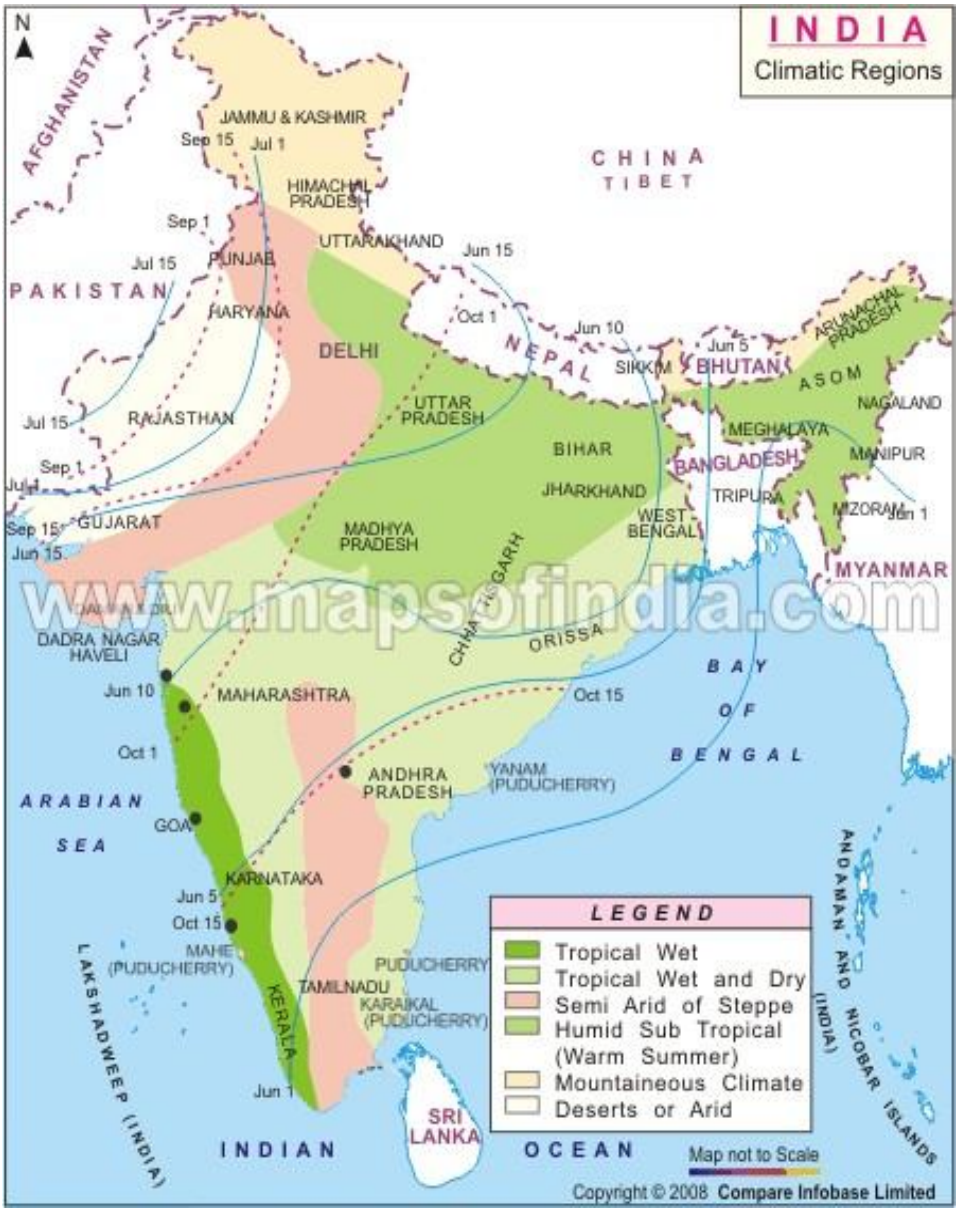

Fig. 10 *Different types of climate over India. Blue line indicates the normal date of onset of south-west monsoon which supply most of the rainfall (Source www.mapsofindia.com)*

Hence, Indian rivers are strongly influenced by the precipitations during both the monsoons and most estuaries receive huge freshwater flux in a limited period of time. This is why the Indian estuaries are referred to as monsoonal estuaries, with the notable exceptions of (i) Ganges-Bhramaputra which is more perennial and, (ii) less seasonal and south-east estuaries since their watershed are spread over arid to semi-arid climate and water is mostly diverted for agriculture and domestic use before reaching estuaries. The Indian subcontinent is bounded by the Arabian Sea on the West and Bay of Bengal on the

East and receives huge suspended material (SPM) and freshwater influx in the Bay of Bengal when compared to Arabian Sea (Fig. 11).

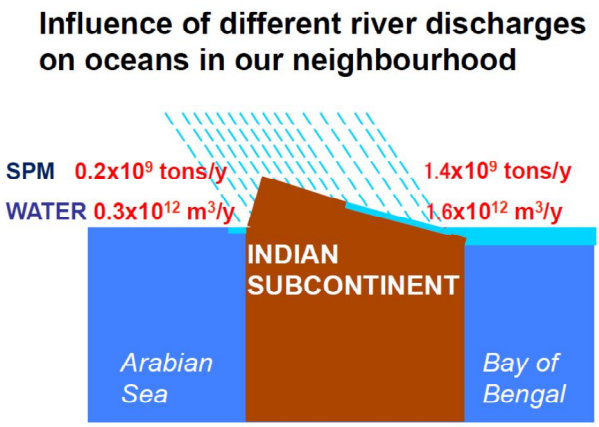

Fig. 11 *Schematic structure of the two contrasted basins of the Indian subcontinent that transport suspended load and fresh water flow at annual scale. Bay of Bengal receives 7 times higher suspended load (SPM) and 5 times more fresh water flow when compared to the Arabian Sea. Source: Nair et al., 1989; Ittekkot et al., 1991.*

3.1 Lithology of River basins

Indian geology is comprised of three major geological units: 1) the Himalayan mountains, 2) the peninsular plateaus and 3) the Indo-Gangetic plains. The geology of Indian subcontinent is diversed from Precambrian hard rock to the most recent alluvium plains. The Himalayan region has a wide mixture of igneous and metamorphic rocks along with tertiary sediments and their proportions varying in the different drainage basins. Moreover, the watersheds in this region are characterized by the presence of silicate rocks (Blum et al. 1998; Quade et al., 2003). The peninsular plateaus are the Deccan traps in the central parts composed of basaltic rocks. The basic lithology of the major river basin is predicted in Table 1 and simplified geology & major watershed in Fig. 12.

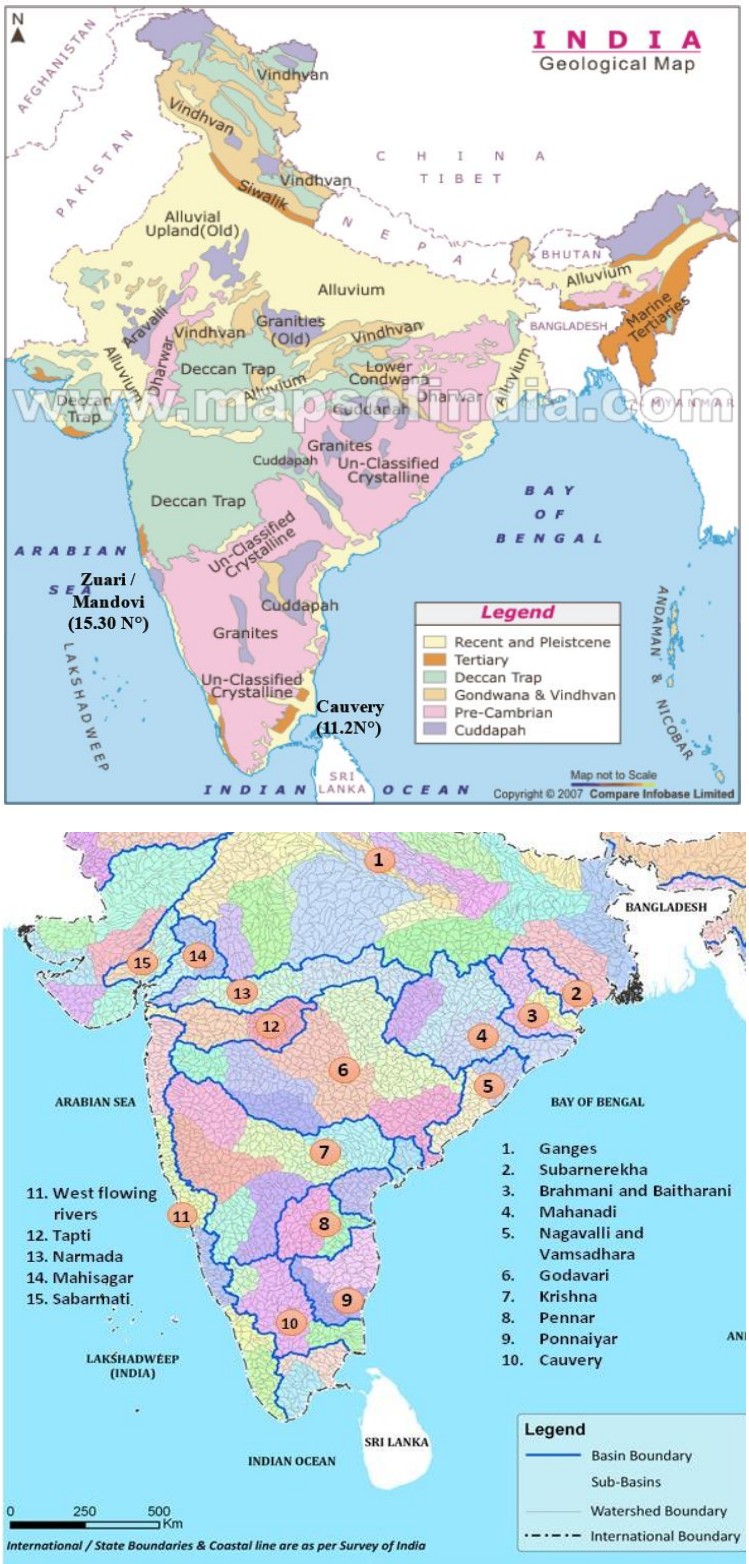

Fig. 12 *Simplified geological and major watershed maps of India (Source: www.mapsofindia.com)*

Major River basin	Basin lithology
Ganges	Upper reaches: granite and other hard and soft rocks 20%, sedimentary rocks 20%, alluvium 60%
Mahanadi	Granite 34%, Sandstone 22%, limestone and shale 17%, charnokite and other hard rocks 20%, coastal sediments 5%.
Godavari	Granite and hard rocks 20%, Deccan basaltic traps 56%, sedimentary rocks 24%.
Krishna	crystalline rocks 78%, Deccan basaltic traps 20%, alluvium 2%
Cauvery	Gneiss 60%, Charnokite 25%, sandstone and limestone 10%, other sedimentary rocks 5 %
Southwest flowing rivers	Granite and other hard rocks 80%, alluvium 20%.
Narmada	Deccan basaltic traps 70%, sedimentary rocks 30%
Tapti	Deccan basaltic traps 70%, sedimentary rocks 30%

Table 1 *The major river basins and their associated lithology of the Indian subcontinent. Table adapted from Subramanian et al, (2006).*

3.2 Why Si cycle in Indian estuaries?

As seen earlier, anthropogenic pressures along the land-ocean continuum and their impacts on Si cycle have been reported by several studies. All these anthropogenic pressures are known to occur in the Indian estuaries (land-ocean continuum). The major problems that could impact the health of the Indian estuarine ecosystems are:

- Increased agricultural activities i.e., 61% of the total watershed area (Central Water Commission report 2014).
- High fertilizer consumption and dumping of excess nutrient (especially N and P) supply in the coastal waters (ministry of Agriculture report, 2012-13).
- Land degradation via erosion. Around 5.3 x 10^9 tons of soil is eroded annually, of which 29% enters into the sea, 10% is retained by the reservoir and the remaining 61% is shifted from one place to another (Ministry of Agriculture report, 2012-13).

- Indian rivers are heavily dammed to meet irrigation, domestic and hydroelectric demands. India ranks fourth in a total number of dams in the world (CWC, 2009).
- Finally, increasing urbanization of the coastal areas due to the increased population growth.

Silicon is rarely studied in the land-ocean continuum. There are no studies existing on ASi dynamics and Si isotopic composition in Indian estuaries (except Ganges basin). We need to focus more on the tropical rivers that supplies 70% of DSi to the ocean to mitigate the risks of ecosystem perturbations. To our knowledge, there are no published studies of the behavior of silicon isotopes in the Indian estuaries.? There are actually only two studies on δ^{30}Si in Indian rivers, both on the Ganges basin (Georg et al., 2009; Frings et al., 2015). This lack of information may hinder the understanding the Si cycle in a land-ocean continuum that controls the Si cycle in adjacent coastal water. Therefore for the first time, seasonal data on silicon isotopes and ASi variability and their associated processes in the Indian estuaries are discussed.

4. Objectives of the study and thesis outline

4.1 Framework

The research leading to these results has been funded by the European Union Seventh Framework Program under grant agreement #294146 (MuSiCC, a Multi-proxy Approach of the Silicon and Carbon cycles, a Marie Curie CIG, cf. http://biogeochemist.eu/musicc/), from the French National INSU programme EC2CO-LEFE (project SINDIA Silicon cycle along the land – ocean continuum in India, funded by Actions CYBER and BIOHEFECT, cf. http://biogeochemist.eu/sindia/). K.R. Mangalaa (Kameswari Rajasekaran Mangalaa) scholarship has been provided by the Erasmus Mundus Action 2 of the European Union (GATE, a mobility project with Asia), the Scientific Department of French Embassy in India and, MuSiCC. Outside LOCEAN the main collaborators of MuSiCC and SINDIA are Dr. V.V.S.S. Sarma (co-supervisor of K.R. Mangalaa's Ph. D.) from National Institute of Oceanography (Regional Centre of Visakhapatnam), Prof. N.S. Sarma from Andhra University and Dr. Jean Riotte (IRD) from the Indo-French Cell of Water Research (IFCWR Bengaluru) and GET (Toulouse).

4.2 Objectives

The main objective of this thesis is to investigate for the first time ASi and Si isotopes and their seasonal dynamics and associated processes in Indian estuaries. More specifically, we looked at the responsible factors and processes that affect the variability of Si dynamics including the climate and anthropogenic activities such as the impact of land use on the different basins that cover different lithologies. We also compare the groundwater vs. upper estuary isotopic compositions. Moreover, the ASi, DSi, LSi fluxes to the downstream and coastal waters is also investigated. Finally we made a more detailed study on two contrasted rivers to better understand the processes setting the Si fluxes and δ^{30}Si signatures before entering the estuaries.

4.3 Thesis outline

- A brief introduction on Si cycle and the present status has been read in this **Chapter 1.**

- To study the ASi and Si isotope variability, the methodologies for the chemical analysis are discussed in **Chapter 2** with the quality control of measurements, inter-calibration exercises are reported. In addition, the chemistry of Si isotope sample preparation and the check for organic matter matrix effect are also discussed.

- In **Chapter 3,** the first look at seasonal, anthropogenic and biogeochemical processes on silicon cycle in 24 and 18 Indian estuaries during the dry and wet period are presented and discussed. The ASi, LSi, DSi variability in all estuaries from different geographical locations is discussed. We categorise the samples based on the season and position along the salinity gradient irrespective of their geographical locations. We perform Principal Component Analysis (PCA) and clustering on PCA results to highlight similarities in biogeochemical functioning of the estuaries. In addition, the impact of land use on the Si cycle is also addressed. Finally, the flux of ASi, LSi and DSi to the coastal North Indian Ocean are discussed to fill the existing knowledge gaps on global Si budget. This chapter has been submitted as an article to *Continental Shelf Research*.

- **Chapter 4** mainly deals with the Si isotopic composition of DSi in Indian estuaries. Their seasonal variability is discussed as well as the processes likely responsible for the changes in Si isotopes.

In addition, ground water Si isotopic compositions are reported and compared. The geochemical processes like weathering/dissolution are discussed using saturation indices of minerals to trace back the source of DSi while diatoms production is estimated based on Rayleigh and steady-state models when applicable.

- In **Chapter 5,** closer look at δ^{30}Si compositions of two geographically contrasting rivers (in terms of topography, climate, length, land use, water use) are studied (Netravathi vs. Cauvery) to understand the processes occurring upstream the estuaries.

- In **Chapter 6** main conclusions and perspectives of this work are presented

- Finally the **Annex/Appendix** are given at the end of the entire manuscript.

5. References

Alexandre, A., Bouvet, M. & Abbadie, L. The role of savannas in the terrestrial Si cycle: A case-study from Lamto, Ivory Coast. *Glob. Planet. Change* **78,** 162–169 (2011).

Alexandre, A., Meunier, J.-D., Colin, F. and Koud, J.-M.: Plant impact on the biogeochemical cycle of silicon and related weathering processes, Geochim. Cosmochim. Acta, **61**(3), 677–682, doi:10.1016/S0016-7037(97)00001-X, (1997).

Attri, S. D. & Tyagi, A. Climate profile of India. *Gov. India Minist. Earth Sci.* 129 (2010). at http://www.imd.gov.in/doc/climate_profile.pdf.

Beckwith, R. S. and Reeve, R.: Studies on soluble silica in soils. The sorption of silicic acid by soils and minerals, Aust. J. Soil. Res., 1, 157–168, (1963).

Berner, R. A., The rise of plants and their effect on weathering and atmo- spheric CO2, Science, **276**, 544–546, (1997).

Berner, R. A., Weathering, plants, and the long-term carbon cycle, Geo- chim. Cosmochim. Acta, **56**, 3225–3231, (1992).

Berner, R.A. Chemical weathering and its effect on the atmospheric CO2 and climate. In: White, A.F., Brantley, S.L. (Eds.), Chemical weath- ering rates of silicate minerals. Rev. Mineral. Mineral. Soc. Am, Washington D.C., pp. 565–583, (1995).

Bianchi TS. Biogeochemistry of Estuaries. Oxford: Oxford Uni- versity Press; (2007).

Blum, J. D., Gazis, C. A., Jacobson, A. D. & Chamberlain, C. P. Carbonate versus silicate weathering in the Raikhot watershed within the High Himalayan Crystalline Series. *Geology* **26,** 411–414 (1998).

Carbonnel, V., Lionard, M., Muylaert, K. & Chou, L. Dynamics of dissolved and biogenic silica in the freshwater reaches of a macrotidal estuary (The Scheldt, Belgium). *Biogeochemistry* **96,** 49–72 (2009).

Carbonnel, V. Silica dynamics and retention in the Scheldt tidal river and estuary (Belgium / The Netherlands). (2009).

Cary, L., Alexandre, A., Meunier, J. D., Boeglin, J. L. and Braun, J. J.: Contribution of phytoliths to the suspended load of biogenic silica in the Nyong basin rivers (Cameroon), Biogeochemistry, 74(1), 101–114, doi:10.1007/s10533-004-2945-1, (2005).

Central Water Commission, Ministry of water resources, Government of India. *Version 2.0*. (2014).

Central Water Commission (CWC), National Register of Large Dams, Government of India (2009).

Clymans W, Struyf E, Govers G, Vandevenne F, Conley DJ. Anthropogenic impact on amorphous silica pools in temperate soils. Biogeosciences **8**:2281–93, (2011).

Cockerton H.E., Street-Perrott F.A., Leng M.J., Barker P.A., Horstwood M.S.A. and Pashley V. Stable-isotope (H, O, and Si) evidence for seasonal variations in hydrology and Si cycling from modern waters in the Nile Basin: implications for interpreting the Quaternary record. Quaternary Science Reviews 66: 4-21. (2013).

Conley, D. J.: Riverine contribution of biogenic silica to the oceanic silica budget, Limnol. Oceanogr., 42(4), 774–777, doi:10.4319/lo.1997.42.4.0774, (1997).

Conley, D. J.: Terrestrial ecosystems and the global biogeochemical silica cycle, Global Biogeochem. Cycles, **16**(4), 68-1-68–8, doi:10.1029/2002GB001894, (2002).

Conley, D.J., Humborg, C., Smedberg, E., Rahm, L., Papush, L., Danielsson, Å., Clarke, A., Pastuszak, M., Aigars, J., Ciuffa, D., Mörth, C.-M. Past, present and future state of the biogeochemical Si cycle in the Baltic Sea. Journal of Marine Systems **73**, 338–346, (2008).

Conley, D.J., Kaas, H., Mølenberg, F., Rasmussen, B., Windolf, J. Characteristics of Danish estuaries. Estuaries **23**, 820–837, (2000).

Coplen, T. B.: Guidelines and recommended terms for expression of stable-isotope-ratio and gas-ratio measurement results., Rapid Commun. Mass Spectrom., 25(17), 2538–2560, doi:10.1002/rcm.5129, (2011).

De La Rocha C. L., Brzezinski M. A. and Deniro M. J. Fractionation of silicon isotopes by marine diatoms during biogenic silica formation. Geochim. Cosmochim. Acta **61**, 5051– 5056, (1997).

Delstanche, S. Opfergelt, S.Cardinal, D. Elsass, F. André, L. Delvaux, B. Silicon isotopic fractionation during adsorption of aqueous monosilicic acid onto iron oxide. *Geochim. Cosmochim. Acta* **73,** 923–934 (2009).

Demarest, M.S., Brzezinski, M.A., Beucher, C.P. Fractionation of silicon isotopes during biogenic silica dissolution. Geochimica et Cosmochimica Acta **73**, 5572-5583 (2009).

Derry L.A., Kurtz A.C., Ziegler K. and Chadwick O.A.. Biological control of terrestrial silica cycling and export fluxes to watersheds. Nature **433**: 728–731, (2005).

Dessert, C., Dupre´ , B., Gaillardet, J., Francois, L.M., Alle´gre, C.J. Basalt weathering laws and the impact of basalt weathering on the global carbon cycle. Chem. Geol. **202**, 257–273, (2003).

Ding, T. P., Ma, G. R., Shui, M. X., Wan, D. F. & Li, R. H. Silicon isotope study on rice plants from the Zhejiang province, China. *Chem. Geol.* **218,** 41–50 (2005).

Ding, T., Wan, D., Wang, C. and Zhang, F.: Silicon isotope compositions of dissolved silicon and suspended matter in the Yangtze River, China, Geochim. Cosmochim. Acta, 68(2), 205–216, doi:10.1016/S0016-7037(03)00264-3, (2004).

Ding, T. P., Gao, J. F., Tian, S. H., Wang, H. B. and Li, M.: Silicon isotopic composition of dissolved silicon and suspended particulate matter in the Yellow River, China, with implications for the global silicon cycle, Geochim. Cosmochim. Acta, 75(21), 6672–6689, doi:10.1016/j.gca.2011.07.040, (2011).

Dove, P.: Kinetic and thermodynamic controls on silica reactivity in weathering environments, in: Chemical weathering rates of silicate minerals, edited by: White, A. and Brantley, S., Miner- alogical Society of America,Washington, DC, 235–290, (1995).

Drees, L. R., Wilding, L. P., Smeck, N. E., and Senkayi, A. L.,. Silica in soils: quartz and disorders polymorphs, in: Minerals in soil environments, Soil Science Society of America, Madison, 914–974, (1989).

Ducklow, H. W., Steinberg, D. K. & Buesseler, K. O. Upper ocean carbon export and the biological pump. *Oceanography* **14,** 50–58 (2001).

Dudgeon, D. Large-Scale Hydrological Changes in Tropical Asia : Prospects for Riverine Biodiversity. *Bioscience* **50,** 793–806 (2000).

Durr, H.H., Meybeck, M., Hartmann, J., Laruelle, G.G., Roubeix, V. Global spatial distribution of natural riverine silica inputs to the coastal zone. Biogeosciences Discussions **6**, 1345–1401 (2009).

Elvidge, C.D, K.E.Baugh, E.A.Kihn, H. W. K. and E. R. D. Mapping city lights with night time data from the DMSP operationational linescan system. *Photogrametric Eng. Remote Sensing* **63,** 727–734 (1997).

Epstein E. The anomaly of silicon in plant biology. Proc. Natl. Acad. Sci. **91**: 11–17 (1994).

Epstein, E. Silicon. An. Rev. Plant Physiol. Plant Molec. Biol. **50**, 641– 664 (1999).

Exley, C. Silicon in life: A bioinorganic solution to bioorganic essentiality. *J. Inorg. Biochem.* **69,** 139–144 (1998).

Faure. G, T. M. Mensing. Isotopes Principles and Applications. John Wiley & Sons, Inc., Hobonken, New Jersey, 3rd edition (2005).

Fraysse F., Pokrovsky O. S., Schott J. and Meunier J. D. Surface properties, solubility and dissolution kinetics of bam- boo phytoliths. Geochim. Cosmochim. Acta **70**, 1939–1951 (2006).

Fraysse F., Pokrovsky O. S., Schott J. and Meunier J. D. Surface chemistry and reactivity of plant phytoliths in aqueous solutions. Chem. Geol. **258**, 197–206, (2009).

Fraysse, F., Pokrovsky, O. S., and Meunier, J. D.: Experimental study of terrestrial plant litter interaction with aqueous solutions, Geochim. Cosmochim. Acta, **74**, 70–84, (2010).

Frings, P. J., De La Rocha, C., Struyf, E., Pelt, D. Van, Schoelynck, J., Hudson, M. M., Gondwe, M. J., Wolski, P., Mosimane, K., Gray, W., Schaller, J. and Conley, D. J.: Tracing silicon cycling in the Okavango Delta, a sub-tropical flood-pulse wetland using silicon isotopes, Geochim. Cosmochim. Acta, **142**, 132–148, doi:10.1016/j.gca.2014.07.007, (2014).

Frings, P. J., Clymans, W., Fontorbe, G., Gray, W., Chakrapani, G. J., Conley, D. J. and De La Rocha, C.: Silicate weathering in the Ganges alluvial plain, Earth Planet. Sci. Lett., 427, 136–148, doi:10.1016/j.epsl.2015.06.049, 2015.

Gaillardet, J., Dupré, B. and Allègre, C. J.: Geochemistry of large river suspended sediments: silicate weathering or recycling tracer?, Geochim. Cosmochim. Acta, **63**(23–24), 4037–4051, doi:10.1016/S0016-7037(99)00307-5, (1999).

Garnier, J., Beusen, A., Thieu, V., Billen, G. & Bouwman, L. N:P:Si nutrient export ratios and ecological consequences in coastal seas evaluated by the ICEP approach. *Global Biogeochem. Cycles* **24,** GB0A05, 1-12 (2010).

Georg, R. B., Reynolds, B. C., West, A. J., Burton, K. W. & Halliday, A. N. Silicon isotope variations accompanying basalt weathering in Iceland. *Earth Planet. Sci. Lett.* **261,** 476–490 (2007).

Georg, R.B, West A.J., Basu A.R., Halliday A.N. Silicon fluxes and isotope composition of direct groundwater discharge into the Bay of Bengal and the effect on the global ocean silicon isotope budget. Earth Planet. Sci. Lett. **203**:67–74, (2009).

Georg, R.B., West, A.J., Basu, A.R., Halliday, A.N. Silicon fluxes and isotope composition of direct groundwater discharge into the Bay of Bengal and the effect on the global ocean silicon isotope budget. Earth Planet. Sci. Lett. **283**, 67–74, (2009a).

Government of India. State of Indian Agriculture. 247 (2012). At http://agricoop.nic.in/sia111213312.pdf.

Guntzer, F., Keller, C. & Meunier, J. D. Benefits of plant silicon for crops: A review. *Agron. Sustain. Dev.* **32,** 201–213 (2012).

Hiemstra T., Barnett M. O. and van Riemsdijk W. H. Interaction of silicic acid with goethite. J. Colloid Interface Sci. **310**, 8–17, (2007).

Howarth, R. Chan, Francis, Conley, Daniel J, Garnier, Josette, Doney, Scott C, Marino Roxanne and Billen Gilles. Coupled biogeochemical cycles: eutrophication and hypoxia in temperate estuaries and coastal marine ecosystems. *Front. Ecol. Environ.* **9,** 18–26 (2011).

Hughes, H.J., Bouillon, S., André, L., Cardinal, D.The effects ofweathering variability and anthropogenic pressures upon silicon cycling in an intertropicalwatershed (Tana River, Kenya). Chem. Geol. 308–309, 18–25, (2012).

Hughes, H. J., Sondag, F., Cocquyt, C., Laraque, A., Pandi, A., André, L. and Cardinal, D.: Effect of seasonal biogenic silica variations on dissolved silicon fluxes and isotopic signatures in the Congo River, Limnol. Oceanogr., 56(2), 551–561, doi:10.4319/lo.2011.56.2.0551, (2011).

Hughes, H. J., Sondag, F., Santos, R. V., André, L. and Cardinal, D.: The riverine silicon isotope composition of the Amazon Basin, Geochim. Cosmochim. Acta, 121, 637–651, doi:10.1016/j.gca.2013.07.040, (2013).

Humborg,C., Pastuszak, M., Aigars, J., Siegmund, H., Mörth ,C.M., Ittekkot, V. Decreased silica land–sea fluxes through damming in the Baltic Sea catchment—significance of particle trapping and hydrological alterations. Biogeochemistry **77**, 265–281, (2006).

Iler, R.K., Silica gels and powders. In: Iler, R.K. (Ed.), The Chemistry of Silica. Wiley, New York, pp. 462–599 (1979).

Ittekkot, V., R. R. Nair, S. Honjo, V. Ramaswamy, M. Bartsch, S. Manganini, and B. N. Desai. Enhanced particle fluxes in Bay of Bengal induced by injection of fresh water, Nature, **351**, 385–387. (1991).

Jennerjahn, T. C. *et al.* Biogeochemistry of a tropical river affected by human activities in its catchment: Brantas River estuary and coastal waters of Madura Strait, Java, Indonesia. *Estuar. Coast. Shelf Sci.* **60,** 503–514 (2004).

Jennerjahn, T. C., Knoppers, B. A., de Souza,W. F. L., Brunskill, G. J., Silva, I. L., and Adi, S.: Factors controlling dissolved silica in tropical rivers, in: The Silicon Cycle – Human Perturbations and Impacts on Aquatic Systems, edited by: Ittekot, V., Unger, D., Humborg, C., and Tac An, N., SCOPE 66, Island Press, Washington, 29–51, (2006).

Jones LHP, Handreck KA. Effects of iron and aluminium oxides on silica in solution in soils. Nature **198**(4883):852–853, (1963).

Keller, C., Guntzer, F., Barboni, D., Labreuche, J. & Meunier, J. D. Impact of agriculture on the Si biogeochemical cycle: Input from phytolith studies. *Comptes Rendus Academ. Sci. - Geosci.* **344,** 739–746 (2012).

Laruelle, G. G., Roubeix, V., Sferratore, A., Brodherr, B., Ciuffa, D., Conley, D. J., Dürr, H. H., Garnier, J., Lancelot, C., Le Thi Phuong, Q., Meunier, J.-D., Meybeck, M., Michalopoulos, P., Moriceau, B., Ní Longphuirt, S., Loucaides, S., Papush, L., Presti, M., Ragueneau, O., Regnier, P., Saccone, L., Slomp, C. P., Spiteri, C. and Van Cappellen, P.: Anthropogenic perturbations of the silicon cycle at the global scale: Key role of the land-ocean transition, Global Biogeochem. Cycles, **23**(4), GB4031, 1-17, doi:10.1029/2008GB003267, (2009).

Li, M., Xu, K., Watanabe, M. & Chen, Z. Long-term variations in dissolved silicate, nitrogen, and phosphorus flux from the Yangtze River into the East China Sea and impacts on estuarine ecosystem. *Estuar. Coast. Shelf Sci.* **71,** 3–12 (2007).

Lionard M. Spatio-temporal phytoplankton dynamics along the Scheldt-North Sea continuum based on HPLC/CHEMTAX pigment analysis. Ph. D. thesis. Univ. of Ghent, Belgium (2006).

Loucaides S, Van Cappellen P, Behrends T. Dissolution of biogenic silica from land to ocean: Role of salinity and pH. Limnol Oceanogr **53**(4):1614-1621, (2008).

Ma, J. F., Yamaji, N., Mitani, N., Tamai, K., Konishi, S., Fujiwara, T., … Yano, M. An efflux transporter of silicon in rice. *Nature*, **448**(7150), 209–12 (2007).

Martin-Jézéquel V, Hildebrand M, Brzezinski MA. Silicon metabolism in diatoms: implications for growth. J Phycol **36**:821-840, (2000).

McKeague J. A. and Cline M. G. Silica in soil solutions: II. The adsorption of monosilicic acid by soil and by other substances. Can. J. Soil Sci. **43**, 83–96, (1963).

McLusky, D. S. Marine and estuarine gradients - An overview. *Netherlands J. Aquat. Ecol.* **27,** 489–493 (1993).

Meunier, J., A. Alexandre, F. Colin, J. Braun. Intérêt de l'étude du cycle biogéochimique du silicium pour interpréter la dynamique des sols tropicaux, Bulletin de la Societe Geologique de France, **172**, 533-538, (2001).

Meunier, J. D., Riotte, J., Braun, J. J., Sekhar, M., Chalié, F., Barboni, D. and Saccone, L.: Controls of DSi in streams and reservoirs along the Kaveri River, South India, Sci. Total Environ., 502, 103–113, doi:10.1016/j.scitotenv.2014.07.107, (2015).

Michalopoulos, P. and Aller, R. C. Early diagenesis of biogenic silica in the Amazon delta: alteration, authigenic clay formation, and storage, Geochim. Cosmochim. Acta, **68**(5), 1061–1085, doi:10.1016/j.gca.2003.07.018, (2004).

Milliman, J. D.: Blessed dams or damned dams?, Nature, **386**(6623), 325–327, doi:10.1038/386325a0, 1997.

Moulton, K.L., West, J., Berner, R.A. Solute flux and mineral mass balance approaches to the quantification of plant effects on silicate weathering. Am. J. Sci. **300**, 539–570, (2000).

Nair, R. R, V. Ittekkot, S. J. Managanini , V. Ramaswamy, B. Hakke, E.T. Degens, B. N. Desai and S. Honjo, Increased particle flux to the deep ocean related to monsoon, Nature, **338**, 749–751 (1989).

Nelson D. M., Treguer P., Brzezinski M. A., Leynaert A. and Queguiner B. Production and dissolution of biogenic silica in the ocean: Revised global estimates, comparison with regional data and relationship to biogenic sedimentation. Global Biogeochem. Cycles **9**, 359–372, (1995).

Oelze, M., von Blanckenburg, F., Hoellen, D., Dietzel, M., & Bouchez, J. Si stable isotope fractionation during adsorption and the competition between kinetic and equilibrium isotope fractionation: Implications for weathering systems. *Chemical Geology*, **380**, 161–171 (2014).

Opfergelt, S. & Delmelle, P. Silicon isotopes and continental weathering processes: Assessing controls on Si transfer to the ocean. *Comptes Rendus - Geosci.* **344,** 723–738 (2012).

Opfergelt, S. *et al.* Silicon isotopic fractionation by banana (Musa spp.) grown in a continuous nutrient flow device. *Plant Soil* **285,** 333–345 (2006).

Opfergelt, S., de Bournonville, G., Cardinal, D., André, L., Delstanche, S. and Delvaux, B.: Impact of soil weathering degree on silicon isotopic fractionation during adsorption onto iron oxides in basaltic ash soils, Cameroon, Geochim. Cosmochim. Acta, **73**(24), 7226–7240, doi:10.1016/j.gca.2009.09.003, (2009).

Opfergelt, S., Eiriksdottir, E. S., Burton, K. W., Einarsson, A., Siebert, C., Gislason, S. R., and Halliday, A. N.: Quantifying the impact of freshwater diatom productivity on silicon isotopes and silicon fluxes: Lake Myvatn, Iceland, Earth Planet. Sci. Lett., **305**, 73–82, doi:10.1016/j.epsl.2011.02.043, (2011).

Parfitt R. L. Anion adsorption by soils and soil materials. Adv. Agron. 30, 1–50, (1978).

Piperno, D. R., Phytolith Analysis — An Archeological and Eeological Perspective, Academic, San Diego, Calif., (1988).

Pogge von Strandmann, P. A. E. Philip A E, Porcelli, Don, James, Rachael H., van Calsteren, Peter Schaefer, Bruce Cartwright, Ian Reynolds, Ben C., Burton, Kevin W.. Chemical weathering processes in the Great Artesian Basin: Evidence from lithium and silicon isotopes. *Earth Planet. Sci. Lett.* **406,** 24–36 (2014).

Pokrovski G. S., Schott J., Farges F. and Hazemann J. L. Iron (III)-silica interactions in aqueous solution: insights from X-ray absorption fine structure spectroscopy. Geochim. Cos- mochim. Acta **67**, 3559–3573, (2003).

Presti, M. & Michalopoulos, P. Estimating the contribution of the authigenic mineral component to the long-term reactive silica accumulation on the western shelf of the Mississippi River Delta. *Cont. Shelf Res.* **28,** 823–838 (2008).

Pritchard, D. What is an estuary: physical view point. In: Lauff, G. (Ed.), Estuaries. AAAS, Washington, DC. (1967).

Quade, J., English, N. & DeCelles, P. G. Silicate versus carbonate weathering in the Himalaya: A comparison of the Arun and Seti River watersheds. *Chem. Geol.* **202,** 275–296 (2003).

Ragueneau, O., D. Conley, A. Leynaert, S. Ni Longphuirt, and C. P. Slomp, Role of diatoms in silicon cycling and coastal marine foodwebs, in The Silicon Cycle, edited by V. Ittekot et al., pp. 163–195, Island Press, Washington, D. C, (2006).

Ran, X. *et al.* Variability in the composition and export of silica in the Huanghe River Basin. *Sci. China Earth Sci.* (2015).

Rao, G. D. and S. V. V. S. Contribution of N_2O emissions to the atmosphere from Indian monsoonal estuaries. *Tellus, Ser. B Chem. Phys. Meteorol.* **1,** 1–9 (2013).

Raven, J. A. & Falkowski, P. G. Oceanic sinks for atmospheric CO2. *Plant, Cell Environ.* **22,** 741–755 (1999).

Reynolds CS. Potamoplankton: paradigms, paradoxes and prognoses. In: Round FE (ed) Algae and the aquatic environment. Biopress, Bristom, pp 285–311 (1988).

Rost, B., Riebesell, U., Röst, B. & Riebesell, U. Coccolithophores and the biological pump: Responses to environmental changes. *Coccolithophores From Mol. Process. to Glob. Impact* 99–125 (2004).

Sabater S. Diatoms. In: Likens GE (eds) Encyclopedia of Inland Waters. Volume 1. Elsevier, Oxford. pp 149-156, (2009).

Sarma, V. V. S. S. Viswanadham, R, Rao, G. D Prasad, V. R, Kumar, B. S K., Naidu, S. A., Kumar, N. a., Rao, D. B., Sridevi, T., Krishna, M. S., Reddy, N. P C., Sadhuram, Y., Murty, T. V R. Carbon dioxide emissions from Indian monsoonal estuaries. *Geophys. Res. Lett.* **39,** (2012).

Schuchardt, B., Haesloop, U. & Schirmer, M. The tidal freshwater reach of the Weser estuary: Riverine or estuarine? *Netherlands J. Aquat. Ecol.* **27,** 215–226 (1993).

Smetacek, V. Diatoms and the ocean carbon cycle. Protist **150**, 25–32, (1999).

Sommer, M., Kaczorek, D., Kuzyakov, Y., and Breuer, J.: Silicon pools and fluxes in soils and landscapes –A review, J. Plant. Nutr. Soil Sc., **169**, 310–329, (2006).

Stone, J., Hutcheon, I.D., Epstein, S., Wasserburg, G.J. Silicon, carbon, and nitrogen isotopic studies of silicon carbide in carbonaceous and enstatite chondrites. In: Tayor, H.P., O'Neill, J.R., Kaplan, I.R. (Eds.), Stable isotope geochemistry. A tribute to Samuel Epstein, 3. Geo- chemical Society, pp. 487–504 (1991).

Struyf E, Conley DJ. Emerging understanding of the ecosystem silica filter. Biogeochemistry **107**(1–3):9–18, (2011).

Struyf E., Van Damme S., Gribsholt B., Bal K., Beauchard O., Middelburg J. J. and Meire P. Phragmites australis and silica cycling in tidal wetlands. Aquat. Bot. **87**, 134–140, (2007).

Struyf, E. Dausse, A.. Van Damme, S. and Bal K.. Gribsholt, B.. Boschker, H. T.S. Middelburg, J. J. Meire, P.. Tidal marshes and biogenic silica recycling at the land-sea interface. *Limnol. Oceanogr.* **51,** 838–846 (2006).

Struyf, E., Smis, A., Van Damme, S., Garnier, J., Govers, G., Van Wesemael, B., Conley, D. J., Batelaan, O., Frot, E., Clymans, W., Vandevenne, F., Lancelot, C., Goos, P. and Meire, P.: Historical land use change has lowered terrestrial silica mobilization., Nat. Commun., **1**(8), 129, doi:10.1038/ncomms1128, (2010).

Stumm, W., Wollast, R. Coordination chemistry of weathering: kinetics of the surface-controlled dissolution of oxide minerals. Rev. Geophys. **28**, 53–69, (1990).

Subramanian V., V. Ittekkot, D. Unger, N. Madhavan. Silicate weathering in South Asian tropical river basins. In : The Silicon Cycle, Human perturbations and impacts on aquatic system (Eds. : V. Ittekkot, D. Uner, C.H. Humborg, N. Tac An). SCOPE Report 66, Island Press, 3-12 (2006).

Sun X, Andersson PS, Humborg C, Pastuszak M, Morth C-M. Silicon isotope enrichment in diatoms during nu- trient-limited blooms in a eutrophied river system. J Geochem Explor **132**:173–180, (2013).

Sun X, Olofsson M, Andersson PS, Fry B, Legrand C, Humborg C, Morth C-M. Effects of growth and dissolution on the fractionation of silicon isotopes by estuarine diatoms. Geochim Cosmochim Acta **130**:156–166, (2014).

Swedlund P. J. and Webster J. G. Adsorption and polymerisation of silicic acid on ferrihydrite, and its effect on arsenic adsorption. Water Res. **33**, 3413–3422, (1999).

Treguer P, Nelson DM, van Bennekom AJ, DeMaster DJ, Leynaert A, Qu´eguiner B. The balance of silica in the world ocean: a re-estimate. Science **268**:375–79, (1995).

Tréguer, P. J. and De La Rocha, C. L.: The world ocean silica cycle., Ann. Rev. Mar. Sci., **5**(1), 477–501, doi:10.1146/annurev-marine-121211-172346, (2013).

Turner, R. E., N. N. Rabalais, D. Justic, and Q. Dortch. Global patterns of dissolved N, P and Si in large rivers, Biogeochemistry, **64**, 297–317, (2003). doi:10.1023/A:1024960007569.

Van Cappellen, P. Biomineralization and global biogeochemical cycles, in Biomineralization, Rev. Mineral. Geochem., vol. **54**, edited by P. Dove, J. DeYoreo, and S. Weiner, pp. 357–381, Mineral. Soc. Am., Washington, D. C, (2003).

Vandevenne, F. I., Delvaux, C., Hughes, H. J., André, L., Ronchi, B., Clymans, W., Barão, L., Cornelis, J.-T., Govers, G., Meire, P. and Struyf, E.: Landscape cultivation alters δ^{30}Si signature in terrestrial ecosystems, Sci. Rep., **5**, 7732, doi:10.1038/srep07732, (2015).

Varela, D. E., Pride, C. J. & Brzezinski, M. A. Biological fractionation of silicon isotopes in Southern Ocean surface waters. *Global Biogeochem. Cycles* **18,** 1–8 (2004).

Velde, B., A. Meunier. The Origin of Clay Minerals in Soils and Weathered Rocks, Springer, Berlin, Germany, (2008).

Vörösmarty, C. J. C., J. Vosmartya, M. Meybeck, B. Feketea, K. Sharmad, P. Greena, J. P.M. Syvitski. Anthropogenic sediment retention: major global impact from registered river impoundments. *Glob. Planet. Change* **39,** 169–190 (2003).

Watteau, F. and Villemin, G.: Ultrastructural study of the biogeochemical cycle of silicon in the soil and litter of a temperate for- est, Eur. J. Soil Sci., **52**, 385–396, (2001).

Wedepohl, K. H. INGERSON LECTURE The composition of the continental crust. *Geochim. Cosmochim. Acta* **59,** 1217–1232 (1995).

Weiss, A., Amann, T. & Hartmann, J. Silica Dynamics of Tidal Marshes in the Inner Elbe Estuary, Germany. *Silicon* **5,** 75–89 (2013).

Weiss, A., De La Rocha, C., Amann, T. & Hartmann, J. Silicon isotope composition of dissolved silica in surface waters of the Elbe Estuary and its tidal marshes. *Biogeochemistry* (2015).

West, A. J., Bickle, M. J., Collins, R. & Brasington, J. Small-catchment perspective on Himalayan weathering fluxes. *Geology* **30,** 355–358 (2002).

Wetzel, F., de Souza, G. F. & Reynolds, B. C. What controls silicon isotope fractionation during dissolution of diatom opal? *Geochim. Cosmochim. Acta* **131,** 128–137 (2014).

White AF, Blum AE. Effects of climate on chemical weathering in watersheds. Geochim Cosmochim Acta **59**:1729–47, (1995).

White, A. Natural Weathering Rates of Silicate Minerals. In: Hol- land, H.D., Turekian, K.K. (Eds.), Geochemistry of Earth surface sys- tems. Acad. Press, Elsevier, London, pp. 205–240, (2011).

Ziegler, K., Chadwick, O. A., Brzezinski, M. A., and Kelly, E. F.: Natural variations of δ^{30}Si ratios during progressive basalt weathering, Hawaiian islands, Geochim. Cosmochim. Acta, **69**, 4597–4610, (2005).

Zinner, E., Tang, M., Anders, E. Interstellar SiC in the Murchison and Murray meteorites: isotopic composition of Ne, Xe, Si, C, and N. Geochim. Cosmochim. Acta **53**, 3273–3290 (1989).

CHAPTER 2

Methodological procedures and quality of measurements

1. Amorphous silica

1.1 Analytical measurements of amorphous Silica (ASi)

Understanding the Si biogeochemical cycle is of growing concern and analysis of Amorphous Si (ASi) has become frequent in aquatic and soil biogeosciences. The correct determination of ASi in the suspended matter is essential to recognize the fate and forms of Si from land to ocean. The measurement of ASi is challenging because of the importance and diversity of silicate minerals especially in estuaries and rivers, which can bias ASi estimates. Among the several existing protocols, the most widely used methods for ASi determination in suspended matter are wet chemical alkaline digestions using Na_2CO_3 (Conley, 1998) or NaOH (Ragueneau et al., 2005). There are several modifications or assumptions in these protocols discussed in earlier studies, such as concentration of alkali used, digestion time, lithogenic correction (Barao et al., 2015). The latter suggest that Na_2CO_3 leaching can overestimate the Biogenic Silica (BSi) content while NaOH leaching might overestimate even more because of the potential dissolution of non-biogenic phases such as volcanic ashes or poorly ordered mineral such as allophanes (Barao et al., 2015). Indeed, it is not possible to differentiate BSi from ASi with these chemical leaching protocols, hence we will use the term ASi (Amorphous silica) to represent the Si extracted by our digestion process. This term includes BSi as well as any other form of amorphous Si. We use the method described by Ragueneau et al. (2005) because it has been developed especially for suspended matter with high silicate mineral contents.

From the total particulate material, a known fraction of filter that represents a mass of particles of 3.3 ± 2.3 mg (dry period) and 11± 21 mg (wet period) was used to perform the chemical leaching for ASi measurement. The filter aliquots were subjected to wet alkaline digestion process, in which, the aluminium released was used to correct the lithogenic contribution. The treatment begins with a first digestion step with 0.2M NaOH (pH 13.3) at 100 ^{o}C for 40 min. For high clay samples, we reduced the time to 15 min. At the end of first leaching, the supernatant was measured for aluminium and silicon concentrations ($[Si]_1$ and $[Al]_1$) using ICP-MS, Agilent Technologies-7500a at the analytical platform Alysés in Bondy (IRD-UPMC). After rinsing and drying the pellet, the filter was subjected to a second digestion same as the one of the first step and $[Si]_2$ and $[Al]_2$ were measured. $(Si:Al)_2$, a characteristic ratio for the quantification of $Si(OH)_4$ extracted from silicate minerals/lithogenic during the second digestion was used to calculate ASi from the first leaching using the Eq. (1):

$$[ASi] = [Si]_1-([Al]_1*[Si: Al]_2) \quad \text{Eq. (1)}$$

This method has three assumptions: 1) All aluminium measured is derived from silicate minerals, 2) All the biogenic silica is dissolved during first digestion, so the second leach should be representative of the Si:Al ratio of silicate minerals only and, 3) Silicate minerals dissolved during second digestion have the same Si:Al ratio as those dissolved during the first digestion.

A third digestion step was added to the above chemistry using 2.9M HF to make sure that no Si was left over after the two leaching processes. Then the lithogenic silicon (LSi) concentration was calculated using the Eq. (2) expressed as µM

$$LSi = ([Si]_1-[ASi]_1) + [Si]_2 + [Si]_3 \quad \text{Eq. (2)}$$

The percentage of LSi in L1 is similar for dry and wet periods with a range of 61 ± 29 and 63 ± 32 respectively. This suggests that there should be no seasonal bias on the use of method. Uncertainty on ASi measurement with this method is estimated to ~10% (Ragueneau et al., 2005). In addition to ICP-MS, all silicon concentrations were measured also by spectrophotometer. Based on standard calibration and certified reference material comparison for Si (PERADE-09, Environment Canada, lot no: 0314, whose Si = 109.96 ± 6.97 µM), the results show that spectrophotometric measurements are more precise with mean Si of 112.8 ± 2.68 µM, n=82 (97.4% reproducibility) and hence have been used for ASi calculations.

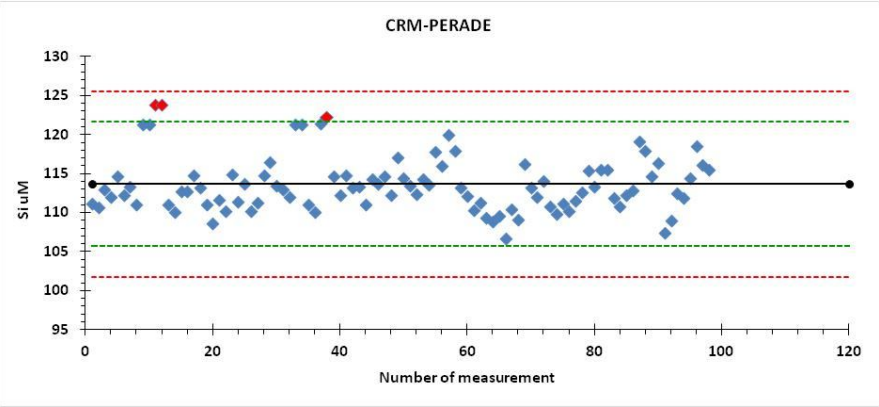

Fig. 1 *Si measurement- Quality check and comparison of certified reference material (PERADE-09) from spectrophotometric measurements. The green line indicates the 2 SD and the red line indicates 3 SD values. Most of the points falling within the 2 SD limits except the points in red color falling on 3 SD limit.*

1.2. GEOTRACES Intercalibration exercise

In addition to the internal lab quality check, we participated to the GEOTRACES (www.geotraces.org) international inter-calibration (IC) exercise for biogenic silica measurements in spring 2014. All the Intercaliberation samples were packed in dry polyethylene clean bags. Three sets of samples have been provided with the details below:

All samples for Biogenic Silica were filtered using 0.8µm polyethersulfone (Supor800) filters and consist of:

1) GT4424S**B**, bSi-IC-1: flow-through **blank** filter (bottom filter from SAFe station)

2) GT4424S**T**, bSi-IC-1: **oligotrophic** (SAFe station), 95m

3) GT4966S**T**, bSi-IC-1: **coastal** (Santa Barbara Basin), 230m.

We digested and analysed all the above IC samples using Ragueneau et al. (2005). The digestion of Intercalibration samples was performed along with the Indian estuarine samples following the same treatment for both. Full triplicate of IC samples was performed and the results were sent to the GEOTRACES inter-calibration committee for comparison (P. Lam). The Table 1 shows the results we measured and our laboratory number is denoted by number 15.

	ID	BSi	1 SD	$BSiO_2$	1 SD
LOCEAN	Sample Identity	nmol/sple after blank and LSi corrections		ug/sple using 67.4 g BSi/mol Si	
IC2	GT 4966 S8T, bsi-IC-15	5523.8	73.0	372.31	4.92
IC3	GT4424 S8T,bsi-IC-15	116.4	2.2	7.85	0.15

Table 1 *Intercalibration (IC) LOCEAN samples of coastal (GT 4966) and oligotrophic (GT 4424) samples and blank corrected BSi values expressed as mol Si by using the molar ratio 67.4g* $BSiO_2$.

We can see that our measurements are highly reproducible with 1 σ_D representing only 1.3 % of BSi in IC2 and 1.9% of BSi in IC3. This is much better than the precision estimated for the method (~10%, Ragueneau et al., 2005; Closset et al., 2015). This better reproducibility can be due to the limited

number of digestion replicates we could perform (n=3). This gives confidence in the applicability of the method since for the estuaries only one full digestion was performed for each sample. However, we should akcnowledge that it does not include the long-term reproducibility and it does not say anything on the accuracy of the method.

The comparative results of all laboratories are yet to finalize (Lam et al., unpub. results). However, as preliminary results, we can see the results from 7 labs, ours being lab # 15 (Fig. 2). Our data agree very well with the mean value, especially when one high outlier (lab 1) is removed from oligotrophic (4424) and two low outliers (labs 3 and 5) from coastal SBB (4966). However, given the limited number of labs, it is difficult to ascribe with certainty labs 1, 3 and 5 as outliers. Overall the results show that the variability can be very high for BSi measurements in marine particulate samples. Our results are likely to be accurate according to their agreement with the majority of labs. However, this calls for the identification of methodological approaches and potential problems. This should be soon done.

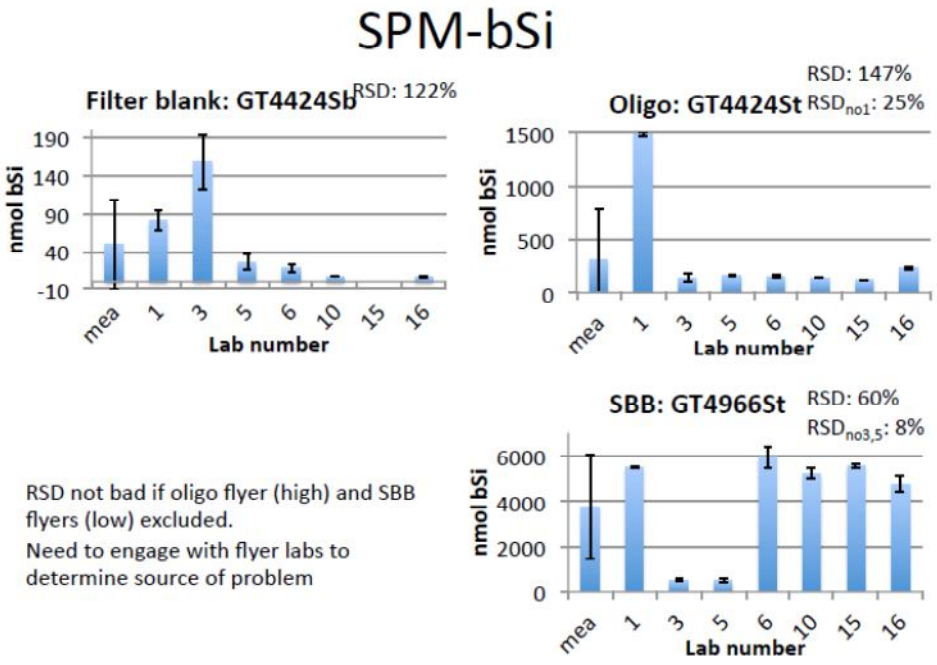

Fig.2 *Preliminary comparison of BSi results from all participated laboratories and our LOCEAN laboratory is reffered as number 15 (P. Lam et al., unpub. results).*

2. Silicon Isotopes

The Si isotopes method has been recently implemented in LOCEAN-LSCE in Paris by I. Closset (Closset et al., 2015, 2016). In the present study we used the same method except for some specific features. In the following sections we briefly summarise the usual method and more fully describe the minor modifications we implemented due to the specificity of our estuarine samples.

2.1 Preconditioning

2.1.1 Pre-concentration

In order to measure the Si isotopic composition, the DSi in the water sample must be pre-concentrated to get increasing concentration and purified from its matrix. A two-step pre-concentration procedure was carried out by adapting the protocol MAGIC- MAGnesium Co-precipitation technique (Karl and Tien, 1992; Reynolds 2006). By adopting this method, pre-concentration of the DSi also reduces the anionic matrix that could interfere during Si isotope measurements (mainly SO_4, Hughes et al., 2011). Since the estuarine and groundwater samples contain less magnesium compared to seawater, we added $MgCl_2$ to obtain similar Mg concentration as seawater. The water samples are treated by adding 2% (v/v) followed by 1% (v/v) of 1M NaOH in two stages. The water sample was left for minimum one hour for each addition of NaOH. The magnesium present in the water sample forms brucite $Mg(OH)_2$ at high pH, to which Si get adsorbed on the surface of the precipitated brucite. Then the brucite precipitate is separated from the supernatant by centrifugation (at 2500 rpm for 10 minutes) and redissolved by the addition of 1M HCl. After the first centrifugation the supernatant followed the second addition of NaOH with the same timing and centrifugation. After the second centrifugation, the supernatant was separated and analyzed for DSi concentration spectrophotometrically (Grasshoff et al., 1999). The second brucite precipitate is dissolved with 1M HCl and merged with the first fraction. The Si recovery is checked in two ways: (i) no detectable quantity of silicic acid remained in the supernatant after the second precipitation indicating 100% adsorption of silicic acid on brucite. (ii) Si recovery analysed on re-dissolved brucite is more >80 %. Indeed 100% recovery is hardly achieved at this step because mechanical loss is more common during the transfer after centrifugation. This should not affect the Si isotopic composition.

2.1.2 Purification of Si

The Si must then be separated from other ions in the sample and this can be achieved for cations by passing the sample solution into the cation exchange resin (BioRad cation exchange resin DOWEX 50W-X12, 200 to 400 mesh, in H^+ form) following the procedure explained by Georg et al, (2006). By performing this protocol, the majority of cations get trapped in the column and Si is released. After the purification process, an aliquot of samples was subjected to major elements analysis (Na, Mg, Ca, Al) by ICPMS (Agilent 7500a) to ensure that the Si/X cations measured weight ratio is always >50, prior to the isotopic measurements to minimize matrix effects in the plasma. Moreover, a small aliquot of purified sample was measured for DSi concentration to check the full Si recovery after column.

Yet, there can still be an anionic matrix in the sample mainly Cl^- and SO_4^{2-}. These anions are thus added in each standard and all samples before measuring the Si isotopic composition similar to Mg doping as explained by Hughes et al. (2011).

The monitoring and correction of analysis mass bias are the key processes for the measurement of precise Si isotopic composition using MC-ICPMS. Samples with different matrices will affect the plasma geometry and ionization efficiency and finally induces an instrumental isotopic mass bias. This creates a problem when using the standard bracketing method to measure in the δ notation if standard and sample do not have the same matrix. Therefore similar matrix between standard and sample need to be maintained to overcome such mass bias problem. This can be achieved either by complete purification of the sample except for the analyte or by adding a known artificial matrix to both sample and standard. Such kind of doping approach is used for Si isotopes measurements. The matrices like presence of anions (SO_4 and Cl) can be corrected by the artificial doping of anions (Suprapur H_2SO_4 and HCl) in all the samples and standard as shown by Hughes et al. (2011) in order to reach the same SO_4 /Si and Cl/Si ratio in the samples and standards.

2.2 Potential dissolved organic carbon (DOC) matrix effect on Si isotopes measurements

Like anions, the presence of DOC in the sample can induce an analytical bias but cannot be eliminated by adding an artificial DOC matrix in the sample and standard because of the variable and complex structure of DOC (Hughes et al. 2011). Moreover, utilization of organic matrix in the solution can clog the nebulizer and the membranes of desolvator and/or disturb the analysis.

Hughes et al. (2011) proposed to oxidise the DOC from stream samples. However this is a time consuming method which is not 100% efficient. In this present study, and for the first time in estuarine and freshwaters, we used the MAGIC method to preconcentrate (a method that was only applied on seawater previously). DOC might then have been partly or totally removed during this preconcentration step. We thus measured the DOC concentration of some samples after the purification process and compared with Si content since impact of matrix does mostly depend on the matrix to analyte ratio. DOC measurements were performed by A. Martinez-Serrano at METIS lab (Jussieu). The 30 samples tested for the DOC measurements were selected based on their high DOC concentration (521 ± 200µM), salinity gradient and the availability of water sample (for Netravathi and Cauvery river samples). They should then be representative of the rest of the samples.

According to Hughes et al. (2011), river sample with DOC/Si ratio at 0.14 does not induce any offset in δ^{30}Si measurement, whereas a stream with a DOC/Si ratio of 0.69 shows a 0.2 ‰ offset in δ measurement. Table 2 represents the list of samples checked for the presence of DOC after purification and prior to the Si isotopic measurements. All measured samples (upper estuaries and rivers) have DOC/Si ratios varying from 0.04 to 0.40 (avg. 0.15 ± 0.1). This suggests that for most of our samples, DOC matrix should be negligible and for some it should lead to an isotopic bias less than 0.2 ‰. We will see in Chapters 4 and 5 that the measured δ^{30}Si in our samples have much higher variability and therefore that matrix effect can be neglected since we will not discuss 0.2 ‰ differences between the samples.

Estuary/River name	Station no.	DSi concentration (ppm)	DOC concentration (ppm)	DOC/Si
After purification				
Netravathi -190		11.2	0.5	0.05
Netravathi -199		12.7	0.7	0.06
Netravathi -208		16.2	0.6	0.04
Netravathi -232		11.1	0.7	0.06
Netravathi -257		14.3	0.6	0.04
Netravathi -270		13.8	0.7	0.05
Netravathi -279		12.3	0.7	0.06
Netravathi -314		13.6	0.7	0.05
Netravathi -332		12.1	0.7	0.06
Netravathi -350		11.2	0.7	0.06
Cauvery dry	1	18.5	1.2	0.07
Krishna dry	8	8.8	1.9	0.21
Krishnaw dry	1	19.4	1.4	0.07
KBW dry	6	4.7	1.7	*0.35*
Haldia dry	2	9.3	1.4	0.16
Vaigai dry	5	9.6	3.9	*0.40*
Mahanadi dry	1	9.7	1.2	0.13
Mahanadi dry	9	6.0	1.2	*0.20*
Cauvery wet	1	21.9	1.9	0.09
Narmada wet	1	23.4	1.3	0.06
Narmada wet	3	7.2	1.6	*0.23*
Zuari wet	1	7.8	1.3	0.17
Zuari wet	5	6.3	2.3	*0.36*
Godavari wet	1	11.8	1.5	0.13
Subernereka wet	3	9.1	1.6	0.17
Haldia wet	3	8.3	1.6	0.19
KBW wet	4	3.3	1.3	*0.38*
Mahisagar wet	3	9.8	2.4	*0.25*
Cauvery river-1767		28.6	3.0	0.10
Cauvery river-1780		14.9	1.7	0.12

Table 2 *Samples from rivers and estuaries measured for DOC concentration after the purification process and the DOC/Si ratio prior to the MC-ICPS analysis Numbers in italics are for samples with DOC/Si ratio > 0.2 for which small but significant isotopic bias could occur (max. 0.2‰).*

2.3 Si isotope measurements

All measurements were done at 2 ppm Si concentration in the samples. The purified estuarine Si samples were injected in Multicollector Inductively Coupled Plasma Mass Spectrometer (MC-ICPMS, Thermo Neptune+) at LSCE, Gif-sur-Yvette, to measure the Si isotopes. The samples were analyzed in dry

plasma mode following standard-sample standard bracketing technique with external Mg doping for mass bias correction (Cardinal et al., 2003; Abraham et al., 2008). The samples were passed through an Apex©, desolvating nebulization system connected with a PFA nebulizer (100 µL min^{-1} uptake rate) and then into the plasma without additional gas. The samples were measured in medium resolution mode (M/ΔM >6000) and optimized to keep the interference of $^{14}N\ ^{16}O$ on ^{30}Si peak (m/z 30) below 0.5%. Moreover, the measurements were carried out on the interference free left side of the peak (Abraham et al., 2008). The $\delta^{29}Si$ and $\delta^{30}Si$ were calculated and expressed in per mil using the formula,

$$\delta^{30}Si\ (‰) = \left[\frac{(^{30}Si/^{28}Si)_{sample}}{(^{30}Si/^{28}Si)_{standard}} - 1 \right] \times 1000$$

These $\delta^{30}Si$ were calculated relative to the Quartz Merck (in-house standard), which is not significantly different from the international reference NBS28 (Abraham et al., 2008). The blank levels were monitored below 1% of the main signal and subtracted for each sample and standard analyzed. The typical analytical settings are provided in Table 3. The interference free measurements were counterchecked for mass-dependent fractionation and the few analyses falling outside the line were excluded from the calculations (Fig. 3). The analytical precision and accuracy were monitored by the long-term measurements of secondary reference material, Diatomite at the frequency of every ten samples. The reproducibility of the measurements was calculated using the standard deviation of 40 standard analyses over one year measurements ($\delta^{30}Si$ =1.28 ± 0.05 ‰, $\delta^{29}Si$= 0.65 ± 0.04 ‰, 1sd; Fig. 4). They are well in agreement with the consensus isotopic composition of diatomite ($\delta^{30}Si$ =1.26 ± 0.1 ‰, $\delta^{29}Si$= 0.64 ± 0.07 ‰, 1sd; Reynolds et al., 2007). We note however that the stability of our measurements indicates a small but significant decreasing signal with time (r= -0.36, n=40, p =0.02) but still within the acceptable range (max. 0.07 ‰ within one year of analyses). This might be an issue to focus from now own, because results from GEOTRACES intercalibration show that at LOCEAN-LSCE, we are 0.1 ‰ lighter than the mean for one of the two seawater samples intercalibrated (Grasse et al., in press).

Moreover, some full duplicate chemical processing and analyses of $\delta^{30}Si$ were carried out on Indian estuaries or rivers. The average reproducibility of all $\delta^{30}Si$ duplicates is 0.1 ‰ (n= 43, SD =0.07‰, Table 4). This is slightly higher than the reproducibility on diatomite. This is not surprising since estuarine water have a very variability of their matrix that could degrade the reproducibility (see next section).

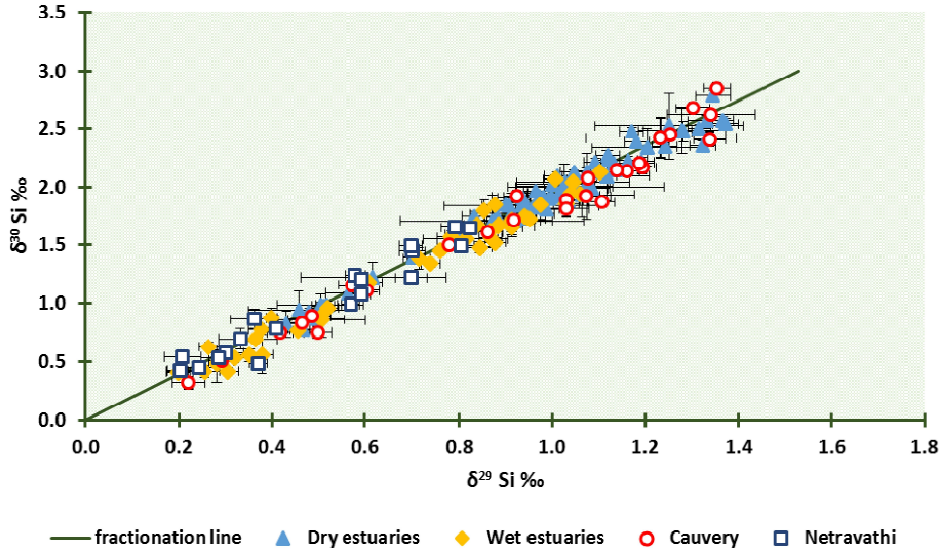

Fig.3 *Mass dependent fractionation of $\delta^{30}Si$ vs $\delta^{29}Si$ of the samples of present study. The points fall on the mass fractionation line with $\delta^{30}Si=1.96 \times \delta^{29}Si$, Young et al, (2002).*

MC-ICPMS Neptune $^{+}$ analytical operational settings	
Resolution	Medium
Forward Power	1200 W
Accelerating voltage	10 kV
Plasma Mode	Dry plasma
Cool Gas Flow Rate	16 L min^{-1}
Auxillary Gas Flow Rate	1.1-1.4 L min^{-1}
Sample Gas Flow Rate	0.9-1 L min^{-1}
Cones type	Nickel X-Skimmer cone + Standard Ni-Sample cone
Desolvator	Apex (ESI)
Nebulizer	PFA microcentric nebuliser 100 µL min^{-1}
Running Concentrations	Si = 2-2.5 ppm, Mg=2-2.5 ppm
Sensitivity	3-4 V ppm^{-1}
Blank Level	≤ 1% signal
^{30}Si Interference	≤ 30 mV

Table 3 *Analytical settings for the measurement of Si isotopic composition in MC-ICPMS.*

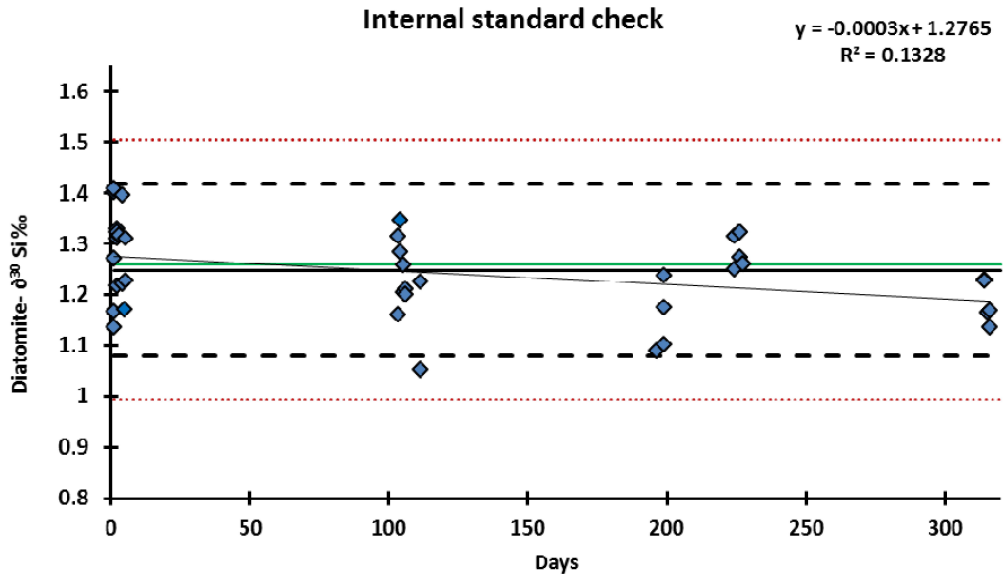

Fig. 4 *Reproducibility and precision of measurements of secondary reference material (Diatomite) during analysis of Si isotopes. Green line is the average of our measurements. Thick black line is the value from intercomparison (Reynolds et al., 2007). The black dashed line represents 2SD and the red line indicates the 3 SD values of present data. Thin black line is the linear regression line of our measurements with time and its equation is provided.*

MC-ICPMS. ref. no	Estuary name	Stn. no	δ^{29} Si-DSi	SD	δ^{30} Si-DSi	SD	Avg. δ^{29} Si-DSi ‰	SD	Avg. δ^{30} Si-DSi ‰	SD
Dry period										
2011	haldia	2	0.9	0.03	1.7	0.03	0.9	0.06	1.7	0.00
2222		2	0.8	0.02	1.7	0.03				
2024	subernereka	1	1.3	0.03	2.5	0.03	1.3	0.02	2.5	0.08
2058		1	1.3	0.02	2.4	0.03				
2010		2	1.1	0.03	2.2	0.04	1.2	0.12	2.3	0.16
2059		2	1.3	0.03	2.4	0.04				
2106	Rushikulya	2	1.0	0.03	1.9	0.05	1.1	0.09	2.1	0.22
2052		2	1.2	0.02	2.3	0.04				
2012	Vamsadhara	5	1.2	0.03	2.2	0.04	1.1	0.17	2.0	0.28
2002		5	1.0	0.03	1.8	0.04				
2007	Nagavalli	2	1.1	0.03	2.0	0.04	1.0	0.13	1.9	0.08
2136		2	0.9	0.03	1.9	0.04				
2224	Mahanadi	1	0.9	0.02	1.9	0.04	0.9	0.02	1.8	0.07
2008		1	0.9	0.03	1.8	0.04				
2021		7	1.1	0.02	2.0	0.03	1.1	0.04	2.0	0.06
2054		7	1.1	0.03	2.0	0.04				
2040		9	1.1	0.03	1.9	0.04	0.9	0.17	1.8	0.12
2225		9	0.8	0.03	1.7	0.04				
2104	krishna	0	1.6	0.03	3.2	0.04	1.5	0.02	3.1	0.15
2129		0	1.5	0.04	3.0	0.05				
2003		2	0.8	0.03	1.6	0.03	0.9	0.09	1.8	0.18
2053		2	1.0	0.03	1.9	0.04				
2064		3	0.9	0.02	1.7	0.03	0.9	0.05	1.7	0.06
2254		3	0.9	0.02	1.8	0.02				
2004		8	1.0	0.02	1.9	0.04	0.9	0.09	1.8	0.10
2219		8	0.9	0.02	1.7	0.03				
1036	Penna	3	1.0	0.05	1.8	0.05	1.1	0.11	1.9	0.20
2017		3	1.1	0.02	2.1	0.03				
2051		5	1.1	0.02	2.0	0.03	1.0	0.07	2.0	0.06
2127		5	1.0	0.03	1.9	0.04				
1035	Ponnaiyar	1	1.2	0.03	2.3	0.03	1.3	0.09	2.5	0.19
2019		1	1.3	0.02	2.6	0.03				
2133		4	1.3	0.03	2.6	0.05	1.3	0.04	2.6	0.05
2109		4	1.4	0.03	2.5	0.04				
2218	Cauvery	1	1.1	0.02	2.1	0.04	1.1	0.00	2.1	0.05
1031		1	1.1	0.03	2.2	0.04				
1033	Ambalayar	1	0.7	0.03	1.6	0.04	0.9	0.20	1.7	0.22
2029		1	1.0	0.03	1.9	0.03				
1032	Vaigai	1	1.1	0.03	2.3	0.04	1.3	0.16	2.5	0.28
2023		1	1.4	0.02	2.7	0.03				
2009		5	1.1	0.03	2.0	0.04	1.0	0.04	2.0	0.07
2056		5	1.1	0.03	2.1	0.04				
2223		5	1.0	0.02	1.9	0.03				
2022		6	1.0	0.02	1.9	0.03	1.1	0.07	2.0	0.08
2057		6	1.1	0.03	2.0	0.04				
1034	Vellar	1	1.0	0.03	1.9	0.04	1.0	0.10	2.0	0.19
2027		1	1.1	0.03	2.1	0.04				
2267	KBW	1	0.5	0.04	0.7	0.06	0.4	0.03	0.8	0.11
2111		1	0.4	0.03	0.9	0.05				
2257		4	0.5	0.02	0.8	0.02	0.5	0.06	0.9	0.06
2110		4	0.5	0.04	0.9	0.06				
2070		6	0.7	0.02	1.3	0.03	0.6	0.15	1.2	0.13
2221		6	0.5	0.02	1.1	0.03				
2015	Bharathapula	1	0.6	0.02	1.0	0.03	0.5	0.09	1.0	0.09
2108		1	0.6	0.03	1.0	0.03				
2131		1	0.4	0.03	0.9	0.05				
2130		2	0.4	0.03	0.8	0.04	0.5	0.11	0.9	0.17
2043		2	0.5	0.02	1.1	0.03				
2042		3	0.6	0.02	1.1	0.03	0.6	0.05	1.1	0.01
2112		3	0.5	0.03	1.1	0.03				
2041		4	0.6	0.02	1.2	0.03	0.6	0.02	1.2	0.07
2055		4	0.6	0.03	1.2	0.04				

Table continued..

MC-ICPMS. ref. no	Estuary name	Stn. no	δ^{29} Si-DSi	SD	δ^{30} Si-DSi	SD	Avg. δ^{29} Si-DSi ‰	SD	Avg. δ^{30} Si-DSi ‰	SD
Wet period										
2153	Haldia	3	0.9	0.03	1.5	0.05	0.8	0.09	1.5	0.00
2233		3	0.7	0.03	1.6	0.03				
2145	Subernereka	3	0.9	0.02	1.8	0.04	0.9	0.08	1.7	0.12
2232		3	0.8	0.02	1.6	0.03				
2194	Rushikulya	4	0.9	0.03	1.6	0.04	0.9	0.06	1.7	0.15
2269		4	1.0	0.03	1.8	0.04				
2231	Godavari	1	0.7	0.02	1.4	0.03	0.7	0.02	1.4	0.09
2261		1	0.7	0.02	1.3	0.03				
2220	Krishna	1	1.0	0.02	1.9	0.04	0.9	0.05	1.9	0.04
2091		1	0.9	0.02	1.9	0.03				
2226	Cauvery	1	0.9	0.02	2.0	0.04	1.0	0.08	2.0	0.03
2087		1	1.1	0.03	2.0	0.04				
2163	KBW	4	0.6	0.03	1.0	0.04	0.5	0.10	0.9	0.15
2202		4	0.4	0.03	0.8	0.04				
2229	Zuari	1	0.3	0.02	0.6	0.04	0.3	0.02	0.5	0.16
2149		1	0.3	0.03	0.4	0.04				
2159		3	0.4	0.03	0.4	0.03	0.4	0.02	0.6	0.17
2195		3	0.4	0.03	0.7	0.05				
2160		4	0.3	0.03	0.7	0.03	0.4	0.04	0.7	0.00
2196		4	0.4	0.03	0.7	0.05				
2161		5	0.4	0.03	0.8	0.03	0.4	0.01	0.9	0.09
2230		5	0.4	0.02	0.9	0.03				
2227	Narmada	1	0.8	0.03	1.9	0.04	0.9	0.01	1.8	0.09
2090		1	0.9	0.03	1.7	0.03				
2162		3	0.8	0.03	1.4	0.04	0.8	0.00	1.5	0.03
2228		3	0.8	0.02	1.5	0.04				
2102	Mahisagar	3	1.1	0.03	2.1	0.04	1.0	0.12	2.0	0.10
2234		3	1.0	0.03	2.0	0.03				
						Avg.SD		0.07		0.11
						SD.SD		0.05		0.07

Table 4 *Duplicate measurements of δ^{30}Si-DSi and δ^{29}Si-DSi (1SD) during dry and wet periods respectively.*

3. Sampling strategy

3.1 Estuarine sampling

24 and 18 estuaries were sampled along the entire coastline of India during the dry (NE monsoon, Jan-Feb 2011) and wet period (SW monsoon, July-August 2014) respectively. In each estuary, generally at least three to five samples were collected across the salinity gradient from near zero salinity to the mouth of estuary. The dry period sampling was carried out by National Institute of Oceanography (NIO), regional centre, Visakhapatnam, India. The wet period sampling was planned and executed by LOCEAN, UPMC Paris (Prof. D. Cardinal and K.R. Mangalaa) with the collaboration of NIO (Dr. V.V.S.S. Sarma) and Andhra University (Prof. N.S. Sarma and Dr. Chiranjeevulu), India. Totally ~4000km of coastal region was

travelled for the sampling of 18 estuaries with the main focus on understanding the Si cycle in monsoonal estuaries. Surface water samples were collected for dissolved inorganic nitrogen (DIN), dissolved inorganic phosphorus (DIP), silicic acid (DSi), total suspended material (TSM), chlorophyll and other phytoplankton pigments by using Niskin (5L) sampler. The DSi, ASi, δ^{30}Si-DSi, TSM (wet period) and major ions were analysed in LOCEAN, UPMC, Paris. The other supplementary biogeochemical parameters like DIN, DIP, TSM (only for dry period), chlorophyll and phytoplankton were carried out by National Institute of Oceanography, India for dry and wet periods respectively.

In addition to estuaries, ground water samples were collected for 13 (out of 18) next to the upstream estuaries samplings in wet season. Most of those samples are from borehole and few from shallow wells (few meters). There analyses were performed by LOCEAN, UPMC-Paris. The surface ground water samples were collected for Si isotopes and major ions to compare with upper estuaries during wet period.

3.2 River sampling

In Cauvery basin (Southeast India), the water samples were collected in 10 riverine and 5 reservoirs stations during summer season (May 2007) and monsoon (July 2007). Sampling and analyses were carried out by Indo-French Cell for Water Sciences (IRD-IISc, Bangalore, PI Dr. J. Riotte) except Si isotopic measurements that were carried out by LOCEAN, UPMC- Paris. All the supplementary parameters (major cations, ASi, DSi and phytoliths) were studied and published earlier by Meunier et al., 2015.

In Netravathi basin (Southwest India), the samples were collected at 9 riverine stations (no reservoirs) during summer season (April 2010) and monsoon (July 2010). For Netravathi basin, the sampling and analytical procedures can be found in Gurumurthy et al. (2012). The DSi concentration and Si isotopic measurements were carried out at LOCEAN, UPMC- Paris. The major ions concentration data were measured by Atomic Absorption Spectroscopy at Geosciences Environment Toulouse (J. Riotte, unpub. data).

The detailed information regarding the location of sampled estuaries and rivers, analytical protocols, reproducibility and precision are discussed under respective chapters.

4. References

Abraham, K., Opfergelt, S., Fripiat, F., Cavagna, A.J., de Jong, J., Foley, S.F., André, L., Cardinal, D. ^{30}Si and ^{29}Si determinations on USGS BHVO-1 and BHVO-2 reference materials with a new configuration on a Nu plasma multi-collector ICP-MS. Geostandards and Geoanalytical Research **32**, 193–202 (2008).

Barão, L. Vandevenne., Floor Clymans, Wim., Frings, Patrick., Ragueneau, Olivier., Meire, Patrick., Conley, Daniel J., Struyf, Eric. Alkaline-extractable silicon from land to ocean: A challenge for biogenic silicon determination. *Limnol. Oceanogr. Methods* **13,** 329–344 (2015).

Cardinal, D., Alleman, L.Y., Jong, J.D., Ziegler, K., André, L. Isotopic composition of silicon measured by multi collector plasma source mass spectrometry in dry plasma mode. Journal of Analytical Atomic Spectrometry **18**, 213–218. (2003).

Closset, I., D. Cardinal, S. G. Bray, F. Thil, I. Djouraev, A. S. Rigual-Hernández, and T. W. Trull (2015), Seasonal variations, origin, and fate of settling diatoms in the Southern Ocean tracked by silicon isotope records in deep sediment traps, Global Biogeochem. Cycles, **29**, 1495–1510, doi:10.1002/ 2015GB005180

Closset, I., Cardinal, D., Rembauville, M., Thil, F., & Blain, S. (2016). Unveiling the Si cycle using isotopes in an iron fertilized zone of the Southern Ocean: from mixed layer supply to export. Biogeosciences, in press. http://doi.org/10.5194/bg-2016-236

Conley, D. J. An inter laboratory comparison for the measurement of biogenic silica in sediments. 39–48 (1998).

Georg, R. B., Reynolds, B. C., Frank, M. & Halliday, a. N. New sample preparation techniques for the determination of Si isotopic compositions using MC-ICPMS. *Chem. Geol.* **235,** 95–104 (2006).

Grasse P., et al., GEOTRACES Inter calibration of the Stable Silicon Isotope Composition of Dissolved Silicic Acid in Seawater. *J. Anal. At. Spectrom.*, in press, doi 10.1039/C6JA00302H

Grasshoff, K., Kremling, K., Ehrhardt, M. Methods of Seawater Analysis. Wiley- VCH, Weinheim, 600 pp (1999).

Gurumurthy, G. P. *K.* Balakrishna, Jean Riotte , Jean-Jacques Braun, Stéphane Audry, H.N. Udaya Shankar, B.R. Manjunatha. Controls on intense silicate weathering in a tropical river, southwestern India. *Chem. Geol.* **300–301,** 61–69 (2012)

Hughes, H. J. C. Delvigne, M. Korntheuer, J. de Jong, L. Andre and D. Cardinal. Controlling the mass bias introduced by anionic and organic matrices in silicon isotopic measurements by MC-ICP-MS. *J. Anal. At. Spectrom.* **26,** 1892 (2011).

Karl, D. M. & Tien, G. MAGIC: A sensitive and precise method for measuring dissolved phosphorus in aquatic environments. *Limnol. Oceanogr.* **37,** 105–116 (1992).

Meunier, J. D., J. Riotte, J.J.Braun, M. Sekhar, F. Chalié, D. Barboni, L. Saccone. Controls of DSi in streams and reservoirs along the Kaveri River, South India. *Sci. Total Environ.* **502,** 103–113 (2015).

Ragueneau, O. N. Savoye, Y. Del Amo, J. Cotten, B. Tardiveau, A. Leynaert. A new method for the measurement of biogenic silica in suspended matter of coastal waters: using Si:Al ratios to correct for the mineral interference. *Cont. Shelf Res.* **25,** 697–710 (2005).

Reynolds, B., Frank, M. & Halliday, a. Silicon isotope fractionation during nutrient utilization in the North Pacific. *Earth Planet. Sci. Lett.* **244,** 431–443 (2006).

Young E. D., Galy A. and Nagahara H: Kinetic and equilibrium mass-dependent isotope fractionation laws in nature and their geochemical and cosmochemical significance. Geochim. Cosmochim. Acta **66**, 1095–1104 (2002).

CHAPTER 3

Seasonal, anthropogenic and biogeochemical processes on silicon cycle in Indian estuaries

K. R. Mangalaa[1], D. Cardinal[1]*, J. Brajard[1], D.B. Rao[2], N.S. Sarma[2], I. Djouraev[1], G. Chiranjeevulu[2], K. Narasimha Murty[2], and V.V.S.S. Sarma[3]

Article submitted to *Continental Shelf Research.*

Seasonal, anthropogenic and biogeochemical processes on silicon cycle in Indian estuaries

K. R. Mangalaa[1], D. Cardinal[1]*, J. Brajard[1], D.B. Rao[2], N.S. Sarma[2], I. Djouraev[1], G. Chiranjeevulu[2], K. Narasimha Murty[2], and V.V.S.S. Sarma[3]

[1] Sorbonne Universités (UPMC, Univ. Paris 06)-CNRS-IRD-MNHN, LOCEAN Laboratory, CP100, 4 place Jussieu, F-75252 Paris cedex 5, France

[2] Marine Chemistry Laboratory, Andhra University, Visakhapatnam - 530 003, India

[3] National Institute of Oceanography, Regional Centre, 176 Lawsons Bay Colony, 530 017 Visakhapatnam, India

* Corresponding author

Abstract

We studied the silicon biogeochemical cycle and its associated parameters in more than 15 Indian estuaries in dry and wet periods. We focus more specifically on dissolved Si (DSi), amorphous Si (ASi,) lithogenic Si (LSi), Particulate Organic Carbon (POC), Total Suspended Material (TSM), Dissolved Inorganic Nitrogen (DIN), salinity and fucoxanthin (a diatom pigment). We showed that the estuaries have high variability of the biogeochemical parameters at all spatial (i.e. even along the salinity gradient or within the same region) and seasonal levels. In dry season, ASi is significantly correlated with fucoxanthin while in the wet season, it is strongly associated to TSM. The wet season supplies more ASi, LSi, POC and TSM. Some regional differences are present but are not necessarily dominant and/or they differ depending on the salinity gradient. Hence, we split the data in five categories according to the salinity and season (for dry and wet: salinity < 5, salinity 5-15 and for dry only, salinity > 15). We then perform Principal Component Analysis (PCA) and clustering on PCA results to group the estuaries according to their similar behaviour. In each category the estuaries do not belong necessarily to the same clusters. We show that even in dry season, the biogeochemical parameters can be significantly associated to the lithogenic supply and, as expected, in wet season this supply is even more dominant. However, along the salinity gradient of wet estuaries, the fate of this huge particulate lithogenic supply varies a lot. Some estuaries encompass important settling, decreasing the particulate fluxes when compared to simple conservative mixing. In contrast for other estuaries, the fluxes dramatically increase above mixing line of conservative mixing, likely resulting from erosion on-going around the estuaries. We then estimate how much the studied estuaries supply LSi, DSi and ASi to the coastal Bay of Bengal and coastal Arabian Sea, taking into account of non-conservativity in the estuaries. Finally we show that

there is an overwhelming control of land use on DSi, LSi, ASi concentrations in the estuaries in the wet season, mostly due to strong positive correlation of agriculture cover with all Si concentrations.

Highlights

High seasonal, inter and intra estuarine variability of biogeochemical parameters

Significant control of diatoms during dry season on Si cycle

Massive control of land use during wet season on dissolved and particulate Si

Non-conservative behaviour of particulate Si fluxes during wet and dry seasons

Keywords

Amorphous silicon

Weathering

Diatoms

Land use

Monsoon

Fluxes to ocean

1. Introduction

Silicon (Si) constitutes 28% in the Earth's crust and is the second most abundant element (Wedepohl, 1995). In aquatic ecosystems, Si is released as dissolved form through chemical weathering and under particulate form through the erosion of particles with high Si contents either as primary residual minerals (e.g. quartz, feldspars) or secondary clay minerals. The particulate Si mineral pool is referred to as lithogenic silicon (LSi) and despite its huge size is often neglected in biogeochemical budget due to its low reactivity. Silicic acid (or dissolved silicon, DSi), is a key nutrient for diatoms, sponges, radiolarians and other aquatic organisms to build their skeleton. Additionally, the terrestrial plants take up DSi and precipitate silica in their cell walls called phytoliths. Diatoms and phytoliths are considered to be the major source of Biogenic Silica (BSi) to the coastal water (Ragueneau et al., 2000). In the ocean, diatoms play a dominant role amongst phytoplankton in carbon uptake (75% of coastal primary production, Nelson et al., 1995) and sediment burial because of their large size and hard structure (Ducklow et al., 2001). Carbon and silicon cycles are thus inter-related since diatoms play currently a dominant role in carbon sequestration while weathering connects C and Si cycles at long-term geological cycles (Berner 1992).

At present, 6.2 ± 1.8 Tmol.yr^{-1} of DSi and 1.1 ± 0.2 Tmol.yr^{-1} of BSi are transported by rivers to the estuaries (Tréguer and De La Rocha, 2013). The amorphous silica (ASi) is mostly of biogenic origin (phytoliths, diatoms, sponge spicules) and relatively dissolvable in the aquatic ecosystems. ASi or BSi transport through rivers has often been neglected compared to DSi, but some studies clearly showed a substantial contribution of ASi flux to the ocean (Conley 1997). For instance, ASi flux in some rivers can represent more than 50% of DSi flux (Frings et al., 2014). Phytoliths can significantly contribute to the BSi pool in tropical rivers (Cary et al., 2005; Ran et al., 2015). According to the revised oceanic silicon cycle, and neglecting LSi, 80% of external Si supply to the ocean is from rivers either as ASi or DSi. About 21% (1.5 ± 0.5 Tmol Si year $^{-1}$) is trapped in the estuaries yielding to a net supply of 5.8 ± 1.9 Tmol Si year^{-1} to the ocean (Tréguer & De La Rocha, 2013). One can notice that there are large uncertainties existing on the above fluxes (ca. ± 33%) due to the poor knowledge on the seasonal cycle of Si in many rivers and nonexistence of data, particularly for ASi and non-conservative behaviour of DSi in the estuaries before entering to the coastal region (Conley, 1993; Chou and Wollast, 2006).

Indeed the estuarine ecosystems are highly productive with rich biodiversity and are characterized by profound changes in the hydro-chemical properties and biological processes. For instance, diatom uptake may reduce the DSi concentration (Admiraal et al., 1990; Conley, 1997; Hughes et al., 2011). In addition, the anthropogenic activities like damming may decrease DSi by favouring BSi retention in the reservoirs (Conley 2002; Friedl et al., 2004; Humborg et al., 2006; Laruelle et al., 2009; Hughes et al 2012). In contrast, deforestation (Conley et al., 2008) and enhanced erosion (Xiangbin et al 2015) may increase the supply of both DSi and BSi to the coastal system. Moreover, increased fertilizer usage (Li et al. 2007), results in supply excess of N and P over Si yielding to development of non-diatoms bloom resulting in Harmful Algal Bloom (HAB) and eutrophication, a major threat to the trophic network (Garnier et al., 2010; Howarth et al., 2011).

A modelling study shows that the Indicator of Coastal Eutrophication Potential (ICEP) is increasing since four decades for Indian estuaries when compared to the temperate and less anthropogenic estuaries (Europe and USA) because of increasing agricultural production, fast urbanization and insufficient sewage treatment (Garnier et al., 2010). ICEP is the N:Si or P:Si of riverine inputs to the coast. Higher ICEP would favour eutrophication since Si would be limiting (Garnier et al., 2010). Hence, ignorance of ASi fate, that could dissolve and partly counterbalance excess of N and P relative to Si, may overestimate the eutrophication potential. Compared to N, P and C, the Si cycle is less known and needs to be more studied by considering the above processes along the land-ocean continuum to better determine the health and functioning of the ecosystem. The lack of data is especially high in the tropical regions, which contribute to 74% of riverine Si input (Tréguer et al. 1995).

Indian estuaries are significantly different from other estuaries in terms of rainfall, discharge and land use. Indian subcontinent is endowed with high mountain ranges, widespread plateaus and extensive plains traversed by large rivers. India has ~220 major and minor estuaries with varying size and shape across the ~7500km Indian coastline (Sarma et al., 2012; Rao et al., 2013). India experiences seasonally reversing monsoonal systems called southwest or summer monsoon (June to September) and northeast or winter monsoon (November to February). In Indian subcontinent, 75% of annual rainfall is received during southwest monsoon and the remaining during northeast/ pre-monsoon (Attri et al., 2010). Except for the glacial rivers, such as Ganges and Brahmaputra, Indian rivers are strongly influenced by the precipitation during southwest and northeast monsoons and most estuaries receive huge freshwater flux in a limited period of time. Hence these estuaries are referred as monsoonal estuaries.

Southwestern India receives more rainfall (~3000mm/yr) than the northeastern (1000-2500mm/yr), southeast (300-500mm/yr) and northwestern India (200-500mm/yr) (Soman and Kumar, 1990). The variability of the estuarine discharge induced by rainfall is discussed in Sarma et al. (2014). During the peak monsoon period, the entire estuary may fill with fresh water without any vertical salinity gradient and exhibits riverine and non-steady state behaviour (Vijith et al., 2009; Sridevi et al., 2015). On the other hand, the upstream estuary gets dried up due to meagre discharge, allowing the penetration of sea water during dry period. Indian subcontinent is bounded by Arabian Sea on the west and Bay of Bengal on the east and receives 0.3×10^{12} m^3 freshwater influx from rivers to the former basin while 1.6×10^{12} m^3 to the latter basin (Krishna et al., 2016). In addition to freshwater influx, the glacial and monsoonal rivers supply enormous suspended load around 1.4×10^9 tons to the Bay of Bengal and 0.2×10^9 tons into the Arabian Sea respectively (Nair et al., 1989; Ittekkot et al., 1991).

Agriculture is the most common land use and economic activity in India (61% of total watershed, Central Water Commission report 2014), with huge consumption of fertilizers (ranks second in the world; source: ministry of Agriculture report, 2012-13), which are dumped in the estuaries and coastal water (Sarma et al., 2014). This may result in imbalanced nutrient supply to the coastal waters (ministry of Agriculture report, 2012-13). Apart from the fertilizer use, an increasing threat is land degradation via erosion. Around 5.3×10^9 tonnes of soil is eroded annually, of which 29 % enters in to the sea, 10% is retained by reservoirs and the remaining 61% are shifted from one place to another (Ministry of Agriculture report, 2012-13). The rivers in India are heavily dammed to meet irrigation, domestic and hydroelectric demands. India ranks fourth in total number of dams in the world (CWC, 2009) and damming may cause nutrient retention via biological uptake and sedimentation, also altering the nutrient supply and finally the phytoplankton diversity and production in the estuaries as well as adjacent coastal ocean. However, despite high consumption of fertilizers in the Indian subcontinent, the concentrations and fluxes of DIN and DIP to the coastal waters are much less than the China Sea. This is probably resulting from high nutrient supply during only 2-3 monsoon months which cannot lead to eutrophication because of high turbidity and quick dilution in the ocean (Rao and Sarma, 2013; Krishna et al., 2016).

So far, there are no studies on ASi and LSi distribution in Indian estuaries except Ganges (Frings et al., 2014). In this present study we mainly focus on 1) Seasonal variability of ASi, DSi and LSi in ~20 estuaries draining into the Bay of Bengal and Arabian Sea. 2) Understanding their associated biogeochemical

processes and the impact of land use. Finally, 3) Estimating the fluxes of ASi, DSi and LSi in to the North Indian coastal ocean and their contribution to the global Si budget.

2. Materials and Methods

In this study the estuaries are first categorized into four groups based on their geographic location: northeast (NE), southeast (SE), southwest (SW), northwest (NW) (Table 1 and details therein). These estuaries were already studied for dissolved inorganic nitrogen (DIN), greenhouse gas fluxes and source of organic matter (Sarma et al., 2012, 2014; Rao and Sarma, 2013; Krishna et al. 2016) respectively. Here we mainly focus on silicon especially amorphous silica (ASi) and Lithogenic Silica (LSi) distribution and its associated processes.

	Name of River/Estuary	Catchment area km^2	Length km	No.of Dams in watershed	% agriculture	% Forest 2005-2006	% Buildup	% waterbodies	Discharge Dry m^3/s	Discharge Wet m^3/s
Rivers flowing in Bay of Bengal, East coast estuaries										
Northeast	Haldia (ganges) (Hal)	22000 (Damodar)	260	NA	65 (ganges)	16 (ganges)	4.3	3.5	NA	1600 *
	Subernereka (Sub)	18951	297	38	54	29	8	2	NA	392 *
	Baitharani (Bai)	10982	355	18	52	34	5	3	NA	903 *
	Rushikulya (Rush)	7700	165	NA	60	26	3	4	3.7	108
	Vamsadhara (Vam)	10830	254	27	"	"	"	"	13.0	149
	Nagavalli (Nag)	9510	256	21	"	"	"	"	16.2	118
	Mahanadi (Maha)	141600	851	253	54	33	3	5	355.4	2922
Southeast	Godavari (God)	312812	1465	921	60	30	2	4	280.2	5576
	Krishna (Kris)	258948	1400	660	76	10	2	4	0	627
	Cauvery (Cau)	81155	800	96	66	21	4	4	158.2	266
	Penna (pen)	55213	597	58	59	20	2	5	7.2	10
	Ponnaiyar (pon)	16019	292	18	67	15	4	9	27.2	51 *
	Vellar (Vel)	8922	210	18	"	"	"	"	44.9	29 *
	Vaigai (Vai)	7741	258	18	"	"	"	"	NA	36 *
	Ambullar (Amb)	NA			NA	NA	NA	NA	NA	28 *
Rivers flowing in Arabian sea, west coast estuaries										
Southwest	Kochi Backwater (KBW)	5243	228	40	51	35	6	4	69.7	455
	Bharathapula (Bha)	5397	251	13	"	"	"	"	4.7	39
	Chalakudi (cha)	1704	130	20	"	"	"	"	0	125
	Netravathi (Net)	3657	103	9	"	"	"	"	12.7	913
	Kali (Kali)	5104	184	1	44	35	3	5	NA	152
	Mandovi (Man)	3600	50		"	"	"	"	6 #	367
	Zuari (Zua)	1000	34	1	"	"	"	"	6 #	258 #
Northwest	Narmada (Nar)	98796	1312	277	57	33	1	3	70.9	911
	Tapti (Tap)	65145	724	356	66	24	1	3	NA	101
	Mahisagar (Mahi)	34842	583	134	64	19	1	4	16.6	353
	Sabarmathi (Sab)	21674	371	50	75	12	2	4	40.0	168

Table 1. *List of estuaries sampled and their respective discharge, length of the river, catchment area, land-use (dams and agriculture) in the river basin. Except for samples with #, discharge dry is Jan-Feb 2012 average (corresponding to the actual sampling period). Except for samples with *, wet discharge is*

*10- year average of June-July (2000-2011) because 2014 discharge was not available *- represents annual mean discharge (because of unavailability of monthly data), taken from Sarma et al 2014. # - represents discharge data taken from Vijith et al 2009. All data are from http://www.india-wris.nrsc.gov.in/* . For some watersheds the land-use data are common for adjacent rivers.

2.1 Sampling and ancillary biogeochemical parameters

24 and 18 estuaries were sampled along the entire coastline of India during the dry (NE monsoon, Jan-Feb 2011) and wet period (SW monsoon, July-August 2014) respectively (Fig. 1). In each estuary, generally at least three to five samples were collected across the salinity gradient from near zero salinity to the mouth of estuary. The details of each watershed are described in Table 1 taken from Water Resource Information System of India (WRIS). Temperature and salinity were measured by using portable CTD for few estuaries (Sea Bird Electronics, SBE 19 plus, USA) and portable pH and conductivity electrode (WTW, MultiLine P4) for other estuaries which was calibrated with CTD to calculate the salinity. Surface water samples were collected for dissolved inorganic nitrogen (DIN), dissolved inorganic phosphorus (DIP), silicic acid (DSi), total suspended material (TSM), chlorophyll and other phytoplankton pigments by using Niskin (5L) sampler. The DIP and DIN samples were preserved with saturated mercuric chloride after filtration to stop bacterial activity and transported to the laboratory for analysis. DIP and DIN were analysed using spectrophotometer following Grasshoff et al. (1999). Depending on the turbidity 100 to 500 ml of water was filtered on cellulose nitrate filter for dry period (pore size 0.45 µm) or polyethersulfone Supor (0.2µm, Pall corporation) filter for wet period. The weight of the total suspended material was calculated using the weight difference of the material. Later these filters were used to measure amorphous silica (ASi) in the particle samples (see §2.3). Another 500 ml of sample was filtered through Glass Fiber (GF/F; 0.7 µm pore size; Whatman) membrane under gentle vacuum for POC. Chlorophyll-a (Chl-a) and other phytoplankton pigments retained on the filter was extracted to dimethyl formamide (DMF) and fluorescence of the extract was measured using Varian Eclipse fluorescence photometer (Varian Electronics, USA) following Suzuki and Ishimaru (1990). The other phytoplankton pigments were measured using High Performance liquid Chromatography (HPLC-series 1200) Agilent technologies proposed by Heukelem and Thomas (2001).

Fig. 1: *Map showing the monsoonal estuaries with main watershed limits (dark blue lines) and rivers (light blue lines). Samples collected during dry (circle) and wet (star) periods. Estuaries with triangles are the 2014 wet period sampling considered as dry because of low discharge (see text).*

2.2 Water Discharge

The water discharge in Indian estuaries highly depends on the monsoonal rainfall and varies between 0-355 m^3s^{-1} and 28-5576 m^3s^{-1} during dry (non-monsoon) and wet (monsoon) periods respectively (Table 1). The discharge data were collected from the gauges near the sampling stations during dry periods (Jan-Feb 2012) corresponding to the sampling year (http://www.india-wris.nrsc.gov.in/). Since no data

are available yet for the wet period sampling (July 2014), 10 years average of June to July period were computed and displayed in the table 1. At the time of sampling, discharge was high during wet period in all estuaries except southeastern estuaries (Ponnaiyar, Vellar, Vaigai and Cauvery) where low discharge remains all year-long because of less rainfall during the southwest monsoon and high water use upstream. Moreover, SW monsoon was particularly late in 2014 and Krishna (SE) estuary was sampled still at low discharge, before typical high discharge monsoon was reached. Hence the "wet" period sampling of these five estuaries will be in the following considered as dry period since discharge was indeed low. During actual dry period sampling, discharge was very low in all the estuaries. The spatial variation of discharge in Indian estuaries is highly variable and depends on the amount of precipitation, water use, length and origin of the river (Sarma et al., 2014).

Since discharge data during our wet period sampling is not available, we used the average monthly discharge data for the period of 2011-2012 (http://www.india-wris.nrsc.gov.in/) to calculate the flux during wet season. For more details on the discharge data calculation refer to supplementary information in Appendix of Chapter 3 (Appendix D).

2.3 Measurement of Amorphous (ASi) and Lithogenic silica (LSi)

Understanding the Si biogeochemical cycle is of growing concern and analysis of ASi has become important in aquatic and soil biogeosciences. The correct determination of ASi in the suspended matter is essential to recognize the fate and forms of Si from land to ocean. The measurement of ASi is challenging because of the importance and diversity of silicate minerals especially in estuaries and rivers, which can bias ASi estimates. Among the several existing protocols, the most widely used methods for ASi determination in suspended matter are wet chemical alkaline digestions using Na_2CO_3 (Conley, 1998) or NaOH (Ragueneau et al., 2005). There are several modifications or assumptions in these protocols discussed in earlier studies, such as concentration of alkali used, digestion time, lithogenic correction (Barao et al., 2015). The latter suggest that Na_2CO_3 can overestimate the BSi content and NaOH overstimates still higher because of the potential dissolution of non-biogenic phases such as volcanic ashes or poorly ordered mineral such as allophanes (Barao et al., 2015). Indeed, it is not possible to differentiate biogenic silica (BSi) from amorphous silica (ASi) with these chemical leaching protocols, hence we will use the term ASi (Amorphous silica) to represent the Si extracted by

digestion process. We use the method described by Ragueneau et al. (2005) because it has been developed especially for suspended matter with high silicate mineral contents.

From the total particulate material, a known fraction of filter was used to perform the chemical leaching for ASi measurement. The filter aliquots were subjected to wet alkaline digestion process, in which, the aluminium released was used to correct the lithogenic contribution. The treatment begins with a first digestion step with 0.2M NaOH (pH 13.3) at 100 ^{o}C for 40 min (and for high clay samples, we reduced the time to 15 min). At the end of first leaching, the supernatant was measured for aluminium and silicon concentrations ($[Si]_1$ and $[Al]_1$) using ICP-MS, Agilent technologies-7500a. After rinsing and drying the pellet, the filter was subjected to a second digestion same as the one of the first step and $[Si]_2$ and $[Al]_2$ were measured. $(Si:Al)_2$, a characteristic ratio for the quantification of $Si(OH)_4$ extracted from silicate minerals/lithogenic during the second digestion was calculated and used to calculate ASi from the first leaching using the Eq. (1)

$$[ASi] = [Si]_1-([Al]_1*[Si: Al]_2) \quad \text{Eq. (1)}$$

This method has three assumptions, 1) All aluminium measured derived from silicate minerals, 2) All the biogenic silica is dissolved during first digestion, so the second leach should be representative of the Si:Al ratio of silicate minerals only and 3) Silicate minerals removed during second digestion have the same Si:Al ratio as those dissolved during the first digestion.

A third digestion step was added to the above chemistry using 2.9M HF to make sure that no Si was left over after the two leaching processes. Then the lithogenic silicon (LSi) concentration was calculated using the Eq. (2) expressed as µM

$$LSi = ([Si]_1-[ASi]_1) + [Si]_2 + [Si]_3 \quad \text{Eq. (2)}$$

Uncertainty on ASi measurement with this method is estimated ~10% (Ragueneau et al., 2005). In addition to ICP-MS, all silicon concentrations were measured also by spectrophotometer. Based on standard calibration and certified reference material comparison for Si (PERADE-09, supplied by environment Canada, lot no: 0314, whose Si = 109.96 ± 6.97 µM), the results show that spectrophotometric measurements are more precise with mean Si of 112.8 ± 2.68 µM, n=82 (97.4%

reproducibility) and hence have been used for ASi calculations. Details of the method and its accuracy are provided in Appendix A. There are some negative values in ASi calculated (both dry and wet periods), mainly because high lithogenic contribution during the first step can lead to an overestimation of the correction in Eq. (1). Those values will be discussed later.

2.4 Statistical analysis

Principal Component Analysis (PCA) and hierarchical clustering on PCA results were performed on the different categories of estuaries during dry (upper, middle and lower) and wet period (upper and middle) respectively (see section 3.4). Since, in wet period, there are only three estuaries falling under the category of high saline water and is not sufficient to perform the PCA analysis for the lower estuary in wet. Before applying the statistical analysis, all the data are log transformed and centred in order to avoid the differences in data dimensions. Likewise, the clustering on PCA provides grouping of estuaries based on their similar behaviour and also delivers the evidence regarding the dominant variable(s) in each group of the clusters obtained. The PCA and clustering were performed using the R statistical program (https://www.r-project.org/) version 0.98.1103. The results of the statistical analysis are discussed in detail below. In our study, PCA combined with cluster analysis provided a synthetic classification of estuaries in response to the respective characterizing variable.

3. Results

Tables 2 and 3 provide the results of DSi, ASi, LSi, TSM, fucoxanthin, DIN and POC concentrations averaged ($\pm \sigma_D$) for each Indian estuary during dry and wet periods respectively while individual data are provided in Appendix B. Significant tests for different populations are performed using T-test assuming unequal variance at the significance level for p-value < 0.05. Standard deviations around mean value are given as $\pm$ 1 σ_D. The significance level for correlations has been calculated with degrees of freedom (number of data) at 95% confidence level.

3.1 Seasonal variability of Dissolved Silicon (DSi)

The average DSi contents of Indian estuaries varied 143 ± 125 and 148 ± 76 µM during dry and wet period, respectively. Such averages are similar to global river average (158 ± 43 µM, Dürr et al., 2011).

Noticeably, there was no significant difference between dry and wet period average (p = 0.34). Due to the potential non-conservative behaviour of DSi in estuaries it is then more appropriate to compare first with the DSi concentration of upper estuaries with the world rivers (salinity <4, considered as representative of the freshwater river end-member). The average DSi concentration of Indian upper estuaries during dry period (213 ± 139 µM) is higher than the world river average (158 ± 43 µM, Dürr et al., 2011) while the average DSi of upper estuaries during wet period (163 ± 88 µM) is similar to the world average. During dry period, the concentration of DSi is more variable compared to wet period. DSi in estuaries may get altered before reaching into the coastal water through several mechanisms: dilution with seawater, biological uptake, dissolution or adsorption - desorption (Struyf et al., 2005; Zhu et al., *2009;* Lehtimäki, et al., 2013; Lu. et al., 2013; Carbonnel et al., 2013; Raimonet et al., 2013). The DSi concentrations in upper estuaries in the present study are similar to earlier studies in Indian rivers (Sharma et al., 2008, Gurumurthy et al., 2012, Meunier et al 2015, Frings et al 2015) and other tropical rivers (Liu et al., 2009; Hughes et al., 2011, 2012, 2013; Ran et al., 2015). No significant relationship was observed between river discharge and DSi concentration in the upper estuaries of wet period (r^2= 0.06, p >0.1).

	Name of river/Estuary	Salinity		DSi		ASi		LSi		TSM		Fucoxanthin		DIN		POC	
		Avg	SD (±)	µM	SD (±)	µM	SD (±)	µM	SD (±)	mg/l	SD (±)	µg/l	SD (±)	µM	SD (±)	µM	SD (±)
	Dry period																
North east	Haldia (ganges)	4.7	0.9	88	42	NA		875	729	143	117	0.35	0.14	28.8	4	231	92
	Subernereka	4.3	0.5	159	12	7.0	7.6	189	109	30	7	1.53	0.50	8.8	1.5	104	20
	Baitharani	17.5	4.4	37	12	0.6	0.7	207	85	56	13	0.70	0.48	10.3	2.8	135	27
	Rushikulya	20.4	2.8	63	28	1.4	0.4	54	12	27	2	0.43	0.08	6.9	2.4	57	17
	vamsadhara	12.4	11.0	189	165	2.2	1.6	48	24	22	8	0.52	0.22	4.1	1	59	8
	nagavalli	6.4	10.2	306	163	3.7	0.6	30	11	8	4	2.08	0.51	11.9	3.1	64	29
	Mahanadi	7.3	4.0	100	48	0.8	0.3	53	30	16	7	0.32	0.17	6.1	2	60	20
South east	Krishna	18.4	9.0	113	97	5.0	4.7	50	42	52	34	1.18	1.40	20.4	20.6	54	9
	Cauvery	9.8	9.6	285	89	8.8	3.6	60	42	23	9	5.21	4.11	6	4.5	127	22
	Penna	16.3	9.2	140	73	3.5	4.0	36	32	14	11	1.91	1.32	13.2	5.5	63	0
	Ponnaiyar	9.8	10.6	389	187	17.4	18.9	105	121	77	25	8.55	7.09	8.5	4.2	106	12
	Vellar	10.1	10.6	298	179	6.9	3.1	105	57	53	37	2.85	2.44	12.8	10.6	203	61
	Vaigai	11.6	8.6	154	59	NA		133	59	67	13	0.32	0.34	10.2	2.9	124	0
	Ambullar	4.2	0.0	317	5	2.5	0.7	40	5	17	14	0.21	0.05	6.7	1.4	95	23
South west	Kochi BW	8.8	9.3	79	33	2.1	1.8	43	28	76	29	1.76	1.99	13.1	6.6	50	12
	Bharathapula	15.5	10.2	74	32	4.9	3.1	78	37	32	18	1.09	1.19	4.7	5.8	98	40
	Chalakudi	14.7	11.9	57	13	1.1	0.7	15	7	17	16	0.51	0.37	6.5	2.6	50	6
	Netravathi	8.0	12.0	90	32	3.4	1.4	115	118	29	25	2.69	1.86	4.5	1.8	74	26
	Kali	1.6	1.5	89	32	1.1	0.8	26	12	63	4	0.44	0.54	20.4	15.2	55	3
	Mandovi	20.9	8.5	38	20	1.8	2.1	29	15	42	19	2.44	3.21	11.5	4.6	45	8
	Zuari	20.7	13.2	42	17	1.9	3.2	30	13	51	17	1.58	1.18	10.2	2.4	66	6
North west	Narmada	3.8	7.3	164	50	NA		171	124	22	16	0.73	0.49	37.3	5.9	NA	NA
	Tapi	9.0	15.3	136	76	NA		1393	1306	418	448	1.20	1.35	29.2	14	NA	NA
	Mahisagar	0.2	0.0	278	4	0.7	0.3	42	21	28	22	0.81	0.90	82.3	0.5	NA	NA
	Sabarmathi	13.5	19.0	127	54	NA		1482	214	209	177	5.15	0.00	49.4	14	NA	NA
	Dry upper overall mean	1.3	1.3	213	139	3.8	5.5	158	330	70	141	2.07	3.36	19.4	19.6	95	78
	Dry middle overall mean	8.8	3.7	139	100	3.6	3.7	136	302	42	42	1.57	2.10	11.6	10	94	59
	Dry lower overall mean	23.6	5.3	80	90	4.2	6.9	142	408	47	48	1.28	1.73	10.6	10	78	49

Table 2: *Variability of Salinity, Dissolved Silicon (DSi), Amorphous silica (ASi), Lithogenic silica (LSi), Total Suspended Matter (TSM), fuxoxanthin, Dissolved inorganic Nitrogen (DIN) and Particulate Organic Carbon (POC) in the estuaries during dry period. NA- represents no data.*

During dry period, there is significant higher DSi concentration in the eastern (179 ± 142 µM) compared to the western (88 ± 63 µM) estuaries ($p<0.001$). In contrast, there was no such significant difference between east (143 ± 43 µM) and west (151 ± 90 µM) during wet period ($p = 0.7$). As weathering is the dominant source of silicon into the estuaries/rivers, the different east vs. west behaviour during dry period can be possibly due to different weathering regimes/climate and also variable residence time of soil which leaches silicon in to the water as observed in other tropical rivers like Tana in Kenya (Dunne, 1978; Hughes et al., 2012). Indeed the east coast Indian estuaries belong to larger watersheds with wider plains where residence time of soil water could be longer compared to the smaller watershed and steeper slopes in the western region (Nayak & Hanamgond, 2010).

	Name of Estuary	Salinity		DSi		ASi		LSi		TSM		Fucoxanthin		DIN		POC	
		Avg	SD (±)	µM	SD (±)	µM	SD (±)	µM	SD (±)	mg/l	SD (±)	µg/l	SD (±)	µM	SD (±)	µM	SD (±)
	Wet period																
North east	Haldia (ganges)	3.6	2.0	113	9	9.8	7.1	2076	367	566	272	0.47	0.09	29.0	18.9	131	35
	Subernereka	6.2	5.5	150	43	12.6	11.5	443	196	67	29	0.66	0.35	18.5	12.3	41	14
	Rushikulya	10.6	9.2	170	77	19.1	29.6	604	932	90	125	0.42	0.52	19.3	11.5	35	37
	Mahanadi	2.6	4.3	134	30	NA		1227	471	185	59	--	--	28.7	31.2	68	8
South east	Godavari	0.6	0.6	147	13	22.3	16.8	1338	193	200	32			54.1	16.9	76	9
	krishna																
	Cauvery																
	Penna	Considered as Dry period because of No runoff and no rainfall during sampling															
	Ponnaiyar																
	vellar																
South west	Kochi BW	4.6	7.0	101	16	NA		294	204	50	30	0.71	0.56	38.0	25.7	100	27
	Netravathi	0.1	0.0	130	19	NA		164	48	30	7	0.46	0.00	23.8	16.6	29	4
	Kali	4.9	3.8	112	8	0.5	0.6	62	28	15	7	0.19	0.08	6.3	1.1	21	5
	Mandovi	3.1	4.9	115	16	0.8	1.1	90	31	20	7	0.17	0.16	15.6	17.2	24	9
	Zuari	4.2	4.4	101	11	NA		233	189	41	30	0.48	0.13	15.9	9.9	37	15
Northwest	Narmada	15.6	12.1	188	105	22.7	22.5	1041	592	334	355	0.38	0.13	37.7	17.6	39	17
	Tapi	12.8	10.2	219	154	44.2	35.1	2925	3366	2104	2109	1.97	0.41	44.2	18.2	37	--
	Mahisagar	6.8	7.9	285	115	12.5	18.6	754	880	151	192	0.51	0.45	39.0	12.4	33	21
	Wet upper overall mean	1.2	1.4	163	88	11.2	15.6	649	727	123	192	0.46	0.40	28.9	20.5	57	38
	Wet Middle overall mean	9.9	3.4	136	54	10.3	11.7	1291	2252	503	1246	0.73	0.68	23.0	18.0	48	33

Table 3. *Variability of Salinity, Dissolved Silicon (DSi), Amorphous silica (ASi), Lithogenic silica (LSi), Total Suspended Matter (TSM), fuxoxanthin, Dissolved inorganic Nitrogen (DIN) and Particulate Organic Carbon (POC) in the estuaries during wet period.*

3.2 Seasonal variability of ASi

The Amorphous silica (ASi) concentration ranges between 0.07 and 80 µM (Appendix B of Chapter 3). Unlike DSi, ASi was significantly different between the seasons ($p<0.001$), with lower average ASi during dry period (4.2 ± 6.3 µM) than during wet period (15.3 ± 20.2 µM). So far, no studies have been carried out on ASi in the Indian estuaries to directly compare. However, the only previous study on ASi in the Ganges river of Indian subcontinent showed that ASi was highly variable (from below detection limit to >

300 µM) and that it does not have solely a biogenic origin (Frings et al., 2014). One step ahead, our study presents the ASi variability from major to minor estuaries and the results are less variable than the Ganges basin. Indeed, our ASi data are well in agreement with those of Frings et al. (2014) when looking at samples with similar TSM (Appendix A of Chapter 3). During dry period, the eastern estuaries showed significantly higher ASi (5.6 ± 7.8 µM) compared to the western estuaries (2.2 ± 2.3 µM) ($p<0.001$). No such significant difference is observed between east (16.4 ± 17.6 µM) and west (14 ± 22 µM) flowing estuaries during wet period. The ASi values observed in the Indian estuaries are in the range of world estuaries and comparable with other tropical estuaries (Table 4).

River/estuary	***ASi µmol/l -range***	***References***
Tropical		
Huanghe river	15.7-285	*xiangbin et al., 2015*
Nyong basin river	0.40-1.16	*Cary et al., 2005*
Congo river	0.9-40.8	*Hughes et al., 2011*
Amazon river	<DL-13.4	*Hughes et al., 2013*
Changjiang river	0.5-4.0	*Cao et al., 2013*
Lake malawi (Shire River outflow)	2.9-69.9	*Bootsma et al., 2003*
Ganges	<DL to 300	*Frings et al., 2014*
Youngjiang	1.7	*Liu et al., 2005*
Indian estuaries-upstream-dry	0.16-36.45	*present study*
Indian estuaries - upstream wet	0.19-62.78	*present study*
Subtropical		
Estuary of Taiwan	4.98-6.05	*Wu, et al., 2003*
Temperate		
Scheldt estuary	7.0-81.0	*Carbonnel et al., 2013*
Baltic sea catchments	0-100	*Humborg et al., 2006*
Oder river	10.4-100.2	*Sun et al., 2013*
Mississippi river USA	14.1	*Conley. 1997*
Daugava river	1.0-12.0	*Aigars et al., 2014*
Rhine river	1.4-5.93	*Admiraal et al., 1990*
Vantaa river estuary	11-192	*Lehtimäki et al., 2013*
Polar		
Lena river	4.0-17.0	*Heiskanen et al., 1996*

Table 4. *ASi/BSi distribution in world rivers/estuary including the present study upper estuaries.*

3.3 Seasonal variability of LSi (Lithogenic silicon) and Total Suspended Material (TSM)

The average concentration of LSi was 143 ± 343 µM and 720 ± 743 µM during dry and wet periods respectively. LSi was found to be particularly high in few estuaries, especially in the northern estuaries Haldia (NE), Tapti and Sabarmathi (NW) even during dry period (Table 2). Otherwise, LSi is relatively higher in all the estuaries during wet compared to the dry period (Table 3). The variability of LSi in Indian estuaries is comparable to Aulne estuary (56-573 µM, France, Ragueneau et al., 2005) and the tropical

Changjiang estuary (560 ± 1410 µM, China, Lu et al., 2013). Unlike the ASi and DSi variability amongst contrasted seasons and regions, LSi does not show any such significant difference between east and west flowing estuaries during the dry ($p=0.27$) and wet ($p=0.16$) periods respectively.

The TSM is highly variable within each estuary across the salinity gradient (Tables 2 and 3) as well as dry (53 ± 87 mg/l) and wet (302 ± 774 mg/l) periods. 95% and 60% of total samples have less than or equal to 100 mg/l of TSM during dry and wet periods respectively. Higher TSM associated with heavy discharge limits the primary productivity in the estuaries (Sarma et al., 2009). The results from Haldia river (566 ± 272 mg/l) and other Indian estuaries are found to be in the range of Ganges, where highly variable TSM concentration were observed in the surface (49 to 2000 $mg.l^{-1}$ Frings et al., 2014). It is also comparable with other European estuaries (varied from few $mg.l^{-1}$ to few $g.l^{-1}$, Middelburg and Herman, 2007). Based on the TSM variability of Indian estuaries, it is clear that most of the estuaries (80% of the samples) have low TSM concentration (50-60 mg/l) suggesting that turbidity is not a limiting factor for primary productivity during dry period as discussed in Sarma et al. (2012). In contrast, a strong positive relationship was observed between TSM and discharge in Indian estuaries during wet period ($r^2=0.70$, $p<0.001$, $n=10$, excluding 3 estuaries), which is similar to earlier observation in Indian estuaries (Sarma et al., 2014). Three estuaries (Mahanadi, Godavari and Tapti) are excluded from this relation because of very high discharge and low TSM concentration. This is counterintuitive and may be due to the use of computed discharge data (10 years average, as described above) instead of the actual discharge at the time of sampling.

3.4 Inter-estuaries biogeochemical and seasonal variability

Apart from seasonal variability, the functioning of each estuary is different from one another in terms of geographical location (climate), topography (e.g., watershed size and slopes), land-use (e.g., type of agriculture, urbanization etc.) with more plains in the eastern parts and smaller rivers and steeper slopes in the southwestern parts. All these processes affect runoff and biogeochemical characteristics, and it is hard to identify the processes controlling the variability when looking at the whole dataset by using only regional average as briefly discussed before. To solve this, we separated all the estuaries in to three main categories: the upper estuary (salinity<4, near freshwater end-member), middle estuary (salinity 5-15) and the lower estuary (salinity >15) respectively. We have chosen these categories for the following reasons: (i) the low salinity can be representative of the freshwater end-member, i.e. what is

supplied to the estuary from rivers with little influence of seawater on concentrations (seawater contribution is max. 11%) as well as on processes like flocculation, turbidity, phytoplankton seeding, etc. (ii) the second category (salinity 5-15) should be indeed the most representative of estuarine processes since it has a large salinity gradient. It should more particularly highlight the processes controlled by seawater intrusion which can have significant influence, e.g. on estuarine turbidity maximum for salinity only slightly above 5 (Schoelhamer, 2001). (iii) For salinity > 15, the seawater contribution is dominant, and therefore, these lower estuaries can better represent the actual supply to the coastal ocean. Henceforth the discussion will be based on the upper, middle and lower estuaries. Since only few or no clear relationships have been identified based on geographical partitioning onto four regional groups (cf. above), we will then apply statistical tools, Principal Component Analysis (PCA) and clustering on PCA to better inter-compare the samples and identify the parameters explaining variability in concentrations of ASi, LSi and DSi.

From the ASi measured in Indian estuaries, there were 46 out of 148 samples for dry and 16 out of 51 for wet samples ASi were below detection limit or yielding to negative value because of too high lithogenic correction. It does not necessarily mean that ASi concentration is low since the detection limit depends more on the LSi contamination during the first leaching (which itself depends on the total LSi concentration) than the ASi content itself. When applying statistical tools, missing or negative data are not allowed. Hence, those missing ASi values were calculated as follows. Since there was a significant positive correlation between ASi and Fucoxanthin during dry period and dominant role of diatoms (r^2 = 0.40), the best linear fit between ASi and fucoxanthin was used to calculate the missing values of ASi during dry period (Fig. 2 and Eq. 3):

$$ASi\ (\mu M) = 0.9261 \times fuco\ (\mu g/l) + 1.6812 \qquad \text{(Eq. 3)}$$

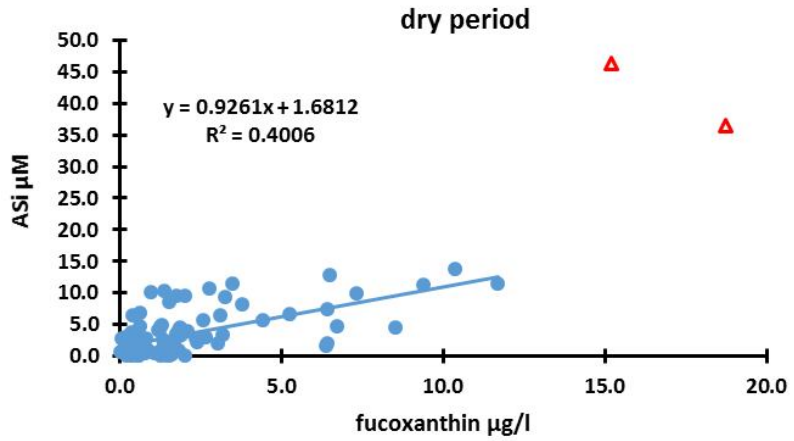

Fig. 2. *Best linear fit of ASi vs. fucoxanthin, to calculate the missing ASi. Two outliers from the small estuary Ponnaiyar (SE estuary) were excluded from the regression because of very high ASi concentrations.*

For the wet period, TSM was used to calculate the missing ASi values, since there is a significant positive relation between ASi and TSM. However, contrary to the ASi vs. fucoxanthin relationship during dry season which holds for all estuaries, independently of salinity, the ASi vs. TSM relationship varies with salinity, and hence the missing values of the upper and lower estuaries are calculated separately (Fig. 3). This improves significantly the correlation (from $r^2 = 0.45$ for the whole wet dataset to $r^2 = 0.70$ and $r^2 = 0.68$ when split into upper and lower, respectively):

Upper (salinity < 4): ASi (µM) =0.1658 x TSM (mg/l) - 2.1553 (Eq. 4)

Middle + Lower estuaries (salinity >5) ASi (µM) =0.0539 x TSM (mg/l) + 2.5494 (Eq. 5)

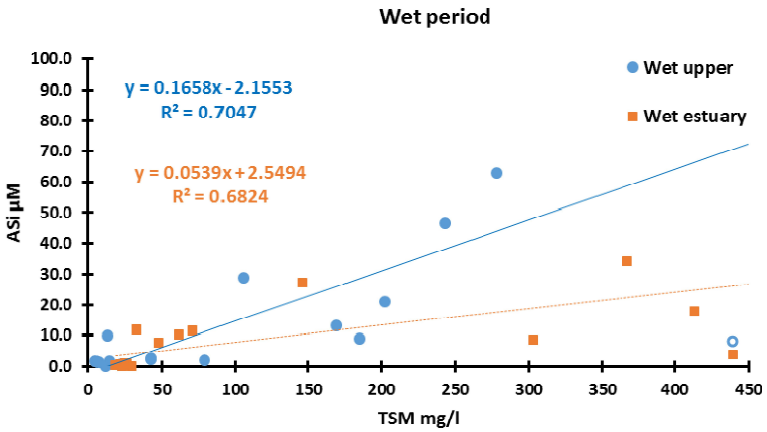

***Fig. 3**: Best linear fit between ASi and TSM for wet season (circles: upper wet, squares: middle and lower wet). The TSM value of estuary Haldia (NE, station 1, blue open circle) is excluded from the regression of wet upper estuaries. Similarly, for middle and lower estuaries, the best fit between ASi and TSM (closed boxes). The TSM value of estuary Tapti (NW, station 3) is excluded from regression because of a TSM concentration more than one order of magnitude higher (3572 mg/l) and not shown in graph.*

4. Discussion

4.1 Main processes controlling the Si pools in the Indian estuaries

Fucoxanthin is considered as representative of the presence of diatoms (Ansotegui et al., 2001; Wysocki et al., 2006; Zhang et al., 2015,). During dry period, a significant positive relation between ASi and fucoxanthin (r^2=0.40, n=104, excluding 2 high values of ASi) suggests that diatom plays major role in ASi contents. Consistent with this, diatom abundance contributes 61 ± 26% of total phytoplankton among all estuaries during dry period (Durgabharathi, 2014). There were no phytoliths counts made to identify their contribution in ASi pool. However, few estuaries particle samples where we have a large salinity gradient e.g., Krishna (SE) and Rushikulya (NE) were observed under SEM (Scanning Electron Microscope) analysis in order to look at the composition of biogenic material during dry and wet periods respectively. It confirms a major presence of healthy diatom cells during dry period and fragmented diatom cells along with clay mineral components during wet period respectively (Annex of Chapter 3).

The contribution of ASi to the total Si pool (ASi/ (ASi+DSi)) was calculated and shows higher ASi contribution during wet (8.8 ± 10 %) when compared to dry (3.5 ± 5 %) season. This is less than the other

world river systems (16%, Conley 1997) and Huanghe River (65% during high flow) (Ran et al., 2015) but comparable with the tropical system like river Congo (6%; Hughes et al., 2011) and slightly higher than Amazon basin (3%; Hughes et al., 2013). Furthermore, in river Congo, amongst the BSi pool, 50% was represented by diatoms (during low flow) and the remaining by phytoliths and sponge spicules (during rainy season). In Indian estuaries too, diatoms seem to explain most of the ASi pool during dry period.

In contrast to dry period, there is a significant positive relationship between TSM and ASi (r^2=0.45, n=34) and TSM vs LSi (r^2=0.86, n=49) in Indian estuaries during wet period. This confirms the dominant role of weathering and erosion of terrigenous material to the particulate Si pool. A similar observation was noticed in river Huanghe, China, where high erosion of top soils was responsible for higher ASi supply (Ran et al., 2015). Increasing TSM and decreasing light penetration ultimately limit the primary productivity in the system (Sarma et al., 2009). This is consistent with the SEM results, carried out in river Rushikulya, where there is higher lithogenic materials (clay minerals) in the upper estuaries and combination of diatom fragments and lithogenic materials in the lower estuaries (Annex of chapter 3).

LSi is chiefly the mineral contribution to the particulate matter, and as such, has a positive significant linear relationship with TSM during dry period (r^2=0.60, n=146, p<0.05, excluding two outliers) and a strong positive relationship with TSM (r^2=0.86, p<0.05, n=49) during wet period. This clearly reflects the dominant role of weathering and erosion on LSi supply especially during wet season. Major diatom contribution to the ASi pool might be an important process considered during dry period (as reflected in total diatom % abundance) as discussed above.

In addition, we attempted to find the relationship between TSM and particulate Si pool (ASi+LSi) for both dry and wet periods to understand the prime controlling process on Si particulate pool. Interestingly, there is significant relationship is noticed during dry period (r^2=0.40, p<0.001, n=145) indicating that, the particulate pool is not solely controlled by terrigenous supply of materials (Fig: Appendix E of Chapter 3, annex F) but might also be impacted by the biological uptake e.g., diatom production (Fig. 2). In contrast, there is a strong positive relation (r^2=0.71, p<0.001) during wet period (Appendix E of chapter 3, annex F) confirming that terrigenous supply of material is the prime process that controls the particulate Si pool in the Indian estuaries. Note that the (ASi+LSi) vs. TSM correlation is less good than LSi only vs. TSM (r2= 0.86 vs. 0.71) which suggests that the origin of ASi during wet does not simply follow LSi. Indeed ASi might be also supplied by plants material and/or diatoms fragments.

4.2 Biogeochemical processes in the dry period

Statistical Approach

The estuaries holding more than one sample point under the same salinity category are averaged and used for statistical interpretations. From the clustering of PCA results, for each cluster, the ratio between the mean of the cluster and the overall mean (hereafter referred to as "$ratio_{(mean)}$") of each category (eg. upper, middle and lower estuaries during dry period) was calculated to reflect the degree of influence of the dominant variables within each cluster. The most influent variables are identified by a $ratio_{mean}$ and that deviate the most from 1 of each cluster under separate category. Therefore, either a strong enrichment ($ratio_{mean}$ >>1) or a strong depletion ($ratio_{mean}$ <<1) indicating the dominating variable of each cluster. Note that all dominant variables were determined at the significance level of $p<0.05$.

Variables	Upper dry (n=21)		Middle dry (n=19)			Lower dry (n=18)		Upper-wet (n=13)		Middle-wet (n=11)	
	PC1 (34%)	PC2 (27%)	PC1 (29%)	PC2 (25%)	PC3 (20%)	PC1 (34%)	PC2 (26%)	PC1 (50 %)	PC2 (20 %)	PC1 (52 %)	PC2 (19 %)
Salinity	**0.47**	-0.26	**-0.65**	0.29	0.38	**-0.48**	0.38	-0.22	**-0.56**	-0.11	**0.57**
Dsi- µM	**-0.55**	**0.61**	**0.73**	-0.39	0.04	**0.77**	-0.27	-0.09	**0.81**	0.51	**-0.80**
TSM- mg/l	**0.87**	0.08	-0.09	**0.86**	0.12	**0.63**	**0.47**	**0.93**	-0.21	**0.92**	-0.03
POC- µM	**0.79**	0.27	**0.77**	**0.46**	-0.08	**0.60**	-0.15	**0.92**	-0.09	**0.58**	0.52
DIN- µM	-0.28	0.14	-0.35	**0.62**	-0.36	**0.59**	**0.62**	**0.78**	0.22	**0.86**	-0.15
ASi- µM	0.16	**0.88**	0.36	-0.03	**0.76**	**0.67**	**-0.59**	**0.85**	0.24	**0.77**	0.07
fuco- µg/l	-0.22	**0.84**	0.01	0.21	**0.84**	0.29	**-0.58**	0.01	**0.69**	**0.68**	0.48
Lsi- µM	**0.80**	0.33	**0.70**	**0.61**	-0.16	**0.52**	**0.72**	**0.95**	-0.16	**0.96**	-0.05

***Table 5**. Correlation (r) between PC axes and variables for dry and wet periods. The values in bold are significant at p<0.05 level.*

4.2.1 Upper estuaries

The estuarine samples with salinity <4, were characterized as upper estuary (n=21). Totally 61% of variability is retained among the variables in the first two axes (PC1 and PC2) and all our variables except DIN, are significantly correlated with PC1 and/or PC2. In the following we will therefore not consider PC3 (explaining only 16% of the variability, not shown) due to its minor influence, especially on silicon associated variables. PC1 explains 34% of the total variability and is essentially correlated with five different variables (Table 5, Fig. 4). PC1 is strongly related in increasing order with salinity, DSi, POC, TSM and LSi (Table 5). A strong positive correlation of TSM, LSi and POC on PC 1 (Fig. 4) relates this axis to variables from terrigenous derived materials supplied via rivers into the upper estuaries. Additionally,

the influence of salinity is also well marked, even though the correlation is less strong but significant (r=0.47) compared to other positive controlling variables. The estuaries falling towards the positive side of axis mainly result from higher lithogenic processes like weathering and erosion as a first order control. Hence PC1 could be considered as indicative of the major role of terrestrial processes on the positive side. Interestingly, the DSi tends towards the negative side of the axis PC 1 (r = -0.55) suggesting that DSi varied opposite to the strength of lithogenic processes. In addition, the angle between the variables represents their correlation with each other. The closeness of the variable arrows LSi, POC and TSM of PC1 (Fig. 4) indicating once again the dominant control of lithogenic processes.

PC2, which accounted for 27% of the variability, is positively correlated with DSi, fucoxanthin and ASi (Table 5). PC 2 is thus primarily influenced by diatom abundance and the estuaries falling under this axis may have a significant control of diatom production on their biogeochemistry.

Based on the PCA results of upper estuary, we obtain three different clusters of estuaries from all geographic locations (Fig 4). The estuaries in each cluster and the dominant variables of each cluster are described in Table 6 and discussed therein. The data table of the upper estuaries and supplementary figures (e.g. individual factor map and hierarchical figures of clustering, figs. C1, C2 and Table. C1) of all categories are provided in Appendix C of Chapter 3.

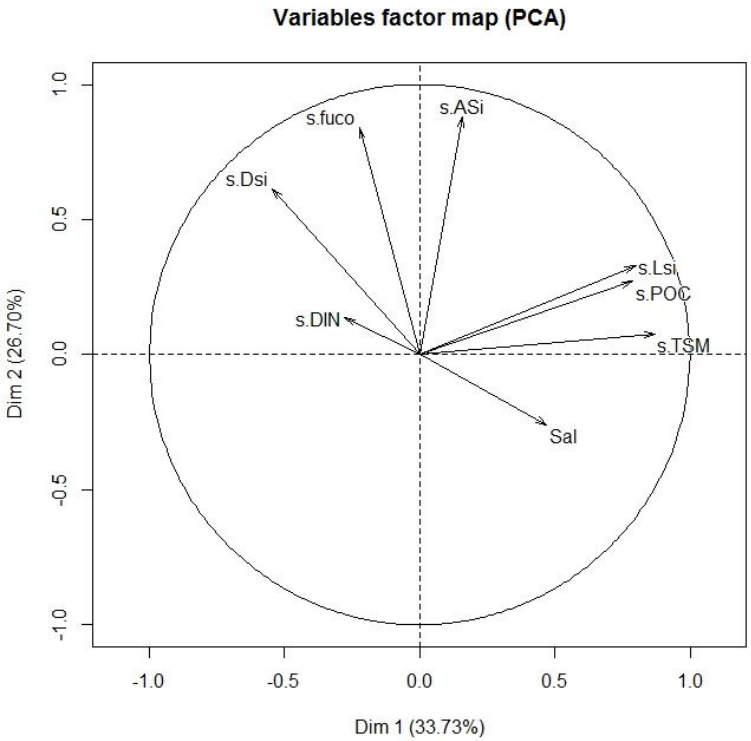

Fig. 4: *Variables factor map describing the parameters and their relationship with other variables and on the PC axis of upper estuaries during dry period.*

	Estuaries	characterized variable	cluster mean	SD	overall mean	SD	ratio $_{(mean)}$
Cluster 1	**NE:** Vam (4), Nag (5), **SE:** Pen (6), Kris (7)	**DSi**	334	74	214	130	1.6
		LSi	27	32	228	385	0.1
		POC	46	25	102	77	0.5
		TSM	7	5	77	133	0.1
Cluster 2	**NE:** Hal (1), Sub (2),Maha (3), **SE:** Vai (11), **SW:** KBW (12), Cha (13), Bha (14),Net (15), Kali (16), Zua (17), **NW:** Nar (18), Mahi (21).	**ASi**	2.05	1.23	3.65	4.06	0.6
		Fuco	0.79	0.7	2.03	2.52	0.4
		DSi	135	75	214	130	0.6
Cluster 3	**SE:** Pon (8), Cau (9), Vel (10), **NW:** Tap (19), Sab (20).	**ASi**	8.36	6.35	3.65	4.06	2.3
		Fuco	5.09	3.4	2.03	2.52	2.5

Table 6: *Clustering results on Dry-Upper estuaries (acronyms of estuaries along with geographical location; samples # refer to the station number with characterized parameter of each cluster including their mean values, standard deviation (SD) and ratio of mean of the cluster to the overall mean for dry upper (ratio $_{(mean)}$). LSi, DIN, POC, ASi, DSi in μM; TSM and fuco are expressed in μg/L.*

The estuaries of cluster 1 belong to eastern regions (n=4) and are dominated by TSM, LSi, POC with ratio$_{(mean)}$ less than 0.5 and DSi with ratio$_{(mean)}$ greater than 1.5 (Table 6). In accordance, cluster 1 is projected towards the negative end of PC1 (Fig. 4) which suggests that there is less influence of lithogenic supply of suspended materials. In contrast, this cluster has +55% DSi enrichment when compared to the mean category. SEM observations of upper dry estuary Krishna, depict the presence of large healthy diatoms (Annex of Chapter 3, Appendix E), which indicates an important diatom production (and no detectable phytoliths). Similarly, high number of diatom cells in these upper estuaries was reported (9.6 ± 7.2 x 10^5 cells/l, n=3, Durgabharathi 2014). Since this cluster is not characterised by specifically high ASi and fucoxanthin concentrations this may indicate that there is a DSi source coming from the dissolution/decomposition of biogenic material (e.g., dead diatoms or phytoliths) that have recently settled in the surface sediments. On the Malebo pool along the Congo river, characterized by low current, it has been estimated that when discharge is low, 80% of ASi produced by diatoms has settled (Hughes et al., 2011). It is also known that ASi dissolution at the sediment – water interface can be a significant supply to DSi in estuaries (Struyf et al., 2006; Delvaux et al., 2013; Raimonet et al. 2013). Our data do not allow quantifying such benthic flux, but we suggest that it should significantly contribute to the high DSi concentration in this cluster.

The cluster 2 mainly consists of estuaries from all geographic locations and is significantly characterized by relatively less fucoxanthin (-61%), ASi (-44%) and DSi (-37%) concentrations compared to the mean upper dry (Table 6). Cluster 2 spreads towards positive on PC1 and negative side on PC2 which suggests that the biogeochemistry of these upper estuaries is not dominated by the diatom production or by the lithogenic processes (Fig. 4, Table 6). This is confirmed by less diatom cells (1.0 ± 1.0 x 10^5 cells/l abundance reported for these upper estuaries, Durgabharathi, 2014).

It is interesting to note that the upper estuary of Haldia (#1 in Fig. 4 and C1) forms very distinctive within the cluster 2 with high concentration of TSM (278 mg/l), POC (322 µM) and LSi (1213 µM). This indicates that Haldia is the only upper dry estuary whose biogeochemistry is largely dominated by lithogenic

processes. Unlike other monsoonal estuaries, Haldia is a tributary of river Hooghly (itself a tributary of Ganges). These rivers can be considered as more perennial than monsoonal, where erosion supplies continuously terrigenous material with high suspended material. This may lead to high organic matter from continental plants along with high LSi, a feature we observed commonly for other estuaries in wet season (see sec. 4.3).

Finally cluster 3 mainly consists of Southeast and Northwest estuaries (Table 6) and is characterised by ASi and fucoxanthin concentrations twice higher than the mean of upper dry estuaries. This should be relative to biological processes especially the diatom production as also supported by the spreading of cluster towards the positive side on PC2 (Fig. 4 and C1). This is also evidenced from high number of diatom cells ($22.4 \pm 16.8 \times 10^{5}$ cells/l, n=3, Durgabharathi 2014) relative to other clusters. Cauvery, Ponnaiyar and Vellar are neighbouring rivers but differ in size, Cauvery being a large river, while two NW estuaries in this cluster (Sabarmati and Tapti) are middle size rivers (Table 1). Our data does not always allow identifying the common process(es) controlling biogeochemical variables within each cluster because they can differ. Indeed, this cluster illustrates well the fact that biogeochemical parameters associated to silicon are not controlled on first order simply by geographical location, but more likely by a combination of climatic (NW and SE regions being the regions receiving the less rainfall), and more local characteristics (e.g. urbanization, topography, etc.).

Overall, in upper dry estuaries, we show that the biogeochemistry of estuaries is dominated by diatoms (cluster 3), the dissolution of biogenic materials (cluster 1) while the others (cluster 2) are characterized by low biological activity and likely dominated by lithogenic processes despite their TSM and LSi concentrations are close to the mean (with the notable exception of Haldia).

4.2.2 Middle estuaries- dry period

The estuarine samples whose salinity is 5 to 15 were considered as middle estuary (n=19). 54% variability of the parameters was explained by the first two PC axes, in which the PC1 axis explained 29% variability (Fig. 5). PC1 is strongly correlated with POC, DSi and LSi towards the positive side of the axis, and salinity towards the negative end of axis (Fig. 5, Table 5). This is, as expected, a clear illustration of sea water impact leading to the dilution of lithogenic supply from land. Therefore mixing with seawater can be considered to be the first order controlling factor of DSi, POC and LSi in the middle estuaries.

Interestingly TSM, DIN, ASi and fuco concentrations are not significantly associated to the PC1 axis, suggesting that salinity and mixing have little impact on these parameters. Indeed, PC2 explained 25 % of variability and is strongly correlated with TSM, DIN, LSi and POC (Table 5) towards the positive side of PC axis (Fig. 5 and C3). This suggests dominant terrestrial processes in PC2. Therefore, the role of lithogenic supply of materials is also significant in the middle estuaries.

Overall 54 % of total variability was explained by first two axes, but we also considered the PC3 axis (20% variability and Eigen values >1) since it is strongly positively correlated with ASi and fuco (Table 5 and Fig. C5). This clearly indicating the high diatom production is the major controlling mechanism. Therefore, three PC axes are primarily considered and the cluster results explained in detail.

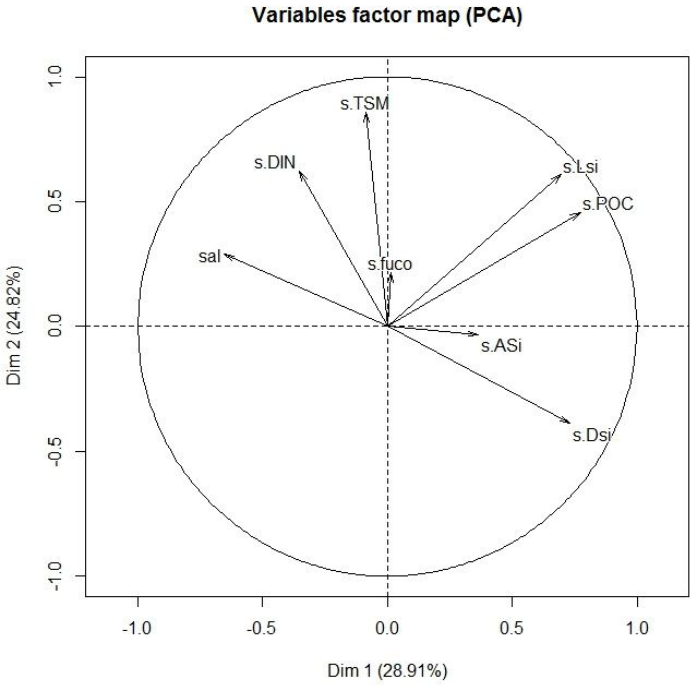

Fig. 5. *Factor map describes the parameters and their relationship with other variables on the principal component axis in the middle estuaries during dry period.*

	Estuaries	characterized variable	cluster mean	SD	overall mean	SD	ratio $_{(mean)}$
Cluster 1	**SE:** Krish (6); **SW:** KBW (12),Bha (14), Zua (17), Man (18); **NW:** Nar (19).	**Sal**	12.5	2.0	9.07	3.4	1.4
		DIN	19	14	13	10	1.5
		POC	56	14	88	47	0.6
Cluster 2	**NE:** Maha (4), Vam (5); **SE:** pen (7), Amb (10); **SW:**Cha (13).	**Fuco**	0.41	0.22	1.53	1.68	0.3
		TSM	16	3	43	27	0.4
Cluster 3	**NE:** Hal (1), Bai (3); **SE:** Vai (11); **SW:** Kali (16).	**LSi**	282	342	110	177	2.6
		TSM	67	29	43	27	1.6
		ASi	1.01	0.80	3.44	2.73	0.3
cluster 4	**NE:** Sub (2); **SE:** Cau (8), Vel (9); **SW:** Net (15).	**fuco**	3.59	2.50	1.53	1.68	2.4
		ASi	7.71	1.64	3.44	2.73	2.2
		DIN	6	3	13	10	0.4

Table 7: *Clustering results on Dry-middle estuaries (acronyms of estuaries along with geographical location; samples # refer to the estuaries station) with characterized parameter of each cluster including their mean values, standard deviation (SD) and ratio of mean of the cluster to the overall mean (ratio $_{(mean)}$). LSi, DIN, POC, ASi, DSi in μM; TSM and fuco are expressed in μg/L.*

Based on PCA results, we obtain four different clusters (Fig. C3 and C4) and the estuaries with characterized variable and ratio$_{(mean)}$ are in Table 7. Clusters 1, 2, 3 and 4 consist of 6, 5 and 4 estuaries respectively.

The cluster 1 belongs to southern and southwestern estuaries (n=6) and spread towards the negative side of PC1 axis (Fig. 5 and C3). Compared to the mean of the middle dry estuaries, the influence of salinity via seawater intrusion is marked (+36% compared to the dry middle mean). Notably, this high salinity is not associated with strong impact on the other biogeochemical variables, except higher DIN (+50% compared to the mean) and lower POC (-36 % compared to the mean). One could have expected for instance that DSi would decrease along with higher salinity due to mixing with low DSi seawater end-member. Lower POC and higher DIN could both result from remineralisation of organic matter.

Cluster 2 consists mostly of eastern estuaries (2 from NE and 2 from SE) and one from south west region and spreads on both PC axes. It was characterized by low fucoxanthin (ratio$_{mean}$ = 0.3) and TSM (ratio$_{mean}$ = 0.4) (Table 7). Low TSM suggests that there is no light limitation, while we know that DSi and DIN are not limiting in these estuaries (DSi > 67 μM and DIN> 4 μM, Table C2). Yet it does not increase diatom

production since ASi is not significantly different from mean, and fucoxanthin is 70% lower. It was also evidenced by moderate diatom cell abundance in these middle estuaries (3.2 ± 2.5 x 10^5 cells/l, n=3, Durgabharathi 2014). Except Mahanadi, the estuaries in cluster 2 have particularly low discharge during dry period (0-13 m^3/s) and thus more prone to local processes that are difficult to identify from our data and they might be dominated by non-diatom species.

Cluster 3 comprises estuaries from northeast, southeast and south west regions respectively (n=4) and spread on positive side of PC2. Compared to the mean of middle dry estuaries, cluster 3 has 2.6 times more LSi (282 ± 342 µM) and 1.5 times higher TSM (67 ± 29 mg/l) and almost three times less ASi (1.0 ± 0.8 µM). Note however the larger variability of LSi and TSM compared to the mean while ASi variability is less. It is interesting to note that, as for the upper dry category, Haldia (sample #1, Fig. C3) seems to behave unique in the cluster with high LSi and TSM. Terrigenous supply associated with high suspended material seems to dominate the estuaries in this cluster. In addition, low ASi that may also be explained by higher turbidity preventing diatom growth.

Finally cluster 4 consists of estuaries from eastern and southwestern estuaries (Table 7) and spreads towards the positive side of PC1. No significant lithogenic variable seems to be in this cluster. Since this cluster is projected towards positive side of PC2 and PC3 (Figs. 5, C3 and Table 5), it is mainly indicative of diatom production with strong positive relation of ASi and fucoxanthin on PC3. ASi and fucoxanthin concentrations are more than two times higher and 60% less DIN than the overall mean of the category respectively (Table 7), suggesting DIN consumption by diatoms. This is supported by high diatom cell abundance (14.1 ± 26.5 x 10^5 cells/l, n= 4, Durgabharathi 2014).

Overall, in middle estuaries, only the estuaries of Suberneraka, Cauvery, Vellar, and Netravathi are considered to be characterized by high diatom production (cluster 4), whereas the remaining estuaries are not. Other processes like mixing with sea water may limit the diatom production (cluster 1). Terrestrial supply of suspended materials and weathering are dominant in cluster 3. In cluster 2, neither diatom production nor lithogenic processes was noticed. A main output from the dry middle category is that despite a large variability of salinity (5-15) it has little impact on the clustering since it is a significant variable only for cluster 1. The different estuaries studied display (dis-)similarities that seem to be generally independent of salinity.

4.2.3 Lower estuaries- dry period

Results from PCA showed that 60% of the total variability in lower estuaries is explained by the two first axes (Table 5). PC1 (34%) was positively correlated with DSi, ASi, TSM, POC, DIN, LSi and negatively with salinity. Being essentially correlated with most of the parameters except fucoxanthin, PC1 could be considered as signature of mixing with sea water characteristics with all the variables (DSi, ASi and POC) dominated by supply from upstream. Axis 2 explains 26 % of total variability and is mainly correlated with LSi, DIN, TSM towards the positive end of PC2 and by ASi and fucoxanthin on the negative end (Table 5). Less supply of suspended material may provide favourable environment for diatom production in the lower estuaries. Indeed, while TSM coming from upstream act as first order control on ASi (both positively correlated on PC1, opposite to salinity), on second order, diatom BSi is favoured by high salinity as can be seen by negative correlation of ASi and fucoxanthin on PC2.

The combined PCA/cluster analysis for lower estuaries allowed for the distinction of three groups/clusters (Figs. 6 and C7). Clusters 1, 2 and 3 accounted for 9, 4 and 5 estuaries respectively.

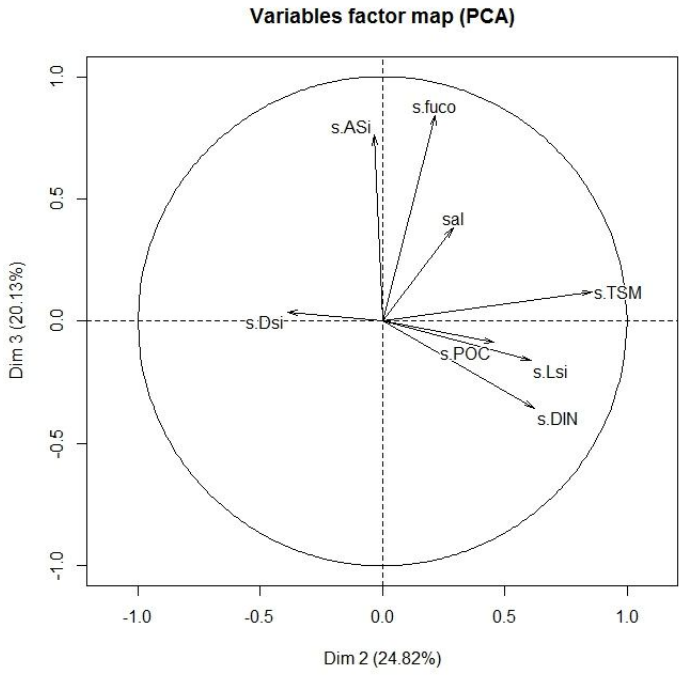

Fig. 6. *Factor map describes the parameters and their relationship with other variables on the principal component axis in the lower estuaries during dry period.*

	Estuaries	characterized variable	cluster mean	SD	overall mean	SD	ratio $_{(mean)}$
Cluster 1	**NE:**Rus (2),Vam (3); **SE:**Kris (5); **SW:** Kbw (11), Cha (12), Bha (13), Net (14), Zua (15), man (16).	LSi	44	17.4	293	693	0.2
		DIN	7	3.6	13	14.6	0.5
		POC	63	20.6	86	42.2	0.7
		ASi	2.22	2.24	4.72	6.32	0.5
		DSi	44	13.3	95	83.7	0.5
Cluster 2	**NE:** Nag (4); **SE:** pen (6), Pon (7), Cau (8).	Dsi	200	110	95	84	2.1
		Asi	11.65	10.33	4.72	6.32	2.5
		fuco	4.33	3.44	2.04	2.20	2.1
		Sal	20.3	2.2	23.9	3.9	0.8
Cluster 3	**NE:** Bai (1); **SE:** Vel (9)**,**Vai (10); **NW:** Tap (17), Sab (18).	LSi	947	1141	293	693	3.2
		TSM	117	122	56	74	2.1
		DIN	26	23	13	15	2.0
		POC	139	18	86	42	1.6

Table 8: *Clustering results on Dry-Lower estuaries (acronyms of estuaries along with geographical location; samples # refer to the estuaries station) with characterized parameter of each cluster including their mean values, standard deviation (SD and the overall mean (ratio $_{(mean)}$). LSi, DIN, POC, ASi, DSi in μM; TSM and fuco are expressed in μg/L.*

The estuaries of cluster 1 (n=9), are from northeastern, southeastern and southwestern regions. They are characterized by low DIN, ASi, POC and DSi parameters and very low LSi (7 times lower than the mean category; Table 8). POC is the less depleted significant variable (-30%). In this cluster, the salinity is similar (25.5 ± 3.9) to the overall mean (23.8 ± 3.9) with little variability. Lower estuaries from this cluster appear to be characteristic of sea water end-member, indicating that most of the lithogenic material has been lost upstream as evidenced by very low LSi. In these estuaries the biogenic contribution is moderate (ASi and fucoxanthin are not different from the mean while POC is lower) and does not seem to control the biogeochemistry of these sites. We can further note the absence of NW estuaries in this cluster.

Estuaries from cluster 2 were all from eastern regions (n=4). Opposite to cluster 1, they are mainly characterized by more than two times higher ASi, fucoxanthin and DSi and slightly lower salinity (Table 8). The estuaries in this cluster seem thus to be favourable for diatom production. It is interesting to note that the conditions seem to be quite constrained by narrow range of salinity (20 ± 2.2) with very

high DSi (> 100 µM). Unfortunately, there is no diatom abundance available to confirm their dominant role.

Finally, cluster 3 comprises the eastern and northwestern estuaries (n=5). This cluster is mainly characterized by three times higher LSi, two fold higher TSM and DIN concentrations than the overall mean of the category. POC is 61% greater than the relative $ratio_{mean}$ while salinity is similar to the overall mean (23.6 ± 3.1). Therefore the materials supplied from the upper estuaries may still control the variability of LSi in these lower estuaries. Moreover, unlike other categories, higher DIN concentration is observed in this cluster, especially in the northwestern estuaries (50.7 ± 13 µM). The anthropogenic effects like supply of domestic waste, agriculture and industrial activity are likely to dominate in these estuaries (150 kg/ha fertilizer usage in Gujarat-NW region compared to other western states like Kerala, 113 kg/h, and Maharashtra 134 kg/h; Ministry of agriculture, 2012-2013). Using nitrogen isotopes as tracer of fertilizer usage, Sarma et al. (2014) reported their higher impact in the northern estuaries.

Overall, in the lower estuaries, Nagavali, Penna, Ponnaiyar and Cauvery estuaries of cluster 2, are mainly controlled by diatom production at specific salinity, whereas the remaining estuaries are mainly dominated by sea water end-member with medium biological production (cluster 1) and terrestrial supply of materials associated with anthropogenic impacts is likely in NW estuaries (cluster 3).

4.3 Biogeochemical processes in Wet period

Similar to dry period, the estuaries of wet period have also been statistically treated to understand the controlling variables and clustering them based on their similar behaviour. However, since only three estuarine samples have been collected for salinity > 15 we will not consider the lower estuary category for wet period and only two categories have been processed for statistics: upper estuary (salinity < 5) and middle estuary (5-15).

4.3.1 Upper estuary- Wet period

Table 5 gives the variables the most strongly correlated to the principal components (PC axis or dimensions) by considering first 2 PC axes (>1 Eigen values). Totally 70 % of variability was retained among the variables in the first two axes (PC1 and PC2). In the first axis, 50% are essentially correlated

with four different variables (Table 5 and Fig. 7): The PC1 is strongly correlated by increasing order with DIN, ASi, POC, TSM and LSi. The strong positive relations of these parameters on axis 1 clearly suggests that monsoonal discharge drives the huge TSM supply along with weathered products (secondary and primary minerals) and organic plant materials in the upper estuaries during wet period.

The PC2 accounted for 20% of the variability and is highly positively correlated with DSi and fucoxanthin and negatively with salinity (Table 5). This indicates that increasing salinity is associated to lower DSi concentration as a result of mixing but this process is second-order control when compared to PC1. Based on the clustering of PCA results, we obtain five distinct clusters (Figs. 7 and C9) with estuaries from east and west coast of India. Clusters 1 (SW-Khali) and 3 (NW-Tapti) are formed with single estuary.

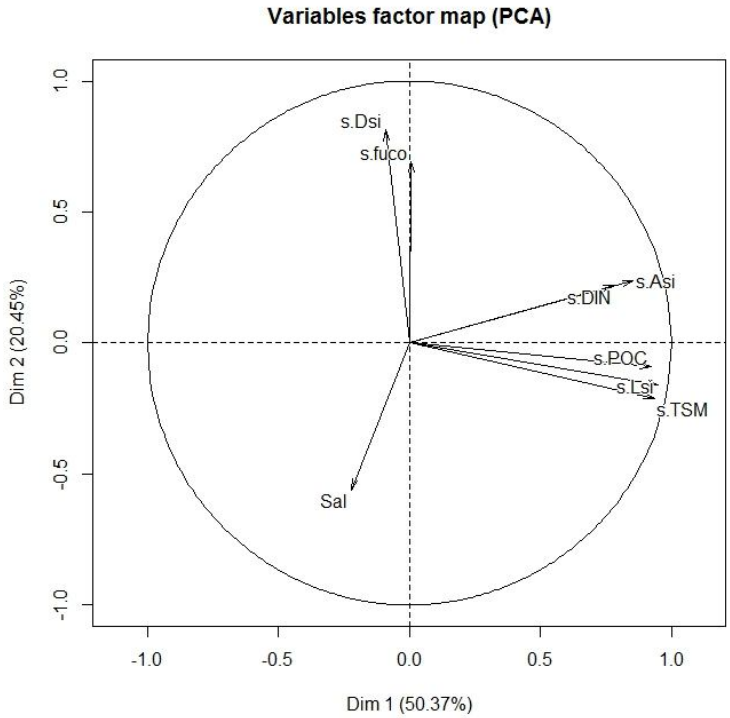

Fig. 7: *Factor map describes the parameters and their relationship with other variables on the principal component axis in the upper estuaries during wet period.*

	Estuaries	characterized variable	cluster mean	SD	overall mean	SD	ratio $_{(mean)}$
Cluster 1	**SW:** Khali (8).	DIN	5		26	14	0.2
Cluster 2	**SW:** Net (7), man (9); **NW:** Nar (11).	NULL					
Cluster 3	**NW:**Tapti (12).	Fuco	1.68		0.47	0.46	3.6
		DSi	443		193	109	2.3
Cluster 4	**NE:** Sub (2); **SW:** Kbw (6), Zua (10); **NW:** Mahi (13).	Sal	1.92	0.56	1.08	0.91	1.8
Cluster 5	**NE:** Hal (1), Rus (3), Maha (4); **SE:** God (5)	TSM	348	241	132	193	2.6
		LSi	1766	452	694	788	2.5
		ASi	31.4	23.0	13.2	17.6	2.4
		POC	94	33	57	38	1.7
		DIN	39	11	26	14	1.5

***Table 9**: Clustering results on Wet-upper estuaries (acronyms of estuaries along with geographical location; samples # refer to the estuaries station number) with characterized variable of each cluster including their mean values, standard deviation (SD) and ratio of mean of the cluster to the overall mean (ratio $_{(mean)}$). LSi, DIN, POC, ASi, DSi in μM; TSM and fuco are expressed in mg/L and μg/L respectively.*

In cluster 1, DIN is the most characterized variable with 79 % lower concentration than the overall mean of the category. Moreover the other variables like, TSM (9 mg/l), LSi (39 µM) and POC (17 µM) are also several folds lower than the overall mean of the category (Table C4) but not significantly characterized by the cluster analysis. The upper Khali estuary was sampled for the wet season (refer to Annex for Chapter 4 sampling pictures) from the shore around mangrove area which may explain this particular data.

On contrary, the cluster 3 is occupied by single estuary Tapti from northwestern region. This cluster is mainly characterized by twofold higher DSi and threefold higher fucoxanthin (Table 9). As for cluster 1, cluster 3 has ca. ten times lower TSM and LSi concentrations than the overall mean (Table C4) even though they are not characteristic variables in Table 9. This suggests a relatively minor lithogenic impact compared to other clusters.

Cluster 2 includes three estuaries from western regions (Table 9) and interestingly there is no significantly characterizing variable governing these estuaries. This means that all the variables are not significantly different from the overall mean and cluster 2 can be considered as representative of the

average upper wet estuaries. Cluster 2 is adjacent to cluster 1 (Fig. C9) but contrary to cluster 1, the relatively high concentration of LSi (170 ± 94 µM), DSi (186 ± 102 µM) indicates the influence of weathering from terrigenous supply.

Cluster 4 includes four estuaries from all regions (Table 9) and is only characterized by higher salinity (1.92 ± 0.56) compared to the overall mean at 0.91. Since no other variable is characterizing this cluster, the other biogeochemical variables are not different from the mean which means high concentrations of LSi (337 ± 126µM), DSi (185 ± 113µM) compared to dry period. The estuaries in this category have all the same level of discharge in wet season (260 – 450 m^3/s), which is medium in our data set (Table 1).

Finally cluster 5 includes only estuaries from the eastern regions (n=4). The estuaries are characterized by high TSM, LSi, ASi, POC and DIN, with $ratios_{mean}$ always greater than unity (Table 9). The discharge driven terrigenous material is the clear controlling mechanism over Si variability during wet period. We further note that it supplies also more ASi, unlikely from live diatoms since this high ASi is not related to high fucoxanthin. This ASi pool may contain diatoms debris (as observed on SEM samples from Rushikulya, Annex of Chapter 3), along with phytoliths and lithogenic ASi. Indeed there should be a common process relating ASi, LSi and TSM in this cluster since these three variables are increased by the same factor (x2.5) compared to the mean, the most likely process being soil erosion. The three estuaries that have the highest discharge during our study belong to this cluster 5 (Haldia, Mahanadi and Godavari, Table 1) and this confirms that higher lithogenic supply is related to higher discharge and erosion.

Overall, a strong control of erosion is observed in the eastern estuaries (cluster 5). The upper wet estuary category presents a high variability of its mean biogeochemical parameters. Surprisingly, this variability does not seem to allow clear grouping of estuaries in different clusters since one cluster does not have characteristic variable and two clusters consist only of one estuary. This is likely the result of high heterogeneity of freshwater end-members during monsoon. Part of this varia-bility seems to be explained by discharge (clusters 4 and 5) while local sampling may have biased one estuary (cluster 1).

4.3.2 Middle estuary- Wet period

Totally 71% of variability is represented by PC 1 and PC2 (Table 5 and Figs. 8 and C11). PC 1 alone explains 52% of variability with strong relationships between LSi, TSM, DIN, ASi, POC and fuco towards the positive end of the axis (Table 5). The remaining 19 % is explained by PC2 with strong relationship of the DSi and salinity towards negative and positive end respectively. The suspended material via river runoff is naturally considered to be the chief controlling mechanism for LSi, ASi, and TSM source to the estuaries during high discharge season. Interestingly, and similar to what we have seen for dry period, despite large variability of salinity in this category (5-15 Table C5), it explains only a minor part of the variability of the biogeochemical data. Therefore intrusion of seawater is only a second order-controlling variable in this category. The clustering of PCA results provides 3 different clusters (Figs. 8 and C11).

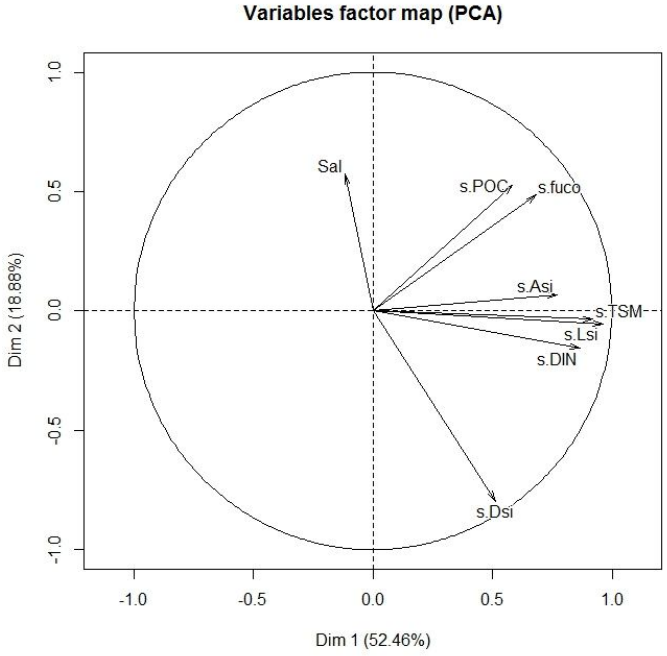

Fig. 8. *Factor map describes the parameters and their relationship with other variables on the principal component axis in the middle estuaries during wet period.*

	Estuaries	characterized variable	cluster mean	SD	overall mean	SD	ratio $_{(mean)}$
Cluster 1	**NE:** Rus (3)**; SW:** Kali (6), Man (7), Zua (8).	POC	26	8	48	33	0.6
		fuco	0.23	0.03	0.73	0.68	0.3
		DIN	7	4	23	18	0.3
		TSM	24	4	503	1246	0.0
		LSi	108	27	1291	2252	0.1
		ASi	0.43	0.38	10.3	11.7	0.0
Cluster 2	**NE:** Sub (2), Maha (4); SW: Kbw (5); **NW:**Mahi (11)	NULL					
Cluster 3	**NE:** Hal (1)**; NW:**Tap (10), Nar (9).	TSM	1603	2284	503	1246	3.2
		LSi	3527	3729	1291	2252	2.7

Table 10*: Clustering results on Wet-middle estuaries (acronyms of estuaries along with geographical location; samples # refer to the estuaries station) with characterized parameter of each cluster including their mean values, standard deviation and ratio of mean of the cluster to the overall mean (ratio $_{(mean)}$). LSi, DIN, POC, ASi, DSi in μM; TSM and fuco are expressed in mg/L and μg/L respectively.*

Cluster 1 comprises estuaries from northeast and southwest regions (Table 10). These estuaries are characterized by variables with ratio$_{mean}$ very much less than unity. The concentration of ASi, TSM and LSi are particularly low compared to the mean (- 90 to - 95%). The concentrations of DIN, fuco and POC (-70 to - 45%) are also lower than the ratio$_{mean}$. Noteworthy, each of these four estuaries belonged to a different cluster in the upper wet category. This shows that the biogeochemical functioning of one estuary can shift from upper to middle estuary category. In this cluster, it indicates that most of the lithogenic supply from upstream has settled and will not reach the coastal ocean. This is particularly obvious for Rushikulya which was characterized for upper wet by very high TSM and LSi (Table C5), while for middle it falls into the low TSM and LSi cluster. Estuaries in this cluster 1 are relatively smaller (Table 1) and influenced by steeper slopes (for SW) and less plains. This may explain higher settling when the high particle load enters the estuary. Moreover the magnitude of discharge determines the amount of organic matter and nutrient supply entering the estuaries in Zuari, Mandovi and Khali (Sarma et al., 2012, 2014).

Opposite to cluster 1, cluster 3 includes estuaries from northern regions that are mainly controlled by the lithogenic supply (Table 10). This was well evidenced by the characterized variables TSM and LSi with concentrations ~3 folds higher than the overall mean of the category. The estuaries under this category

are usually larger in size and run in wider plains with heavy runoff during monsoon period. Actually, the average TSM and LSi of cluster 3 are much higher than TSM and LSi measured in the same estuaries upstream. Because of the larger size and longer length of these estuaries, it is possible that lithogenic supply from land surrounding the estuary (i.e. not coming from upstream estuaries) is significant and contributes to increase particle load. Moreover, the NW estuaries (Tapti, Narmada), watersheds are characterized by semi-arid climate and vegetation that should favour erosion.

Cluster 2 includes estuaries from northeast, south west and northwest regions (Table 10). Similar to upper estuaries (in clusters 4 and 2), there is no dominating biogeochemical variable in this cluster. Indeed, three of these lower estuaries were already under this group for upper (Zuari being now replaced by Mahanadi, Tables 9 and 10). High range of concentrations was clearly observed for LSi (797 ± 664 µM), TSM (156 ± 145 mg/l) and ASi (15.88 ± 12.07 µM) which are very similar from upper mean wet estuaries. Therefore, particulate material supplied from freshwater end-member is efficiently transferred into middle estuary with little modification in this category.
Overall, the middle wet estuaries are mainly controlled by the lithogenic processes but different fate and origins of this lithogenic material are identified: middle estuaries with efficient sediment trapping in the estuary (cluster 1) or in contrast efficient transfer to the coastal ocean (cluster 2) while some large estuaries are getting enriched in lithogenic particles coming locally from the estuarine watershed (cluster 3).

4.4 Fluxes of ASi, LSi and DSi from Indian estuaries to North Indian Ocean

The knowledge on riverine contributions of dissolved and particulate materials to the oceans is essential to understand the element fluxes and balances on a global scale. Uncertainties on Si river fluxes to the ocean, especially in tropical environments have been recently highlighted (Tréguer & De La Rocha, 2013).

4.4.1 Bulk fluxes

Here, we calculate the total flux of DSi, ASi and LSi delivered by our studied estuaries to the North Indian Ocean by considering the upper estuaries of wet period. Details of the calculation for discharge data are provided in Appendix D and fluxes (expressed in moles/wet season) shown in Table 11. We estimated

that the Indian monsoonal upper estuaries sampled in our study supply 26 ± 2.9, 1.3 ± 1.0, and 144 ± 34 x 10^{6} kmol of DSi, ASi and LSi to the Northern Indian Ocean during wet season, in which, 54% of DSi, 93% of ASi and 92% of LSi respectively is supplied to the Bay of Bengal and the rest to the Arabian Sea. It is interesting to note that the supply of DSi to Arabian Sea and Bay of Bengal are similar, but the ASi and LSi supply are ~25 and 10 times higher in the Bay of Bengal when compared to the Arabian sea. Similarly, ~10 times more of TSM is supplied to the Bay of Bengal than to the Arabian Sea based on upper wet data.

4.4.2 Net fluxes

However, we have seen from the discussion above and from the data for each estuary that ASi, LSi, DSi and TSM do not necessarily follow a conservative behaviour along salinity gradient in wet season (Appendix B). Therefore we corrected the upper wet fluxes for non-conservativity mechanism to have more relevant estimates of silicon fluxes to the coastal North Indian Ocean. This is achieved by calculating the fraction of non-conservative Si by assuming 5µM (avg) of DSi in the coastal water (Naqvi et al., 2010). Finally, this fraction and the flux of upper estuaries are used to calculate the net fluxes to the coastal ocean. By taking into account of non-conservativity, 12 ± 1.3, 0.4 ± 0.3, and 115 ± 24 x 10^{6} kmol of DSi, ASi and LSi are supplied to the Bay of Bengal and 12 ± 1.4, 5.3 ± 3.3, and 270 ± 222 x 10^{6} kmol of DSi, ASi and LSi to the Arabian Sea respectively during wet season.

The non-conservative net fluxes do not modify much the bulk DSi fluxes because during wet, most of DSi variability can be explained by conservative mixing. However this is not the case for particles. The north-west estuaries have been identified as endowing a dramatic increase of particle supply within the salinity gradient (see cluster 3, section 4.3.2 for Narmada and Tapti). Consequently this leads to a large increase of ASi, TSM and LSi fluxes to the Arabian Sea which are now higher than to the Bay of Bengal (Table 11).

Estuaries	Discharge	Bulk fluxes to upper estuaries								Net fluxes to ocean (taking into account of non-conservativity)							
		DSi	*sd*	ASi	*sd*	LSi	*sd*	TSM flux	*sd*	DSi	*sd*	ASi	*sd*	LSi	*sd*	TSM flux	*sd*
	(m^3 x 10^9. wet season)	10^6 kmol/wet season						10^6 kg/wet season		10^6 kmol/wet season						10^6 kg/wet season	
Haldia	16	0.35	0.03	0.02	0.01	6.97	0.60	1.92	0.95	0.47	0.04	0.05	0.02	6.35	0.55	2.19	1.08
Subernereka	4	0.15	0.02	0.01	0.02	0.44	0.24	0.06	0.03	0.12	0.02	0.01	0.01	0.38	0.21	0.07	0.03
Rushikulya	1	0.33	*0.03*	0.09	*0.06*	2.73	*1.26*	0.38	*0.20*	0.23	*0.02*	0.04	*0.03*	0.53	*0.24*	0.12	*0.06*
Mahanadi	39	5.72	0.81	NA	NA	56	16	8.10	2.26	4.63	0.66	NA	NA	55.76	15.70	8.42	2.35
Godavari	50	7.36	0.64	1.11	0.83	67	10	9.98	0.02	6.47	0.56	0.33	0.24	51.68	7.45	7.25	0.01
Kochi-BW	3	0.38	0.03	NA	NA	1.01	0.86	0.16	0.12	0.46	0.04	NA	NA	6.06	5.16	1.06	0.80
Kali	2	0.05	0.001	0.0003	0.0003	0.02	0.00	0.004	0.00	0.06	0.00	0.0001	0.0001	0.04	0.01	0.01	0.00
Netravathi	9	1.18	0.20	0.01	*0.00*	1.49	0.40	0.28	0.10	0.90	0.15	0.01	*0.0043*	2.51	0.68	0.42	0.15
Mandovi	5	0.62	0.03	0.01	*0.01*	0.39	0.11	0.09	0.02	0.62	0.03	0.00	*0.0004*	1.11	0.31	0.21	0.04
Zuari	5	0.52	0.05	NA	NA	1.36	0.99	0.23	0.16	0.78	0.07	NA	NA	1.13	0.83	0.27	0.19
Narmada	20	6.03	*0.60*	0.05	*0.03*	5.27	*2.42*	0.84	*0.44*	7.37	*0.74*	4.63	*3.10*	120.20	*55.29*	73.98	*39.21*
Tapti	2	0.70	*0.07*	0.02	*0.01*	0.09	*0.04*	0.02	*0.01*	0.44	*0.04*	0.20	*0.13*	8.44	*3.88*	2.78	*1.47*
Mahisagar	6	2.25	0.38	0.01	0.00	1.70	2.03	0.27	0.34	1.69	0.29	0.44	0.04	130.63	155.82	38.16	47.34
Total flux to Arabian Sea	*52*	*12*	*1.4*	*0.1*	*0.05*	*11*	*7*	*1.9*	*1.2*	*12*	*1.4*	*5.3*	*3.3*	*270*	*222*	*117*	*89*
Total flux to Bay of Bengal	*110*	*14*	*1.5*	*1.2*	*0.9*	*133*	*27*	*20*	*3.5*	*12*	*1.3*	*0.4*	*0.3*	*115*	*24*	*18*	*3.5*
Total flux to Indian ocean	*162*	*26*	*2.9*	*1.3*	*1.0*	*144*	*34*	*22*	*5*	*24*	*2.7*	*5.7*	*3.6*	*385*	*246*	*135*	*93*
Extrapolated flux to total discharge																	
Flux to Arabian sea	*300*									*68*	*8.0*	*30.0*	*19.0*	*1543*	*1268*		
Flux to Bay of Bengal	*1600*									*171*	*19*	*5.7*	*4.3*	*1643*	*343*		

Table 11. *ASi, LSi, DSi and TSM fluxes of Indian estuaries draining in to the Bay of Bengal and Arabian sea during wet period. Fluxes to the left have been calculated using upper wet concentrations. Fluxes to the right are estimates of fluxes to the coastal ocean calculated taking into account the non-conservativity of the variables along the salinity gradient.*

Our results do not mean that total sediment supply to Arabian Sea is larger than to the Bay of Bengal. It is well known that it is the reverse. There is indeed a total 1.4 x 10^{12} kg of sediment supplied to the entire Bay of Bengal and 0.2 x 10^{12} kg into the entire Arabian Sea respectively (Nair et al., 1989; Ittekkot et al., 1991). Indeed the estuaries sampled in our study represent a discharge to the Arabian sea for wet season of 52 x 10^9 m^3 which is 17.3 % of the total discharge in to Arabian sea, while for the Bay of Bengal the discharge for wet season is 110 x10^9 m^3 which covers 7% of the total discharge to Bay of Bengal (Table 11). So we have oversampled 2.5 times more fluxes to Arabian Sea relative to Bay of Bengal. Moreover, for the Bay of Bengal, we miss the Ganges-Brahmaputra which by far the largest river to the east Indian coast. However if we extrapolate the fluxes to 100% of discharge (300 and 1600 x10^9 m^3 to Arabian Sea and Bay of Bengal respectively) indicate fluxes of Si is greater in Bay of Bengal (except ASi) than the Arabian Sea respectively (Table.11) .

4.5. Impact of land use on Si cycle

Being an agricultural country with ~1.3 billion inhabitants, an attempt has been made to visualize the impact of land use, especially the effect of agriculture, forest cover, build-up lands and the water bodies on Si cycle in the Indian estuaries, since earlier studies have shown anthropogenic impacts on continental Si cycle (e.g. Humborg et al. 2006, Conley et al. 2008; Struyf et al. 2010). The PCA analysis was performed to envisage the relationship among the variables and the prevailing effect of land use in the Indian estuaries. The impact of land use can be better evidenced by the terrestrial supply strappingly associated with discharge during wet period. Therefore the impact of land use was studied only on the Si parameters (ASi, DSi and LSi) during wet period on mean estuary. Before performing the PCA analysis, the % of different land use values are centered to make dimensionless unit. The land use data has been taken from http://www.india-wris.nrsc.gov.in/ and is shown in the Table 1. Note that for some adjacent watersheds, the NRSC-WRIS website gives same land uses which are regional averages (e.g. same land-use for Khali, Mandovi, Zuari).

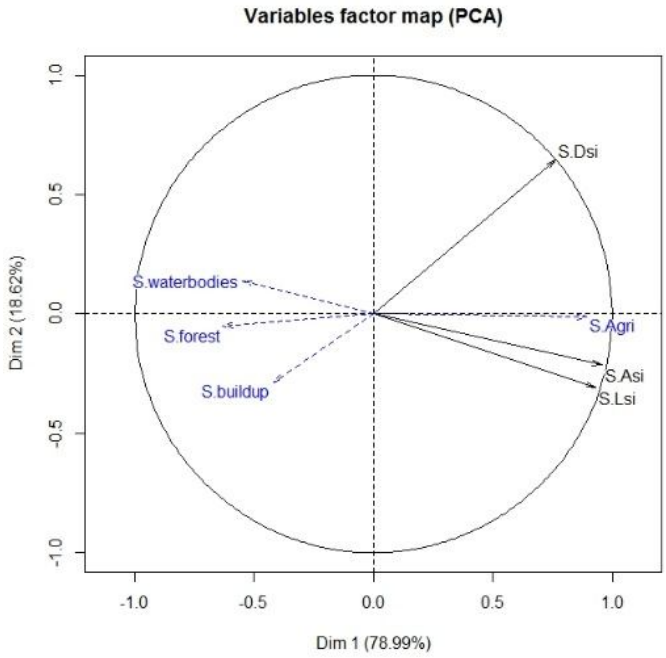

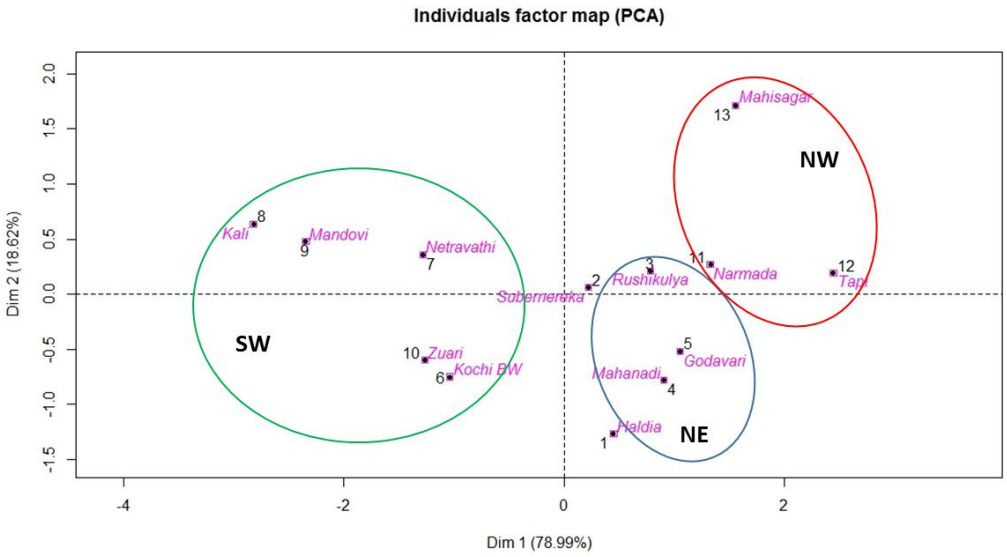

***Fig. 9a and b**, PCA analysis on the impact of land use in the Indian estuaries during wet period. A) Relationship among the variables and b) Individual factor map with Indian estuaries based on PCA results.*

The PCA results explain 79% of the overall variability along the first axis and the 19% along the second axis. PC 2 shows less variability with Eigen value <1 and no significant correlation between PC2 and variables was observed. The positive site score (PC axis) indicates the strong increase in ASi, LSi and to a lesser extent in DSi concentration correlated with increase in agriculture (Fig. 9, Table 12). The negative score (PC axis) indicates the decrease in ASi, DSi and LSi concentration with increase in forest, build-ups and water-bodies (along with decrease in agriculture). Hence PC1 explains best the relationship among variables and impact of land use. The northern estuaries (NE and NW) are congregated towards the positive end of PC1, whereas the Southern (SW) estuaries towards the negative side of PC1. This clearly indicates that, relatively more forest cover (Avg 35%) along the SW region (Western Ghats-chain of mountains) and steeper rivers reduce the Si supply to the coastal water in the SW estuaries (Kochi BW, Zuari, Mandovi, Kali and Netravathi) compared to the other estuaries (avg. forest covers 26%). Moreover, increased forest cover in SW region, reduces the soil erosion thereby limiting the lithogenic supply of Si parameters to the estuaries relative to the eastern estuaries. On the contrary, the wider plains with more agriculture practice along the eastern and Northwestern regions (avg 60%), than the SW (avg 47%) favours more supply of land derived Si (via biogenic) to the Bay of Bengal when compared to Arabian Sea. In addition, a significant positive relationship between DIN and % of agriculture (r^2=0.46,

n=13, p<0.1 Appendix for chapter 3 and Annex G) prominence the impact of fertilizers from agriculture but need further studies to rate the impact extent.

Finally, increasing urbanization can also alter the Si cycle (e.g. deforestation) and changes the Si supply in to estuaries. It is interesting to note that there is no significant relation of "build-up" on the PC axis (Table 12) and on Si variables.

Variables	Wet period (n=13)	
	PC 1	**PC 2**
ASi	**0.95**	-0.21
LSi	**0.93**	-0.30
Dsi	**0.76**	**0.64**
Buildup	-0.41	-0.28
Agriculture	**0.89**	-0.01
Forest	**-0.63**	-0.05
Water bodies	**-0.55**	0.13

***Table 12**. Correlation of land use and Si variables on PC axis 1 and 2 during wet period.*

5. Conclusions

Indian estuaries are highly diversified in terms of geographical situations (climate), topography (e.g., larger watershed and more plains in the eastern parts and smaller rivers and steeper slopes in the western parts), water runoff and land use practices. In this study, we have looked at the variability of amorphous, lithogenic and dissolved silicon as well as of the main biogeochemical parameters relevant to Si in several Indian estuaries in wet and dry seasons. The processes responsible for the variability are mainly the diatom uptake and lithogenic supply during dry period when looking at whole dataset. However, no dominant process was noticed when applying solely a categorisation based on location (NE, NW, SE, SW regions). To decipher between intra-estuary and inter-estuary variability, we separate our data in three categories i) upper (salinity <5), ii) middle (salinity 5 to 15) and iii) lower estuaries (salinity >15) for dry and wet period respectively and performed PCA and clustering on PCA results. We show that during dry period in upper estuaries diatom production is commonly present with possible dissolution in eastern and few western estuaries. ASi is mostly controlled by diatoms as seen by the significant correlation with fucoxanthin. In addition strong lithogenic impact was observed in northwest, especially in Haldia estuary. In dry middle estuaries only four estuaries show dominant role of diatoms on biogeochemical parameters. Surprisingly, mixing with seawater does not seem to control the

variability of biogeochemical parameters. In lower dry estuaries, the control of diatoms is dominant only in four estuaries, the rest of estuaries are either characterised by supply of terrestrial materials or low particulate content due to mixing with seawater.

In wet season, a strong control of erosion is observed, especially in the eastern estuaries. The amount of discharge seems to be the main relevant parameter on particulate concentrations. In the middle wet estuaries, the lithogenic supply continues to dominate. However contrasted fate of Si supplied is observed: in some estuaries (especially northwest), the continental supply increases dramatically while in other, sediment settling decreases the supply to the coast. Overall we show that estuaries have strong variability of their biogeochemical parameters at seasonal and along the salinity gradient, as well as between estuaries. Indeed the clustering of estuaries varies a lot.

We estimated the net Si fluxes to the northern Indian Ocean (Bay of Bengal and Arabian sea) by correcting the upper estuaries fluxes for non-conservativity: the estuaries studied supply 12 ± 1.3, 0.4 ± 0.3 and 115 ± 24 of DSi, ASi and LSi respectively to Bay of Bengal and 12 ± 1.4, 5.3 ± 3.3 and 270 ± 222 x 10^6 kmol/ wet season to Arabian sea respectively. Taking into account of the contribution of our estuaries sampled which represent 17.3% of Indian riverine discharge to Arabian Sea and 7% to Bay of Bengal; we then extrapolate these fluxes to 100 % discharge and find Bay of Bengal supplies more flux of DSi and LSi than Arabian sea.

Finally, the impact of land use was studied on ASi, LSi and DSi. Clearly, increasing agriculture activities play major role in the Si biogeochemical cycle and increasing all Si fluxes. In contrast relatively more forest cover prevents the soil erosion and reduces the supply of silicon in the southwestern estuaries. The present work is the first study on ASi, LSi variability in estuaries at the Indian subcontinent scale and suggests that silicon cycle is largely impacted by the anthropogenic activities. Therefore temporal monitoring of individual estuaries is needed for better understanding or modifications of the Si cycle and its impacts on the health of the estuarine and coastal ecosystems.

Acknowledgements

The research leading to these results has received funding from the European Union Seventh Framework Program under grant agreement #294146 (MuSiCC Marie Curie CIG), from the French

National INSU programme EC2CO-LEFE (project SINDIA funded by Actions CYBER and BIOHEFECT). K.R. Mangalaa scholarship has been provided by the Erasmus Mundus Action 2 of the European Union (GATE project), the Scientific Department of French Embassy in India and, MuSiCC. The authors would like to thank M. Benrahmoune (LOCEAN, CNRS) for managing the clean lab and performing colorimetric analyses.

6. References

Admiraal, W., Breugem, P., Jacobs, D. M. L. H. a. & Steveninck, E. D. Fixation of dissolved silicate and sedimentation of biogenic silicate in the lower river Rhine during diatom blooms. *Biogeochemistry* **9,** 175–185 (1990).

Aigars, J., Jurgensone, I. & Jansons, M. Dynamics of silica and phytoplankton population under altered conditions of river flow in the Daugava River, Latvia. *Est. J. Ecol.* **63,** 217 (2014).

Ansotegui, a. The Use of Pigment Signatures to Assess Phytoplankton Assemblage Structure in Estuarine Waters. *Estuar. Coast. Shelf Sci.* **52,** 689–703 (2001).

Barão, L. *et al.* Alkaline-extractable silicon from land to ocean: A challenge for biogenic silicon determination. *Limnol. Oceanogr. Methods* **13,** 329–344 (2015).

Attri, S. D. & Tyagi, A. Climate profile of India. *Gov. India Minist. Earth Sci.* 129 (2010). at http://www.imd.gov.in/doc/climate_profile.pdf.

Berner, R. A. Weathering, plants, and the long-term carbon cycle. *Geochimica et Cosmochimica Acta*, *56*(8), 3225–3231. (1992).

Bootsma, H. A., Hecky, R. E., Johnson, T. C., Kling, H. J. & Mwita, J. Inputs, Outputs, and Internal Cycling of Silica in a Large, Tropical Lake. *J. Great Lakes Res.* **29,** 121–138 (2003).

Carbonnel, V., Vanderborght, J. P., Lionard, M. & Chou, L. Diatoms, silicic acid and biogenic silica dynamics along the salinity gradient of the Scheldt estuary (Belgium/The Netherlands). *Biogeochemistry* **113,** 657–682 (2013).

Cary, L., Alexandre, A., Meunier, J. D., Boeglin, J. L. & Braun, J. J. Contribution of phytoliths to the suspended load of biogenic silica in the Nyong basin rivers (Cameroon). *Biogeochemistry* **74,** 101–114 (2005).

Central water commission report. National Register of Large Dams – 2009. (2009).

Chou L. and R. Wollast. Estuarine silicon dynamics. In: The Silicon Cycle. Human Perturbations and Impacts on Aquatic Systems. Edited by V. Ittekkot, D. Unger, C. Humborg and N. Tac An. Scope 66, pp. 93- 120, Island Press, Washington, Covelo, London (2006).

Commission, C. W., Remote, N. & Centre, S. Watershed Atlas. (2014).

Conley, D. J. An interlaboratory comparison for the measurement of biogenic silica in sediments. 39–48 (1998).

Conley, D. J. *et al.* Deforestation causes increased dissolved silicate losses in the Hubbard Brook Experimental Forest. *Glob. Chang. Biol.* **14,** 2548–2554 (2008).

Conley, D. J. Riverine contribution of biogenic silica to the oceanic silica budget. *Limnol. Oceanogr.* **42,** 774–777 (1997).

Conley, D. J. Terrestrial ecosystems and the global biogeochemical silica cycle. *Global Biogeochem. Cycles* **16,** 1–8 (2002).

Conley, D. J., Schelske, C. L. & Stoermer, E. F. Modification of the biogeochemical cycle of silica with eutrophication. *Mar. Ecol. Prog. Ser.* **101,** 179–192 (1993).

Delvaux, C. *et al.* Controls on riverine δ30Si signatures in a temperate watershed under high anthropogenic pressure (Scheldt — Belgium). *J. Mar. Syst.* 1–12 (2013).

Ducklow, H. W., Steinberg, D. K. & Buesseler, K. O. Upper ocean carbon export and the biological pump. *Oceanography* **14,** 50–58 (2001).

Dunne, T. Rates of chemical denudation of silicate rocks in tropical catchments. *Nature* **274,** 244–246 (1978).

Durga bharathi. 'Variability in composition and diversity of phytoplankton in the Indian estuaries and coastal Bay of Bengal '. Ph.D. thesis (2014).

Dürr, H. H., Meybeck, M., Hartmann, J., Laruelle, G. G. & Roubeix, V. Global spatial distribution of natural riverine silica inputs to the coastal zone. *Biogeosciences* **8,** 597–620 (2011).

Friedl, G., Teodoru, C. & Wehrli, B. Is the Iron Gate I reservoir on the Danube River a sink for dissolved silica? *Biogeochemistry* **68,** 21–32 (2004).

Frings, P. J. *et al.* Silicate weathering in the Ganges alluvial plain. *Earth Planet. Sci. Lett.* **427,** 136–148 (2015).

Frings, P. J., Clymans, W. & Conley, D. J. Amorphous Silica Transport in the Ganges Basin: Implications for Si Delivery to the Oceans. *Procedia Earth Planet. Sci.* **10,** 271–274 (2014).

Garnier, J., Beusen, A., Thieu, V., Billen, G. & Bouwman, L. N:P:Si nutrient export ratios and ecological consequences in coastal seas evaluated by the ICEP approach. *Global Biogeochem. Cycles* **24,** GB0A05, 1–12 (2010).

Government of India. State of Indian Agriculture. 247 (2012). http://agricoop.nic.in/sia111213312.pdf.

Grasshoff K., K. Kremling, M. Ehrhardt. *Methods of Seawater Analysis 3rd Edison completely Revised and Extended edition.* Wiley- VCH. ISBN 3-527-29589-5, (1999).

Gurumurthy, G. P. *et al.* Controls on intense silicate weathering in a tropical river, southwestern India. *Chem. Geol.* **300-301,** 61–69 (2012).

Heiskanen, A. S. & Keck, A. Distribution and sinking rates of phytoplankton, detritus, and particulate biogenic silica in the Laptev Sea and Lena River (Arctic Siberia). *Mar. Chem.* **53,** 229–245 (1996).

Heukelem. Van, L. & Thomas, C. Computer-assisted high-performance liquid chromatography method development with applications to the isolation and analysis of phytoplankton pigments. *J. Chromatogr. A* **910,** 31–49 (2001).

Howarth, R. *et al.* Coupled biogeochemical cycles: eutrophication and hypoxia in temperate estuaries and coastal marine ecosystems. *Front. Ecol. Environ.* **9,** 18–26 (2011).

Hughes, H. J. *et al.* Effect of seasonal biogenic silica variations on dissolved silicon fluxes and isotopic signatures in the Congo River. *Limnol. Oceanogr.* **56,** 551–561 (2011).

Hughes, H. J., Bouillon, S., André, L. & Cardinal, D. The effects of weathering variability and anthropogenic pressures upon silicon cycling in an intertropical watershed (Tana River, Kenya). *Chem. Geol.* **308-309,** 18–25 (2012).

Hughes, H. J., Sondag, F., Santos, R. V., André, L. & Cardinal, D. The riverine silicon isotope composition of the Amazon Basin. *Geochim. Cosmochim. Acta* **121,** 637–651 (2013).

Humborg, C. *et al.* Decreased Silica Land–sea Fluxes through Damming in the Baltic Sea Catchment – Significance of Particle Trapping and Hydrological Alterations. *Biogeochemistry* **77,** 265–281 (2006).

Ittekkot, V., R. R. Nair, S. Honjo, V. Ramaswamy, M. Bartsch, S. Manganini, and B. N. Desai. Enhanced particle fluxes in Bay of Bengal induced by injection of fresh water, Nature, 351, 385–387. (1991).

Krishna, M. S. *et al.* Export of dissolved inorganic nutrients to the northern Indian Ocean from the Indian monsoonal rivers during discharge period. *Geochim. Cosmochim. Acta* **172,** 430–443 (2016).

Laruelle, G. G. *et al.* Anthropogenic perturbations of the silicon cycle at the global scale: Key role of the land-ocean transition. *Global Biogeochem. Cycles* **23,** 1–17 (2009).

Lehtimäki, M., Tallberg, P. & Siipola, V. Seasonal Dynamics of Amorphous Silica in Vantaa River Estuary. *Silicon* **5,** 35–51 (2013).

Li, M., Xu, K., Watanabe, M. & Chen, Z. Long-term variations in dissolved silicate, nitrogen, and phosphorus flux from the Yangtze River into the East China Sea and impacts on estuarine ecosystem. *Estuar. Coast. Shelf Sci.* **71,** 3–12 (2007).

Liu, S. M., Hong, G.-H., Ye, X. W., Zhang, J. & Jiang, X. L. Nutrient budgets for large Chinese estuaries and embayment. *Biogeosciences Discuss.* **6,** 391–435 (2009).

Lu, C. A. O., Sumei, L. I. U. & Jingling, R. E. N. Seasonal variations of particulate silicon in the Changjiang (Yangtze River) Estuary and its adjacent area. *Acta Oceanol. Sin.* **32,** 1–10 (2013).

Meunier, J. D. *et al.* Controls of DSi in streams and reservoirs along the Kaveri River, South India. *Sci. Total Environ.* **502,** 103–113 (2015).

Michalopoulos P, AllerRC. Rapid clay mineral formation inAmazondelta sediments: reverse weathering and oceanic elemental cycles. Science 270:614–17. (1995).

Michalopoulos, P. & Aller, R. C. Early diagenesis of biogenic silica in the Amazon delta: alteration, authigenic clay formation, and storage. *Geochim. Cosmochim. Acta* **68,** 1061–1085 (2004).

Middelburg, J. J. & Herman, P. M. J. Organic matter processing in tidal estuaries. *Mar. Chem.* **106,** 127–147 (2007).

Nair, R. R, V. Ittekkot, S. J. Managanini , V. Ramaswamy, B. Hakke, E.T. Degens, B. N. Desai and S. Honjo (1989), Increased particle flux to the deep ocean related to monsoon, Nature, 338, 749–751.

Nayak, G. N. & Hanamgond, P. T. India. *Encycl. World's Coast. Landforms* **2010,** 1065–1070 (2010).

Naqvi, S. W. A. *et al.* The Arabian Sea as a high-nutrient, low-chlorophyll region during the late Southwest Monsoon. *Biogeosciences* **7,** 2091–2100, 2010

Nelson, D. M., Tréguer, P., Brzezinski, M. A., Leynaert, A. & Quéguiner, B. Production and dissolution of biogenic silica in the ocean: Revised global estimates, comparison with regional data and relationship to biogenic sedimentation. *Global Biogeochem. Cycles* **9,** 359–372 (1995).

Ragueneau, O. *et al.* A new method for the measurement of biogenic silica in suspended matter of coastal waters: using Si:Al ratios to correct for the mineral interference. *Cont. Shelf Res.* **25,** 697–710 (2005).

Ragueneau, O. *et al.* A review of the Si cycle in the modern ocean: Recent progress and missing gaps in the application of biogenic opal as a paleoproductivity proxy. *Glob. Planet. Change* **26,** 317–365 (2000).

Ragueneau, O. *et al.* Direct evidence of a biologically active coastal silicate pump: Ecological implications. *Limnol. Oceanogr.* **47,** 1849–1854 (2002).

Raimonet M., Andrieux-Loyer F., Ragueneau O., Michaud E., Kerouel R., Philippon X., Nonent M., Mémery, L. Strong gradient of benthic biogeochemical processes along a macrotidal temperate estuary: focus on P and Si cycles. Biogeochemistry (2013).

Ran, X. *et al.* Variability in the composition and export of silica in the Huanghe River Basin. *Sci. China Earth Sci.* (2015).

Rao, G. D. and S. V. V. S. S. Contribution of N 2 O emissions to the atmosphere from Indian monsoonal estuaries. *Tellus, Ser. B Chem. Phys. Meteorol.* **1,** 1–9 (2013).

Sharma. S.K and V. Subramanian. Hydrochemistry of the Narmada and Tapti Rivers, India. *Hydrol. Process.* **22,** 3444–3455 (2008).

Sarma, V. V. S. S. *et al.* Carbon dioxide emissions from Indian monsoonal estuaries. *Geophys. Res. Lett.* **39,** (2012).

Sarma, V. V. S. S. *et al.* Distribution and sources of particulate organic matter in the Indian monsoonal estuaries during monsoon. **119,** 1–17 (2014).

Sarma, V. V. S. S. *et al.* Influence of river discharge on plankton metabolic rates in the tropical monsoon driven Godavari estuary, India. *Estuar. Coast. Shelf Sci.* **85,** 515–524 (2009).

Schoellhamer, D.H., 2001, Influence of salinity, bottom topography, and tides on locations of estuarine turbidity maxima in northern San Francisco Bay, in McAnally, W.H. and Mehta, A.J., ed., Coastal and Estuarine Fine Sediment Transport Processes: Elsevier Science B.V., p. 343-357.

Soman, M. K. & Kumar, K. K. Some aspects of daily rainfall distribution over India during the south-west monsoon season. *Int. J. Climatol.* **10,** 299–311 (1990).

Sridevi, B., Sarma, V. V S S., Murty, T. V R., Sadhuram, Y., Reddy, N. P C., Vijayakumar, K., Raju, N. S N., Jawahar Kumar, C. H., Raju, Y. S N., Luis, R., Kumar, M. D., Prasad, K. V S R. Variability in stratification and flushing times of the Gautami–Godavari estuary, India. *J. Earth Syst. Sci.* **124,** 993–1003 (2015).

Struyf, E., Van Damme, S., Gribsholt, B., Middelburg, J. J. & Meire, P. Biogenic silica in tidal freshwater marsh sediments and vegetation (Schelde estuary, Belgium). *Mar. Ecol. Prog. Ser.* **303,** 51–60 (2005).

Sun, X., Andersson, P. S., Humborg, C., Pastuszak, M. & Mörth, C. M. Silicon isotope enrichment in diatoms during nutrient-limited blooms in a eutrophied river system. *J. Geochemical Explor.* **132,** 173–180 (2013).

Tréguer, P. *et al.* The silica balance in the world ocean: a re-estimate. *Science* **268,** 375–379 (1995).

Tréguer, P. J. & De La Rocha, C. L. The world ocean silica cycle. *Ann. Rev. Mar. Sci.* **5,** 477–501 (2013).

Vijith, V., Sundar, D. & Shetye, S. R. Time-dependence of salinity in monsoonal estuaries. *Estuar. Coast. Shelf Sci.* **85,** 601–608 (2009).

Wedepohl, K. H. INGERSON LECTURE The composition of the continental crust. *Geochim. Cosmochim. Acta* **59,** 1217–1232 (1995).

Wu, J. T. & Chou, T. L. Silicate as the limiting nutrient for phytoplankton in a subtropical eutrophic estuary of Taiwan. *Estuar. Coast. Shelf Sci.* **58,** 155–162 (2003).

Wysocki, L. A., Bianchi, T. S., Powell, R. T. & Reuss, N. Spatial variability in the coupling of organic carbon, nutrients, and phytoplankton pigments in surface waters and sediments of the Mississippi River plume. *Estuar. Coast. Shelf Sci.* **69,** 47–63 (2006).

Zhang. A.Y, J. Zhang, J.Hu, R. F. Zhang, and G. S. Z. School. Journal of Geophysical Research : Oceans. *J. Geophys. Res. Ocean. Res.* 1–16 (2015).

Zhu, Z.-Y. *et al.* Estuarine phytoplankton dynamics and shift of limiting factors: A study in the Changjiang (Yangtze River) Estuary and adjacent area. *Estuar. Coast. Shelf Sci.* **84,** 393–401 (2009).

CHAPTER 4

Seasonal silicon isotope compositions of surface and ground waters in Indian estuaries

K. R. Mangalaa, D. Cardinal, A. Dapoigny, S. Caquineau, Shangyao Guo, V.V.S.S. Sarma et al.

Article in preparation for *Biogeosciences*

1. Introduction

Silicon (Si) is the second most abundant element next to oxygen with 28.8% in the Earth's crust (Wedepohl, 1995). The Si contained in the rocks is released by physical and chemical weathering and results either in congruent dissolution or in the formation of clay minerals. As a result of chemical weathering, Si is split into two reservoirs: a secondary mineral fraction (clay minerals) and the dissolved silicon (DSi) while some primary minerals remain unmodified and are referred to as residual primary minerals (e.g. quartz, feldspar). Around 80% of DSi supplied to the ocean is delivered by rivers (Treguer and De la Rocha, 2013). This release of DSi to the hydrosphere is controlled by several factors, including lithology, climate, terrain, slope and vegetation (Dessert et al., 2003; Beusen et al., 2009; Roelandt et al., 2010). A schematic representation of weathering processes and the type of clay minerals formation with respect to the climate is depicted in the figure 2 of chap. 1. Moreover, Si is strongly intertwined in biogeochemical processes in both the terrestrial and aquatic ecosystems since it is taken up by plants and is an absolute nutrient for diatoms to build their silica frustules that are abundant and freshwater and marine ecosystems.

According to the revisited Si budget, proposed by Treguer and De la Rocha. (2013), 21% (1.5 ± 0.5 Tmol year $^{-1}$ of Si is trapped in the estuaries before entering into the coastal zone. Estuaries are dynamic ecosystems characterised by a salinity gradient with higher nutrient supply from upstream and varying primary production. The supplied DSi may not behave conservatively and can be controlled by various natural (biological and geochemical reactions) and anthropogenic processes (different land-use) in estuaries before entering into the ocean. The variability of ASi (amorphous silica), DSi (dissolved silicon) and LSi (lithogenic silicon) was discussed in the previous chapter and the significant impact of land use was noticed in the Indian estuaries. It is estimated that the DSi trapped within the estuaries (21%, Treguer and De La Rocha. 2013) is due to biological uptake (De la Rocha et al., 1997; Loucaides et al., 2008; Sun et al., 2013) and may be by adsorption/desorption processes (Delstanche et al., 2009, Ding et al., 2011). Moreover, increasing eutrophication of coastal waters due to the anthropogenic increase of N and P nutrients supply from the fertilizers usage for agriculture, combined with reduced Si supply due to damming may alter the phytoplankton diversity at the expenses of diatoms and thereby producing harmful algal blooms (Garnier et al., 2010). Indian estuaries are monsoonal estuaries and serve as the best example to study the natural (with diversified lithology associated weathering cf. Chapter 1) and

anthropogenic impact on the Si cycle on tropical rivers which are the major sources of DSi to the ocean (Treguer et al 1995).

Besides its ubiquitous nature of Si, the anthropogenic impacts on Si cycle are not studied well. The stable Si isotopes (^{28}Si, ^{29}Si and ^{30}Si) serve as useful tool to trace the biotic (e.g., biological uptake, De La Rocha et al., 1997; Sun et al., 2013), abiotic (e.g., weathering), physical mixing and anthropogenic (e.g. Delvaux et al., 2013) processes that control the Si fluxes. So far, there are only few studies existing on estuarine Si isotope studies. For example in Tana estuary conservative mixing controls the δ^{30}Si-DSi (Hughes et al., 2012). In the tidal freshwater estuary of Scheldt river there is control of diatom uptake on the δ^{30}Si-DSi composition during summer and simple mixing during winter (Delvaux et al., 2013).

As discussed in the earlier Chapter 3, there is a wide variability of ASi and DSi concentrations within as well as among regional estuaries controlled by several processes irrespective to their geographic positions. However, the impact of land-use on Si variability seems to be first order control as seen in previous chapter, which emphasizes the natural and anthropogenic pressures along the land-ocean continuum Si cycle. Apart from estuaries, studies on groundwater remain particularly scarce despite groundwater is a major source of fresh water and nutrient supply, including Si (Ziegler et al., 2005; Georg et al., 2009a,b; Opfergelt et al., 2011; Pogge von Standmann et al., 2014). Globally Si supply to the ocean by submarine groundwater discharge has indeed ± 100% uncertainty due to the lack of measurements (Tréguer and De La Rocha 2013). Regionally it has been estimated that the groundwater may constitute up to 40 % of the Si flux to the Bay of Bengal (Georg et al., 2009).

With the greater contribution of Si fluxes along the land-ocean continuum over tropical regions, we propose first to explore the Si isotopic signature of DSi at both spatial and seasonal scale over Indian estuaries. We will then try to identify whether the behaviour of DSi is conservative or influenced by biological uptake, dissolution within the estuaries during both seasons. Finally, we make an attempt to understand the impact of land use on the Si isotopic composition in the Indian monsoonal estuaries.

2. Materials and methods

The climatic Indian setting and the existing anthropogenic pressures were discussed already in Chapter 3. As in the previous chapter, 24 and 18 estuaries were sampled along the entire coastline of India

during the dry (Jan-Feb 2011) and wet period (July-August 2014) respectively for main hydrological and biogeochemical parameters including temperature, salinity, nutrients and the Si parameters (DSi and particulate ASi and LSi). In each estuary, generally 3 to 4 samples were collected across the salinity gradient from near zero salinity to the mouth of the estuary during both seasons (refer to Chapter 3 for more details regarding sampling). In this Chapter 4, we considered only estuaries where the Si isotopes samples are available. 16 and 13 estuaries have been studied for dry and wet period respectively (Fig. 1). Moreover, the estuaries sampled during dry and wet period are generally different except for the estuaries Haldia, Subarnarekha, Rushikulya, and Mahanadi (from northeast) and Kochi Back Waters (KBW, from the southwest) that have been sampled during both the seasons.

Fig. 1 *Estuaries with main watershed limits (dark blue lines) and rivers (light blue lines). Samples collected during dry (circle) and wet (star) periods. Estuaries with triangles are the 2014 wet period sampling considered as dry because of low discharge event (see text under water discharge section or Chapter 3 for more details). Filled blue diamonds represent the groundwater samples collected during the wet period.*

In addition, 14 surface groundwater samples were also collected from the municipal and domestic wells (mostly boreholes) next to the upstream sampling of each estuary (Fig. 1). The sampling procedures for biogeochemical parameters like nutrients, suspended materials, temperature and salinity were

presented in Chapter 3. The Nalgene Polypropylene bottles used for Si isotopes were acid pre-cleaned, dried and rinsed well with filtered sampling water before sample collection. The surface water samples were collected using 5l Niskin sampler. Depending on the turbidity 100 to 500 ml of water was filtered on cellulose nitrate filter for the dry period and polyether sulfone Supor ®200 (0.2µm, Pall corporation) paper for the wet period. Then the samples were preserved at room temperature until preparation for isotopic analysis. The DSi concentration was measured following Grashoff et al. (1992). The results were compared with Certified Reference Material for Si (PERADE-09, supplied by environment Canada, lot no: 0314, whose Si = 109.96 ± 6.97 µM) and the measurements were found to be more precise with mean Si of 112.8 ± 2.68 µM, n=82 (97.4% reproducibility). More details about the precision of the methods are discussed in Chapter 2. The pictures of the estuaries sampling sites during wet period are given in the Annex of chapter 4. Note that some were sampled in the middle of the flow (using boat or ferry or pirogue) and some from the shore when weather was too rough or boat unavailable.

Total cations

For cations measurements, around 10 ml of filtered samples are collected and preserved by adding supra pure HNO_3. In the laboratory, the major cations (Na, Ca, Mg, K, Fe, Al) were measured using a ICPMS (Agilent 7700 series, LOCEAN, IRD-UPMC) and Cl concentrations were measured by ion chromatography (ISTEP, UPMC). The major cations concentration of estuaries was not corrected for the atmosphere/seawater input because this generally resulted in negative concentration. We ascribe this is due to the fertilizers impact (see discussion the annexure A of Chapter 4). However, these major cations uncorrected concentrations were used to calculate the mineral saturation indices within estuaries (cf below).

Saturation Indexes

Based on major ion chemistry data, the Saturation Indexes (SI) with respect to relevant minerals in the upper estuarine samples and groundwater (salinity <5) were calculated with the phreequ program-version 2 (Parkhurst and Appelo, 1999). The Saturation Index indicates whether a mineral will tend to dissolve or precipitate in the surrounding water according to thermodynamic laws. Negative SI indicates that minerals are under-saturated and may dissolve while positive values indicate oversaturation and mineral should precipitate or remain stable if present.

Clay minerals

We studied the clay mineralogy composition with X-Ray diffraction on our particulate samples from Indian estuaries during wet period (Table 3, data from Master student S. Guo, 2016). Absolute quantification of clay minerals is very difficult to achieve on particulate suspended matter, but the relative abundance of clay minerals can be estimated using Caquineau et al. (1997) which has been adapted from Biscaye et al. (1965).

Si isotopes

Methodological procedures such as sample preparation, purification and measurement of δ^{30}Si-DSi are explained in detail in Chapter 2. The reproducibility, precision and quality of the data are also discussed under Chapter 2.

Water discharge

Since the Indian estuaries are monsoonal estuaries, they generally receive maximum freshwater runoff (>80%) during monsoon (June-September) as discussed in Chapter 3. Therefore, a huge supply of land-derived material transport occurs only during wet (monsoon) period and this can be considered as more representative of the land-derived processes. The discharge during dry (non-monsoon) period is much less due to the water consumption for several domestic and irrigation purposes upstream and reflects more estuarine or riverine processes (e.g., discussion in Chapter 5).

There is no discharge data available for the wet period sampling (June-July 2014) and hence, we used the wet period total discharge data (i.e., 3 to 5 months of 2011-2012). The data was obtained from the gauge measurements at the upstream end of the estuary and can be downloaded from the Water Resources Information System of India (http://www.india-wris.nrsc.gov.in/wris.html). More details about the discharge data were discussed in Chapter 3, (under § on 2.2 and 4.4) flux calculations. At the time of sampling, discharge was high during wet period in all estuaries except southeastern estuaries (Penna, Ponnaiyar, Vellar and Cauvery) where low discharge remains all year-long because of less rainfall during the southwest monsoon and high water use upstream. In addition to the above-mentioned estuaries, southwest monsoon was particularly late in 2014 and Krishna (southeast) estuary was sampled still at low discharge before typical high discharge monsoon was reached. Hence the “wet” period sampling of these 5 estuaries is considered as dry period since discharge was indeed low and shown in Figure 1 (cf. pictures in Annex of Chapter 4).

3. Results

3.1 General trend on DSi

Contrary to Chapter 1, here we present the DSi concentration on lesser estuaries because of less Si isotopes samples availability. Therefore the variability of DSi, in this chapter can slightly differ from the Chapter 3. The DSi concentrations of Indian estuaries considered here are notably higher and variable (200 ± 140 µM) during dry period (Table 1) than the wet period (148 ± 76 µM, Table 2) with significant seasonal variability ($p = 0.007$). Note that this is partly due to the comparison of estuaries which are not the same between both the periods (only five estuaries have been sampled at the two seasons). Yet, this seasonal variability could also be explained because of the dilution effect during heavy discharge. However, there is no significant relationship between DSi and discharge during wet period. Throughout dry period, the east-flowing estuaries are distinguished by higher DSi concentration (220 ± 142 µM, n=69) compared to the southwestern estuaries (85 ± 28 µM, n=12) with significant difference ($p <0.001$). This major difference is likely due to the topographical nature of the eastern (wider plains and more soil water residence time) and western (steeper slopes) estuaries respectively which was discussed earlier (Chapter 3). Yet, this hypothesis will be conferred in this chapter along with weathering processes. Noteworthy the 5 common estuaries during both seasons do not show any significant seasonal difference in DSi concentration ($p =0.2$, n=19).

3.2 General trend on Silicon isotopes (δ^{30}Si-DSi)

The isotopic data are all consistent with the mass dependent fractionation line shown under section 2.2 of Chapter 2. The δ^{30}Si-DSi of Indian estuaries vary from 0.8 to 2.8‰ with an average of 1.9 ± 0.47 ‰ during dry period (n= 74) and 0.4 to 2.1 ‰ with an average of 1.3 ± 0.55 ‰ during wet period (n= 46) (Tables 1 and 2). This seasonal difference is significant with $p <0.001$ when considering all estuaries. However, as also noticed for DSi concentration when considering only the common estuaries of both seasons (Haldia, Subarnarekha, Rushikulya, Mahanadi, and KBW) there was no significant seasonal difference ($p= 0.2$) in the Si isotopic composition. This suggests that most of the seasonal isotopic variation we observe might rather result from inter-estuary difference than from a seasonal imprint.

The east-flowing estuaries (2.1 ± 0.32 ‰) are heavier by +1‰ in δ^{30}Si-DSi compared to the west flowing estuaries (1.0 ± 0.17 ‰) with a significant difference ($p < 0.001$) during dry period. Likewise, the significant difference between eastern (1.6 ± 0.22‰) and western estuaries (1.1 ± 0.61 ‰) is observed during wet period ($p < 0.001$). This indicates the importance of location of estuaries in India with respective to Si isotopes. Combining east and west flowing estuaries, there is no relationship between discharge and Si isotopes. Nevertheless, a strong significant negative relationship between discharge and δ^{30}Si-DSi is observed for northern estuaries, whereas relatively less significant ($p < 0.1$, n=4, except "Mandovi") relationship is observed for the southern estuaries (Fig. 2). There exist only a few δ^{30}Si-DSi data in estuaries and overall, our results are consistent and comparable with other estuaries studied so far. For example, in Changjiang estuary the δ^{30}Si-DSi varies from 1.48 to 2.35 ‰ (Zhang et al., 2015), in Tana estuary 2.00 ± 0.1 ‰ (Hughes at al., 2012), in Elbe estuary 1.71 to 3.18 ‰ (Weiss et al., 2015) and in Scheldt estuary 1.05 ± 0.35 ‰ (Delvaux et al., 2013).

3.3 Major cations

The concentrations of major cations of Indian estuaries are highly variable with decreasing order of Cl>Na>SO4>Mg>Ca>K>Al>Fe during dry and Cl>Na>SO4>Mg>K>Ca>Al>Fe during wet periods respectively (Table 2). The groundwater major cations concentrations are less variable than the estuaries (Table 4) with decreasing order of Na>Cl>SO4>Ca>K>Mg>Al>Fe.

3.4 Clay mineralogy

Based on XRD study, there is a presence of relatively high percentage of smectite (especially in the east flowing estuaries and northwest estuaries), kaolinite (southwest estuaries- Kochi BW, Netravathi, and Kali), illite (northeast estuaries- Haldia and Subernereka). We further note the presence of gibbsite in the south-west flowing estuaries (Table 3). This clay mineralogy composition is comparable with earlier studies on Indian estuaries (Deepthy and Balakrishnan, 2005; Kessarkar et al., 2013).

	Estuary	Salinity	DSi (µM)	ASi (µM)	δ^{30}Si-DSi ‰	SD	δ^{29}Si-DSi ‰	SD	Na	Mg	Al	K	Ca	Fe	Cl	SO_4
									ppm							
Northeast	Haldia	6.8	138	NA	1.9	0.03	1.0	0.02	1896	244	0.06	77	101	0.09	3758	480
		5.5	131	NA	1.7	0.00	0.9	0.06	1464	189	0.05	60	83	0.04	3040	391
	Subarnerekha	7.0	143	2.91	2.5	0.08	1.3	0.02	1913	243	0.04	77	92	0.05	3861	492
		4.2	170	3.22	2.3	0.16	1.2	0.12	912	118	0.03	38	53	0.03	2344	295
		5.3	157	18.42	2.4	0.03	1.2	0.03	1401	179	0.03	57	70	0.03	2965	370
		3.7	164	3.37	2.5	0.04	1.2	0.03	987	127	0.03	41	57	0.02	2039	262
	Baitharani	21.3	59	1.63	1.9	0.04	1.0	0.03	4221	744	0.08	239	239	0.04	11858	1445
	Rushikulya	26.3	96	1.62	2.1	0.22	1.1	0.09	5256	1022	0.03	331	327	0.05	14612	1803
	Vamsadhara	28.8	50	0.68	1.9	0.03	0.9	0.03	5801	1093	0.02	359	348	0.01	16026	2010
		2.3	358	4.07	1.9	0.04	1.0	0.03	707	92	0.02	31	50	0.01	1292	177
		1.0	378	3.76	2.0	0.28	1.1	0.17	270	39	0.01	15	35	0.01	530	64
	Nagavali	3.4	381	4.27	1.9	0.08	1.0	0.13	979	132	0.15	40	65	0.15	1863	232
		5.2	418	3.05	1.8	0.04	1.0	0.03	1370	180	0.02	55	78	0.03	2906	371
	Mahanadi	2.5	153	1.13	1.8	0.07	0.9	0.02	665	87	0.03	29	42	0.01	1409	182
		4.4	152	0.75	1.8	0.04	0.8	0.03	1309	167	0.05	54	70	0.04	2458	300
		3.2	148	1.00	2.1	0.04	1.0	0.03	996	127	0.02	42	54	0.01	1781	266
		10.0	120	0.71	2.0	0.06	1.1	0.04	1969	340	0.02	109	120	0.01	5564	673
		10.6	116	0.23	2.1	0.03	1.0	0.03	2143	356	0.02	113	122	0.01	5877	731
		15.8	77	0.70	1.8	0.12	0.9	0.17	3126	562	0.05	181	185	0.01	8773	1076
Southeast	Krishna	0.1	327	0.93	1.9	0.04	0.9	0.05	92	24	0.01	4	15	0.01	76	56
		10.9	239	9.49	2.0	0.04	1.0	0.03	3672	546	0.01	135	177	0.01	6063	780
		16.3	166	10.81	1.7	0.03	0.9	0.02	5766	682	0.02	214	262	0.02	9035	1134
		24.1	59	2.62	1.7	0.03	0.9	0.02	6281	1024	0.03	328	342	0.09	13371	1662
		32.4	33	1.33	1.8	0.08	0.9	0.07	11030	1540	0.03	437	411	0.02	18018	2241
	Penna	0.2	233	2.01	1.8	0.05	1.0	0.03	110	20	0.01	4	26	0.01	85	72
		0.3	211	0.60	1.9	0.20	1.1	0.11	113	17	0.03	5	34	0.03	166	45
		17.3	121	4.79	2.0	0.03	1.1	0.02	6013	806	0.01	221	225	0.01	9609	1247
		1.2	212	NA	1.9	0.05	1.0	0.03	365	47	0.03	15	43	0.05	667	111
		22.5	81	11.59	2.2	0.03	1.2	0.02	7282	1040	0.04	288	287	0.01	12522	1576
		21.8	80	4.29	NA	NA	NA	NA	8171	1081	0.01	302	298	0.01	NA	NA
		7.4	178	0.87	2.0	0.06	1.0	0.07	2212	279	0.06	89	112	0.02	4122	539
	Ponnaiyar	0.4	544	2.79	2.5	0.19	1.3	0.09	87	27	0.02	6	37	0.01	198	34
		0.5	326	36.45	2.8	0.05	1.3	0.04	363	47	0.03	11	26	0.03	282	204
		0.6	578	6.48	2.6	0.05	1.3	0.04	177	38	0.03	9	43	0.04	328	43
		2.1	530	7.38	2.6	0.03	1.4	0.02	537	82	0.02	24	55	0.02	1150	121
		24.2	138	46.27	2.8	0.04	1.6	0.02	8248	872	0.03	312	296	0.02	13442	1620
	Cauvery	0.2	334	2.23	2.1	0.05	1.1	0.00	54	19	0.03	4	32	0.03	119	24
		0.2	368	6.79	2.3	0.05	1.1	0.03	657	194	0.26	46	326	0.44	125	25
		2.7	358	11.50	2.1	0.03	1.1	0.02	762	107	0.04	30	59	0.04	1485	190
		2.7	349	2.93	2.0	0.03	1.0	0.08	1018	114	0.02	38	64	0.03	1481	203
		4.9	332	10.04	2.2	0.03	1.1	0.02	1363	181	0.05	51	79	0.05	2740	337
		7.6	298	11.41	2.0	0.04	1.0	0.03	2129	284	0.03	80	109	0.02	4226	532
		13.9	197	10.41	2.3	0.03	1.2	0.03	4759	554	0.01	183	215	0.01	7748	971
		17.5	173	10.15	2.5	0.04	1.4	0.03	5877	738	0.01	226	270	0.33	9732	1267
		26.9	97	9.54	2.4	0.04	1.3	0.03	9559	1121	0.03	381	368	0.03	14967	1847
	Ambullar	0.3	314	2.04	1.7	0.22	0.9	0.20	89	22	0.03	4	17	0.03	142	18
		0.3	321	2.98	1.9	0.04	1.0	0.03	99	23	0.02	4	31	0.02	163	19
	Vaigai	1.3	258	1.80	2.5	0.28	1.3	0.16	264	41	0.17	13	32	0.11	732	75
		8.1	95	0.48	2.5	0.04	1.3	0.02	2522	286	0.03	65	118	0.01	4520	505
		11.1	141	1.78	2.0	0.07	1.0	0.04	3695	410	0.02	106	155	0.01	6155	745
		14.8	191	1.84	2.0	0.08	1.1	0.07	5370	637	0.05	169	241	0.02	8196	1185
	Vellar	0.4	519	2.69	2.1	0.04	1.1	0.03	301	45	0.03	4	27	0.02	247	110
		2.1	431	4.81	2.0	0.19	1.0	0.10	2675	301	0.07	87	116	0.09	1142	148
		2.6	427	5.70	2.2	0.03	1.1	0.03	7584	945	0.21	283	311	0.11	1424	182
		3.2	390	9.57	2.1	0.04	1.1	0.03	NA	NA	NA	NA	NA	NA	1794	234
		NA	347	6.59	NA	NA	NA	NA	1667	214	0.03	55	59	0.03	NA	NA
		6.9	357	5.80	2.2	0.04	1.2	0.03	6674	743	0.04	251	222	0.03	3855	577
		19.7	37	12.79	0.8	0.04	0.5	0.03	11086	1597	0.01	441	399	0.01	10958	1404
		34.1	45	6.95	2.1	0.03	1.1	0.02	NA	NA	NA	NA	NA	NA	18950	2311

Table continued...

Southwest	KBW	0.4	112	0.16	0.8	0.11	0.4	0.03	81	11	0.03	4	16	0.06	231	20
		0.5	111	NA	0.9	0.04	0.5	0.03	118	16	0.02	5	14	0.06	278	29
		2.6	100	NA	1.0	0.03	0.5	0.02	691	88	0.04	27	36	0.03	1459	177
		2.4	102	1.72	0.9	0.06	0.5	0.06	612	78	0.02	24	32	0.02	1359	153
		5.7	84	4.64	1.0	0.03	0.5	0.02	1939	245	0.03	73	84	0.04	3179	444
		11.4	62	3.98	1.2	0.13	0.6	0.15	3939	436	0.10	130	145	0.02	6307	751
	Bharathapuzha	4.1	103	0.72	1.0	0.09	0.5	0.09	995	125	0.03	39	43	0.07	2282	258
		0.9	101	NA	0.9	0.17	0.5	0.11	203	27	0.03	9	13	0.04	496	40
		4.2	93	3.42	1.1	0.01	0.6	0.05	1301	164	0.03	50	55	0.03	2307	293
		6.2	79	4.81	1.2	0.07	0.6	0.02	1990	251	0.02	75	83	0.01	3455	478
		NA	43	8.56	NA	NA	NA	NA	5415	660	0.03	195	214	0.02	NA	NA
		31.2	25	7.11	1.4	0.03	0.7	0.02	9688	1201	0.04	364	391	0.02	17333	2157

Table 1 *Concentrations of DSi, ASi (in µM), major elements (in ppm) and δ^{30}Si-DSi composition (in ‰ along with 1 σ_{SD}) of surface estuarine samples during dry period. NA indicates the data not available.*

	Estuary	Salinity	ASi (µM)	DSi (µM)	δ^{30}Si-DSi ‰	SD	δ^{29}Si-DSi ‰	SD	Na	Mg	Al	K	Ca	Fe	Cl	SO_4
									ppm							
Northeast	Haldia	2.0	8.1	101	1.6	0.04	0.87	0.03	630	85	0.07	26	34	0.050	901	121
		2.1	NA	118	1.7	0.03	0.89	0.02	674	67	0.03	30	35	0.01	948	130
		4.2	3.8	120	1.5	0.00	0.81	0.09	1471	150	0.02	59	63	0.02	1725	260
		6.1	17.6	112	1.8	0.04	0.88	0.03	2104	271	0.02	76	72	0.012	2945	335
	Subernereka	0.1	28.9	202	1.7	0.03	0.94	0.03	9	5	1.18	2	12	0.906	5	9
		3.9	2.4	161	1.6	0.03	0.81	0.02	1333	173	0.01	49	52	0.008	1652	243
		7.6	7.7	137	1.7	0.12	0.89	0.08	2566	362	0.03	101	94	0.023	4495	550
		13.1	11.3	100	1.7	0.04	0.91	0.02	4520	647	0.02	177	149	0.005	7949	957
	Mahanadi	0.1	NA	164	1.5	0.03	0.88	0.02	7	4	0.09	2	11	0.057	4	5
		0.1	NA	134	1.6	0.03	0.87	0.02	9	4	0.03	3	13	0.03	7	9
		7.6	NA	105	1.5	0.04	0.84	0.03	2688	285	0.02	104	99	0.01	3614	518
	Rushikulya	0.1	62.8	242	1.9	0.04	1.03	0.03	51	11	0.04	5	20	0.032	52	11
		7.2	0.8	203	2.0	0.04	1.04	0.03	2554	265	0.07	101	99	0.04	3582	525
		12.9	1.1	170	NA	NA	NA	NA	4520	520	0.02	182	180	0.02	NA	NA
		22.0	11.8	64	1.7	0.15	0.91	0.06	9219	960	0.04	341	311	0.03	13434	1626
	Godavari	0.1	46.5	167	1.4	0.09	0.71	0.02	9	4	0.04	2	13	0.03	5	6
		0.3	20.8	137	1.3	0.03	0.74	0.02	76	10	0.03	5	16	0.01	111	18
		0.7	9.1	146	1.1	0.04	0.58	0.02	178	21	0.03	9	19	0.02	253	37
		1.5	13.0	140	1.2	0.05	0.61	0.03	441	60	0.02	18	26	0.008	617	82
Southwest	KBW	0.0	NA	105	0.6	0.04	0.26	0.02	3	1	0.03	1	2	0.033	3	1
		0.7	NA	113	NA	NA	NA	NA	191	20	0.02	10	12	0.02	NA	NA
		2.6	NA	109	1.0	0.03	0.52	0.02	854	109	0.01	33	30	0.007	1247	160
		14.9	10.1	77	0.9	0.15	0.51	0.10	4441	729	0.02	204	174	0.010	8617	1010
	Khali	0.0	1.4	114	0.8	0.04	0.42	0.03	8	2	0.02	1	3	0.018	8	2
		4.0	0.2	117					1350	137	0.04	51	43	0.03	NA	NA
		9.0	0.1	100	0.9	0.03	0.51	0.02	3112	418	0.01	115	101	0.010	4243	609
		6.5	0.4	117	0.8	0.04	0.46	0.03	2336	300	0.02	83	72	0.013	3593	448
	Netravathi	0.1	0.7	142	0.8	0.04	0.38	0.03	7	3	0.04	1	7	0.053	7	4
		0.1	NA	141	0.6	0.05	0.35	0.04	16	2	0.03	1	3	0.03	22	4
		0.1	NA	108	0.5	0.04	0.32	0.03	23	3	0.05	2	3	0.04	31	5
	Mandovi	0.1	NA	129	NA	NA	NA	NA	14	3	0.03	1	3	0.029	19	3
		0.2	1.6	124	0.4	0.034	0.201	0.028	38	5	0.03	2	4	0.02	57	6
		2.0	NA	116	0.4	0.03	0.31	0.02	640	84	0.02	25	21	0.007	806	126
		10.3	0.1	92	0.4	0.04	0.20	0.02	3451	390	0.03	141	126	0.01	5632	686
	Zuari	0.2	NA	114	0.5	0.16	0.28	0.02	46	6	0.12	3	3	0.133	67	9
		2.3	NA	90	0.4	0.05	0.25	0.03	652	65	0.04	28	25	0.03	999	125
		2.9	NA	106	0.6	0.17	0.38	0.02	948	98	0.02	39	37	0.01	1442	180
		3.8	NA	106	0.7	0.00	0.37	0.04	1330	168	0.02	49	41	0.014	1696	252
		11.8	0.4	91	0.9	0.09	0.40	0.01	4042	559	0.02	156	140	0.004	6476	781
Northwest	Narmada	0.4	2.5	305	1.8	0.09	0.85	0.01	44	21	0.11	3	22	0.089	24	6
		5.4	27.0	249	2.1	0.03	1.10	0.02	1807	174	0.10	78	82	0.08	2665	339
		19.3	8.6	110	1.9	0.04	1.06	0.03	7209	963	0.02	269	270	0.021	11293	1350
		27.1	52.7	89	1.5	0.03	0.76	0.00	9899	1455	0.04	411	372	0.009	16937	2106
	Tapti	0.3	9.8	443	2.1	0.04	1.01	0.02	38	21	0.01	3	26	0.009	33	20
		9.3	NA	195	1.8	0.03	0.97	0.03	3106	331	0.04	129	126	0.03	4322	666
		18.6	80.1	143	1.7	0.04	0.84	0.03	6636	916	0.02	259	254	0.021	10762	1284
		23.1	42.8	97	1.6	0.05	0.78	0.03	8352	1181	0.02	335	333	0.017	14435	1766
	Mahisagar	0.9	1.6	389	1.7	0.05	0.95	0.03	40	16	0.02	3	19	0.02	25	17
		3.7	1.9	305	NA	NA	1.37	0.03	1227	122	0.03	60	42	0.02	1589	242
		15.8	34.0	162	2.0	0.10	1.05	0.12	5574	613	0.03	231	200	0.03	9809	1194

Table 2 *Concentrations of DSi, ASi (in µM), major elements (in ppm) and δ^{30}Si-DSi composition (in ‰ along with 1 σ_{SD}) of surface estuarine samples during wet period.*

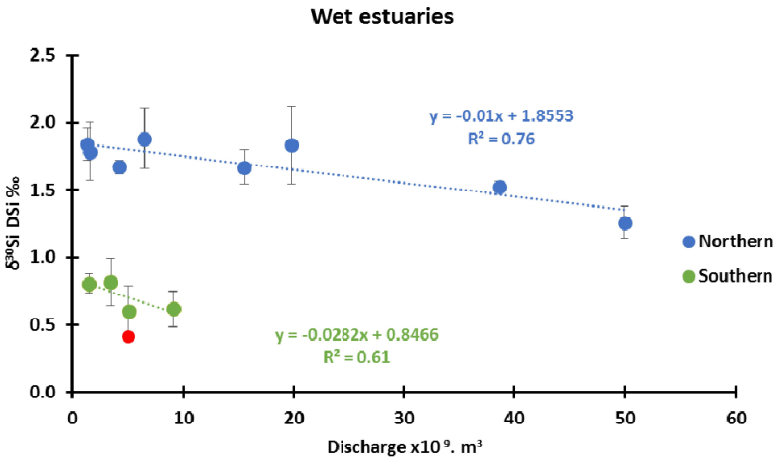

Fig. 2. *δ^{30}Si-DSi vs. discharge during the wet period of Indian estuaries. The red point "Mandovi" estuary is excluded from the linear relationship. Data points are the average for each estuary of δ^{30}Si-DSi of several samples along the salinity gradient and error bars indicate* $\pm 1\sigma_D$

4. Discussion

The processes that control the Si isotopes will be discussed for upper and within estuaries separately for both seasons under each section.

4.1 Wet season

4.1.1 Geochemical processes in all estuaries: An overview

There is a wide variability of DSi and heavier isotopic signature in northern estuaries due to salinity gradient when compared to the southwestern estuaries (Fig. 3). In addition, as discussed in Chapter 3, heavy discharge and terrestrial supply of suspended materials limit the light availability for the diatoms to grow in the system and hence the diatom uptake may not be the plausible mechanism occurring during wet period.

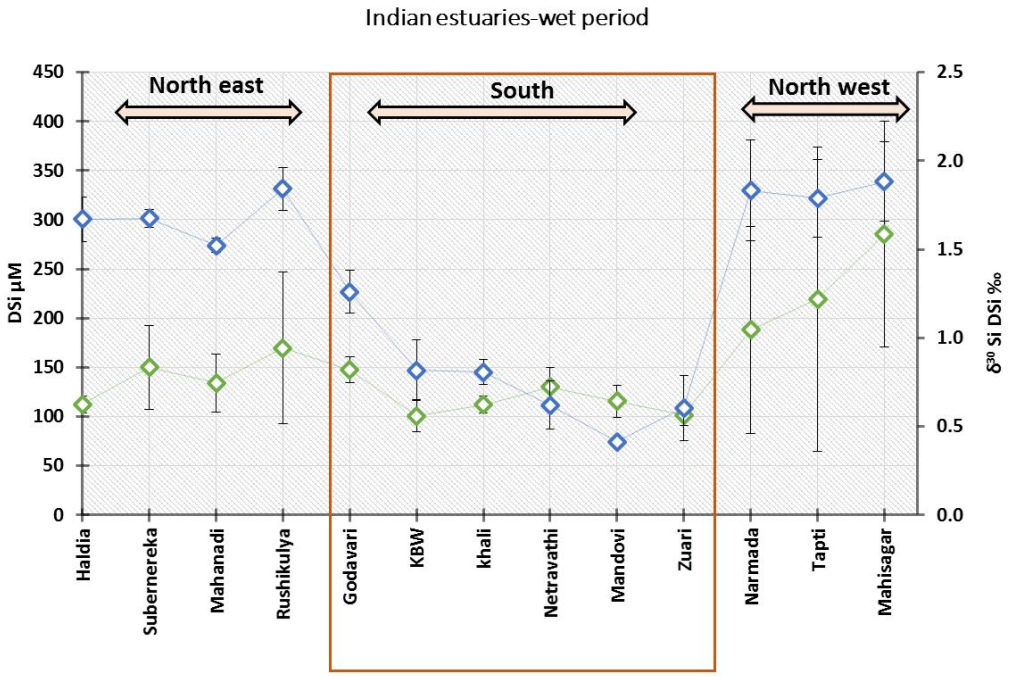

Fig. 3 *DSi (µM) and δ^{30}Si-DSi (1SD) in the Indian estuaries of wet period. All data for each estuary have been averaged and ± 1σ_D shown by the error bars. Blue open diamond: δ^{30}Si-DSi and green open diamond: DSi concentration. High error bars are due to larger salinity gradient sampled of those estuaries.*

The δ^{30}Si-DSi of all Indian estuaries are always enriched relative to the continental crust. The δ^{30}Si-DSi range from -0.1 ‰ up to 3.4 ‰ reported in most of the continental aquatic systems (e.g., De La Rocha et al., 2000; Ding et al., 2004; Alleman et al., 2005; Ziegler et al., 2005; Georg et al., 2006; Cardinal et al., 2010; Hughes et al., 2012, 2013). The positive signatures of Si isotopes in continental waters are mainly due to the two processes. 1) Weathering and successive clay mineral formation and 2) Biological uptake. Therefore the effects of these processes on Si isotopes are discussed in detail.

A significant ($p < 0.01$, $n=13$) positive correlation is observed between the DSi and δ^{30}Si-DSi in the Indian estuaries during wet period (Fig. 4). This is typical from weathering signature which preferentially incorporates light Si isotopes in clay minerals while relatively heavier isotopes are released in the solution (De La Rocha et al., 2000). The estuaries in the northern regions are heavier than the southwestern estuaries likely due to the processes associated with weathering and lithology. For example, the estuaries on the north are relatively longer in size with wider plains when compared to the

southwestern estuaries with steep slopes on their watershed (cf. Table 1 of Chapter 3). This topography also alters the degree of weathering (Gurumurthy et al., 2012). Note that there is no data on Southeastern estuaries for wet sesason because these estuaries never reach high discharge regime since rainfall is low all year long and water demand for agriculture and domestic uses extremely high.

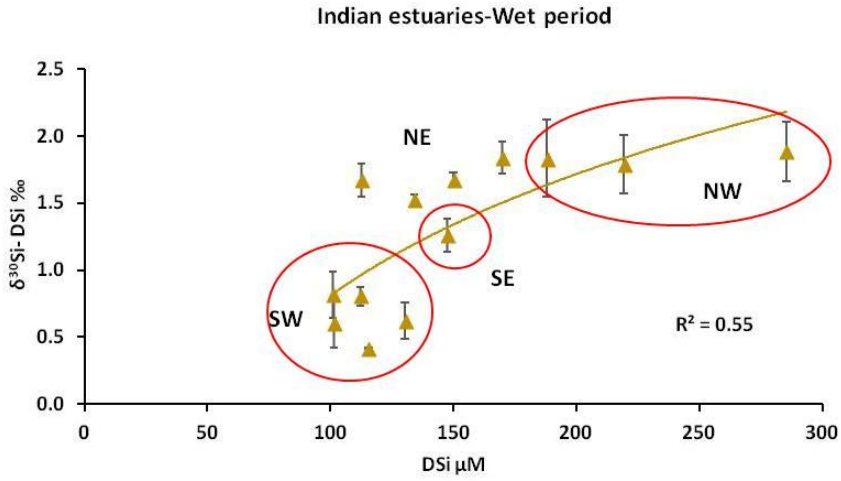

Fig. 4 *δ^{30}Si-DSi vs. DSi concentration (µM) of Indian estuaries during wet period. The main regions of the estuaries are grouped and encircled. NW, NE, and SW represent northwest, northeast and southwest estuaries respectively. Data points are the average for each estuary of δ^{30}Si-DSi of several samples along the salinity gradient and error bars indicate ± 1σ_D*

It is interesting to note the influence of discharge over δ^{30}Si-DSi during wet period of Indian estuaries with strong negative relationship (Fig. 2). As explained by Dunne (1978), discharge or runoff plays dominant control on weathering and dissolution rates. It also generally dilutes the concentration of dissolved elements, a simple process that cannot impact the isotopic compositions. So, the leaching of superficial soils is greater with increased discharge and it mobilizes soil surface water with shorter residence time. In contrast, low discharge is associated to leaching of deeper soil water with higher residence time. As a result, not only the residence time of water differs but also the type of minerals (i.e. those in contact with saprolite during low discharge). Such type of observation was noticed in the tropical river Tana by Hughes et al. (2012) where the residence time of water and rainfall control weathering and in fine the Si isotopic composition of the river. Indeed the Indian estuaries are monsoonal estuaries: the higher runoff of fresh water increases the intensity weathering processes as seen in river Netravathi (Gurumurthy et al., 2012).

Though the control of weathering is evidenced in the Indian estuaries, there is no clear information regarding the degree of weathering that influences the Si isotopic composition. In order to understand such processes, we consider only the upper estuaries, since they represent the riverine end-member. The upper estuaries are considered as the samples whose salinity ≤ 5.

4.1.2 Upper estuaries

The strong positive relationship between DSi and δ^{30}Si-DSi (r= 0.71, p<0.01, n=13) confirms the dominance of weathering on δ^{30}Si-DSi signatures in the upper estuaries (Fig. 5). Since, we could not use the DSi/Na* as weathering index due to over estimation of atmospheric correction of major cations, we used clay mineralogy composition and saturation indices under this section.

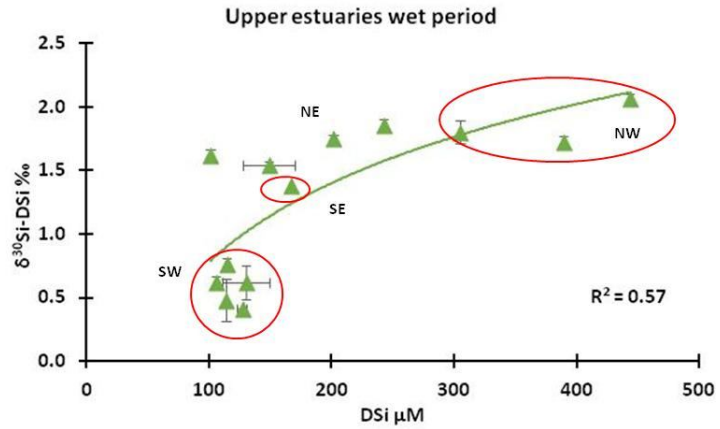

Fig. 5 *δ^{30}Si-DSi vs. DSi concentration (µM) of upper estuaries during wet period. When several samples from the same upper estuary have been analyzed, the data points are the average and error bars indicate ± 1σ_D.*

Interestingly, the linear significant relationships between δ^{30}Si-DSi and relative percentage of clay minerals in the particle samples indicate the good consistency between these parameters (Fig. 6). The Si isotopic composition of river DSi is enriched with increasing contribution of smectite in particles, especially in the northern estuaries when compared to the south. In contrast there are negative relationships of δ^{30}Si-DSi with % of kaolinite & chlorite (Fig. 6b and c). Indeed, we observe an increasing relative percentage of kaolinite with lighter Si isotopic signature in the southwestern upper wet estuaries (Fig. 6b and c). It is well known that the intensity of weathering is highly climate dependent (cf.

Chapter 1) and in humid tropical climate heavy rainfall favors intense weathering with Kaolinite-gibbsite formation (cf. Chapter 5). Due to the heavy rainfall, the leaching of superficial soils (e.g. oxisols) decreasing the fraction of Si incorporating into the clay minerals and leaving lighter isotopic composition. On contrary, during the base flow (mainly groundwater), the increased residence time of soil water and the interaction of base flow waters with bed rock favours secondary mineral formation by incorporating lighter isotopes in the clay minerals. This mechanism occurs in the semi-arid climatic zones with less rainfall. This is consistent with the climatic patterns occurring on the Indian estuaries watersheds. The southwest estuaries are located in humid areas where heavy precipitation (2000-4000 mm/yr, cf. Fig. 6b of Chapter 1) is associated with high runoff, favoring the intense weathering of clay minerals leaching the superficial soil. This may dissolve clay minerals such as kaolinite which could explain the lighter isotopic composition (Fig. 6). Indeed, the negative relationship of Si isotopes with % kaolinite in suspended material cannot be explained by increasing Kaolinite formation since this would on the contrary leave heavier isotopic composition in southwest estuaries.

However, we could not measure the isotopic composition of clay minerals since there exist so far no method to separate clays mineral from river particles. It has been reported that increasing kaolinite is associated to lighter Si isotopic composition in clay soils minerals (e.g. Ziegler et al., 2005; Opfergelt et al., 2010). It remains unclear if this comes from a larger (more negative) fractionation factor for kaolinite and/or lower DSi fraction released in soil solution (Hughes et al., 2013). If the fractionation factor was more important for kaolinite, this should release heavier DSi in solution for increasing kaolinite contribution to clay minerals. Our results are opposite with this since we have lighter δ^{30}Si-DSi for higher kaolinite contribution and do not support a different fractionation factor for kaolinite than other clays. However one should remind that our isotopic and clays mineral data are from upper estuaries, i.e. far from the clay formation sites so this could also be due to a sampling bias since δ^{30}Si-DSi do not necessarily have the same origin as the suspended clay we sampled. For instance, clay minerals can partly originates from local erosion and/or sediment resuspension while δ^{30}Si-DSi can result from a mixing of weathering over the whole river watershed in addition to local processes (e.g. uptake-dissolution, adsorption – erosion, groundwater discharge…). Moreover, dissolution of isotopically light minerals (either primary or secondary, which are even lighter) could also explain the variability of δ^{30}Si-DSi. Therefore in the following, we now discuss the most likely precipitation – dissolution processes of minerals.

	Rivères	Pourcentage relative				
		Smectite	Illite	Kaolinite	chlorite	Gibbsite
NE	1 Haldia	33.4	49.2	10.2	7.2	-
	2 Surbarnereka_1	28.7	47.0	17.6	6.6	-
	3 Mahanadhi	66.7	19.3	12.9	1.1	-
	4 Rushikulya_1	62.3	21.8	15.9	0.0	-
SE	5 Godavari_1	72.2	9.8	14.5	3.5	+
	6 Krishna	44.9	43.2	5.4	6.5	+
	7 Vellar	86.4	7.7	5.9	0.0	-
	8 Cauvery	58.9	26.9	9.1	5.2	+
SW	9 Kochi_1	0.0	21.9	60.4	17.6	+
	10 Nethravathi	0.0	15.3	84.7	0.0	++
	11 Khali_1	4.4	36.3	53.1	6.2	++
	12 Zuari_1	52.0	16.4	24.2	7.5	+
	13 Mandovi_1	31.3	30.1	30.1	8.5	+
NW	14 Tapti_1	88.1	5.8	3.6	2.5	+++
	15 Narmada_1	90.4	5.4	3.1	1.0	-

***Table 3**. Relative abundance of clay minerals in the particle samples of upper Indian estuaries during wet period (data from S. Guo, 2016). During wet period, the discharge of southeast estuaries (Krishna, Vellar and Cauvery) is very meagre due to the all year less rainfall during southwest monsoon and high water usage in the upstream. We then considered Krishna, Vellar and Cauvery as dry period (see chapter 3 for more details).*

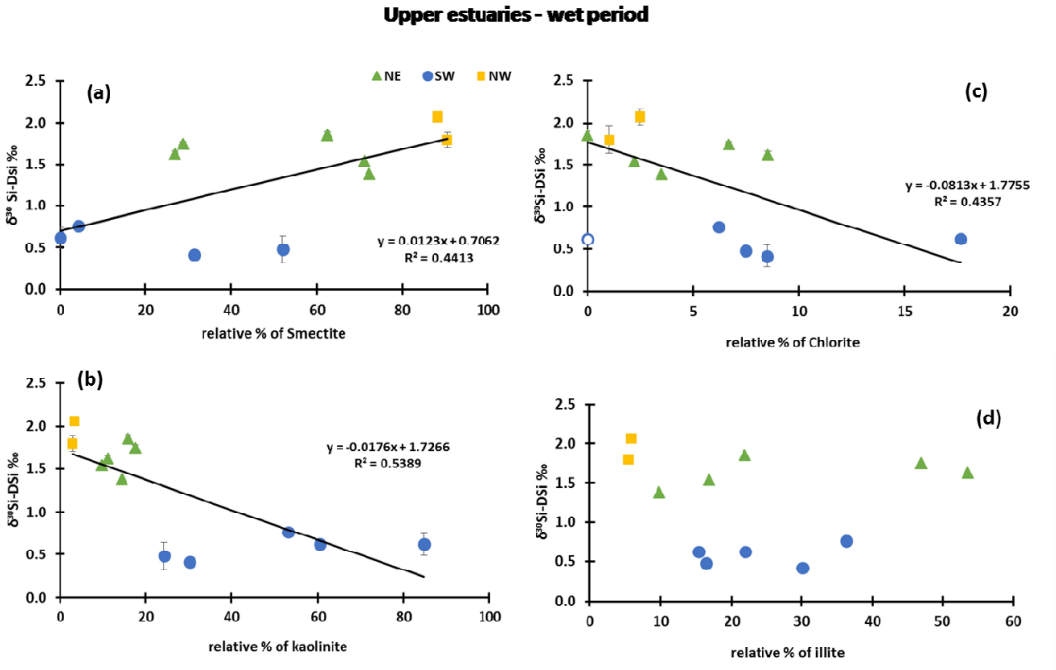

***Fig. 6**. The δ^{30}Si-DSi (±1 σ_D when several samples are available for salinity < 5) vs. the relative abundance of clay minerals in %) in the particle samples of Indian upper estuaries during wet period (a: smectite; b: kaolinite; c: chlorite; d: Illite). In (c), the open circle from Netravathi has been removed from the linear equation. Linear correlations are all significant with p-value < 0.05.*

Saturation index

The variability of saturation indexes (SI) of minerals are predicted in the Figures 7a, b, and 7c for primary, secondary minerals and oxy-hydroxides respectively. Undersaturation of albite and K-feldspar in all the estuaries and oversaturation (slightly greater than zero) of Ca-montmorillonite (except Haldia), illite and kaolinite were noticed (Fig. 7a and b). This is consistent with the clay mineral formation process and associated with heavy isotopic signature in the northern estuaries (Fig. 7). We also note that there is relatively lighter isotopic composition in the southwest estuaries.

The estuaries of Southwest regions (Fig. 7a, b) have greater undersaturation of both primary minerals (e.g., albite) and clay minerals (e.g., illite). Since, the southwest estuaries are fed by heavy monsoon rainfall and favour leaching of superficial soil minerals and results intense weathering. Since the water fed in to the basin is young (rain water) and readily dissolves the weathered clay minerals from the surface soil. Therefore possible dissolution of kaolinite (due to their higher relative % abundance) clay minerals release lighter isotopic composition in the solution at the same time erosion will increase the clay minerals in the suspended material. This is consistent with the earlier studies on weathering mechanisms of southwest regions (Western Ghats) that suggest that weathering occurs in the superficial soil (e.g., ultisols and oxisols) zone by leaving the parent rock unaltered in the southwest regions (Deepthy and Balakrishnan, 2005). In addition, the oversaturation of Fe-Al oxy-hydroxides in all estuaries with variable SI (Fig. 7c) was noticed in Indian upper estuaries. This indicates the occurrence of hydroxides in the surface water. Since these minerals can adsorb silicic acid with a preferential adsorption of light Si isotopes (Delstanche et al., 2009; Oelze et al., 2014) their oversaturation could also favor heavy δ^{30}Si-DSi.

The relationship between δ^{30}Si-DSi with saturation indices of primary and secondary minerals are depicted in Fig. 8. The positive relationship between saturation index and δ^{30}Si-DSi of primary minerals indicates the possible dissolution and concurrent clay mineral formation associated with heavier isotopic signature in the northern estuaries. However, there is no clear evidence for the dissolution of heavily

weathered superficial clay minerals (e.g., kaolinite). The significant positive relationship ($p < 0.01$) with chlorite suggests the possible congruent dissolution of chlorite type minerals. It is interesting to note that the south west estuaries do not provide any clear information regarding the dissolution of secondary minerals. However, one need to consider that the clay mineral formation site is far from the upper estuarine sampling locations and does not necessarily provide information regarding dissolution and clay formation process. Hence, the saturation index of southwest estuaries indicates the possible dissolution of secondary minerals (e.g. chlorite) and explains the lighter δ^{30}Si-DSi. Therefore, the nature of source water and its interaction with the type of minerals determine the δ^{30}Si-DSi composition within the wet period. Indeed, intense weathering and kaolinite formation decreasing the fraction of silicon incorporated into the clay minerals leaving lighter isotopic signature has been noticed in the riverine regime of Netravathi basin (cf. Chapter 5).

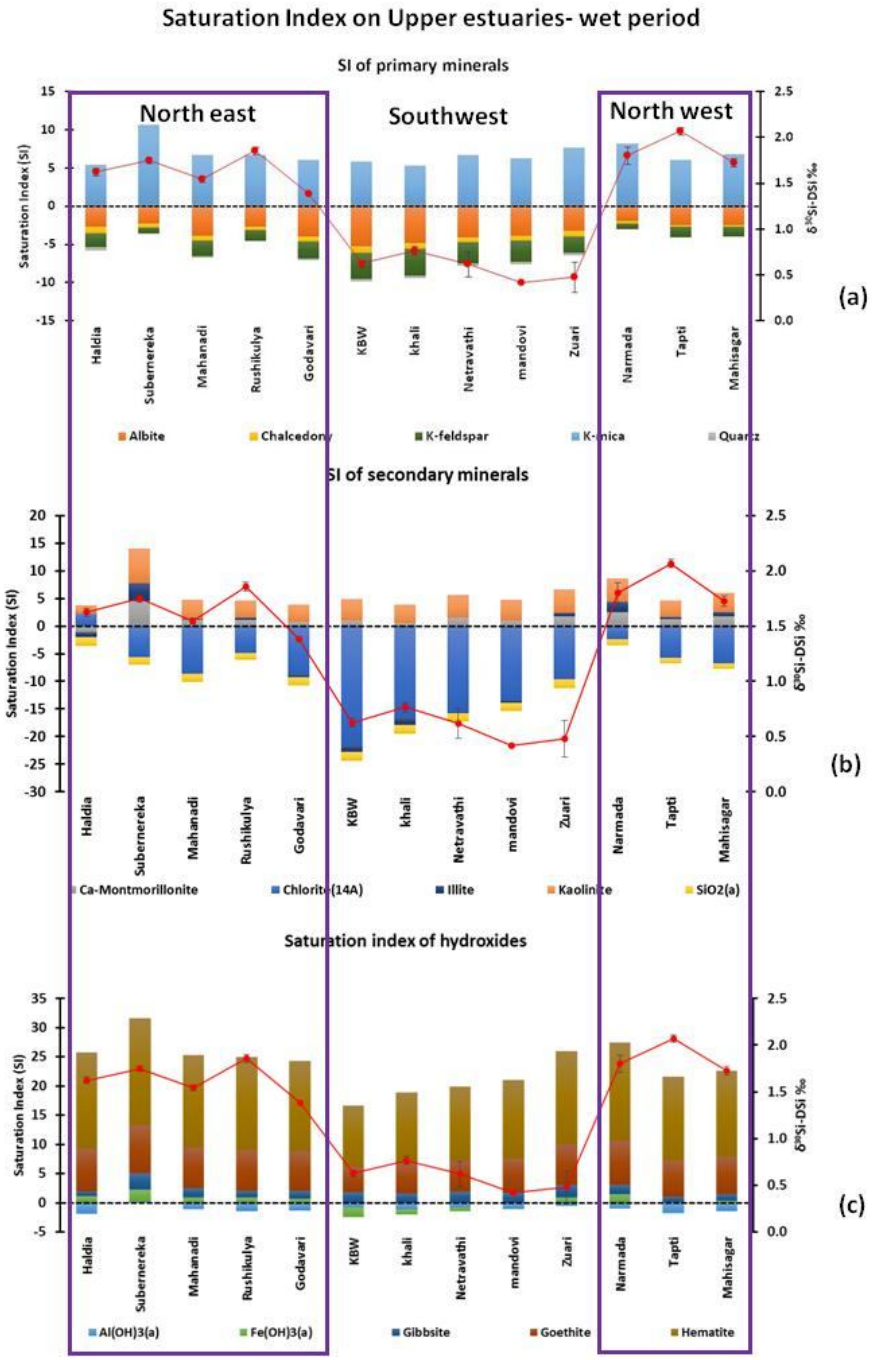

Fig. 7*. The saturation index of primary minerals (a), clays and amorphous silica (b) oxi-hydroxides of aluminium and iron minerals (c). δ^{30}Si-DSi (1SD) along the upper estuaries of wet period (red filled circles and line).*

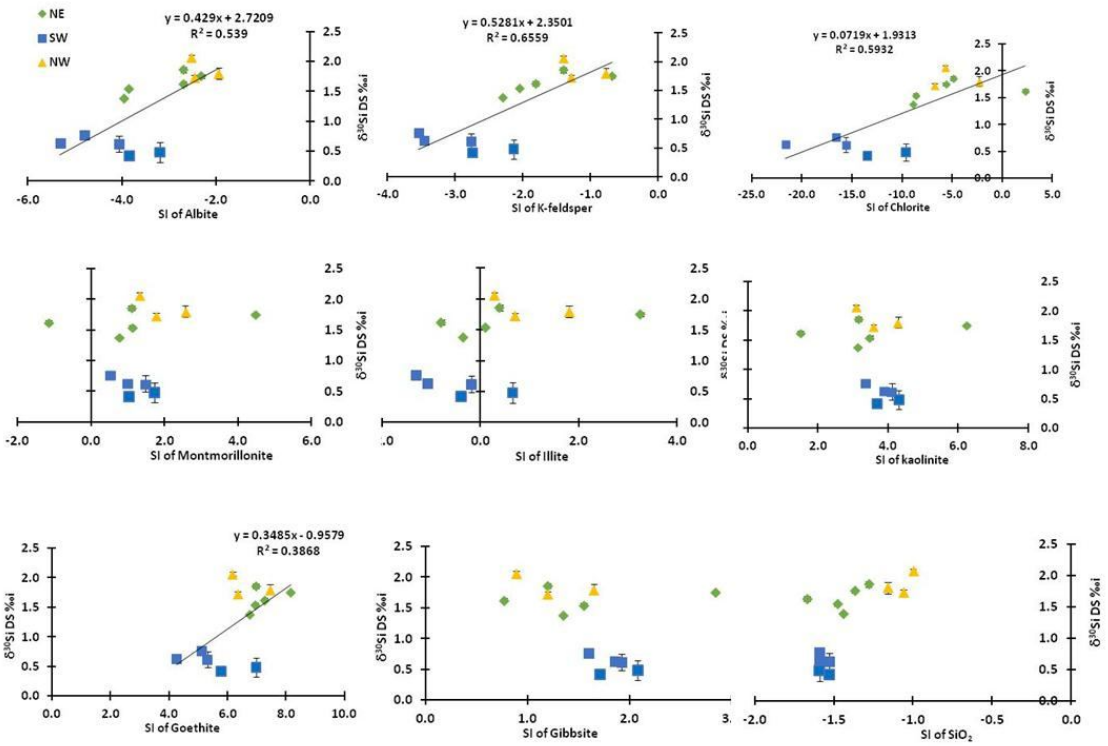

Fig. 8 *The relationship of δ^{30}Si-DSi vs primary and secondary minerals saturation indices of upper estuaries during wet period. The positive relationship between the δ^{30}Si-DSi and saturation index indicates, the possible dissolution of primary or secondary minerals.*

Apart from the clay mineral formation and dissolution processes, DSi can also be withdrawn from the solution by adsorption onto aluminium and iron oxy-hydroxides with a preferential adsorption of light Si isotopes (Delstanche et al., 2009; Oelze et al., 2014). Oxy-hydroxides are ubiquitous in the soil or weathered rocks and sediments (Schwertmann and Taylor, 1989), especially in warm and wet environment and they partly control the concentration of DSi in the solution by adsorbing on their surface OH groups (McKeague and Cline, 1963; Gehlen and Van Raaphorst, 2002; Opfergelt et al. 2009). The over saturation of iron and aluminum oxy-hydroxides in all the upper estuaries indicate the possibility for the presence of oxy-hydroxides that could partly control δ^{30}Si-DSi (Fig. 8). It does not seem to be the case since e.g. Zuari (SW) and Narmada (NW) are amongst the most oversaturated with respect to goethite while they bear highly contrasted δ^{30}Si-DSi (0.5 vs. 1.8 ‰ respectively). Moreover, there is no clear relationship between δ^{30}Si-DSi and dissolved Fe concentration that could indicate that dissolution of oxy-hydroxide (i.e. high dissolved Fe) is associated to lighter δ^{30}Si-DSi (not shown).

Nevertheless, Indian estuaries are discharge-controlled during the wet period and the residence time of water will be less with more flushing rate (Vijith et al., 2009; Sarma et al., 2010, 2014). Overall, it seems unlikely that adsorption – desorption of Si onto oxy-hydroxides as a significant control onto δ^{30}Si-DSi in upper wet Indian estuaries. The role of weathering with dissolution – precipitation on Si-bearing primary and secondary minerals seems dominant in the upper estuaries.

4.1.3 Land use

Besides the effect of weathering on Si cycle, land use can impact the Si isotopic composition. In the terrestrial environment, the plants and crops can affect the DSi supply via uptake, BSi precipitation in the tissue and finally BSi dissolution (Alexandre et al., 1997). During the plant growth, the vegetation uptake the DSi from water and converts it in to phytoliths. In the litter, the phytoliths return to the soils (Farmer et al., 2005). This BSi supply also contributes to the DSi release in the soil waters and finally to rivers and estuaries (Derry et al., 2005; Struyf et al., 2010). Since plants preferentially uptake the light Si isotopes, as weathering, they also contribute to enrich the δ^{30}Si-DSi signature in the soil solutions (Ziegler et al., 2005; Opergelt et al., 2006). Therefore δ^{30}Si of phytoliths is also related to the degree of soil weathering (Opfergelt et al., 2008). However, no change in the DSi concentration of soil water can be expected when the soil – plant is at steady state. The Si accumulated by the plants may vary from 0.1 % to 10% of their dry weight and this is greatly species dependent (Hodson et al., 2005; Gerard et al., 2008). The studies carried out by Ding et al. (2004, 2008) indicated that crops could alter the Si cycle via phytoliths formation, leaving isotopically heavier and decreased DSi supply to the rivers. Hence, in addition to the weathering variability, the land use may also partly explain the Si isotopic variability. The percentages of different land uses such as agriculture, forest, built-up areas and water bodies of each river basin were presented in Table 1 of Chapter 3. It is noteworthy that there is a higher percentage of agriculture in the northern watershed (and the Godavari) than on the southwestern watersheds and vice-versa for forest cover (Table 1 of Chapter 3). Interestingly, there is a high positive relationship (R^2=0.73, n=13, p<0.001) between the extent of agriculture and the δ^{30}Si-DSi (Fig. 9). This would be consistent with the heavier isotopic composition resulting from the agricultural crop uptake (e.g., rice, sugarcane etc.). In addition, the percentage of forest cover also provides negative relationship with δ^{30}Si-DSi (Fig. 9b) (R^2=0.48, n=13, p<0.001). Increasing forest cover enhances clay dissolution because of high organic matter and lower pH in the forest soils. It results in the lighter isotopic composition in the solution (Cardinal et al., 2010; Cornelis et al., 2010; Engstrom et al., 2010; Delvaux et al., 2013). This is

also consistent with the lighter isotopic composition of the southwest estuaries. Note that for some adjacent watersheds, the NRSC-WRIS website gives same land uses which are regional averages (Table 1 of Chapter 3). Being an agricultural country, with major rice cultivation in the east and Si is the essential nutrient for rice cultivation, it is very likely that crop - in addition to weathering mechanisms, alter the Si cycle over India as the Si isotopic signatures in the Indian estuaries suggest. It is interesting to remind the results from Chapter 3 where the variability of ASi and DSi concentrations were mainly controlled by the land use especially by agriculture in the north east and northwest estuaries rather by forest cover in the southwest estuaries. This was consistent with the earlier studies on Indian estuaries by Sarma et al, (2014), suggesting less $\delta^{15}N_{PN}$ in the northern estuaries due to the artificial N supply via fertilizers consumption for agriculture than the southern estuaries.

Therefore, agriculture and clay mineral formation strengthen more DSi supply with enriched Si isotopic signature in the estuaries especially in the northern estuaries. On contrary, weathering of secondary minerals and relatively less agricultural land use with more forest cover control the reduced supply of Si and lighter isotopic signature of characteristic southwest estuaries.

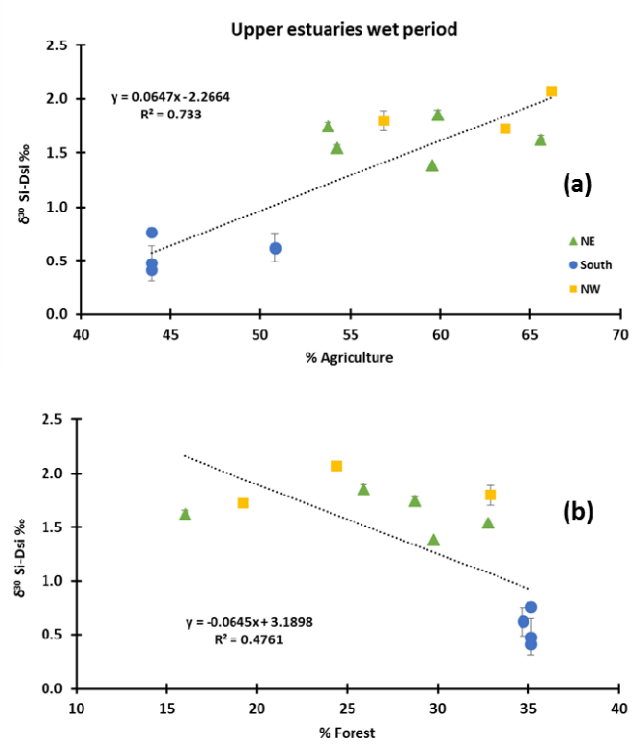

Fig. 9 a and b *δ^{30}Si-DSi (1SD) and % of agricultural land use (a) and % of forest cover (b) on the each estuarine basin, indicating the impact of agriculture on Si isotopes.*

4.2 Variability within estuaries (wet)

The monsoonal rainfall and associated high discharge result in dwelling of more fresh water in the estuaries (Vijith et al., 2009; Sridevi, 2015). Consequently, it was impossible to sample along the complete salinity gradient (high salinity often found beyond the coastline and being inaccessible for sampling due to rough sea). Only three estuaries have been sampled with salinity more than 15 during the wet season (Table 2). Generally, DSi concentration does not behave conservatively (Fig. 10a, Annex C of Chapter 4 for individual estuaries) instead, a clear north – south difference was noticed with DSi and observed to be sink/source along salinity gradient respectively. In addition, there is no clear positive linear relationship between δ^{30}Si-DSi and 1/DSi that should result solely from mixing (Fig. 10b). However, to see mixing on δ^{30}Si-DSi would require samples with higher salinity end-member. Indeed since seawater has very low DSi content (Avg. 5 µM in coastal India; Naqvi et al., 2010) it requires a large dominance of seawater fraction to modify the isotopic composition of the mixture (seawater end-member should have heavy δ^{30}Si-DSi with high 1/DSi). This was already seen in Tana estuary with unchanged δ^{30}Si-DSi from salinity 0 to 29 (Hughes et al., 2012). Therefore, in several estuaries where δ^{30}Si-DSi are near constant are indeed consistent with mixing indicating devoid of any other processes such as dissolution or adsorption (Rushikula, Mahanadi, Subarnareka, Khali, Mandovi, Figure 10b). For those estuaries, the δ^{30}Si-DSi is thus mainly controlled by the signature of weathering coming from upstream. Interestingly, the estuaries Narmada and Tapti (northwest) seem to be the sink for DSi (Fig. 10a) and showing inverse relationship between δ^{30}Si-DSi vs 1/DSi (Fig. 10b). In addition to mixing of seawater, possible adsorption mechanism may be responsible for this inverse relation but it was not reflected with decreasing DSi concentration associated by increasing isotopic composition. However, one should also note that the estuary Tapti is greatly influenced by the human settlements (slum areas with heavily polluted) and the dredging activities has been noticed during our sampling (cf. pictures in Annex). Therefore, the conservativity or non-conservativity of Indian estuaries remains unclear due to the lack of sea water end-member and also the discrepancies of sampling during wet period.

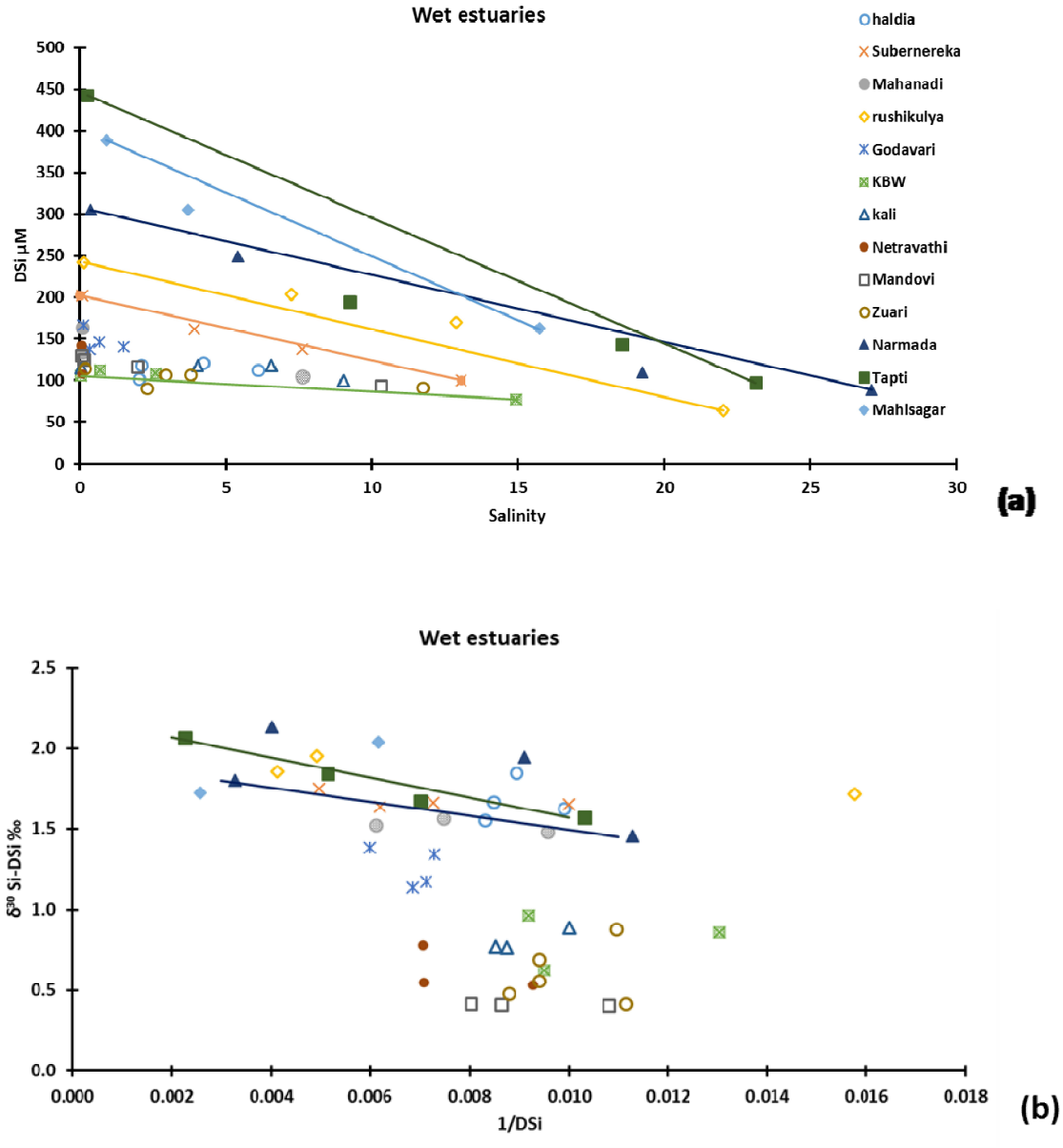

Fig. 10. *The conservative and non-conservative behavior of DSi (a) and* δ^{30}Si-DSi *(b) in the Indian estuaries during wet period. The upper estuary is considered as fresh water end member and lower estuary as sea water end-member. The lines represent the mixing line of the estuaries Narmada and Tapti indicating the adsorption like processes within the estuaries during wet period.*

4.3 Groundwater

The Si isotopic composition of shallow groundwaters varies between -0.25 and 1.47 ‰ and is consistent with the Ganges shallow groundwater isotopic composition (from 1 to 1.3‰) but also with deep groundwater (-0.15 to 1.2‰, Georg et al., 2009). The groundwater DSi concentration ranged from 69 to 839 µM and is several folds higher than the estuarine concentrations (Table 4). All the groundwater δ^{30}Si-DSi is lighter (except 2) and all have higher DSi concentration than the surface upper estuarine samples (Figs. 11 and 12). Higher DSi concentrations and lighter δ^{30}Si-DSi of groundwater have already been observed and are generally attributed to the dissolution of primary or secondary minerals which supplies DSi with lighter Si isotopes in the solution (Georg et al., 2009; Pogge von Strandmann et al., 2014). Yet, the occurrence of overall (all sampled groundwater) positive relationship between δ^{30}Si-DSi of groundwater and DSi concentration emphasis also the role of weathering (Fig. 11). Such positive relationship between isotopes and DSi concentration of groundwater has not been reported earlier (Pogge von Strandmann et al., 2014).

4.3.1 Groundwater and upper estuaries

Dissolution is the major process responsible for lighter isotopic signature with more DSi concentration in groundwater. In order to check this we compare our groundwater dataset with upper estuarine isotopic signature. We calculated the difference of δ^{30}Si-DSi of groundwater and upper estuarine surface water ($\Delta^{30}Si = \delta^{30}Si\text{-}DSi_{GW} - \delta^{30}Si\text{-}DSi$) and compare it with the fraction of DSi enrichment (DSi_{Gw} /DSi). If dissolution is the sole process that supplies DSi to the groundwater, then one should expect negative linear relationship between Δ^{30}Si and fraction of DSi enrichment. Surprisingly, a strong positive relationship is found for southern groundwater samples (R^2=0.83, n=9, p <0.001 Fig. 12) whereas the northern groundwater samples do not reflect any relationship with isotopic composition. This suggests that high DSi enrichments are associated with smaller isotopic difference between surface and groundwater (i.e. Δ^{30}Si near 0, and even positive for 2 samples indicating heavier δ^{30}Si in ground waters than the surface water). This could indicate that dissolution of minerals is not the only process controlling δ^{30}Si in the groundwater.

	Groundwater	δ^{30}Si-DSi ‰	SD	δ^{29}Si-DSi ‰	SD	DSi µM	Na	Mg	Al	K	Ca	Fe	Cl	SO_4
							ppm							
NE	Haldia	-0.3	0.03	-0.1	0.02	576	153	26	0.01	3.3	54	0.01	43	16
NE	Subernereka	0.8	0.04	0.5	0.03	729	14	9	0.01	0.5	13	0.03	12	11
NE	Mahanadi	1.3	0.03	0.7	0.02	753	85	24	0.02	19.3	47	0.01	96	50
NE	Rushikulya	0.9	0.05	0.4	0.03	839	136	41	0.01	281.8	90	0.01	216	77
SE	Godavari	0.4	0.05	0.2	0.03	328	671	65	0.02	16.6	59	0.02	472	196
SE	Krishna	1.5	0.04	0.8	0.03	691	239	129	0.02	106.3	156	0.02	261	170
SE	Ponnaiyar	1.0	0.04	0.5	0.02	328	42	8	0.00	1.7	17	0.03	16	14
SE	Cauvery	1.4	0.04	0.7	0.03	517	145	60	0.01	13.1	97	0.01	257	75
SE	Vellar	NA	NA	NA	NA	624	283	51	0.03	4.1	64	0.02	NA	NA
SW	KBW	1.4	0.03	0.8	0.03	464	32	8	0.02	11.6	23	0.01	34	19
SW	Kali	0.9	0.03	0.5	0.03	430	43	12	0.02	2.8	30	0.02	32	42
SW	Netravathi	-0.1	0.04	0.0	0.03	240	15	5	0.02	4.8	26	0.30	13	7
SW	Mandovi	0.0	0.03	0.0	0.02	270	32	2	0.03	2.0	35	0.02	21	8
SW	Zuari	NA	NA	NA	NA	69	7	2	0.09	0.6	7	0.05	NA	NA

Table 4 *The individual estuaries and their concentration of DSi, major elements (in ppm) and δ^{30}Si-DSi composition (in ‰ along with 1 σ_{SD}) of ground water samples during wet period.*

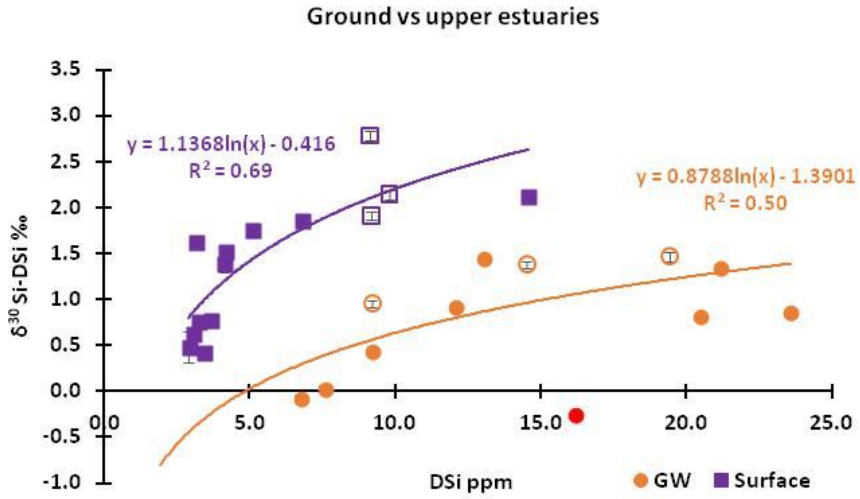

Fig. 11 *The δ^{30}Si-DSi (1SD) vs. DSi concentration (ppm) of groundwater (closed orange circles) and upper estuaries (closed squares) of wet period. The open rectangles and circles represent the estuaries sampled during wet but considered as dry. The red point is excluded from the correlation of groundwater.*

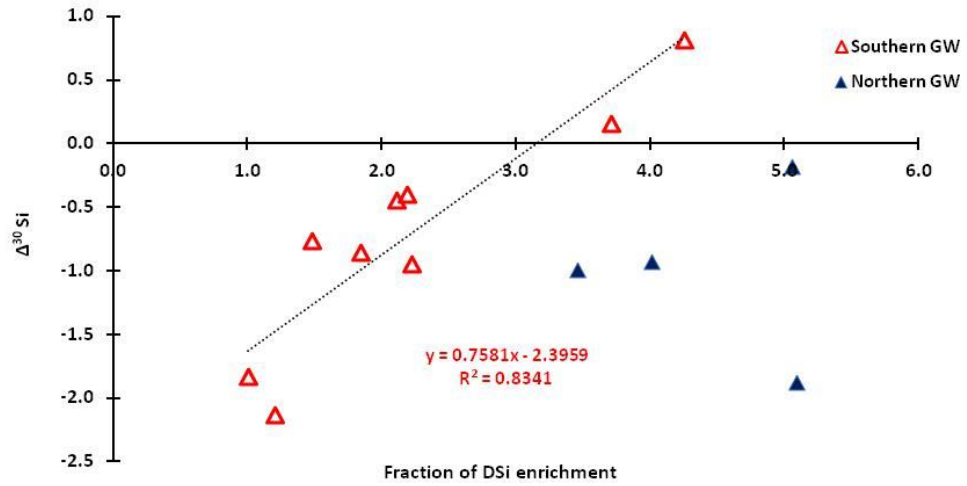

Fig. 12 *Δ^{30} Si (= δ^{30}Si-DSi of groundwater minus δ^{30}Si-DSi of the upper wet estuary) and the fraction of DSi enriched (DSi of groundwater divided by DSi of the upper wet estuary). Linear correlation is only on Southern samples.*

Saturation indexes

As for upper estuaries, saturation indexes (SI) of primary minerals, clay minerals and hydroxides were calculated for groundwater (Fig. 13). Similar to surface upper estuaries, in all groundwater samples, albite, and amorphous silica are undersaturated while Ca-montmorillonite, K-mica, illite and kaolinite are oversaturated (Figs. 13a and b). This indicates that albite ($NaAlSi_3O_8$) could be weathered with the subsequent clay mineral formation. In addition, the positive δ^{30}Si-DSi of most ground water and the positive relationship with DSi (Fig. 11) suggests that groundwater also underwent weathering with concurrent secondary minerals formation. This signal is, however, different from the one in the surface (for both δ^{30}Si and DSi, Fig. 11). The Δ^{30}Si also follows a similar trend as δ^{30}Si of groundwater DSi (Fig. 13a, b and c). However, the variability between Δ^{30}Si and δ^{30}Si of ground water is relatively smaller in the southwest estuaries when compared to the eastern estuaries (Fig. 13a, b and c). This indicates that the southwestern estuaries are more interconnected with ground water rather than the eastern estuaries. Yet, there is no clear overall relationship between δ^{30}Si of groundwater and saturation index of primary and secondary minerals (Fig. 14). Noteworthy, there is a positive relationship between δ^{30}Si and undersaturation of amorphous SiO_2 (R^2 =0.45, n=11, p <0.02, Fig. 14) suggesting the possible dissolution of amorphous SiO_2 that could control the δ^{30}Si-DSi composition (with heavier signature relative to the primary or secondary minerals) and higher DSi concentration in the groundwater during wet period (Fig.

14, except Haldia). In addition, near zero or slight over saturation of smectite (Ca-Montmorillonite) in all groundwater samples, indicates the possible formation of smectite minerals that might contribute to the high DSi load and release of heavy isotopes. This could explain the positive general relationship in Fig. 11. Moreover, as for upper estuaries, the oversaturation of hydroxides in all groundwater samples also indicates possible adsorption fractionating the Si isotopes. However, similar to the ground waters of Arizona (Georg et al., 2009a), the shifts in the saturation of clay minerals indicating the dissolution of clay coatings could be responsible for the supply of lighter Si isotopes in groundwater and could explain the relationship in Fig. 14. Therefore, the Si isotopic composition of ground water seems to reflect the change of DSi origin from primary to increasing contribution from secondary sources. Yet, the studies on groundwater are still sparse and detailed study on each groundwater system is necessary to decipher chemical weathering vs. dissolution processes. This is important since groundwater contributes 40% of Si flux in Bay of Bengal (Georg et al., 2009).

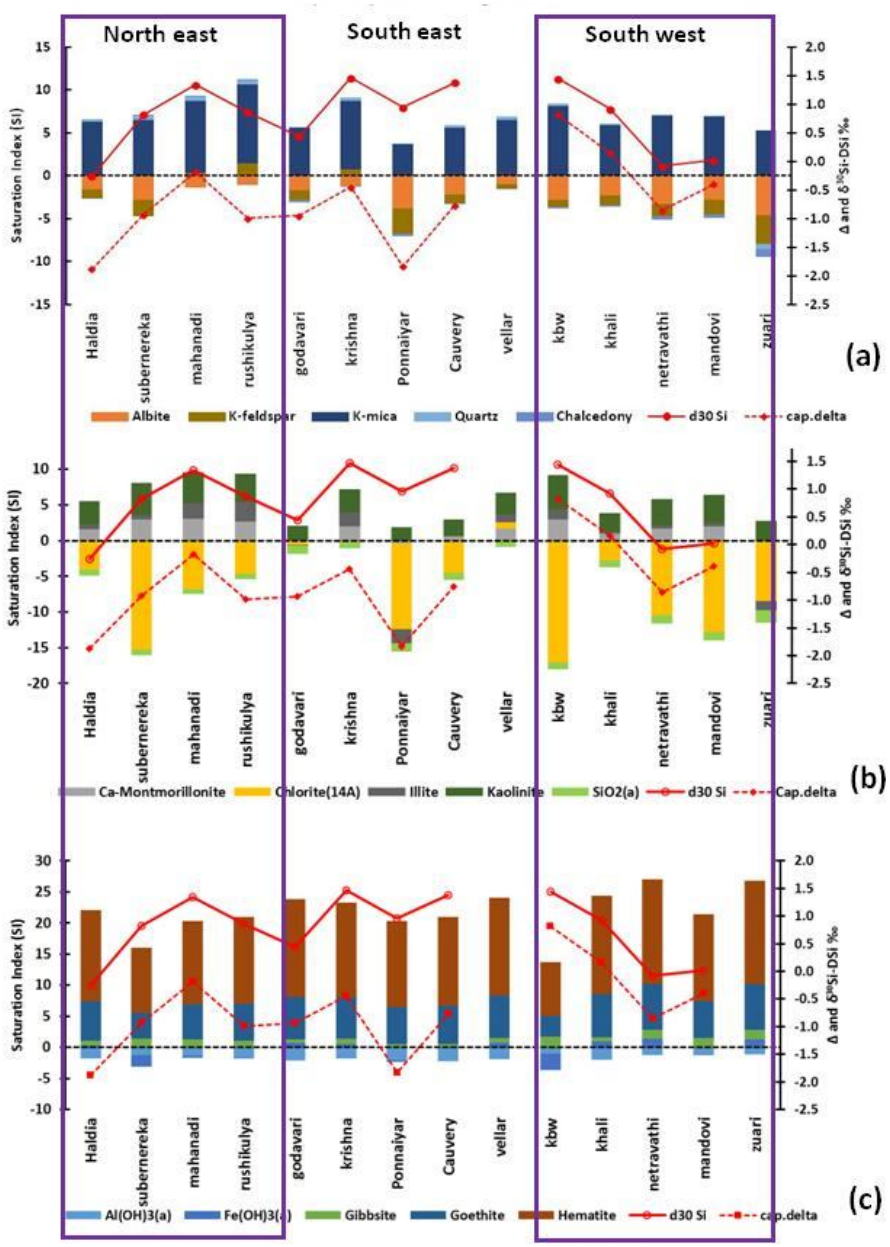

Fig. 13. *Saturation indexes of primary minerals (a) secondary minerals (b) and of Fe-Al oxy-hydroxides minerals (c) along with the variability of δ^{30}Si-DSi and Δ^{30} Si (δ^{30}Si of ground water - δ^{30}Si of surface water) in the ground waters during wet period.*

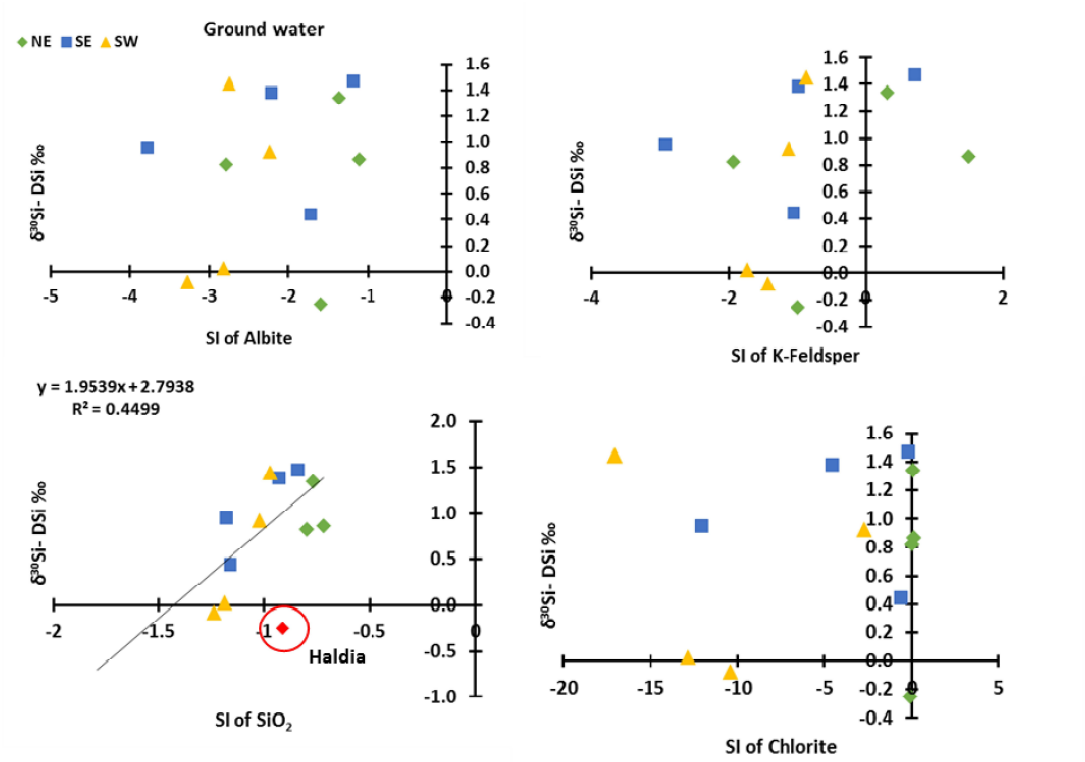

Fig. 14 *The relationship between Saturation indexes of primary minerals and secondary minerals and* δ^{30}*Si-DSi in the ground waters during wet period. A significant positive relationship between* δ^{30}*Si groundwater and saturation index of* SiO_2 *indicates possible dissolution of amorphous Si with lighter isotopic composition relative to the surface water. The point encircled with the red font is removed from the linear equation calculation.*

In addition adsorption could increase the Si isotopic composition in the solution by incorporating light isotopes as discussed elsewhere (Delstanche et al., 2009). Lower DSi and Fe concentrations in the dissolved phase could indicate the formation of Fe oxy-hydroxides that could adsorb Si and alternatively enrich the Si isotopic signature. There is indeed a strong negative relationship between DSi and dissolved Fe concentrations (Fig. 15) that could result from Si adsorption onto Fe-oxy-hydroxides which are oversaturated in all ground waters. However, there is no clear relationship between SI with δ^{30}Si (Figure not shown) and it is not possible to conclude whether adsorption – desorption modifies δ^{30}Si of groundwater. We would need a more direct estimate of the abundance of Fe-Al oxy-hydroxides to conclude on this aspect since just SI or dissolved Fe concentrations may not be directly linked to the abundance of oxides in aquifers. Note that there is no significant relation between dissolved Al and DSi or δ^{30}Si (not shown).

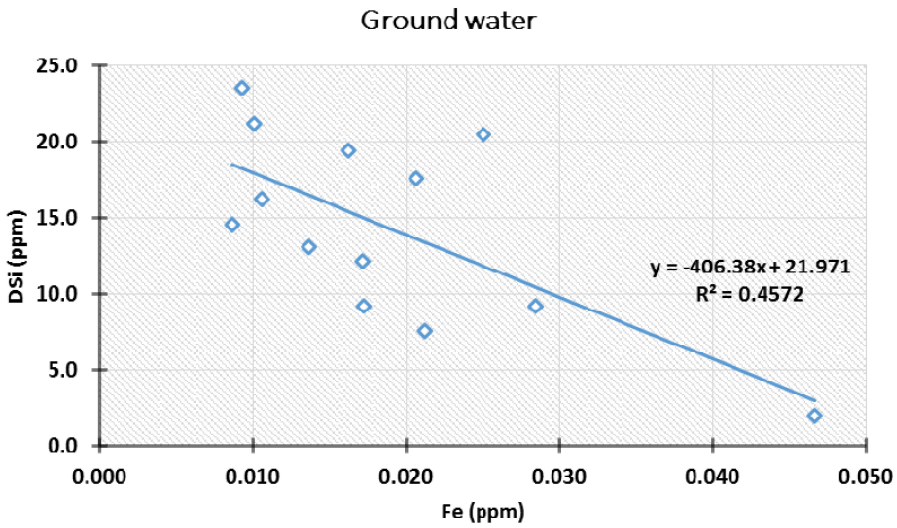

Fig. 15 *DSi and dissolved Fe concentration (ppm) in the groundwater. A negative relationship indicates the possible formation of iron hydroxides in the groundwater.*

4.4 Dry period

4.4.1 Upper dry and comparison with upper wet

Similar to wet period, the upper dry estuaries are also categorised based on the salinity ≤ 5 by assuming that there is a negligible effect from seawater. The estuaries sampled during dry and wet periods are different except Haldia, Subernereka, Rushikulya, Mahanadi and Kochi BW. These common five estuaries will be compared and discussed separately. Overall the δ^{30}Si-DSi of dry period upper estuaries is heavier (0.2 to 0.7‰) than those of the wet season (Fig. 16). Unlike wet period, the water is mostly originating from base flow (e.g., groundwater) because of no rainfall and less or meagre discharge (as discussed in chapter 3) during dry period.

Similar to upper wet estuaries, there is positive relationship between DSi and δ^{30}Si-DSi (r= 0.57, p =0.02, n=14). However they are significantly heavier (p =0.006) during dry period indicating the possible formation of secondary minerals. Even though similar kind of mechanism was noticed in wet period, the isotopic composition during dry period is heavier than the wet season. This is mainly due to the fact that during weathering it is not the same soil solution that is leached. Therefore this solution may be in

contact with different minerals during both seasons. Since the atmospheric input correction for major elements based on Cl was not possible we calculated the saturation index for upper estuaries as indicator of weathering potential processes. Once again under saturation of primary minerals (e.g., albite, K-feldspar) and over saturation of secondary minerals (e.g., Ca-montmorillonite, illite and kaolinite) is observed (Fig. 17). This suggests the dissolution of Na-containing primary minerals and the subsequent formation of secondary clay minerals that could strongly control the isotopic composition. The δ^{30}Si of southwestern estuaries are significantly ($p<0.001$) lighter than the other estuaries during both the seasons. This could once again be due to the residence time of water and interaction with type of minerals that determines the Si isotopic composition. In addition, the intensity of weathering is higher in the south west region due to the humid tropical wet climate and responsible for the lighter isotopic composition when compared to semi-arid climatic regions (cf. Chapter 5). It is interesting to note that the δ^{30}Si-DSi of eastern estuaries is less variable (~0.5 ‰, except Subernereka, Ponnaiyar and Vaigai, Fig. 17). The saturation indices of primary minerals are near zero (Figs. 17 and 18) and over saturation of kaolinite (Fig.17) indicates a similar type of weathering of primary minerals and subsequent clay mineral formation possible in the eastern estuaries.

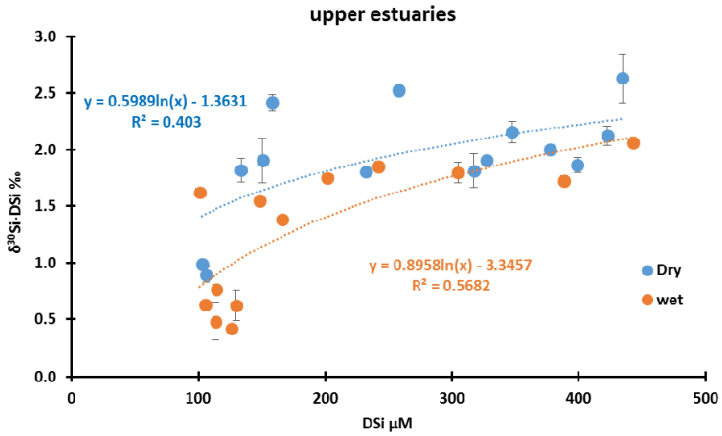

Fig. 16. *Comparison of δ^{30}Si-DSi and DSi (µM) concentration in dry and wet upper estuaries. All data for each estuary have been averaged and ± 1σ_D shown by the error bars*

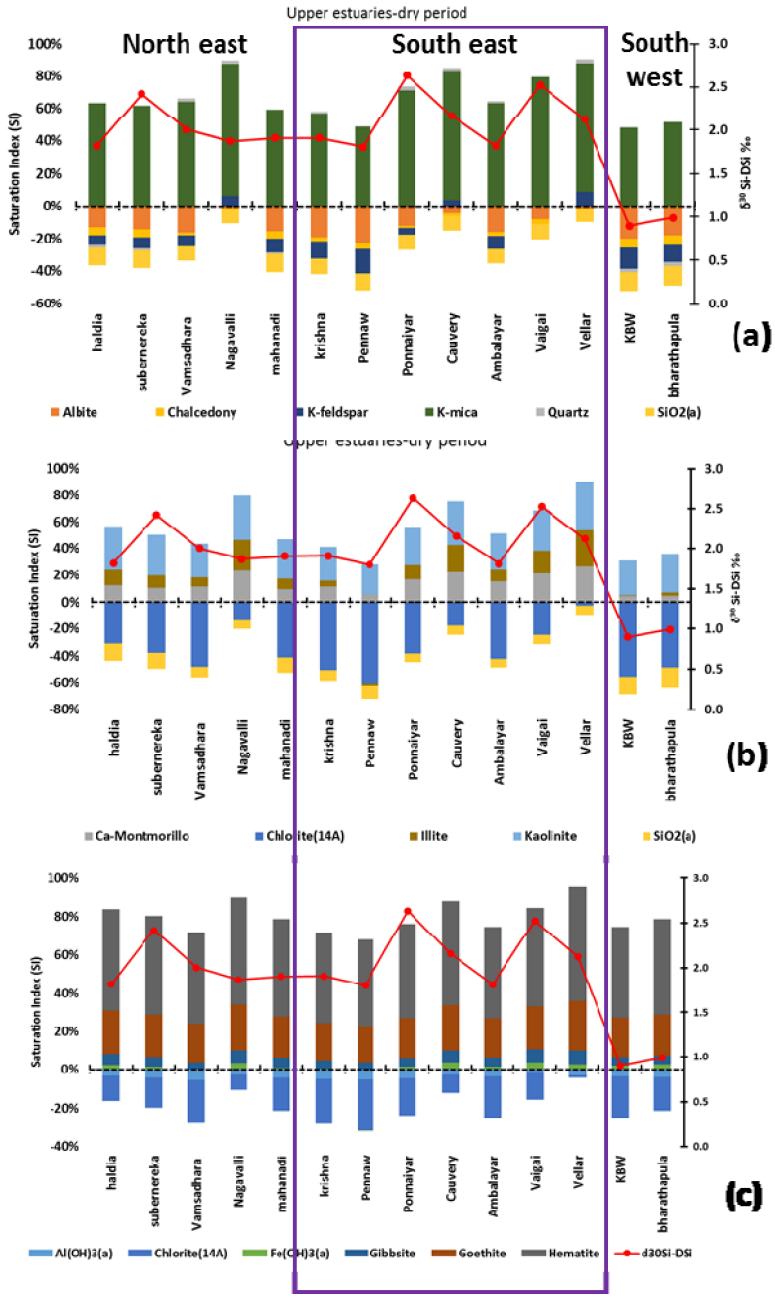

Fig. 17. *Saturation index of primary (a) secondary minerals (b) and hydroxides (c) of upper estuaries during dry period. The line represents the variability of* δ^{30}*Si-DSi.*

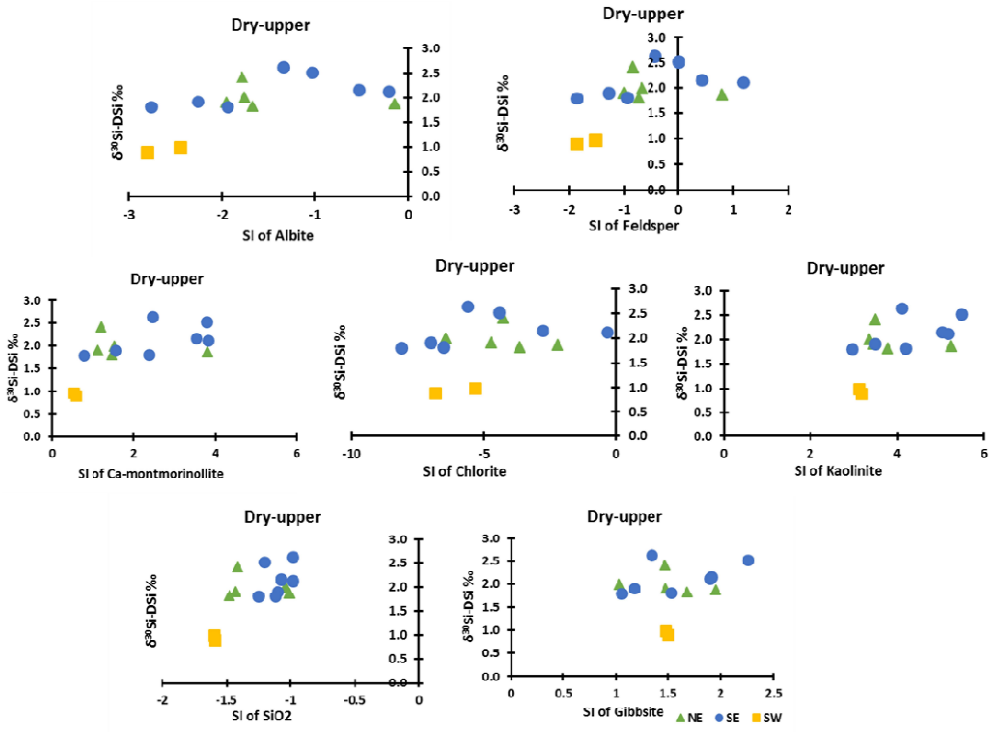

Fig. 18. *Relationship of δ^{30}Si-DSi vs Saturation index of primary (a) secondary minerals (b) and hydroxides (c) of upper estuaries during dry period indicating the possible clay mineral formation uniformly with less variable nature of δ^{30}Si-DSi (except southwest).*

4.4.2 Conservativity vs. non-conservativity within all estuaries

Apart from weathering mechanisms discussed earlier for upper estuaries during both seasons, there are several other processes such as biological uptake that need to be taken into account. For example, during dry period relatively less suspended material with increasing light penetration favour diatom growth. In addition, mixing with sea water should also control the Si variability. The two end-members can be used to evaluate the conservative or non-conservative behaviour of DSi. If the estuarine system is in steady state, the material fluxes remain constant at both end-members and are just diluted by increasing seawater contribution with lower DSi. In order to check the conservative mechanism, we considered the low saline sample as fresh water end-member and sample with salinity at least > 15 as seawater end-member. There is a conservative behaviour of DSi in estuaries like Penna (except 1 point), Mahanadi, KBW (Fig. 19). The other estuaries like Cauvery, Vellar and Krishna show non-conservative

behavior with some points above the mixing line in Cauvery (i.e. indicative of DSi release) and some below the mixing line in the Vellar and Krishna (i.e. indicative of DSi uptake) (Fig. 19a). The remaining estuaries from northeast and southeast do not have enough points to check conservativity. If there is simple mixing of two members, then it should be also reflected in the linear positive δ^{30}Si-DSi with 1/DSi. Those above mentioned conservative estuaries were examined for the mixing effect over δ^{30}Si-DSi (Fig. 19b). Surprisingly, no clear mixing signature was noticed but instead steady δ^{30}Si-DSi with 1/DSi in Vellar (excluding one point), Krishna, Vamsadhara and Subernereka (Fig. 19b) indicate the absence of other processes such as biological uptake or dissolution that could modify the Si isotopes within the estuary. In addition, Cauvery and Vaigai also exhibit less variability of δ^{30}Si-DSi (<0.5 ‰) within the estuaries (Table 1 and see annex B of Chapter 4 for the graphs of individual estuaries). Penna and KBW estuaries showed clear mixing signature with positive relationship between δ^{30}Si-DSi with 1/DSi (Fig.19b). Therefore, all the estuaries of dry period are not strictly conservative in terms of Si isotopic composition, but the stable δ^{30}Si-DSi composition within the estuaries indicates the possible upstream signature are conserved in the estuaries with similar signature. Indeed, we need further investigation on δ^{30}Si-DSi and 1/DSi along the complete salinity gradient to understand the mixing process.

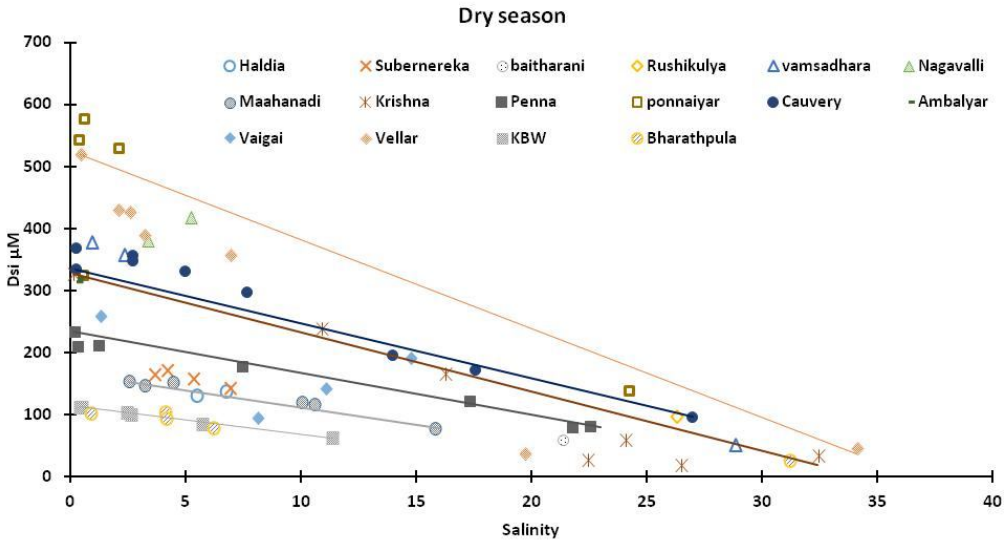

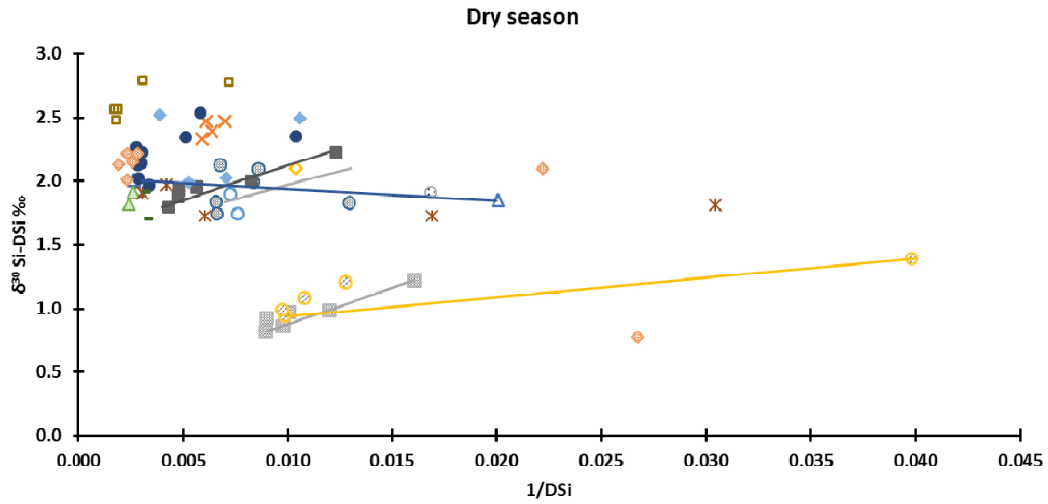

Fig. 19 *DSi concentration vs. salinity (a) and δ^{30}Si-DSi vs 1/DSi (b) in the Indian dry season estuaries. The mixing lines were drawn only for the estuaries with sample(s) at salinity ≥15 (a) and where the only positive relation between δ^{30}Si-DSi and 1/DSi to explain the mixing (b) respectively.*

Biological uptake

The estuaries showing uptake like signature are Vellar, Cauvery, Penna (2 samples), KBW (2 samples) and Bahrathapula (Fig. 20). In order to quantify such uptake, we calculate the amount of ASi needed to explain the increase of δ^{30}Si based on the calculation provided by Hughes et al. (2011) for the Congo basin. This calculation rewrites the existing two models Rayleigh and Steady state by assuming f_{Si}= DSi/ (DSi+ASi) as,

Rayleigh: $BSi = DSi \times [\exp(\delta^{30}Si_0 - \delta^{30}Si/\varepsilon) - 1]$ 2

Steady state $BSi = DSi \times [\varepsilon/(\delta^{30}Si - \delta^{30}Si_0 + \varepsilon) - 1]$ 3

$\delta^{30}Si_0$ is used from upstream end-member value and the fractionation factor (ε) has been taken from the earlier studies as -1.2 ‰ (Alleman et al., 2005; Fripiat et al., 2011). Before estimating the calculated ASi, we nullified the dilution effect on DSi concentration because mixing with sea water reduces the DSi concentration in the estuaries and cannot be attributed to uptake. Therefore the DSi concentration due to conservativity can be corrected assuming the average coastal DSi concentration (avg 5µM). The calculated ASi is 2 to 10 folds (Rayleigh model) and 2 to 12 folds (Steady state) higher than the measured ASi (except Penna, Table. 5). This is very similar to what has been reported earlier by Hughes et al.

(2011) in the Congo basin. Our results show that the measured suspended amorphous silica is not sufficient to explain the changes in the Si isotopic signature in the estuaries. This likely result from the settling of diatoms in the sediments. It indicates that the majority (up to 90%) of diatoms have settled.

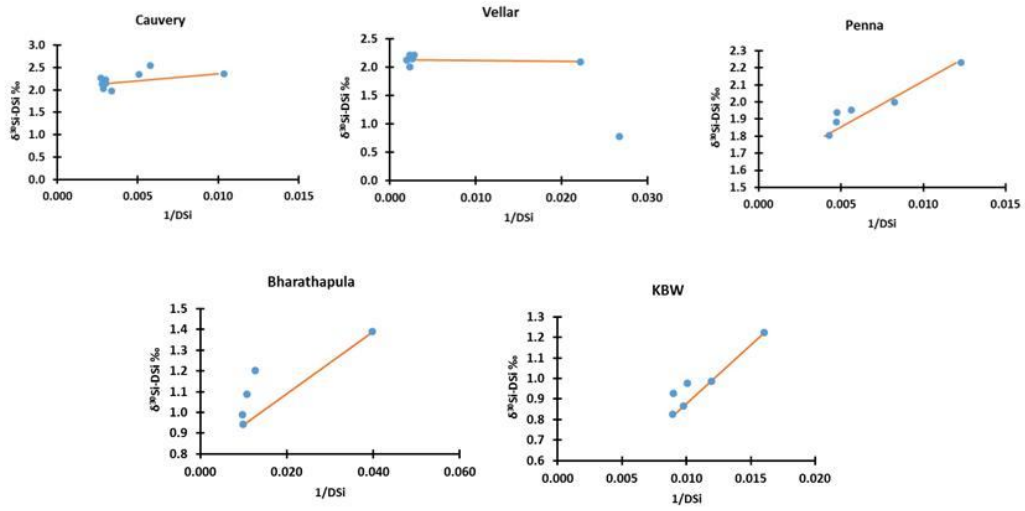

Fig. 20 *The conservative behavior of Si isotopes with 1/DSi and the points above the mixing line indicates the possible biological uptake mechanism. The estuaries with points above mixing line are studied separately for the biological uptake process.*

Estuary	salinity	Conservative DSi (µM)	δ^{30}Si-DSi ‰	SD	DSi (µM)	Measured ASi (µM)	Calculated Asi Rayleigh model (µM)	Calculated ASi Steady state model (µM)	Ratio calculated ASi versus measured ASi	
									Rayleigh	Steady state
KBW	2.4	104	0.9	0.06	102	1.7	3.8	3.8	2.2	2.2
	5.7	94	1.0	0.03	84	4.6	14.7	15.8	3.2	3.4
	11.4	77	1.2	0.13	62	4.0	38.4	48.5	9.7	12.2
Bharathapula	6.2	86	1.2	0.07	79	4.8	22.6	25.9	4.7	5.4
Cauvery	13.9	212	2.3	0.03	197	10.4	102.3	121.8	9.8	11.7
Vellar	3.2	390	2.1	0.04	390	9.6	53.8	57.5	5.6	6.0
Penna	0.3	231	1.9	0.20	211	0.6	24.7	26.3	41	44
	7.4	185	2.0	0.06	178	0.9	30.0	32.1	34	37
	22.5	86	2.2	0.03	81	11.6	97.2	125.6	8.4	10.8

Table 5 *Diatom uptake process in the southern estuaries during dry period. The measured ASi on filters are data from Chapter 3. The calculated ASi concentrations are calculated from the eq. 2 and 3. Conservative DSi is calculated by removing the dilution effect on DSi concentration using the average*

surface salinity of sea water and DSi concentration of coastal Indian water of 5 µM (Naqvi et al., 2010). The estuaries are selected based on the points that falling above the mixing line between δ^{30}Si-DSi &1/DSi and also the heavier δ^{30}Si-DSi associated by concurrent reduced DSi concentration respectively.

Dissolution or DSi supply

Apart from dissolution of minerals, dissolution of phytoliths also releases DSi but for phytoliths with heavier Si isotopic signature in to the solution. This should lead to δ^{30}Si-DSi points falling below the mixing line (Annex for chapter 4). The estuaries that belong to such category are Mahanadi (one sample), Krishna, Vaigai and Vellar. Unfortunately, there is no more information to confirm such process. However, the under saturation of amorphous SiO_2 in the upper estuaries (Fig. 18) showed a positive relation with increasing δ^{30} Si-DSi (especially in southeast estuaries) indicating the possible dissolution process with heavier isotopic signature in the solution relative to the clay minerals. Moreover, higher agriculture activities on the eastern estuaries are possibly the source of amorphous Si that could eventually dissolve. Yet, we need further studies to confirm such process. The Scanning Electron Microscope (SEM) pictures of suspended particles sampled in Krishna (southeast) do not indicate the occurrence of phytoliths suggesting that the dissolution of phytoliths is unlikely within that estuary (as discussed in Chapter 3) but this could have occurred upstream river. On contrary, in another study, the river Cauvery (southeast) showed the presence of phytoliths evidencing the possibility for phytolith dissolution (Meunier et al., 2014). One must be aware that the eastern estuaries are well known for the huge rice cultivation that may probably alter the Si cycle. Therefore, it is difficult to conclude about the source via dissolution process but there is possibility for the influence of phytoliths on δ^{30}Si-DSi of Indian estuaries. We would need further studies with special reference to each basin to better quantify such mechanisms.

4.5 Common estuaries

The common estuaries sampled for the two seasons are Haldia, Subernereka, Mahanadi, Rushikulya, and KBW. The (non-)conservative behavior of above-mentioned estuaries has been discussed earlier in the respective dry and wet sections. In summary, there is non-conservativity of δ^{30}Si-DSi between both the seasons along the salinity gradient sampled in all the common estuaries. In addition, there is no sample with salinity above 7 to estimate the sea water end-member during dry period (Haldia, Subernerekha, and Rushikulya with one point). Indeed, the δ^{30}Si-DSi within estuary remains stable indicating no

significant process occurring within estuaries. However, non-availability of sea water end-member restricts to describe the conservativity mechanism. In addition the other common estuary KBW exhibits imprint of DSi uptake and has been discussed earlier (under biological uptake section). There is no significant variability of δ^{30}Si-DSi along the salinity gradient (< 0.2‰) during wet period. This suggests that there is no process that takes place within the estuarine system to modify the δ^{30}Si-DSi. In addition, there is no clear seasonal difference of δ^{30}Si-DSi between both the periods (p=0.2). Indeed the process of weathering and concurrent clay mineral formation mainly influences the δ^{30}Si-DSi composition in the upstream.

5. Conclusions

Knowing the scarcity of studies on Si isotopes in the estuaries, a crucial link between land and ocean trapping 21 % of total Si supply to the ocean, the present study proposed to understand the δ^{30}Si-DSi variability in the tropical estuaries. The major and minor Indian monsoonal estuaries are studied for the first time using the δ^{30} Si-DSi proxy (except Ganges river basin, Frings et al., 2014) during dry and wet seasons. Indian estuarine Si isotopic compositions varied widely from 0.41 ‰ to 2.78 ‰ during both seasons and are comparable with other global estuarine and riverine studies. During wet period, the positive relationship between the δ^{30}Si-DSi and clay mineral composition of the particle samples of upper estuaries clearly suggest the weathering of smectite minerals especially in the northern estuaries (note that there is no data for southeast estuaries). On contrary, in southwest estuaries, the lighter δ^{30}Si-DSi could be due to the dissolution of kaolinite in upper soil horizons when surface flow is high (humid tropical) and undersaturation of young water supplied by rain. Indeed, the saturation indexes of primary and secondary minerals of upper estuaries indicate the dissolution of primary minerals associated with clay mineral formation. In addition, the undersaturation of chlorite minerals (KBW, Kali and Netravathi) and positive relation with δ^{30}Si-DSi suggest congruent dissolution of chlorite minerals in the southwest estuaries. Moreover, the oversaturation index of hydroxides minerals indicates the possible adsorption of DSi on hydroxides that favor incorporation of lighter Si isotopes leaving a heavier isotopic signature in the solution. Therefore, the variability of δ^{30}Si-DSi of Indian estuaries is mainly based on climatic zone and weathering regime over the river basin (e.g., humid, heavy rainfall and intense weathering in south-west region and vice-versa). In addition, the longer residence time of water in deeper saprolite (dry season and/or semi-arid climate and/or low topography) compared to surface soil water (wet season and/or humid climate and/or mountains) seems to have a dominant control on Si

isotopic variability. For instance, in southeast and north the presence of wider plains should favour leaching of more dissolved elements along with clay mineral formation (e.g., smectite kind of minerals). This major mechanism could explain the variability of δ^{30}Si-DSi during both seasons. Likewise, the soil solutions that interact with the soil minerals are not the same during both seasons. This determines the type of mineral leached and is reflected in the isotopic composition of upper estuaries. In addition, we see clear evidence of diatom uptake (southern estuaries- Penna, Vellar, Cauvery, Bharathapuzha and KBW). Mixing with sea water adds to the δ^{30}Si-DSi variability within the estuaries especially during dry period even though weathering is the major factor that controls the δ^{30}Si-DSi of Indian estuaries.

In addition, land use especially intense agricultural practice in the eastern regions (>60% watershed area) can also contribute to the δ^{30}Si-DSi variability, with the heavier isotopic composition in the eastern and north-western upper estuaries. Relatively less agricultural activities with more forest cover in the southwest regions could enhance clay dissolution because of high organic matter and low pH in the forest soils as noticed in other tropical (e.g., Congo) and European estuaries (e.g., Scheldt).

We also measured the δ^{30}Si-DSi of 13 upper estuarine shallow ground water samples during wet season and the values are comparable with Ganges groundwater isotopic composition. Surprisingly we noticed a positive relationship of δ^{30}Si-DSi with DSi concentration indicating a typical weathering signature. At the same time, the lighter δ^{30}Si-DSi and higher in DSi concentration than the surface suggest the dissolution of primary and secondary minerals.

6. References.

Alexandre, A., Meunier, J.-D., Colin, F. and Koud, J.-M.: Plant impact on the biogeochemical cycle of silicon and related weathering processes, Geochim. Cosmochim. Acta, 61(3), 677–682, doi:10.1016/S0016-7037(97)00001-X, 1997.

Alleman, L. Y., Cardinal, D., Cocquyt, C., Plisnier, P.-D., Descy, J.-P., Kimirei, I., Sinyinza, D. and André, L.: Silicon Isotopic Fractionation in Lake Tanganyika and Its Main Tributaries, J. Great Lakes Res., 31(4), 509–519, doi:10.1016/S0380-1330(05)70280-X, 2005.

Berner, R. A., Weathering, plants, and the long-term carbon cycle, Geo- chim. Cosmochim. Acta, 56, 3225–3231, 1992

Beusen, a. H. W., Bouwman, a. F., Dürr, H. H., Dekkers, a. L. M. and Hartmann, J.: Global patterns of dissolved silica export to the coastal zone: Results from a spatially explicit global model, Global Biogeochem. Cycles, 23(4), 1–13, doi:10.1029/2008GB003281, 2009.

Biscaye, E. P.: Mineralogy and Sedimentation of Recent Deep-Sea Clay in the Atlantic Ocean and Adjacent Seas and Oceans, Geological Society of America Bulletin, 76, 803-832, 1965.

Caquineau, S., Magonthier, C. M., Gaudichet, A., and Gomes, L.: An improved procedure for X-ray diffraction analysis of low-mass atmospheric dust sample, Eur. J. Mineral, 9, 157-166, 1997.

Cardinal, D., Gaillardet, J., Hughes, H. J., Opfergelt, S., and André, L.: Contrasting silicon isotope signatures in rivers from the Congo Basin and the specific behaviour of organic-rich waters, Geophys. Res. Lett., 37(12), 1–6, doi:10.1029/2010GL043413, 2010.

Chou L**.** and R. Wollast Estuarine silicon dynamics. In: The Silicon Cycle. Human Perturbations Island Press, Washington, Covelo, London 66, pp. 93- 120, 2006.

Cornelis, J.T., Delvaux, B., Cardinal, D., André, L., Ranger, J., and Opfergelt, S.: Tracing mechanisms controlling the release of dissolved silicon in forest soil solutions using Si isotopes and Ge/Si ratios, Geochim. Cosmochim. Acta 74, 3913–3924, 2010.

Cornelis, J.-T., Delvaux, B., Georg, R. B., Lucas, Y., Ranger, J., and Opfergelt, S.: Tracing the origin of dissolved silicon trans- ferred from various soil-plant systems towards rivers: a review, Biogeosciences; 8, 89–112, 2011.

De La Rocha C.L., Brzezinski M.A. and DeNiro M.J.: Fractionation of silicon isotopes by marine diatoms during biogenic silica formation, Geochimica et Cosmochimica Acta 61: 5051-5056, 1997.

De La Rocha, C. L.,M. A. Brzezinski, and M. J. DeNiro.: A first look at the distribution of the stable isotopes of silicon in natural waters, Geochim. Cosmochim. Acta, 64, 2467–2477, 2000

Deepthy, R. and Balakrishnan, S.: Climatic control on clay mineral formation: Evidence from weathering profiles developed on either side of the Western Ghats. *J. Earth Syst. Sci.* **114,** 545–556, 2005.

Delstanche, S., Opfergelt, S., Cardinal, D., Elsass, F., André, L. and Delvaux, B.: Silicon isotopic fractionation during adsorption of aqueous monosilicic acid onto iron oxide, Geochim. Cosmochim. Acta 73, 923–934, 2009.

Delstanche, S., Opfergelt, S., Cardinal, D., Elsass, F., André, L. and Delvaux, B.: Silicon isotopic fractionation during adsorption of aqueous monosilicic acid onto iron oxide, Geochim. Cosmochim. Acta, 73(4), 923–934, doi:10.1016/j.gca.2008.11.014, 2009.

Delvaux, C., Cardinal, D., Carbonnel, V., Chou, L., Hughes, H. J. and André, L.: Controls on riverine δ30Si signatures in a temperate watershed under high anthropogenic pressure (Scheldt — Belgium), J. Mar. Syst., 1–12, doi:10.1016/j.jmarsys.2013.01.004, 2013.

Demarest, M.S., Brzezinski, M.A. and Beucher, C.P.: Fractionation of silicon isotopes during biogenic silica dissolution, Geochimica et Cosmochimica Acta 73: 5572-5583, 2009

Derry, L. A., Kurtz, A. C., Ziegler, K., and Chadwick, O. A.: Biological control of terrestrial silica cycling and export fluxes to watersheds, Nature, 433, 728–731, 2005.

Dessert,C., Dupré, B., Gaillardet, J., François, LM. and Allègre, CJ.: Basalt weathering laws and the impact of basalt weathering on the global carbon cycle, Chem Geol; 202:257–73, 2003.

Ding, T., Wan, D., Wang, C and Zhang, F.: Silicon isotope com- positions of dissolved and suspended matter in the Yangtze, Geochim. Cosmochim. Acta, 68, 205–216, doi:10.1016/S0016-7037(03)00264-3, 2004.

Ding, T.P., Zhou, J.X., Wan, D.F., Chen, Z.Y., Wang, C.Y., and Zhang, F.: Silicon iso- tope fractionation in bamboo and its significance to the biogeochemical cycle of silicon, Geochim. Cosmochim. Acta 72, 1381–1395, 2008.

Dunne, T.: Rates of chemical denudation of silicate rocks in tropical catchments, *Nature* **274,** 244–246, 1978.

Engström, E., Rodushkin, I., Ingri, J., Baxter, D.C., Ecke, F., Osterlund, H. and Ohlander, B.: Temporal isotopic variations of dissolved silicon in a pristine boreal river, Chem. Geol. 271, 142–152, 2010.

Farmer, V. C., Delbos, E., and Miller, J. D.: The role of phytolith formation and dissolution in controlling concentrations of silica in soil solutions and streams, Geoderma, 127, 71–79, 2005.

Fripiat, F., Cavagna, AJ., Savoye, N., Dehairs, F., Andre, L ., Cardinal, D.: Isotopic constraints on the Si-biogeochemical cycle of the Antarctic Zone in the Kerguelen area (KEOPS), Mar Chem 123(1–4):11–22, 2011.

Garnier, J., Beusen, A., Thieu, V., Billen, G. and Bouwman, L.: N:P:Si nutrient export ratios and ecological consequences in coastal seas evaluated by the ICEP approach, Global Biogeochem. Cycles **24,** GB0A05, 1-12, 2010.

Garnier, J., Sferratore, A., Meybeck, M., Billen, G., and Dürr, H.: Modeling silicon trans- fer processes in river catchments. In: Ittekkot, V., Unger, D., Humborg, C., Tac An, N. (Eds.), The Silicon Cycle: Human Perturbations and Impacts on Aquatic Systems. Island Press, Washington, pp. 139–162, 2006.

Gehlen, M. and Van Raaphorst, W.: The role of adsorption– desorption surface reactions in controlling Si(OH)4 concentra- tions and enhancing Si(OH)4 turn-over in shallow shelf seas, Cont. Shelf Res. 22, 1529–1547, 2002.

Georg, R. B., Reynolds, B. C., Frank, M. and Halliday, A. N.: New sample preparation techniques for the determination of Si isotopic compositions using MC-ICPMS, Chem. Geol., 235(1–2), 95–104, doi:10.1016/j.chemgeo.2006.06.006, 2006.

Georg, R. B., West, a. J., Basu, a. R. and Halliday, a. N.: Silicon fluxes and isotope composition of direct groundwater discharge into the Bay of Bengal and the effect on the global ocean silicon isotope budget, Earth Planet. Sci. Lett., 283(1–4), 67–74, doi:10.1016/j.epsl.2009.03.041, 2009.

Georg, R.B., Zhu, C., Reynolds, B.C. and Halliday, A.N.: Stable silicon isotopes of groundwater, feldspars, and clay coatings in the Navajo Sandstone aquifer, Black Mesa, Arizona, USA, Geochimica et Cosmochimica Acta 73: 2229-2241, 2009.

Gérard, F., K. U. Mayer, M. J. Hodson, and J. Ranger (2008), Modelling the biogeochemical cycle of silicon in soils: Application to a temperate forest ecosystem, Geochim. Cosmochim. Acta, 72(3), 741–758.

Grashoff, K.,: Methods of Seawater Analysis. Verlag Chemie, New York, NY, 419 pp 1992.

GUO, S. *Rapport de stage, Master, Origines et transferts de matières en suspension dans les estuaires indiens,* 2016.

Gurumurthy, G. P., Balakrishna, K., Riotte, J., Braun, J.-J., Audry, S., Shankar, H. N. U. and Manjunatha, B. R.: Controls on intense silicate weathering in a tropical river, southwestern India, Chem. Geol., 300–301, 61–69, doi:10.1016/j.chemgeo.2012.01.016, 2012.

Hodson, MJ., White, PJ., Mead, A., Broadley, MR.: Phylogenetic Variation in the Silicon Composition of Plants, Annals of Botany 96: 1027–1046, 2005.

Hughes, H. J., Delvigne, C., Korntheuer, M., de Jong, J., André, L. and Cardinal, D.: Controlling the mass bias introduced by anionic and organic matrices in silicon isotopic measurements by MC-ICP-MS, J. Anal. At. Spectrom., 26(9), 1892, doi:10.1039/c1ja10110b, 2011.

Hughes, H. J., Sondag, F., Santos, R. V., André, L. and Cardinal, D.: The riverine silicon isotope composition of the Amazon Basin, Geochim. Cosmochim. Acta, 121, 637–651, doi:10.1016/j.gca.2013.07.040, 2013.

Hughes, H.J., Bouillon, S., André, L. and Cardinal, D.: The effects ofweathering variability and anthropogenic pressures upon silicon cycling in an intertropicalwatershed (Tana River, Kenya), Chem. Geol. 308–309, 18–25, 2012.

Kessarkar, P.M., Shynu, R., Rao, V.P., Chong, F., Narvekar, T. and Zhang, J.: Geochemistry of the suspended sediment in the estuaries of the Mandovi and Zuari rivers, central west coast of India, Environment Monitoring Assessment, 185, 4461–4480, 2013.

Loucaides, S., Van Cappellen, P. and Behrends T.: Dissolution of biogenic silica from land to ocean: Role of salinity and pH, Limnology and Oceanography 53: 1614-1621, 2008.

McKeague, J.A. and Cline, M.G.: Silica in soil solutions. I. The form and concentration of dissolved silica in aqueous extracts of some soils, Can. J. Soil Sci. 43: 70–82, 1963.

Meunier, J. D., Riotte, J., Braun, J. J., Sekhar, M., Chalié, F., Barboni, D. and Saccone, L.: Controls of DSi in streams and reservoirs along the Kaveri River, South India, Sci. Total Environ., 502, 103–113, doi:10.1016/j.scitotenv.2014.07.107, 2015.

Naqvi, S. W. A. *et al.* The Arabian Sea as a high-nutrient, low-chlorophyll region during the late Southwest Monsoon. *Biogeosciences* **7,** 2091–2100, 2010.

Oelze M., von Blanckenburg F., Hoellen D., Dietzel M. and Bouchez J. Si stable isotope fractionation during adsorption and the competition between kinetic and equilibrium isotope fractionation: Implications for weathering systems. Chemical Geology 380: 161-171, 2014.

Opfergelt S., Cardinal D., Henriet C., Draye X., André L. and Delvaux B. Silicon isotopic fractionation by banana (Musa spp.) grown in a continuous nutrient flow device. Plant and Soil 285: 333-345, 2006.

Opfergelt S., Eiriksdottir E., Burton K., Einarsson A., Siebert C., Gislason S. and Halliday A. Quantifying the impact of freshwater diatom productivity on silicon isotopes and silicon fluxes: Lake Myvatn, Iceland. Earth and Planetary Science Letters 305: 73-82, 2011.

Opfergelt, S., Cardinal, D., Andr´e, L., Delvigne, C., Bremond,L., and Delvaux, B.: Variations of [delta]30Si and Ge/Si with weathering and biogenic input in tropical basaltic ash soils under monoculture, Geochim. Cosmochim. Acta, 74, 225–240, 2010

Opfergelt, S., Delvaux, B., André, L. and Cardinal, D.: Plant silicon isotopic signature might reflect soil weathering degree, Biogeochemistry, 91, 163–175, doi:10.1007/s10533-008-9278-4, 2008.

OPFERGELT, S., G.DE BOURNONVILLE,D. CARDINAL,L.ANDRE´,S. DELSTANCHE, AND B. DELVAUX. Impact of soil weath- ering degree on silicon isotopic fractionation during adsorp- tion onto iron oxides in basaltic ash soils, Cameroon. Geochim. Cosmochim. Acta 73: 7226–7240, doi:10.1016/ j.gca.2009.09.003, 2009.

Parkhurst, D. L., and C. A. J. Appelo, User's guide to PHREEQC (Version 2)—A computer program for speciation, batch-reaction, one- dimensional transport, and inverse geochemical calculations, U.S. Geol. Surv. Water Resour. Invest. Rep., 99–4259, 312 pp, 1999.

Pogge von Strandmann P.A.E., Porcelli D., James R.H., van Calsteren P., Schaefer B., Cartwright I., Reynolds B.C. and Burton K.W. Chemical weathering processes in the Great Artesian Basin: Evidence from lithium and silicon isotopes. Earth and Planetary Science Letters 406: 24-36, 2014.

Roelandt, C., Goddéris, Y., Bonnet, M.P., Sondag, F. Coupled modeling of biospheric and chemical weathering processes at the continental scale. Global Bio- geochemical Cycles 24; GB2004, 2010.

Sarma, V. V. S. S., *M.S. Krishna, V.R. Prasad, B.S.K. Kumar, S.A. Naidu, G.D. Rao, R. Viswanadham, T. Sridevi, P.P. Kumar, N.P.C. Reddy.* Distribution and sources of particulate organic matter in the Indian monsoonal estuaries during monsoon. **119,** 1–17, 2014.

Sarma, V. V. S. S., Prasad, V. R., Kumar, B. S. K., Rajeev, K., Devi, B. M. M., Reddy, N. P. C., Sarma, V. V., et al. Intra-annual variability in nutrients in the Godavari estuary, India. Continental Shelf Research, 30, 2005–2014, 2010.

Schwertmann U. and Taylor R. M. Iron oxides. In Minerals in Soil Environments (eds. J. B. Dixon and S. B. Weed). Soil Science Society of America Madison, Wisconsin, pp. 379–438, 1989.

Sridevi, B.,Sarma, V. V S S, Murty, T. V R, Sadhuram, Y., Reddy, N. P C, Vijayakumar, K., Raju, N. S N, Jawahar Kumar, C. H., Raju, Y. S N, Luis, R., Kumar, M. D., Prasad, K. V S R. Variability in stratification and flushing times of the Gautami–Godavari estuary, India. *J. Earth Syst. Sci.* **124,** 993–1003, 2015.

Stallard, R. & Edmond, J. Geochemistry of the Amazon: 3. Weathering chemistry and limits to dissolved inputs. *J. Geophys. Res.* **92,** 8293–8302, 1987.

Struyf, E., Smis, A., Van Damme, S., Garnier, J., Govers, G., Van Wesemael, B., Conley, D. J., Batelaan, O., Frot, E., Clymans, W., Vandevenne, F., Lancelot, C., Goos, P. and Meire, P.: Historical land use change has lowered terrestrial silica mobilization., Nat. Commun., 1(8), 129, doi:10.1038/ncomms1128, 2010.

Stumm, W., Wollast, R. Coordination chemistry of weathering: Kinetics of the surface-controlled dissolution of oxide minerals. Revs. Geophysics; 28: 53–69, 1990.

Sun X., Andersson P.S., Humborg C., Pastuszak M. and Mörth C.-M. Silicon isotope enrichment in diatoms during nutrient-limited blooms in a eutrophied river system. Journal of Geochemical Exploration 132: 173-180, 2013.

Tréguer, P. *et al.* The silica balance in the world ocean: a reestimate. *Science* **268,** 375–379, 1995.

Tréguer, P. J. and De La Rocha, C. L.: The world ocean silica cycle. Ann. Rev. Mar. Sci., 5(1), 477–501, doi:10.1146/annurev-marine-121211-172346, 2013.

V. Ittekkot, D. Unger, C. Humborg and N. Tac An. Scope Berner, R. A., The rise of plants and their effect on weathering and atmo- spheric CO2, Science, 276, 544–546, 1997.

Vijith, V., Sundar, D. and Shetye, S. R.: Time-dependence of salinity in monsoonal estuaries, Estuar. Coast. Shelf Sci., 85(4), 601–608, doi:10.1016/j.ecss.2009.10.003, 2009.

Wedepohl K.H. 1995. The composition of the continental crust. Geochim. Cosmochim. Acta 59; 1217–1232.

Weiss A., De La Rocha C., Amann T. and Hartmann J. Silicon isotope composition of dissolved silica in surface waters of the Elbe Estuary and its tidal marshes. Biogeochemistry: 1-19, 2015.

Zhang, A. Y., J. Zhang, J. Hu, R. F. Zhang, and G. S. Zhang. Silicon isotopic chemistry in the Changjiang Estuary and coastal regions: Impacts of physical and biogeochemical processes on the transport of riverine dissolved silica, J. Geophys. Res. Oceans, 120, 6943– 6957, 2015.

Ziegler K., Chadwick O.A., Brzezinski M.A. and Kelly E.F. Natural variations of δ30Si ratios during progressive basalt weathering, Hawaiian Islands. Geochimica et Cosmochimica Acta 69: 4597-461, 2005.

Ziegler K., Chadwick O.A., White A.F. and Brzezinski M.A. δ30Si systematics in a granitic saprolite, Puerto Rico. Geology 33: 817-820, 2005b.

CHAPTER 5

Seasonal, biological and weathering processes controlling silicon cycle along the land-ocean continuum in two contrasted rivers of India (Cauvery and Netravathi)

K.R. Mangalaa, D. Cardinal, A. Dapoigny, G.P. Gurumurthy, J. Riotte, V.V.S.S. Sarma, *et al.*

Article in preparation for *Geochimica et Cosmochimica Acta*

1. Introduction

Silicon (Si), is the second most abundant element in the Earth's crust and is present as particulate and dissolved forms in rivers, estuaries and ocean. Weathering is the major source for Si supply to the terrestrial and aquatic systems. During chemical weathering of primary minerals, due to its intermediate atomic radius-to-charge ratio (r/z), silicon is partly released as a solute (dissolved silicon, DSi) - a behaviour typical of soluble elements with low r/z that form oxyanions (such as S, P, N, C), while the other fraction is incorporated into insoluble secondary clay minerals (moderate r/z, such as Al). In aquatic systems, DSi is largely dominated by orthosilicic acid, H_4SiO_4 (>98% at pH <8) and serves as an important nutrient for aquatic and terrestrial plants for making their rigid cell wall. Indeed vegetation plays an important role in Si biogeochemical cycle via phytoliths formation (amorphous silica) that are recycled into the soil or exported to rivers through erosion (Alexandre et al., 1997, Derry et al., 2005). Likewise, diatom uptake alters the Si biogeochemical cycle via conversion of DSi to biogenic silica (BSi) in aquatic ecosystems (Conley 1997). Consequently, these continental processes alter the Si supply to the estuaries and coastal waters. This might have a significant impact on the functioning and health of the coastal ecosystem since diatoms contribute commonly up to ~75% of coastal primary production (Nelson et al., 1995). On the other hand, urbanization and anthropogenic activities like agriculture and construction of reservoirs can alter the natural Si cycle by reducing the supply of Si load into the estuarine and coastal ecosystems. These effects were well evidenced in several aquatic environments (Conley 2000; Humborg et al., 2002; Hughes et al., 2012). In contrast, deforestation and increasing agriculture can enhance the soil erosion and lead to the increasing DSi supply into the aquatic ecosystems (Struyf et al., 2010; Vandevenne et al., 2012). Therefore, recently the increasing anthropogenic activities have drawn much attention to understanding these effects on the global Si cycle. Tropical areas are known for high DSi concentration (Dürr et al., 2011) because of hot and wet climates especially when they are associated with high mountains, favoring high weathering intensity, runoff, and erosion (Meunier et al., 2015). Hence the understanding of the Si cycle in tropical regions is of particularly high relevance in this context.

In recent years, Si isotopes have been proved to be a valuable tool for tracing several processes affecting the Si biogeochemical cycle. For example, secondary mineral formation (Georg et al., 2007), mixing of the different DSi sources (Georg et al., 2006), biological uptake (Ding et al., 2004, Engstrom et al., 2010),

anthropogenic effects such as damming (Hughes et al., 2012) and land use (Delvaux et al., 2013) have been studied using silicon isotopes.

Despite their importance as the main suppliers of DSi to the ocean due to their geological and climatological settings, tropical rivers remain understudied. This results in large uncertainties on the DSi fluxes to the ocean (±30 %, Tréguer and De La Rocha et al., 2013). Therefore, in the present work, we propose to study the Si cycle in two contrasted tropical rivers of Southern India, the Cauvery and the Netravathi. Both river headwaters originate from the Western Ghats but the Cauvery basin is draining eastward to the Bay of Bengal while the Netravathi flows westward to the Arabian Sea. Because of the very humid climate along the western coast, the Netravathi basin is experiencing extreme weathering intensity and is responsible for high Si supply to the coast (Gurumurthy et al., 2012). The upper Cauvery basin is characterized by a sharp rainfall gradient, from 3000mm/yr to about 500mm within 100km. Most of the basin is under semi-arid to sub-humid conditions (Meunier et al., 2015). The major contrasting features of both basins are summarised in Table 1. They include:

(i) For Cauvery: longer and wider watershed with agriculture relying on irrigation from several large reservoirs along the main channels (rice and sugarcane as major crops) or from bore well irrigation in the semi-arid and sub-humid parts of the basin. The management of water in the reservoirs is highly controlled and discharge to the middle and lower parts (i.e., from Karnataka to Tamil Nadu states) is still a major dispute e.g. with violent riots in September 2016 (http://indianexpress.com/article/explained/cauvery-water-dispute-karnataka-tamil-nadu-supreme-court-3043193/). Currently, water diversion for irrigation accounts for about 80% of the total discharge to the sea, which thereby decreases the Si flux. In addition to irrigation, there is a huge human settlement in the Cauvery basin with more than 1500 km^{-2} as per 2001 census (WRIS. Cauvery Basin Report: Gov. of India 2014). Meunier et al. (2015) report no change in the chemical composition of the dissolved load since three decades.

(ii) In contrast, the Netravathi basin is much smaller (4.5 % of Cauvery basin) with 397 inhabitants km^{-2} and only 48% of the basin is cultivated (Pradhan et al., 2014 cited from ground water information booklet 2009, 2010) with no heavy water management as seen in the Cauvery basin.

This contrasted land uses and rainfall intensities in these two tropical rivers makes the comparison of both systems particularly interesting for the study of Si cycle and how it get affected via natural (weathering) and anthropogenic (land use) pressures.

Netravathi- SW	Cauvery- SE
Netravathi originates in the Western Ghats, flows West around 147 km and empty into the Arabian Sea.	Cauvery (Kaveri) originates in the Western Ghats and runs about 765km south-east and drains in to the Bay of Bengal.
Annual discharge = 12 Km^3 /yr and maximum during SW monsoon.	Average discharge= 4.5 km^3/ yr. receives water mainly during SW and partially from NE monsoon.
Poor water flow regulation. 94% of total discharge drains in to the sea.	Water flow is strongly controlled and maximum used for irrigation purpose (80%).
51% of agricultural land and 35% forest area.	66% of agricultural land and 20% forest area
Total number of dams=9	Total number of dams= 96
Inhabitants = 397 km^{-2}	Inhabitants= 1500 km^{-2}
No studies on eutrophication potential	13-54% pollution index and less or no eutrophication potential

Table 1 *Contrasting features of Cauvery (southeast) and Netravathi (Southwest) basin of Indian subcontinent.*

Therefore, we propose 1) to determine the seasonal variability of silicon isotopic signature for the first time in these two river systems and to understand the factors that drive the Si isotopic compositions in the Cauvery and Netravathi basins in order to 2) understand the effect of weathering, climate, and anthropogenic activities on Si cycle before entering into estuaries.

2. Study area and materials

2.1 River Settings, climate and hydrology

Cauvery basin – located between 10^0 07 'N to $13^0$28' N and 75^0 28'E to 79^0 52'E, runs about 765 km towards the southeast and drains an area of 81,155 km^2 from the Western Ghats to the Bay of Bengal (Fig. 1a). Cauvery drains three different states of India with 42% in Karnataka (origin of Cauvery, Thalakaveri), 54% in Tamil Nadu and the remaining 4 % in Kerala. Cauvery river basin covers the major part of the South Indian peninsula and is constituted by three sub-basins namely upper (Karnataka), middle (Karnataka and Tamil Nadu) and lower basins (Tamil Nadu). The important tributaries joining the Cauvery are, Hemavathi (H1), Kabini (K1), Shimsha (S) and Arakavathy (A), Bhavani (Fig. 1a). The Cauvery river basin experiences tropical monsoonal climate and influenced by southwest (SW) monsoon (June to September) in the upper basin and northeast (NE) monsoon in lower basin. The Western Ghats create rain shadow region and affect the SW monsoonal flow winds in the east inducing a sharp rainfall gradient from West (humid) to East (semi-arid). Therefore, Cauvery basin receives maximum rainfall during SW monsoon mainly in the upper reaches and partly in middle reaches which are responsible for 80% of the annual water flow and sediment load (Pattanaik et al., 2013). In contrast, lower reaches are influenced mainly by NE monsoon. Hence, mean rainfall distribution varies widely depending on locations from 6000 mm yr^{-1} in the Western Ghats to 300 mm yr^{-1} in the eastern parts during NE monsoon (Meunier et al., 2015). The tributaries like Arakavathy and Shimsha are less sensitive to the monsoonal effect and consequently are exposed to the pollution effects, especially Arakavathi river considered as polluted (35 to 45 % pollution index, Meunier et al., 2015) because it is acting as a drain for domestic and industrial effluents (Lele et al*.,* 2013). The average runoff of the basin was found to be 21.3 km^3 yr^{-1} (Integrated Hydrological Data Book 2012, cited by Meunier et al., 2015) but the diversion of water is extremely high to meet domestic and irrigation demands (80% of total runoff), yielding to a discharge to the sea as low as 4.5km^3 yr^{-1} (Meunier et al., 2015). Agriculture is the major land use on the basin with 66% of the total area and followed by forest cover (20%, WRIS. Cauvery Basin Report: Gov. of India 2014).

The Netravathi basin – lies between $12^0$29'11''N to $13^0$11'11''N and 74^0 49'08''E to $75^0$47'53''E and is surrounded by Tunga-Bhadra bain in North, Cauvery basin in the east and by the Arabian Sea in the West. It originates from densely forested Western Ghats (Chikmagalore) and runs about 147 km southwest to the Arabian Sea forming a common estuary with Gurupur river at Mangalore (Fig: 1b). The total drainage area of the basin is 3657 km^2. The major tributaries of Netravathi basin are Shanthimageru (Sha), Gundiya hole (Gun), Shishila hole (Shi) and Neriya hole (Ner) (Fig. 1b). The basin is characterized by high humidity and heavy rainfall (3600 - 4200 mm yr^{-1}, from http://www.imd.gov.in

cited by Gurumurthy et al., 2012). Likewise the upper Cauvery basin, the river flow is controlled by the SW monsoon and about 93% of total discharge occurs during June to October (Gurumurthy et al., 2012, 2014). The annual discharge from the river Netravathi is 12 km^3yr^{-1} (Karnataka irrigation Department 1986 cited by Gurumurthy et al., 2012). Since the basin is located in the Western Ghats, the upper basin is densely covered with forest cover limiting erosion probability (Ganasri et al., 2015) in the basin.

2.2 Geology of Cauvery and Netravathi Basin

Cauvery – The upper and middle reaches of the basin are composed of a silicate Precambrian basement comprising peninsular gneiss, charnockites and granitic rocks associated with metasedimentary and mafic rocks (Naqvi and Rogers, 1987; Shadakshara Swamy et al., 1995). Granulites and migmatitic gneisses are visible in the middle reaches. The lower reach of Shimsha drain mafic granulite, foliated charnockites and granitoid gneisses (Pattanaik et al., 2013). The lower reaches of Cauvery flow through the Cretaceous deposits composed of conglomeratic sandstone, limestone, shale and finally the alluvium plains (Pattanaik et al., 2007). The weathered layer (regolith) consists in thick laterite in the humid zone, ferralsol / vertisol developed on saprolite in the semi-arid zone of upper and middle and, alluvium in the lower reaches.

Netravathi – the basin primarily drains the metamorphic changeover zone of west dharwar craton comprising trondhjemite – tonalite - granodiorite suite (Naqvi and Rogers, 1987). Overall, the basin is composed of 83% migmatites and granodiorites, 6% metasediments, 5% charnockites and 2% laterites and amphibolites (Gurumurthy et al., 2012, 2015) [Fig. 1b]. The regolith cover is composed of thick laterites (Gurumurthy et al., 2012).

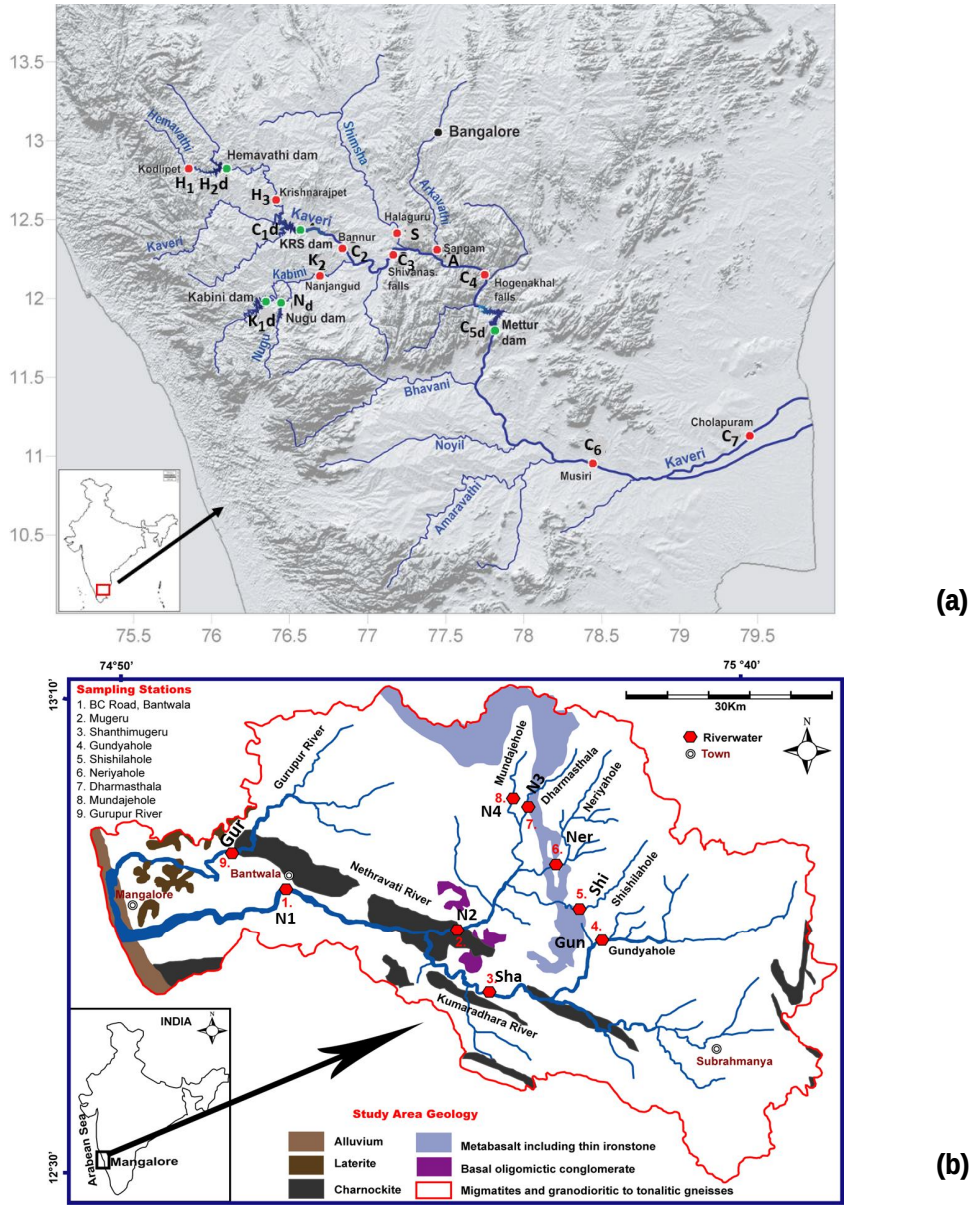

Fig. 1*, Location map of Cauvery (a) and Netravathi (b) basins showing the sampling stations. (a) Sample locations with the first letter for the river name (C = Cauvery, H = Hemavathi, S: Shimsa, K: Kabini, A: Arkavathi); dams are indicated in green by the suffix "d"; suffix numbers indicate station downstream. (b) Netravathi mainstream sampling stations are indicated by the letter "N" and the numbers are the station number. Tributaries of Netravathi basin are indicated by their first three letters (for example, Sha=Shanthimugeru, Gun= Gundyahole etc.). Finally "Gur" represents the river Gurupur, flowing adjacent to the Netravathi basin (modified from Meunier et al., 2015 and Gurumurthy et al., 2012).*

2.3. Materials

In Cauvery basin, the water samples were collected in 10 riverine and 5 reservoirs stations during summer season (May 2007) and monsoon (July 2007). In Netravathi basin, the samples were collected at 9 riverine stations (no reservoirs) during summer season (April 2010), monsoon (July 2010) and post monsoon (Dec-2010). Dissolved cations were measured by Atomic Absorption Spectroscopy at Geosciences Environnement Toulouse while silicic acid was determined by spectro-photometry (blue method) at the Indo-French Cell for Water Sciences (IRD-IISc, Bangalore). The sample collection procedures, details of parameters and analysis information (dissolved load concentration) are described in Meunier et al. (2015) for Cauvery basin. For Netravathi basin, the sampling and analytical procedures can be found in Gurumurthy et al. (2012). The DSi concentration and Si isotopic measurements were carried out at LOCEAN, UPMC- Paris. The sample preparation and procedures for Si isotope measurements were discussed in Chapter 2. The reproducibility of Si isotopic analyses of the 43 (river and estuarine) samples have been fully replicated with an average reproducibility of ± 0.1 ‰ (±1 σ_D, cf. Chapter 2 for complete details about analytical precision). The significant tests are performed using T-stat and the p-values are always given.

Major cations

In order to assess the contribution of bedrock weathering to the flux exported by the river, cations concentrations are usually corrected from atmospheric deposits assuming seawater origin according to the equation (1):

$$X^* = X_{river} - Cl^-_{river} * (X / Cl^-)_{Seawater} \quad \text{Eq. (1)}$$

The X_{river} and Cl^-_{river} are the concentrations of element X and Cl^- in the river water respectively and $(X/Cl^-)_{Seawater}$ is the element X to Cl ratio of seawater. The atmospheric corrected (indicated by *) major cations are depicted in the Tables 1 and 2.

We also employed another proxy of silicate weathering degree, the Re index proposed by Boeglin and Probst (1998). Re index is mainly based on the silicate-derived dissolved cations during weathering and Si concentration in the river (Equation 4)

$$Re = (3Na^+ + 3K^+ + 1.25Mg^{2+} + 2Ca^{2+} - DSi) / (0.5\,Na^+ + 0.5K^+ + 0.75\,Mg^{2+} + Ca^{2+}) \quad (2)$$

The coefficients used in the above formula correspond to the average granite containing feldspar, mica and Mg-silicate minerals such as amphiboles on the numerator while the release of Na and K from carbonate induced weathering is corrected with the denominator. Re index is also equivalent to the molar ratio (DSi/Al_2O_3) of secondary mineral formation within the soil profile (Tardy, 1971).

Weighted average calculation

The data for sampling discharge of Netravathi (we used the year 2012 due to lack of data during 2010) and Cauvery (during 2007) rivers are from http://www.india-wris.nrsc.gov.in/wris.html , government of India. Discharge weighed Si isotopic composition supplies to the coastal areas are calculated using the formula:

Weighted isotopic composition ‰ = [(δ^{30}Si-DSi $_{dry}$ x DSi supply $_{dry}$ / DSi supply $_{(dry+wet)}$) + (δ^{30}Si-DSi $_{wet}$ x DSi supply $_{wet}$ / DSi supply $_{(dry+wet)}$)].

3. Results

3.1 Dissolved load concentrations

3.1.1 Dissolved silicon (DSi)

The DSi concentrations of individual samples studied for Cauvery and Netravathi basins are provided in Tables 2 and 3 respectively. The DSi concentration of Cauvery and Netravathi basins varied 289 ± 143 µM and 196 ± 61 µM respectively. Though the origin of both rivers is the Western Ghats, the DSi concentrations of both complete river basins are significantly different (p=0.002) irrespective to the seasons.

	Cauvery	δ^{30}Si-DSi ‰	std err	DSi µM	Na*	Ca*	K*	Mg*	ΣC+ *	DSi / (Na+K)*	DSi / (Na)*	Re index
	Dry season				**(µM) adopted from Meunier et al 2015**							
	Reservoirs											
H_{2d}	Hemavathi dam	2.1	0.05	208	90	211	28	114	443	1.8	2.3	2.0
C_d	Cauvery dam			309	432	596	30	518	1576	0.7	0.7	2.4
$_{Nd}$	Nugu dam	2.8	0.04	231	107	234	55	147	544	1.4	2.2	2.1
K_{1d}	Kabini Dam	1.9	0.05	234	76	165	26	107	373	2.3	3.1	1.8
C_{5d}	Cauvery dam	2.4	0.06	296	621	460	44	527	1652	0.4	0.5	2.8
	River + tributaries											
H_1	Hemavathi river	1.9	0.04	352	116	139	40	118	412	2.3	3.0	1.8
H_3	Hemavathi	2.2	0.05	232	109	292	33	165	599	1.6	2.1	2.0
K_2	Kabini river	1.9	0.05	320	269	481	29	404	1183	1.1	1.2	2.2
C_2	Cauvery river	2.1	0.04	362	360	890	43	603	1896	0.9	1.0	2.2
C_3	Cauvery river	1.8	0.07	393	475	600	29	557	1660	0.8	0.8	2.4
S	Shimsha river	2.1	0.05	697	2266	423	79	801	3568	0.3	0.3	3.7
A	Arakavathi river	2.4	0.04	602	791	839	86	689	2405	0.7	0.8	2.5
C_4	Cauvery river	1.9	0.05	427	557	594	30	612	1793	0.7	0.8	2.4
C_6	Cauvery river	2.4	0.17	397	486	416	57	481	1440	0.7	0.8	2.5
C_7	Kollidam	2.7	0.05	393	415	656	86	553	1711	0.8	0.9	2.4
	Overall Average	*2.2*		*363*	*478*	*466*	*46*	*426*	*1417*	*1.1*	*1.4*	*2.4*
	SD	*0.3*		*136*	*541*	*233*	*22*	*235*	*876*	*0.6*	*0.9*	*0.5*
	Wet season											
	Reservoirs											
H_{2d}	Hemavathi dam	1.6	0.04	159	142	149	35	81	407	0.9	1.1	2.6
C_d	Kaveri dam	1.2	0.04	160	56	185	27	92	359	1.9	2.9	1.9
$_{Nd}$	Nugu dam	2.2	0.04	227	69	182	60	109	421	1.7	3.3	2.0
K_{1d}	Kabini Dam			131	14	85	26	41	166			1.5
C_{5d}	Kaveri dam	1.5	0.04	198	264	353	38	280	935	0.7	0.7	2.5
	River + tributaries											
H_1	Hemavathi river	0.3	0.05	145	21	55	12	34	122	4.5	7.0	1.1
H_3	Hemavathi	1.1	0.05	153	32	119	30	62	243	2.5	4.9	1.8
K_2	Kabini river	0.8	0.04	158	21	89	25	46	182	3.4	7.5	1.5
C_2	Cauvery river	0.5	0.04	172	49	190	24	91	355	2.3	3.5	1.8
C_3	Cauvery river	0.8	0.04	176	49	281	25	86	441	2.4	3.6	1.9
S	Shimsha river	2.6	0.01	540	2270	531	87	850	3738	0.2	0.2	3.7
A	Arakavathi river	0.8	0.04	191	92	244	30	128	494	1.6	2.1	2.1
C_4	Cauvery river	0.9	0.03	260	106	261	34	136	535	1.9	2.5	2.0
C_6	Cauvery river				352	507	52	328	1239			2.8
C_7	Kollidam	1.7	0.01	246	298	473	48	300	1119	0.7	0.8	2.4
	Overall Average	*1.2*		*208*	*256*	*247*	*37*	*178*	*717*	*1.9*	*3.1*	*2.1*
	SD	*0.7*		*103*	*568*	*155*	*18*	*209*	*902*	*1.2*	*2.3*	*0.6*

Table 2 *Si isotopes, DSi and dissolved cations (atmospheric corrected *) measured in the Cauvery river basin during dry and wet periods respectively. The Ratio of DSi/ (Na+K), DSi/Na* and Re index are used to characterise the proportion of Si remaining immobilized in the secondary minerals and the type of weathering in the basin.*

	Netravathi	δ^{30}Si-DSi ‰	std err	DSi	Na*	Ca*	K*	Mg*	ΣC+ *	DSi/ (Na+K)	DSi/ (Na)*	Re index
	Dry period - April 2010					**µM**						
N1	Bantwal BC Road											
N2	Mugeru	1.6	0.04	220	115	109	41	63	328	1.4	1.9	2.3
Sha	Shanthimageru	NA	NA	240	101	98	40	89	329	1.7	2.4	2.1
Gun	Gundyahole	1.7	0.04	268	115	111	43	86	355	1.7	2.3	2.1
Shi	Shishilahole	0.5	0.03	163	58	55	21	33	167	2.1	2.8	1.9
Ner	Neriyahole	1.4	0.04	250	111	78	26	61	277	1.8	2.2	2.1
N3	Dharmasthala	NA	NA	232	112	103	31	54	300	1.6	2.1	2.2
N4	Mundaje Hole	1.5	0.04	307	146	98	25	58	328	1.8	2.1	2.1
Gur	Gurupura River	NA	NA	166	99	108	36	64	306	1.2	1.7	2.4
	Wet-Monsoon-July 2010											
N1	Bantwal BC Road	0.8	0.04	169	36	48	18	31	134	3.1	4.7	1.3
N2	Mugeru	0.6	0.05	155	46	54	16	32	148	2.5	3.4	1.7
Sha	Shanthimageru	0.5	0.06	141	34	48	16	35	133	2.8	4.2	1.5
Gun	Gundyahole	NA	NA	147	35	46	15	34	130	2.9	4.2	1.4
Shi	Shishilahole	0.5	0.07	170	42	52	14	36	145	3.0	4.0	1.4
Ner	Neriyahole	0.4	0.06	173	53	49	13	34	149	2.6	3.3	1.5
N3	Dharmasthala	0.7	0.09	182	55	63	15	37	171	2.6	3.3	1.6
N4	Mundaje Hole	0.9	0.09	198	64	60	15	37	177	2.5	3.1	1.6
Gur	Gurupura River	0.4	0.04	389	26	40	14	19	99	9.8	15.1	-2.2
	Post monsoon- Dec 2010											
N1	Bantwal BC Road											
N2	Mugeru	1.0	0.03	160	94	77	17	58	246	1.4	1.7	2.3
Sha	Shanthimageru	1.2	0.05	176	66	65	15	64	209	2.2	2.7	1.8
Gun	Gundyahole	1.1	0.03	159	100	73	17	71	261	1.4	1.6	2.3
Shi	Shishilahole	1.2	0.03	153	82	68	14	74	238	1.6	1.9	2.1
Ner	Neriyahole	NA	NA	158	74	65	14	72	224	1.8	2.1	2.0
N3	Dharmasthala	NA	NA	144	116	88	18	56	277	1.1	1.2	2.6
N4	Mundaje Hole	1.5	0.03	122	107	82	16	57	262	1.0	1.1	2.6
Gur	Gurupura River	1.2	0.03	249	63	69	18	46	195	3.1	4.0	1.3
	Overall Average	*1.0*		*196*	*78*	*72*	*21*	*52*	*224*	*2.4*	*3.2*	*1.8*
	SD	*0.4*		*61*	*33*	*22*	*10*	*19*	*76*	*1.7*	*2.7*	*0.9*

Table 3 *Si isotopes, DSi and dissolved cations (atmospheric corrected *) measured in the Netravathi river basin during dry, wet and post monsoon periods respectively. The Ratio of DSi/ (Na+K)*, DSi/Na* and Re index are used to characterise the proportion of Si remaining immobilized in the secondary minerals and the type of weathering in the basin.*

In *Cauvery* – the DSi concentration of the main stream (Fig. 2a, samples named as "C") samples are homogenous 387 ± 27 µM and 200 ± 50 µM during dry and wet seasons respectively with a significant

seasonal difference ($p < 0.001$). The tributaries Hemavathi "H3" and Kabini "K2" (232 and 320 µM) are comparable to the mainstream, while tributaries Shimsha "S" and Arakavathi "A" (697 and 602µM) are ~3 folds higher than the mainstream during dry period (Fig. 2a). Likewise, during wet season, all tributaries showed similar DSi concentration (167 ± 21 µM), consistent with the main stream except "S" (540 µM) because this sub-watershed, located in the semi-arid area, did not have received much rain at the period of sampling (Fig. 2a). However, the reservoirs (H_2d- C_5d) are less variable with significant seasonal variation during dry and wet periods (256 ± 44 and 175 ± 38 µM, respectively, t stat= 3.1, p=0.01). It is interesting to note that the DSi concentration of reservoirs/dams is significantly less than the main stream during dry period (t stat= 5.8, p=0.001), but there is no such decrease of DSi load during wet period which exhibit similar concentration as mainstream.

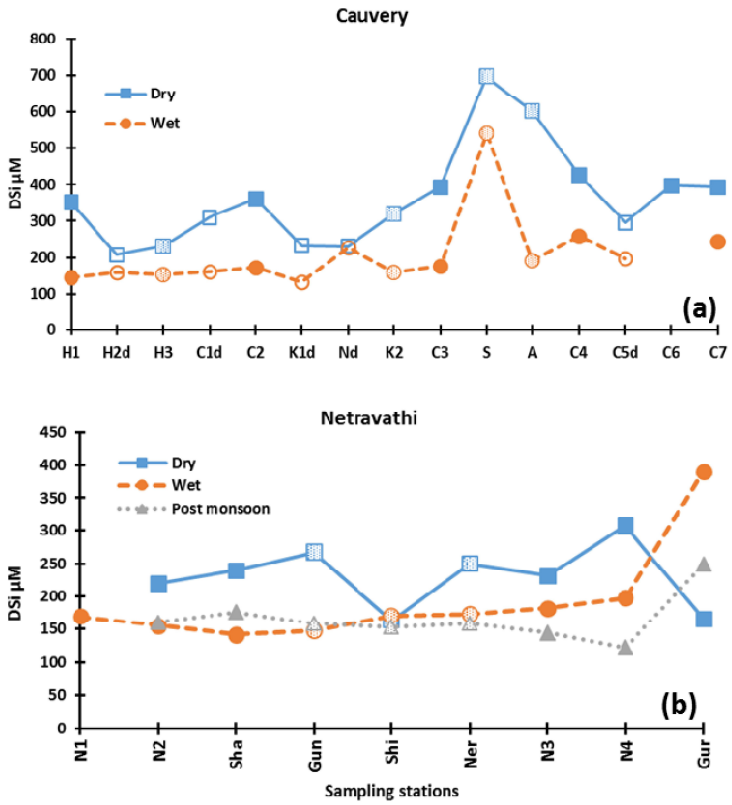

Fig. 2 *Spatial and seasonal variability of DSi (µM) concentration in the Cauvery (2a) and Netravathi (2b) river basins during dry and wet periods. Water flow is from left to right. The open squares and circles represent the dams, dotted squares and circles represent the tributaries, filled squares and circles represent the main stream during dry (blue squares) wet (orange circles) and post-monsoon (grey triangles) periods respectively. . The numbers refer to different stations starting from 1 then downstream.* ***(a)*** *Each capital letter represents the river sampled: C for Cauvery mainstream and other*

letters for tributaries (H = Hemavathi, S: Shimsa, K: Kabini, A: Arkavathi). The subscript letter "d" refers to damsRefer to table 1 for full names of rivers and dams. ***(b)*** *The Netravathi mainstream is indicated by the letter "N" followed by the station number downstream. The tributaries are indicated by their first three letters (for example, Sha= Shanthimugeru). Refer to table 2 for full names of tributaries. "Gur" represents the river Gurupur, joining the river Netravathi forming common estuary.*

In Netravathi – Similar to Cauvery, the DSi concentrations of main stream (Fig. 2b, samples with "N") samples are homogenous with 250 ± 39 µM, 169 ± 22 µM and 151 ± 23 µM during dry, wet and post monsoon periods respectively. The concentrations are significantly different between dry and wet periods of the main stream (p =0.02). The Gurupur river (sample "Gur") exhibits more variable DSi concentration than Netravathi, with 166, 389 and 249 µM during dry, wet and post monsoon seasons respectively (Table 3, Fig. 2b). In contrast, the other tributaries exhibit similar concentrations to the mainstream during dry, wet and post monsoon seasons (230 ± 46, 158 ± 16 and 161 ± 10 µM, respectively). Except for the seasonal difference, the entire Netravathi basin appears to be relatively homogenous excluding Gurupur tributary which is mostly draining lowland area.

3.1.2 Dissolved cations load

For Cauvery basin, the concentrations of dissolved cations were taken from Meunier et al., (2015) for the same samples. The average total dissolved cation concentration ($\Sigma C+^* \pm 1\ \sigma_D$) of the Cauvery basin is 1417 ± 876 µM and 717 ± 902 µM during dry and wet periods respectively and for Netravathi, 299 ± 58, 143 ± 23 µM and 239 ± 28 µM during dry, wet and post monsoon seasons respectively (Fig. 3a and b). River Cauvery exhibits a wide range of variability with ~ 5 folds higher $\Sigma C+^*$ concentration than the Netravathi basin. As expected, the solutes of both basins tend to be less concentrated during wet period because of the dilution effect (Ramanathan et al., 1994; Pattanaik et al., 2013). Nevertheless there are significant changes between these two basins (p=0.02) that could possibly explain the different water sources. This hypothesis will be tested in the following discussion. In addition, a significant seasonal difference of $\Sigma C+^*$ concentration (Fig. 3a and 3b) noticed for both Cauvery ($p < 0.05$) and Netravathi ($p < 0.001$) basin. It is also notable that the $\Sigma C+^*$ of the mainstream and tributaries of Cauvery basin tend to clearly increase towards the lower reaches (Fig. 3a) during both seasons (relatively higher during dry) and exceptionally very high concentration in Shimsa ("S" for both seasons) and Arakavathi ("A" for dry

season). In contrast, in Netravathi, the ΣC+* tend to be similar in the entire basin during all seasons except "Shi" of dry period (Fig. 3b).

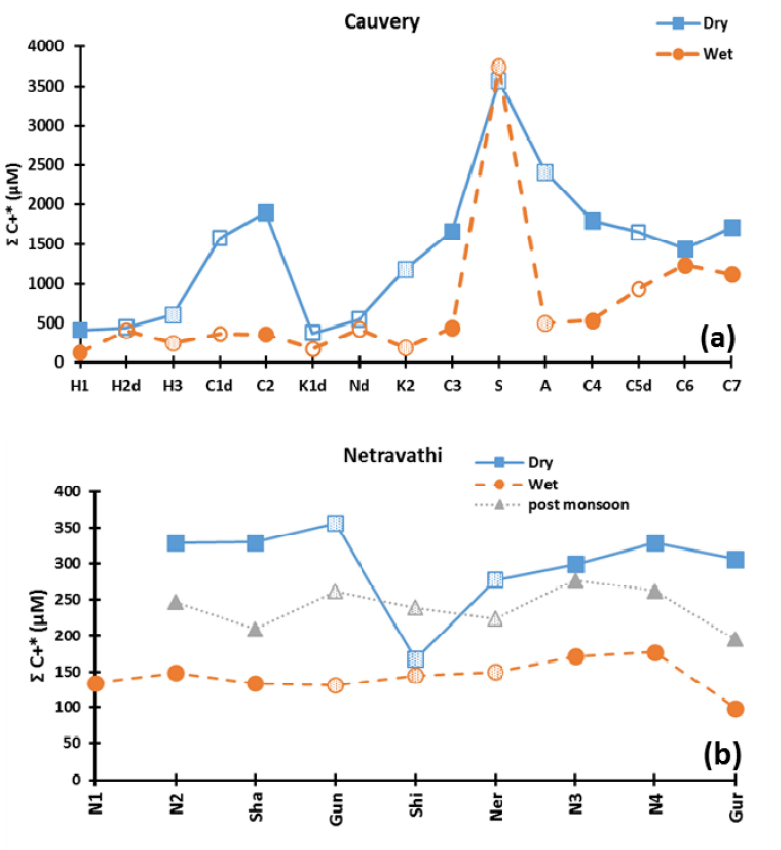

Fig. 3 *Spatial and seasonal variability of dissolved cations (atmospheric corrected- Σ C+*in µmol/L) concentration in the Cauvery (a) and Netravathi (b) river basins during dry and wet periods respectively. The open squares and circles represent the dams, dotted squares and circles represent the tributaries, filled squares and circles represent the main stream during dry (blue squares) wet (orange circles) and post-monsoon (grey triangles) periods respectively.* ***(a)*** *Each capital letter represents the river sampled: C for Cauvery mainstream and other letters for tributaries (H = Hemavathi, S: Shimsa, K: Kabini, A: Arkavathi). The subscript letter "d" refers to dams. The numbers refer to different stations starting from 1 then downstream. Refer to table 1 for full names of rivers and dams.* ***(b)*** *The Netravathi mainstream is indicated by the letter "N" followed by the station number downstream. The tributaries are indicated by their first 3 letters. Refer to table 2 for full names of tributaries. "Gur" represents the river Gurupur, joining the river Netravathi forming common estuary.*

3.2 Seasonal variability of δ^{30}Si in Cauvery and Netravathi basins

The Si isotope compositions of Cauvery and Netravathi river basins are given in Tables 2 and 3. All δ^{30}Si-DSi follow the mass dependent fractionation line of Si as shown in Chapter 2, which allows ruling out isobaric interferences during MC-ICP-MS measurements. All the samples of Cauvery and Netravathi basins carry a positive value of δ^{30}Si-DSi consistent with previous studies showing that weathering and biological processes fractionate Si, by incorporating lighter isotope in secondary clays and in plants and deviate from the average igneous δ^{30}Si of -0.3 to 0.3 ‰ (Ding et al., 1996) leaving heavier isotopic composition in DSi (De la Rocha et al., 2000, Ding et al., 2004). The average δ^{30}Si-DSi of the river Cauvery (1.73 ± 0.71 ‰) is ~0.7 ‰ heavier than the Netravathi basin (0.99 ± 0.43 ‰), a difference which is significant ($p < 0.001$) (Fig. 4a and b). The δ^{30}Si-DSi of the Cauvery and Netravathi basins are comparable with the world tropical rivers (Fig. 5). Cauvery basin is found to be slightly heavier than other tropical, subtropical, and temperate basins with wide variability but comparable to Ganges-Brahmaputra basin whereas river Netravathi is similar to the other tropical basins.

In Cauvery basin, the seasonal influence is well evidenced between dry (base flow) and wet (high flow) seasons with δ^{30}Si ~1‰ heavier during dry period ($p < 0.001$) [Fig. 4a]. The Si isotopic composition is heavier during the dry season (2.2 ± 0.3 ‰) than in the wet season (1.2 ± 0.7 ‰) which likely indicates the effect of monsoon on type of solution leached as discussed later. Similar to dissolved load concentrations, the slight enriching trend of silicon isotopes towards lower reach might enlighten the presence of biogeochemical processes within rivers in both the seasons as discussed later. Noteworthy, there is no significant variability of silicon isotopes between reservoirs, tributaries and mainstream except Nugu dam (Nd) where the heaviest isotopic composition was measured during dry period (+2.8 ‰; Table 1 and Fig. 4a). Unlike dry period, during wet period the silicon isotope compositions are variable but not significantly different among tributaries (1.3 ± 0.9 ‰), reservoirs (1.6 ± 0.4 ‰) and mainstream (0.9 ± 0.5 ‰).

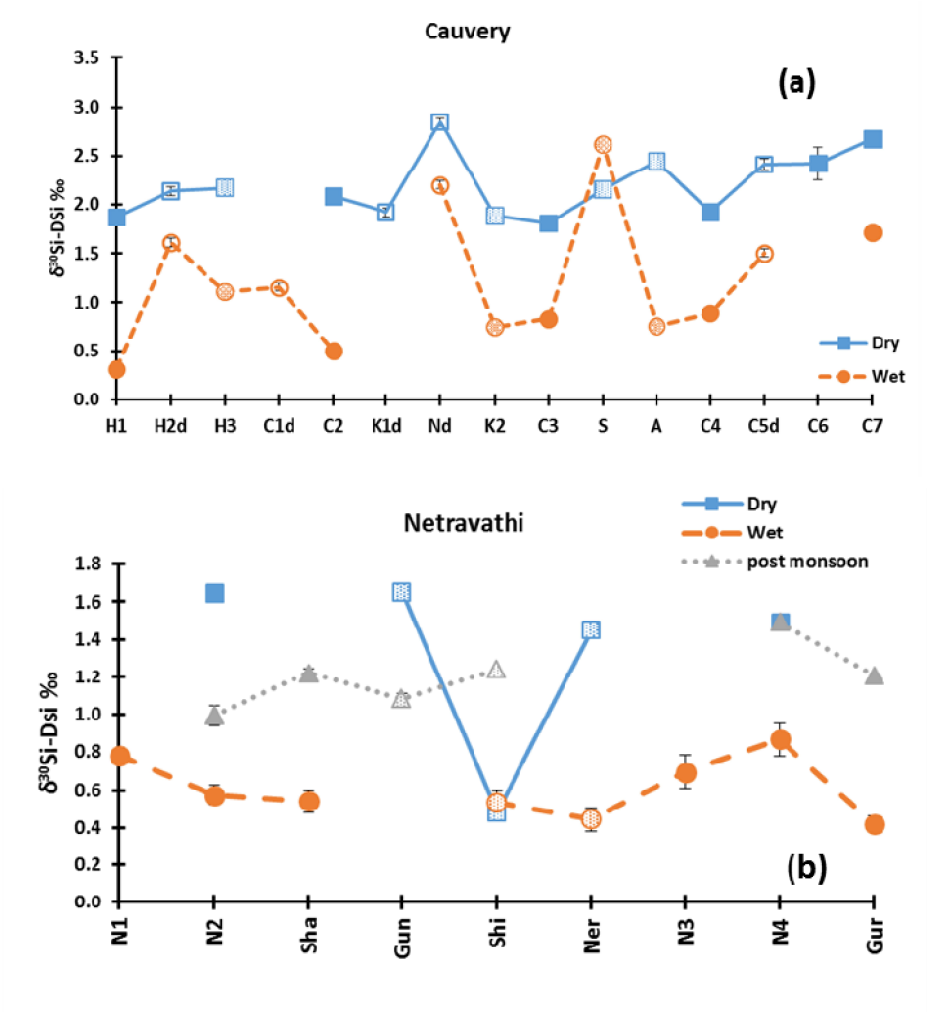

Fig. 4 *Spatial and seasonal variability of silicon isotopes of DSi (δ^{30}Si-DSi ‰) composition in the Cauvery (a) and Netravathi (b) river basins during dry and wet periods respectively. The open squares and circles represent the dams, dotted squares and circles represent the tributaries, filled squares and circles represent the main stream during dry (blue squares) wet (orange circles) and post-monsoon (grey triangles) periods respectively.* ***(a)*** *Each capital letter represents the river sampled: C for Cauvery mainstream and other letters for tributaries (H = Hemavathi, S: Shimsa, K: Kabini, A: Arkavathi). The subscript letter "d" refers to dams. The numbers refer to different stations starting from 1 then downstream. Refer to table 1 for full names of rivers and dams.* ***(b)*** *The Netravathi mainstream is indicated by the letter "N" followed by the station number downstream. The tributaries are indicated by their first 3 letters of the tributary name. Refer to table 2 for full names of tributaries. "Gur" represents the river Gurupur, joining the river Netravathi forming common estuary.*

In Netravathi basin there is a significant seasonal impact ($p < 0.05$), but no significant difference in spatial variability of Si isotope compositions (1.6 ± 0.1‰) in the entire basin except tributary (Shishilahole,"Shi") during dry period which is particularly light (0.5 ‰, Table 2 and Fig. 4b). It is interesting to note that the dissolved load concentration of "Shi" also remains lower when compared to the other stations during the dry period (163 μM, Fig. 4b). No such lower dissolved load concentration and lighter isotopic composition were noticed at "Shi" during the wet season (Fig. 4b). The variability of isotope composition lies close to the analytical reproducibility (± 0.11 ‰) indicating that the processes responsible for the δ^{30}Si signatures in the various parts of the watershed are quite homogeneous during wet and post monsoon seasons respectively.

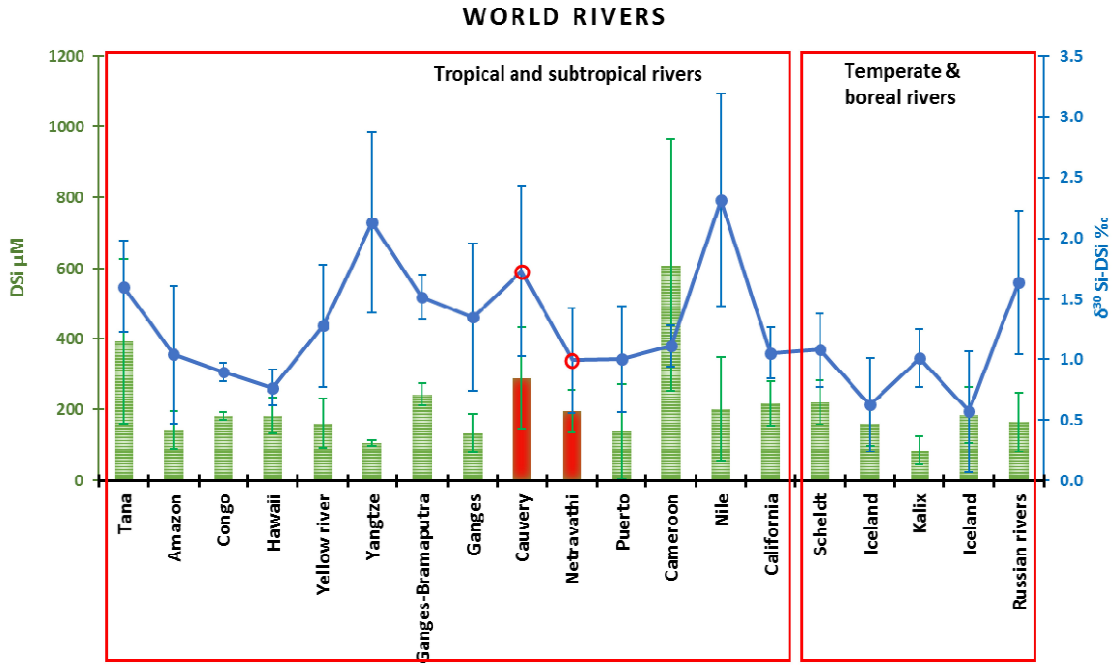

Fig. 5 *Comparison of World Rivers DSi concentration and dissolved Si isotopic composition with standard deviations. The data from the present study are highlighted in red. Rivers Tana (Hughes et al., 2012), Amazon (Hughes et al., 2013), Congo (Hughes et al., 2011; Cardinal et al., 2010), Hawaii (Ziegler et al., 2005), Yellow river (Ding et al., 2011), Yangtze (Ding et al., 2004), Ganges-Brahmaputra (Georg et al., 2009), Ganges (Fontorbe et al., 2013), Puerto (Ziegler et al., 2005), Cameroon (Opfergelt et al., 2009), Nile (Cockerton et al., 2013), California (De La Rocha et al., 2000), Scheldt (Delvaux et al., 2013), Iceland rivers (Georg et al 2007), Kalix (Engstrom et al., 2010), Iceland (Opfergelt et al., 2013) and Russian rivers (Pokrovski et al., 2013).*

4. Discussion

4.1 General overview

The riverine dissolved silicon of this study is always enriched in heavier isotopes relative to the mean continental crust and lies within the range (-0.1 ‰ up to 3.4 ‰) of world rivers reported so far (e.g., De la Rocha et al., 2000, Ding et al., 2004, Alleman et al., 2005, Cardinal et al., 2010 and Hughes et al., 2012). Generally, the positive isotopic signatures are explained as the resulting from two main processes: 1) weathering and secondary clay mineral formation (Georg et al., 2007) and 2) biological silica production (e.g. diatom uptake in rivers and plant uptake in soils forming phytoliths). These processes preferentially mobilize light Si isotopes and result in the heavy isotopic composition of Si remaining in the dissolved phase. The influence of these two major processes on different seasons in the rivers Cauvery and Netravathi are discussed in the next sections.

4.1.1 Cauvery

The Western Ghats receive maximum rainfall from SW monsoon which is responsible for 80% of the total annual flow in the upper reach of the Cauvery River (Pattanaik et al., 2013). Therefore, the lower concentration of solutes during monsoon is possibly due to 2 major reasons (Fig. 2a): 1) dilution effect and 2) different sources of water during both seasons and their interaction with bedrock and regolith (loose unconsolidated rock which includes soil). The contribution of SW monsoon flow decreases towards lower reach which receives water only during the NE monsoon in the Shimsha and Arakavathy rivers (S, A) respectively (Pattanaik et al., 2013). Moreover, the diversion of water for irrigation and domestic purpose represent 80% of the total runoff on the Cauvery Basin (21.3 km^3 yr^{-1}, Kumar et al., 2005) leaving a low runoff of 4.5 km^3yr^{-1} into the sea (Meunier et al., 2015). Undoubtedly, the diversion of water flow for irrigation purpose and water storage may modify the intensity of geochemical processes (mainly weathering) by increasing the soil-water residence time and may alter the Si signature before entering the estuary. Therefore, exceptionally heavier isotopic composition at S- Shimsha river on the lower reach in both the seasons (+2.6‰, Table 1 and Fig. 4a) may be due to the absence of discharge. In river Tana (East Africa) Hughes et al. (2012) noticed that the increased residence time of soil water due to less water flow led to concentrated minerals in the river. Simultaneously, it favors the

formation of clay minerals incorporating lighter isotopes and increasing the δ^{30}Si of DSi in the river. Our data are thus consistent with such process.

During the wet period, the dilution effect is generally seen in dissolved load concentration, but the Si isotopic composition is variable which cannot be explained by dilution (Fig. 4a). Indeed, the Si isotopic signature of the mainstream is gradually getting heavier towards the lower reach, while the tributaries and reservoirs exhibit higher variability during wet period (Fig. 4a). The rainfall as well as the water flow are important factors controlling the intensity of weathering and erosion and might be responsible for the Si isotope variations under different weathering regimes. The δ^{30}Si signature of the dissolved silicon (DSi) exported to the Cauvery estuary for the studied period is estimated at 1.34 ‰ (weighed for DSi flux) which is heavier than the Amazon basin reported by Hughes et al, 2013 (0.92 ‰).

4.1.2 Netravathi

Unlike Cauvery, the absence of spatial variability of dissolved load and Si isotopic compositions (except "Shi" during dry period) suggests the homogeneity of this much smaller basin (Fig. 4b). The reduced dissolved load and lighter isotopic composition in "Shi" during dry is quite notable since, contrary to all other samples, it is similar to the wet composition. The low ΣC+, δ^{30}Si and DSi for dry-Shi might be explained by the different minerals of this catchment from others for e.g., Na-poor minerals (6% metasediments, Gurumurthy et al., 2012). For the other samples, the Si isotopes indicate that discharge-driven processes like dilution (on concentrations only) and intensity of weathering are the controlling processes in this basin with particularly high runoff 3300 mm yr^{-1} (Gurumurthy et al., 2012). The δ^{30}Si signature of the dissolved silicon (DSi) exported to the Netravathi estuary for the studied period is estimated at 0.61 ‰ (weighed for DSi flux, discharge of the 2012 period is used from http://www.indiawris.nrsc.gov.in/WRIS.html) which is two times less than Cauvery basin and lighter than Amazon and Congo basins or estimated world river average (around 0.74 ‰, Frings et al. 2016).

4.2 Weathering process

Apart from monsoonal variability, in order to understand the processes that control the Si isotope composition we compared δ^{30}Si with other geochemical proxies of weathering. Weathering and successive clay formation are the important processes driving the riverine δ^{30}Si and it has been well

observed in several tropical and temperate systems (e.g., Swiss rivers-Georg et al., 2006, Amazon basin-Hughes et al., 2013).

In *Cauvery,* we observe generally good correlations on the entire basin between $\delta^{30}Si$, DSi and ΣC+* concentrations (Fig. 7a and b). This is consistent with the preferential incorporation of light Si isotopes in the secondary weathering products whereas heavier Si isotopes are released in the dissolved phase along with highly soluble cations relative to the parent silicate material (Ziegler et al., 2005). Therefore the $\delta^{30}Si$ compositions are mainly controlled by weathering and clay mineral formation in the whole basin. However the overall positive correlation between Si isotopes and DSi concentration appears mainly because of the seasonal difference (Fig. 7a and b). Indeed, there is no clear relationship between $\delta^{30}Si$, DSi concentration and ΣC+* during dry period only. In general, the ratios of major cations are more conservative and serve as a proxy for weathering reactions. Unlike other major cations, dissolved Na* and K* (* indicates atmospheric corrected) mainly originate from their direct solubilisation during silicate bedrock weathering. Therefore, Na* and K * are considered as a proxy to identify the weathering of primary minerals. A study on the Amazon basin used the DSi/(Na*+K*) ratio to determine the proportion of Si remaining immobilized in the secondary minerals (Hughes et al., 2013). Thus, a lower ratio in solution indicates a higher proportion of Si remaining immobilized in secondary clay minerals.

A ratio lower than 2, is indicative of smectite formation (bisiallitization with formation of 2:1 clays), ratio from 2 to 3.5 indicates kaolinite formation (monosiallitization with formation of 1:1 clays) and ratio greater than 3.5 indicates that all silicon is leached which results in gibbsite formation (allitization process) (Tardy 1971; Hughes et al., 2013). However, K is possibly incorporating into the clay minerals like Illite and by vegetation as their plant nutrients. This may deviate the ratio and may change the interpretation of the type of chemical weathering. Therefore it might be more accurate to use DSi/Na* because Na is an excellent marker for the first stage of weathering of primary minerals (e.g., Na-Plagioclase) since it is highly soluble and not incorporated in the secondary minerals. However, if we use DSi/Na*, we do not have the threshold values to explain the type of clay minerals formation as explained by Hughes et al (2013). Therefore we compare both the ratios (DSi/Na* and DSi/(Na+K)*) to understand the clay mineral formation.

The Figure 7c and d show, as expected, the negative relationship between $\delta^{30}Si$ and DSi/(Na*+K*) or DSi/ Na*. This confirms that high proportion of Si remaining immobilized in the clay minerals (low ratio)

is associated with heavier Si isotopic signatures of DSi released. Most samples have DSi/(Na*+K*) or DSi/Na* ratios consistent with the smectite type weathering (bisiallitization), some with kaolinite type of weathering and one with alitilization process. Bisiallitization type of weathering occurs during dry period (base flow) with increased residence time of soil water in the deeper weathering front and interaction with the bed rock (saprolite) leaches more cations and higher DSi concentration in the solution. During this process the lighter isotopes are incorporated in to clay minerals formed leaving with heavier isotopic composition in the solution. This similar mechanism also noticed in the lower reaches of the wet period (including the dams) (Fig. 7c and d). Likewise, the monosiallitization type of weathering occurs during wet period (rainfall amount increases). During this period, the interaction of soil water (young water) with the superficial soil from heavily weathered minerals and it is referred as intense weathering because of the kaolinite formation by leaving lighter Si isotopic composition in the solution (Fig. 7c and d). Therefore, the isotopic composition is greatly governed by the interaction of soil water and type of weathering occurring in the basin. In addition, a strong negative relationship between δ^{30}Si and increasing discharge during wet period (R^2 =0.76, n=5, $p<0.05$, excluding "S", Fig. 8) suggests the influence of monsoon (young rain water) with lighter isotopic signature due to the higher flushing rate and interaction with superficial soils. In contrast, there is no relationship between δ^{30}Si and discharge during dry period since the discharge is very meagre (Fig. 8) but with heavier isotopic signature indicating the higher residence time of soil water (old base flow water) might favour weathering and concurrent clay mineral formation.

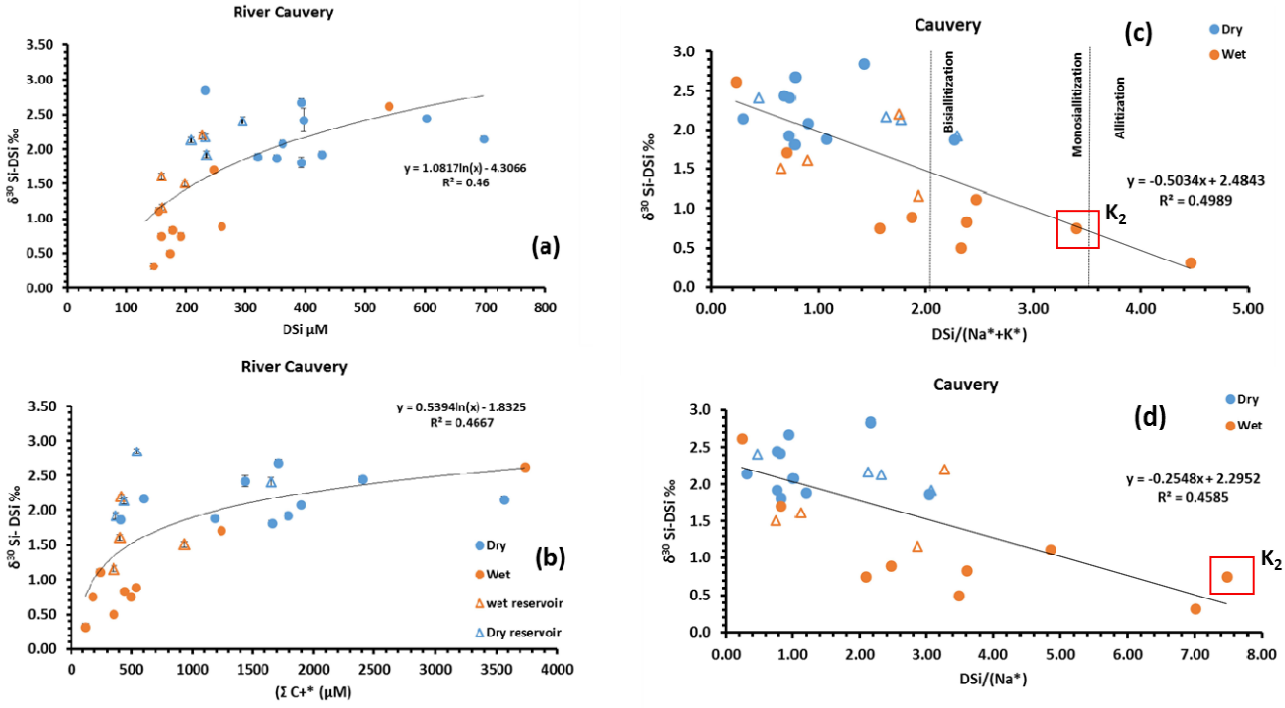

Fig. 7 *Si isotopic signature in the river Cauvery during dry and wet periods, (a) with dissolved Si concentration. (b) With the sum of major cations (corrected for atmospheric inputs). (c) with DSi/(Na*+K*) ratio or (d) DSi/Na* ratio depending on the Si remaining immobilized in secondary minerals and also the type of clay mineral formation during weathering process and their relationship with Si isotopes. The dashed lines representing the limits of different clay mineral formation processes (section 4.3 for details). The reservoirs are represented by open triangles during dry and wet period respectively. The red encircled values from the station K_2 (Kabini) showing a huge shift from monosiallitzation (DSi/(Na+K)* to Allitization (DSi/Na*) process after removing the K intrusion.*

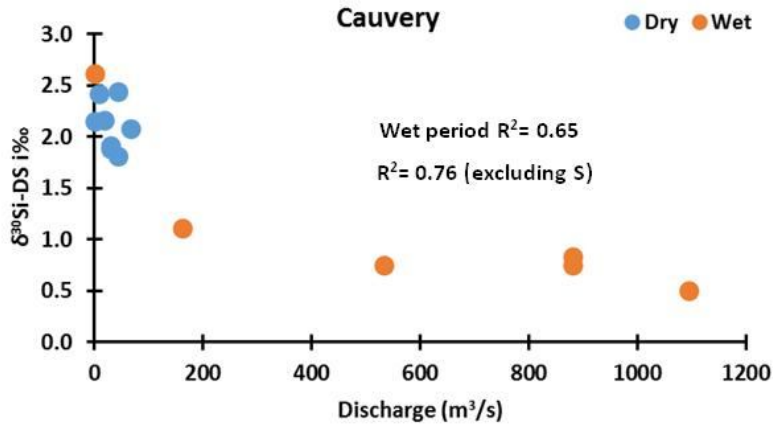

Fig. 8 *Relationship between $\delta^{30}Si$ and discharge in the Cauvery river during both seasons. Strong negative relationship indicates the different source of water (young rain water and old base flow water) that interacts with the respective Si minerals.*

In *Netravathi* basin – a similar positive relationship between $\delta^{30}Si$ and DSi or ΣC+* concentrations (Fig. 9a and b) likely results also from the lighter isotopes incorporated in secondary clay minerals and leaving an enriched isotopic signature in the solution. As explained above, the intensity of weathering may change the isotopic composition of the basin. Likewise to Cauvery basin, the relationship between $\delta^{30}Si$ and DSi/(Na*+K*) or DSi/Na* (Fig. 9c and d) is shown in order to identify the type of clay formation in the Netravathi basin. Similar to Cauvery basin, there is a ratio < 2 for dry and post monsoon periods. This once again indicates the leaching of base flow water from the deep saprolite (near to bedrock) zone i.e., the formation of smectite type of minerals with more proportion of Si immobilized in the secondary minerals associated with the heavier isotopic composition in the dissolved phase (Fig. 9c and d). In contrast, during wet period, a ratio > 2 indicates that DSi is mostly released from the superficial weathered secondary minerals (e.g. Kaolinite) leading to lighter isotopic composition in the solution (Fig. 9c and d). Overall, these major elements, as well as the $\delta^{30}Si$ data are highly consistent with those on the Amazon basin and tributaries where same behavior has been observed, including the seasonal variations (Hughes et al., 2013).

During dry period, unlike other stations, the sample "Shi" exhibits less dissolved load and lighter Si isotopic signature (as described in the results section) associated with high DSi/(Na+K)* indicating intense weathering of kaolinite type of minerals. The reasons for the intense weathering in that

particular tributary (Shi) during dry period remains unclear. In addition, the two highlighted values from the figure 9a, having higher DSi with low isotopic signature (Gur) and low DSi value with heavy isotopic signature (N_4) is noticed. Yet the DSi/(Na+K)* values of the above highlighted stations indicate allitization process (with one sample (Gur) with a high ratio of 9.82, not shown in figure 9c and d) may explain the congruent dissolution of secondary minerals with gibbsite formation in the Gurupur (Gur) during wet period and bisiallitization process (with less ratio 0.99, included in the linear relation of the figure 9c and d) in the N_4 mainstream during post monsoon period.

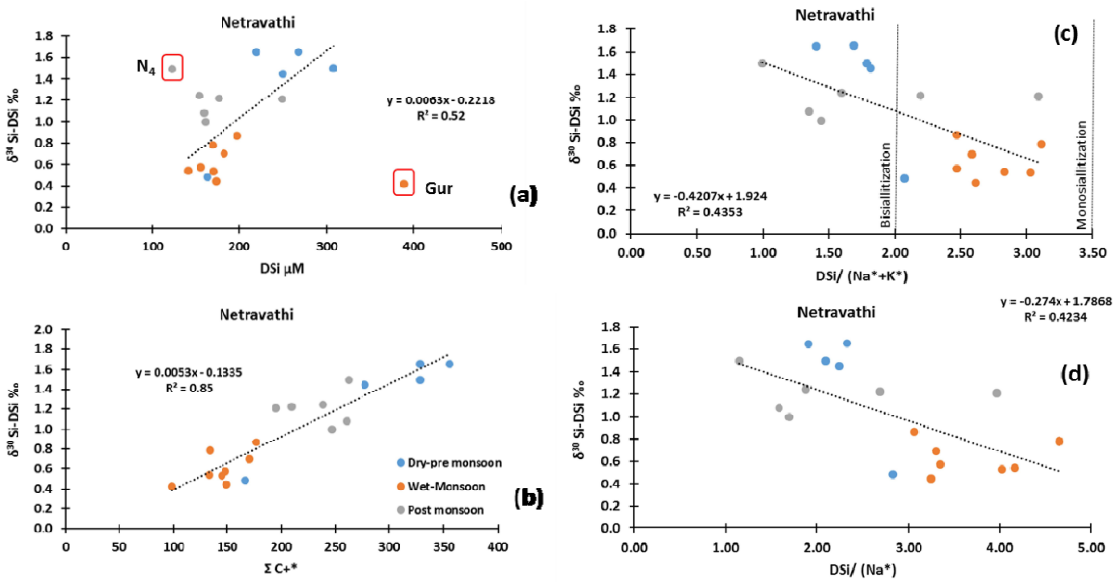

Fig. 9 *Evolution of the isotopic signature in the river Netravathi during dry, wet and post monsoon periods respectively, (a) with dissolved Si concentration. Encircled points are removed from the linear relationship. (b) with the sum of major cations (corrected for atmospheric inputs). (C) with the ratio between DSi and (Na*+K*) and with Na*(d) variability depending on the Si remaining immobilized in secondary minerals and also the type of clay mineral formation during weathering process and their relationship with Si isotopes. The sample value of "Gur"-monsoon period (DSi/(Na+K)*=9.82) is removed from the figure 9c and not shown. The dashed lines representing the limits of different clay mineral formation processes (section 4.3 for details). The red encircled values in 9a are from Gur and N_4, Gur not included in the linear equation calculation in all figures because of its higher values (refer table 2 for the individual values) and N_4 values are included in all linear equations except in fig.9a.*

Degree of silicate rock weathering using Re index

Actually, there might be few flaws associated with the DSi/(Na*+K*) ratio in the determination of the type of weathering. They are 1) Quartz dissolution, 2) Ignorance of Ferro-magnesium minerals (e.g.; amphiboles) 3) the influence of biological uptake. The presence of the magnesium-silicate mineral (e.g., amphiboles) in both basins, as well as some carbonate in the Cauvery Basin can be the most problematic (Braun et al., 2009, Gurumurthy et al., 2012) since we will discuss the likely minor role of biological uptake under next section.

Lithologies of both basins encompass gneissic and schist belts in the Netravathi and peninsular gneiss, granitic rocks along with amphibolites in Cauvery. This confirms the pertinence to consider the Re index for the present study. If the Re= 0, the weathering is intense and forms gibbsite (allitization), if Re= 2, kaolinite is essentially formed (monosiallitization), if Re= 4, the weathering products are mainly smectites (bisiallitization). The Re values of Cauvery and Netravathi samples are presented in the Tables 2 and 3 and the behavior of Si isotope to the respective Re-index was studied.

The Re calculated for Cauvery basin ranges from 1.77 to 3.73 (2.35 ± 0.47) and 1.09 to 3.76 (2.10 ± 0.62) during dry and wet periods respectively. The relationship between δ^{30}Si and Re index (Fig. 10) confirms that more smectite is associated with heavier isotopic signature during dry and kaolinite-gibbsite with lighter Si isotopic signature during wet period. The changes in Re across the basin are helpful to understand the variability of δ^{30}Si-DSi. These results are consistent with the DSi/(Na*+K*) ratio as explained earlier. Therefore, it is clear that the increased soil-water residence time and the interaction of base flow waters with the bed rock favours the secondary mineral formation by preferential incorporation of lighter isotopes leaving enriched in solution during dry period. On contrary, intense weathering process decreasing the fraction of silicon incorporated into clay minerals and leaving the solution with lighter Si isotopic composition is noticed during wet period. Globally, a clear seasonal effect is seen with higher Re values during low flow period and vice versa in the high flow period except few points (Fig. 10). We studied the clay minerals composition on upper estuarine particle samples that showed the presence of high relative percentage of smectite (59 %) > Illite (27%) > Kaolinite (9%) > Chlorite (5%) during dry period of Cauvery basin confirming the bisiallitization process once again (refer Table 3 of chapter 4).

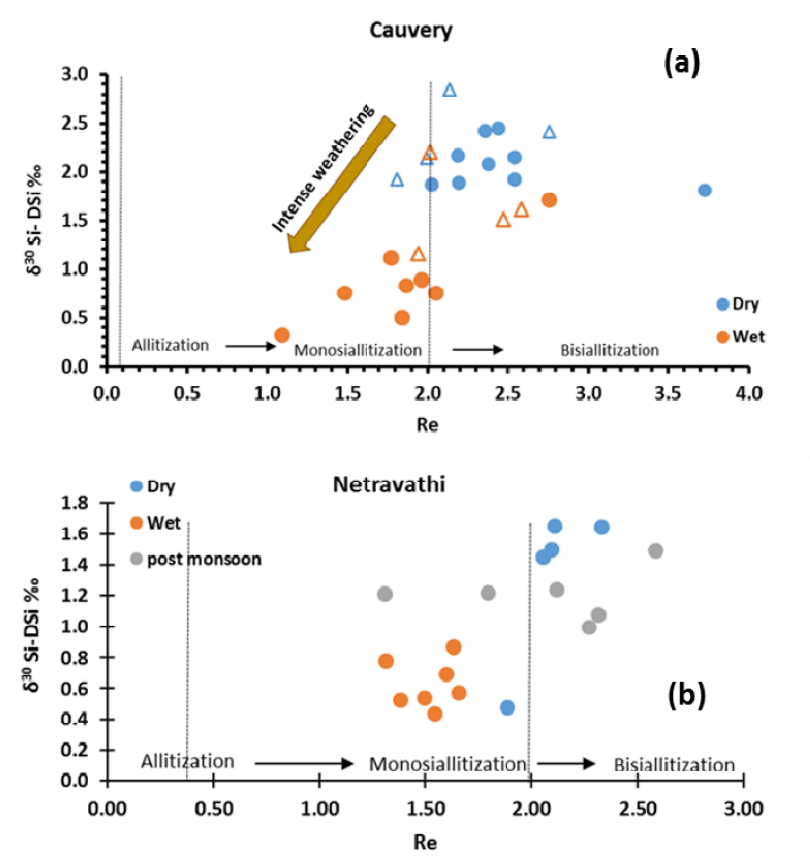

Fig. 10 *The relationship between $\delta^{30}Si$ and Re index in the river Cauvery (a) and Netravathi (b) during dry and wet periods respectively. The open triangles represent the dam samples of the basin. The dashed line indicates the limits of different clay minerals formation.*

In Netravathi the Re index ranges from 1.9 to 2.4, 1.3 to 1.7 and 1.3 to 2.6 during dry, wet and post monsoon respectively (Table. 2). There is a significant seasonal difference of the Re index between dry and wet periods with lower Re-index during wet period ($p < 0.001$). Likewise to Cauvery basin, the relationship between $\delta^{30}Si$ and Re index (Fig. 10b) indicates that heavier $\delta^{30}Si$ of dry period are associated with the weathering of primary cation-rich minerals and with the probable smectite formation (Re>2). Re <2, indicates the intense weathering and dissolution of primary minerals with the probable formation of kaolinite-gibbsite, that supplies lighter isotopes in the solution during wet period. These results are consistent with the DSi/(Na*+K*) ratio discussed earlier. The Re-index of present study is relatively higher than the previous study in Netravathi basin from same sites but samples were collected in 2006-2007 in Gurumurthy et al. (2012), where the Re index at the outlet was -0.6 during

peak flow season and 2.4 during dry season. They reported intense weathering that result in gibbsite formation. On contrary, on our data there is no clear evidence for intense gibbsite formation as reported earlier because of higher Re values (1.9 ± 0.4) favoring kaolinite-gibbsite (during wet period, Re= 1.5 ± 0.1) and smectite (during dry period, Re= 2.1 ± 0.2) formation. This is mainly due to the difference in the water flow due to the rainfall in the basin. The total rainfall in the Netravathi basin at Chikmagalur (origin of Netravathi) was 2,319 mm yr^{-1} during 2010 (monthly rainfall data, http://www.indiawaterportal.org), which is less than 2006-2007 (3600-4200 mm yr^{-1}, Gurumurthy et al., 2012). Therefore, the intensity of the monsoon determinates the runoff and in turn, controls the weathering regime in the basin. Moreover, the clay mineralogy studies on estuarine particle samples (from wet period) also confirm the presence of high relative percentage of kaolinite (85%), illite (15%) and absence of smectite in the particle samples with the presence of noticeable gibbsite in the sample (see Table 3 of Chapter 4). One explanation for the absence of smectite may be that the base flow is sustained by groundwater, i.e. in depth, closer to the weathering front than during the monsoon. If smectite can form at the weathering front, these particles cannot be exported contrary to the top soil which has been leached.

Therefore the significant changes of isotopic composition between these two basins are mainly defined by the origin of water i.e., the river is either fed by surface or subsurface flows from different weathering profiles. The reduced water flow during dry period (especially very low in the Cauvery basin due to the diversion of water for domestic and irrigation purpose) increases the residence time of soil water via groundwater as base flow. This favors the weathering of bedrock resulting in the high supply of dissolved load, associated with secondary mineral smectite formation. As evidenced from the Re index, the proportion of Si immobilized in the clay minerals results in heavier isotopic signature in the solution. In contrast, during wet period, intense runoff (2319 $mm.yr^{-1}$ in Netravathi basin, Gurumurthy et al., 2012) increases the intensity of weathering resulting on long scales to the formation of kaolinite. On seasonal scale, heavy rain leads to the dissolution of kaolinite present in shallow soil horizons since rain is under saturated which therefore might release lighter Si isotopes in the solution and concomitantly less dissolved Si load due to dilution effect. The present study Re weathering indexes are comparable and similar to the calculated Re values of other global rivers (discussed in Gurumurthy et al., 2012): Ganges-Brahmaputra (2.2), Amazon (2.1) and Congo-Zaire (2.1) are similar to Cauvery basin, whereas, the Orinoco (1.6), Parana (1.4) and Mekong (1.7) are more comparable to the Netravathi basin.

One should notice the impact of land use in both basins as discussed in the previous chapter. Higher agricultural activities can lead to more incorporation of lighter Si isotopes in the plants leaving heavier Si isotopic signature in the solution. Such mechanism was well evidenced in the upper estuaries with a positive correlation (Fig. 9a of Chapter 4). In addition, less agriculture is generally associated with more forest cover and light isotopic signature as evidenced in the Netravathi basin (Fig. 9b of chapter 4). The comparison of weathering intensity between both the basins and the relationship with Si isotopic signature (Fig. 11) indicates intense weathering in the Netravathi (kaolinite formation) when compared to the Cauvery basin (smectite - kaolinite formation) and minor biological allochtonous input. It is also interesting to note from the Figure 11, that the two Indian tropical contrasted basins are behaving exactly as the tributaries and mainstream from the Amazon basin (data adapted from Hughes et al., 2013), Congo river (Hughes et al., 2011), Tana river (Hughes et al., 2012) indicating that weathering is the major process that controls the Si isotopic variability despite its size and pristine nature (e.g., less anthropogenic impact on Amazon basin). On contrary, the Yellow river is behaving different from other tropical rivers and this could be mainly due to the first order control of biological uptake via phytoliths formation on δ^{30}Si-DSi variability (Ding et al., 2011). Likewise, In Ganges combination of both above mentioned processes (Fontorbe et al., 2013) control the δ^{30}Si-DSi variability. It should also be noted that weathering explains 40-50% of δ^{30}Si-DSi variability (Fig. 7 and 9) and the remaining can be due to other processes. The residues from the relationships between δ^{30}Si-DSi and DSi/(Na+K)* have been calculated and used to check the relationship with DSi or ASi to explain secondary-order processes such as biological uptake. No significant relationship was found between the residues and other Si parameters (fig. not shown). This indicates a very unlikely control of biological uptake over δ^{30}Si-DSi variability. Therefore, the δ^{30}Si-DSi of two Indian contrasted river basins is primarily controlled by the weathering and might get altered in the downstream.

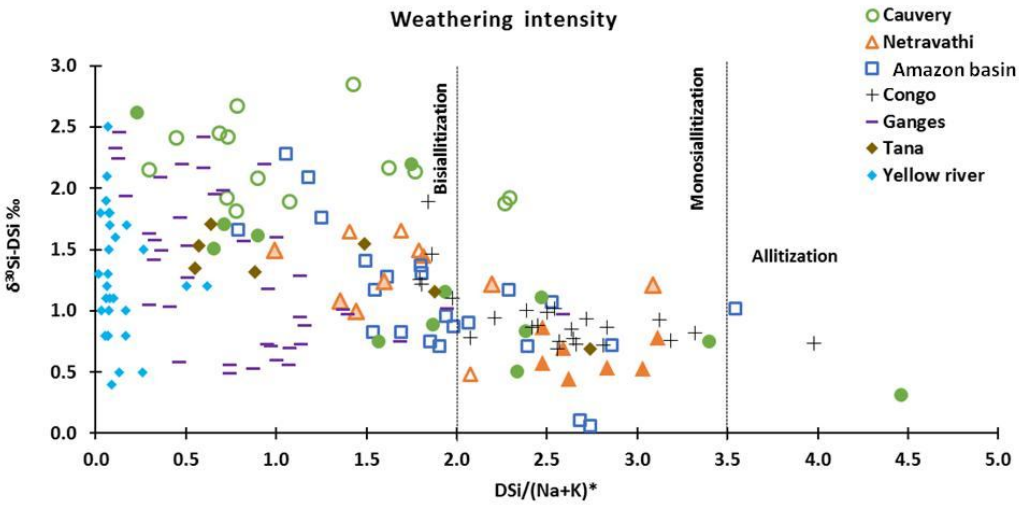

Fig. 11 *δ^{30}Si-DSi and DSi/(Na+K)* ratio of the present study Cauvery (green open circles) and Netravathi (orange open triangles) basins compared with the largest watershed Amazon (blue open squares data from Hughes et al., 2013). The open and closed circles represent Cauvery basin dry and wet periods respectively. The open and filled triangles represent Netravathi basin dry and wet periods respectively. The faded filled triangles represent the post monsoon of Netravathi basin.*

4.3 Biological processes

The absence of both overall positive correlation between δ^{30}Si and the concentration of amorphous silica in suspended matter (ASi, data from Meunier et al., 2015) of the Cauvery River and decrease of DSi concentration in the river, suggest a minor influence of diatom uptake. However, the relationship between ASi and δ^{30}Si are not straightforward as shown by Hughes et al. (2011) in the Congo river because of the importance of fast settling of diatoms in the sediment. Yet, excluding two points the occurrence of a positive relation between ASi and δ^{30}Si ($r=0.77$, $n=7$, $p=0.02$) in the Cauvery river (mainstream and tributary) might be indicative of the significant effect of diatom uptake on dissolved δ^{30}Si (Fig. 6).

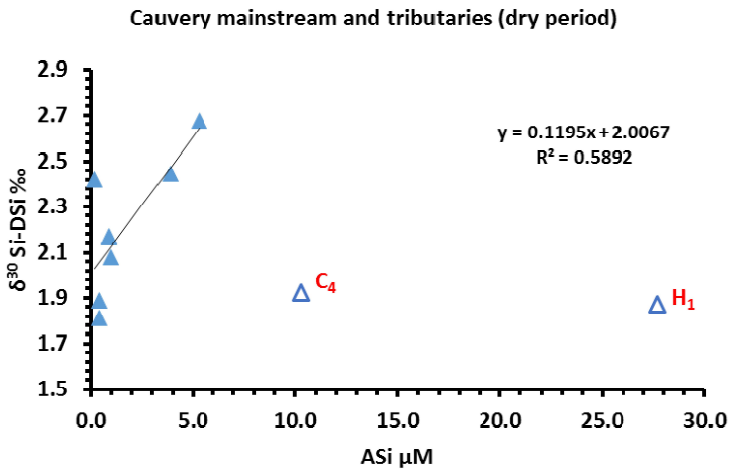

Fig. 6 *δ^{30}Si-DSi vs. ASi in the Cauvery basin. The open triangles are removed from the linear equation calculation (C_4 and H_1. See Table 2 for their complete names).*

To quantify such potential diatom uptake, we use the different approaches explained by Hughes et al. (2011). Here, we assume that the heavier isotopic composition of Cauvery basin in dry season results from the diatom uptake and the δ^{30}Si is used as a proxy to quantify the uptake mechanism. Based on our assumption, the production of BSi (Biogenic silica) as the only main output of DSi for the given water, then f_{Si} = DSi/ (DSi + BSi), and one can rewrite the Rayleigh and Steady state equations (presented in Chap. 1 and 4) as:

$$\text{Rayleigh:} \quad BSi = DSi \times [\exp((\delta^{30}Si_0 - \delta^{30}Si) / \varepsilon) - 1] \qquad (2)$$

$$\text{Steady state:} \quad BSi = DSi \times [(\varepsilon / \delta^{30}Si - \delta^{30}Si_0 + \varepsilon) - 1] \qquad (3)$$

$\delta^{30}Si_0$ is considered as 1.81 ‰, which is the lightest in the river stream during dry period. The fractionation factor (ε) is -1.2 ‰ (Fripiat et al., 2011, Alleman et al., 2005 and Georg et al., 2006).

Based on both the models of Rayleigh and Steady state, the calculated BSi varied 174 ± 165 and 294 ± 350 µM in the mainstream and tributaries of Cauvery respectively whereas the measured ASi values varied 5.6 ± 8.9 µM (Meunier et al., 2015). Moreover, no relation is observed between measured ASi and calculated BSi. Indeed, it is not realistic to have such high BSi production by diatoms to explain the

isotopic composition in the basin because the residence time of the water in the stream is too short to allow such dense growth of diatoms. Moreover this mechanism is even true for the reservoirs due to the quick usage of water for irrigation. On contrary, in river Congo, higher stability of water flow made favorable for diatom growth was noticed by Hughes et al, (2011) and that could explain the relationship between Si isotopes and ASi. This suggests that the influence of diatom uptake is unlikely to explain solely the variability of δ^{30}Si in Cauvery basin during the dry season.

It is interesting to note that the dams are exhibiting heavier isotopic signature with remarkably heavier in N_d (+2.8 ‰, Table 2, Fig. 4a). For this sample, it is consistent with high measured ASi (73.8 µM) and decreasing DSi (231 µM) concentration relative to the other adjacent reservoirs (Fig. 2a, 4a). Moreover, the higher diatom abundance (94%) in Nd (Nugu reservoir) was also reported by Meunier et al. (2015) and considered only as allochthonous input. We do not have sample upstream that could be considered as the DSi source to the Nugu reservoir however, we have a very nearby river, Kabini, which bears a δ^{30}Si of 1.9 ‰. Using this isotopic composition as the $\delta^{30}Si_0$ and applying Equations (2) and (3), gives calculated BSi of 258 µM and 693 µM for Rayleigh and steady-state respectively. The value obtained by the Rayleigh model is larger but comparable to the highest value calculated in Malebo pool by Hughes et al, (2011) in which 215 µM of DSi has been consumed, and appears realistic for diatom production in a tropical lake during summer.

Hence biological uptake may have impacted δ^{30}Si signature only in one reservoir. Therefore, except of this sample, our Si isotopic signature suggest diatom uptake as negligible in the Si biogeochemical cycle from headwater to upper estuaries both in Cauvery basin, whatever the season. In addition, there are no measured ASi values for Netravathi basin to explain the biological uptake process. Indeed, there are few dams in basin to allow a significant modification of Si biogeochemical cycle due to diatom growth. Moreover, the lighter isotopic signature of Netravathi basin (dry period 1.6 ± 0.1‰) than the Cauvery basin may unlikely results from the diatom uptake process.

5 Conclusions

In this study, we report the first dataset of riverine δ^{30}Si signatures in the Cauvery and Netravathi basin originating from the Western Ghats, flowing east and west directions in India. Both the basins are seasonally well influenced and the Cauvery river is ~1 ‰ heavier than the Netravathi river. This results in

a weighed δ^{30}Si of DSi exported to estuary which is twofold heavier in Cauvery (1.31 ‰) than in Netravathi (0.61 ‰). Diatoms uptake in the Cauvery stream is negligible and it was only observed for some reservoirs of the Cauvery basin in dry season. There are no measured ASi values in the Netravathi basin to estimate the presence of diatoms. However, it is unlikely to have significant diatom uptake within the basin because there are few reservoirs and moreover the δ^{30}Si-DSi is lighter than Cauvery basin. The δ^{30}Si-DSi in Cauvery basin is mainly controlled by the weathering regime and the water flow at spatial and seasonal scales. i.e., longer soil water residence time and soil water release closer to the weathering front and with heavier δ^{30}Si (Hughes et al., 2013). In addition, heavy runoff during wet period intensifies weathering decreasing the fraction of silicon incorporated into secondary mineral and, leaving the solution with lighter Si isotopic signature. The Re-index of Cauvery basin confirms the formation of smectite and kaolinite during dry and wet seasons respectively and controlling the Si isotopic signature. Likewise, the Re index of Netravathi basin indicates relatively more intense weathering than Cauvery basin with the release of DSi characteristically from smectite and kaolinite during dry while DSi release during wet is from solution in which kaolinite-gibbsite formation has been favored. The present study Re weathering indexes are comparable and similar to the calculated Re values of other global rivers and seem to behave similarly to Amazon basin tributaries. This study emphasized the utility of Si isotopic signature as a good proxy for understanding the Si mobility based on the type of weathering in the system.

6. References

Alexandre, A., Meunier, J.-D., Colin, F. & Koud, J.-M. Plant impact on the biogeochemical cycle of silicon and related weathering processes. *Geochim. Cosmochim. Acta* **61,** 677–682 (1997).

Alleman, L. Y. *et al.,* Silicon Isotopic Fractionation in Lake Tanganyika and Its Main Tributaries. *J. Great Lakes Res.* **31,** 509–519 (2005).

Boeglin, J. L. & Probst, J. L. Physical and chemical weathering rates and CO2 consumption in a tropical lateritic environment: the upper Niger Basin. *USDA For. Serv. - Gen. Tech. Rep. RMRS-GTR* **148,** 137–156 (1998).

Braun, J. J., Marc Descloitres., Jean Riotte., Simon Fleury., Laurent Barbiero., Jean-Loup Boeglin., Aurelie Violette., Eva Lacarce., Laurent Ruiz., M. Sekhar., M.S. Mohan Kumar., S. Subramanian., Bernard Dupre. Regolith mass balance inferred from combined mineralogical, geochemical and geophysical studies: Mule Hole gneissic watershed, South India. *Geochim. Cosmochim. Acta* **73,** 935–961 (2009).

Cardinal, D., Gaillardet, J., Hughes, H. J., Opfergelt, S. & André, L. Contrasting silicon isotope signatures in rivers from the Congo Basin and the specific behaviour of organic-rich waters. *Geophys. Res. Lett.* **37,** 1–6 (2010).

Cockerton, H., E., Street-Perrott F. A., Leng M. J., Barker P. A., Horstwood M. S. A. and Pashley V *et al.,*. Stable-isotope (H, O, and Si) evidence for seasonal variations in hydrology and Si cycling from modern waters in the Nile Basin: Implications for interpreting the quaternary record. *Quat. Sci. Rev.* **66,** 4–21 (2013).

Conley, D. J., Per Pitkanen, Heikki Wilander, Anders Stålnacke, Per Pitkänen, Heikki. The transport and Retention of dissolved Silicate by Rivers in Sweden and Finland. *Limnol. Oceanogr.* **45,** 1850–1853 (2000).

Conley, D. J. Riverine contribution of biogenic silica to the oceanic silica budget. *Limnol. Oceanogr.* **42,** 774–777 (1997).

De La Rocha, C. L., Brzezinski, M. A. & Deniro, M. J. A first look at the distribution of the stable isotopes of silicon in natural waters. *Geochim. Cosmochim. Acta* **64,** 2467–2477 (2000).

Delvaux, C., D. Cardinal, V. Carbonnel, L. Chou, H.J. Hughes, L. André. Controls on riverine δ30Si signatures in a temperate watershed under high anthropogenic pressure (Scheldt — Belgium). *J. Mar. Syst.* 1–12 (2013). doi:10.1016/j.jmarsys.2013.01.004.

Derry, L. a, Kurtz, A. C., Ziegler, K. & Chadwick, O. a. Biological control of terrestrial silica cycling and export fluxes to watersheds. *Nature* **433,** 728–731 (2005).

Ding, T. P., Gao, J. F., Tian, S. H., Wang, H. B. & Li, M. Silicon isotopic composition of dissolved silicon and suspended particulate matter in the Yellow River, China, with implications for the global silicon cycle. *Geochim. Cosmochim. Acta* **75,** 6672–6689 (2011).

Ding, T., Wan, D., Wang, C. & Zhang, F. Silicon isotope compositions of dissolved silicon and suspended matter in the Yangtze River, China. *Geochim. Cosmochim. Acta* **68,** 205–216 (2004).

Ding, T.,Wan,D., Li, J., Jiang, S., Song,H., Li,Y., Liu, Z. Silicon Isotope Geochemistry. Geological Publishing House, Beijing (1996).

Dürr, H. H., Meybeck, M., Hartmann, J., Laruelle, G. G. & Roubeix, V. Global spatial distribution of natural riverine silica inputs to the coastal zone. *Biogeosciences* **8,** 597–620 (2011).

Engström, E. Ilia Rodushkin, Johan Ingri, Douglas C. Baxter , Frauke Ecke , Heléne Österlund, Björn Öhlander. Temporal isotopic variations of dissolved silicon in a pristine boreal river. *Chem. Geol.* **271,** 142–152 (2010).

Fontorbe, G., Rocha, C. L. D. La, Chapman, H. J. & Bickle, M. J. The silicon isotopic composition of the Ganges and its tributaries. *Earth Planet. Sci. Lett.* **381,** 21–30 (2013).

Fripiat, F., Cavagna, A.-J., Savoye, N., Dehairs, F., André, L., Cardinal, D., 2011. Isotopic constraints on the Si-biogeochemical cycle of the Antarctic Zone in the Kerguelen area (KEOPS). Marine Chemistry 123, 11–22.

Ganasri, B. P. & Ramesh, H. Assessment of soil erosion by RUSLE model using remote sensing and GIS - A case study of Nethravathi Basin. *Geosci. Front.* 1–9 (2015). doi:10.1016/j.gsf.2015.10.007.

Garnier, J., Beusen, A., Thieu, V., Billen, G. & Bouwman, L. N:P:Si nutrient export ratios and ecological consequences in coastal seas evaluated by the ICEP approach. *Global Biogeochem. Cycles* **24,** GB0A05, 1-12 (2010).

Georg, R. B., Reynolds, B. C., Frank, M. & Halliday, a. N. Mechanisms controlling the silicon isotopic compositions of river waters. *Earth Planet. Sci. Lett.* **249,** 290–306 (2006).

Georg, R. B., Reynolds, B. C., West, A. J., Burton, K. W. & Halliday, A. N. Silicon isotope variations accompanying basalt weathering in Iceland. *Earth Planet. Sci. Lett.* **261,** 476–490 (2007)

Georg, R. B., West, a. J., Basu, a. R. & Halliday, a. N. Silicon fluxes and isotope composition of direct groundwater discharge into the Bay of Bengal and the effect on the global ocean silicon isotope budget. *Earth Planet. Sci. Lett.* **283,** 67–74 (2009).

Gurumurthy, G. P. *K.* Balakrishna, Jean Riotte , Jean-Jacques Braun, Stéphane Audry, H.N. Udaya Shankar, B.R. Manjunatha. Controls on intense silicate weathering in a tropical river, southwestern India. *Chem. Geol.* **300–301,** 61–69 (2012)

Gurumurthy, G. P. K. Balakrishna, M. Tripti, Stéphane Audry, Jean Riotte, J. J. Braun & H. N. Udaya Shankar. Geochemical behaviour of dissolved trace elements in a monsoon-dominated tropical river basin, Southwestern India. *Environ. Sci. Pollut. Res.* **21,** 5098–5120 (2014).

Hughes, H. J. Francis Sondag, Christine Cocquyt, Alain Laraque, Albert Pandi, Luc Andre and Cardinal.D. Effect of seasonal biogenic silica variations on dissolved silicon fluxes and isotopic signatures in the Congo River. *Limnol. Oceanogr.* **56,** 551–561 (2011).

Hughes, H. J., Bouillon, S., André, L. & Cardinal, D. The effects of weathering variability and anthropogenic pressures upon silicon cycling in an intertropical watershed (Tana River, Kenya). *Chem. Geol.* **308–309,** 18–25 (2012).

Hughes, H. J., Sondag, F., Santos, R. V., André, L. & Cardinal, D. The riverine silicon isotope composition of the Amazon Basin. *Geochim. Cosmochim. Acta* **121,** 637–651 (2013).

Humborg, C. Blomqvist S, Avsan E, Bergensund Y, Smedberg E. Hydrological alterations with river damming in northern Sweden: Implications for weathering and river biogeochemistry. *Global Biogeochem. Cycles* **16,** 12-1-12–13 (2002).

Lele, S, Srinivasan, V, Jamwal, P., Thomas, B.K., Eswar, M., Zuhail, T.Md. Water Management In Arkavathy Basin: A situational analysis. Environment and Development Discussion Paper (2013).

Meunier, J. D., J. Riotte, J.J.Braun, M. Sekhar, F. Chalié, D. Barboni, L. Saccone. Controls of DSi in streams and reservoirs along the Kaveri River, South India. *Sci. Total Environ.* **502,** 103–113 (2015).

Monthly rainfall data 2004-2010, http://www.indiawaterportal.org

Naqvi, S.M., Rogers, J.W., 1987. Precambrian Geology of India. Clarendon Press, Oxford University Press, New York.

Nelson, D. M., Tréguer, P., Brzezinski, M. A., Leynaert, A. & Quéguiner, B. Production and dissolution of biogenic silica in the ocean: Revised global estimates, comparison with regional data and relationship to biogenic sedimentation. *Global Biogeochem. Cycles* **9,** 359–372 (1995).

Opfergelt, S., G. de Bournonville, D. Cardinal, L. Andre, S. Delstanche, B. Delvaux. Impact of soil weathering degree on silicon isotopic fractionation during adsorption onto iron oxides in basaltic ash soils, Cameroon. *Geochim. Cosmochim. Acta* **73,** 7226–7240 (2009).

Opfergelt, S., Burton, K. W., Pogge von Strandmann, P. A. E., Gislason, S. R. & Halliday, A. N. Riverine silicon isotope variations in glaciated basaltic terrains: Implications for the Si delivery to the ocean over glacial–interglacial intervals. *Earth Planet. Sci. Lett.* **369–370,** 211–219 (2013).

Pattanaik J. K., Balakrishnan S., Bhutani R. and Singh P. (2007) Chemical and Sr isotopic composition of Kaveri, Palar and Ponnaiyar rivers: significance to weathering of Granulites and Granitic gneisses of southern Peninsular India. Curr. Sci. 93(4), 523–531.

Pattanaik, J. K., Balakrishnan, S., Bhutani, R. & Singh, P. Estimation of weathering rates and CO2 drawdown based on solute load: Significance of granulites and gneisses dominated weathering in the Kaveri River basin, Southern India. *Geochim. Cosmochim. Acta* **121,** 611–636 (2013).

Pokrovsky, O. S., Reynolds, B. C., Prokushkin, A. S., Schott, J. & Viers, J. Silicon isotope variations in Central Siberian rivers during basalt weathering in permafrost-dominated larch forests. *Chem. Geol.* **355,** 103–116 (2013).

Pradhan, U. K., Wu, Y., Shirodkar, P. V. & Zhang, J. Seasonal nutrient chemistry in mountainous river systems of tropical Western Peninsular India. *Chem. Ecol.* **31,** 1–18 (2014).

Ramanathan AL, Vaithiyanathan P, Subramanian V, Das BK. Nature and transport of solute load in the Cauvery River basin, India.Water Res 1994; 28:1585–93.

Shadakshara Swamy N, Jayananda M, Janardhan AS. Geochemistry of Gundlupet gneisses, Southern Karnataka: a 2.5 Ga old reworked sialic crust. In: YoshidaM, Santosh M, Rao AT, editors. India as a fragment of East Gondwana. Gondwana Research Group; 1995.

Struyf, E., Mrth, C. M., Humborg, C. & Conley, D. J. An enormous amorphous silica stock in boreal wetlands. *J. Geophys. Res. Biogeosciences* **115,** 1–8 (2010).

Tardy, Y. Characterization of the principal weathering types by the geochemistry of waters from some European and African crystalline massifs. *Chem. Geol.* **7,** 253–271 (1971).

Tréguer, P. J. & De La Rocha, C. L. The world ocean silica cycle. *Ann. Rev. Mar. Sci.* **5,** 477–501 (2013).

Vandevenne, F., Struyf, E., Clymans, W. & Meire, P. Agricultural silica harvest: Have humans created a new loop in the global silica cycle? *Front. Ecol. Environ.* **10,** 243–248 (2012).

WRIS. Cauvery Basin Report: Gov. of India - MoWR. 141 (2014).

Ziegler, K., Chadwick, O. A., White, A. F. & Brzezinski, M. A. δ30Si systematics in a granitic saprolite, Puerto Rico. *Geology* **33,** 817–820 (2005).

Chapter 6

General conclusions and perspectives

1. Conclusions

Increasing studies on silicon cycle in the past two decades highlighted the importance of the global Si cycle due to its ubiquitous nature in the Earth's crust; it's coupling with carbon cycle and its role in key aquatic and continental ecosystems. At present, the revisited Si budget emphasis knowledge gaps and uncertainties due to the lack of data more particularly from the tropical regions that contribute 75% of external Si supply to the ocean. In addition, increasing anthropogenic pressures and altering the ecosystem health have been noticed and are now of growing concern. By trying to fill some of the existing gaps along the land-ocean continuum, we proposed in this present study to understand the Si cycle and its controlling factors in the tropical Indian estuaries.

In terms of methodological developments, while performing the Si isotopes measurements, we used for the first time brucite preconcentration on fresh and estuarine water samples. Matrix effect was taken care using the standard sampling standard bracketing technique. Since the estuarine and riverine samples were having high DOC concentration, we check the potential influence on Si isotope measurements. Yet all our measured samples (upper estuaries and rivers) have DOC/Si ratio varied about 0.15 ± 0.1, and suggests a negligible matrix effect due to DOC.

The major conclusions from the present thesis begin with the seasonal and spatial variability of different Si forms (ASi, DSi and LSi) and the associated processes that control their variability (**Chapter 3**) in major and minor estuaries draining in to Bay of Bengal and Arabian Sea. Our data showed that the Indian estuaries varied widely with respect to their climate (based on their geographic locations), topography (steeper slopes in south west and wider plains in the eastern and northwestern) and discharge (controlled by monsoonal rainfall). Overall, the Indian estuaries contribute 8.8 ± 10% and 3.5 ± 5% of ASi to the total Si pool during dry and wet periods respectively. This contribution is similar to the Congo basin (6%, Hughes et al., 2012) and higher than the Amazon basin (3%, Hughes et al., 2013). The ASi pool of Indian estuaries is mainly controlled by biological uptake during dry period. Indeed, there is no single dominant process such as biological uptake or mixing that responsible for the variability Si parameters when looking at the whole dataset or even applying solely a categorisation based on their location (NE, NW, SE, SW). Therefore, we separated our data in three categories: i) upper (salinity <5), ii) middle (salinity 5 to 15) and, iii) lower estuaries (salinity >15) for dry and wet period respectively and performed

PCA and clustering on PCA results. The results showed that the variability was controlled by four main mechanisms namely:

- Biological uptake mainly by diatoms
- Mixing with seawater
- Lithogenic supply of suspended materials via erosion and weathering
- Impact of land use especially the agriculture and forest cover

1.1 Controlling of biotic and abiotic factors

1.1.1 Dry period (base flow season)

During dry period, the ***diatom uptake*** process is evidenced by positive relationship between ASi and fucoxanthin in the upper (Ponnaiyar, Cauvery, Vellar, Tapti and Sabarmati), middle (Subarnarekha, Cauvery, Vellar and Netravathi) and lower (Nagavali, Penna, Ponnaiyar, Cauvery, KBW, Bharathapuzha, Netravathi, Zuari and Mandovi) estuaries irrespective of the geographical positions. This is consistent with the δ^{30}Si-DSi composition of southern estuaries (Penna, Vellar, Cauvery, Bharathapuzha and KBW) [Fig.1a and b]. Even though the measured ASi was not sufficient to explain the isotopic variability likely due to fast diatom settling as noticed in Congo basin (Hughes et al., 2012). Yet, there is no availability of Si isotopes on Nagavali, Netravathi, Sabarmathi to characterise diatom uptake during dry period. Indeed, one can confirm that the diatom uptake in the southern estuaries controls the δ^{30}Si-DSi during dry period.

Mixing with seawater generally does not seem to control the variability of biogeochemical parameters except for few estuaries (e.g., KBW, Penna). In addition, the δ^{30}Si-DSi showed the mixing with sea water on the above mentioned estuaries with a positive relationship between 1/DSi and δ^{30}Si-DSi. In addition, stable isotopic composition along the salinity gradient (e.g., Krishna, Vellar) indicating absence of any other significant biogeochemical process occurring in the estuaries. However, non availability of δ^{30}Si-DSi values of high salinity end member samples restricts us to predict the clear mixing process.

Otherwise, the rest of estuaries during dry period were either mostly controlled by the supply of ***terrestrial materials*** (e.g., Haldia), anthropogenic activities (e.g., fertilizer usage, Tapti and Sabarmati)

(Fig. 1a). It is interesting to utilize the δ^{30}Si-DSi tool to trace the source of the terrestrial geochemical process. The δ^{30}Si-DSi of upper estuaries indicates that weathering with clay mineral formation is the important mechanism that controls the Si isotopic composition of upper estuaries (positive relationship between DSi and δ^{30}Si-DSi, r= 0.57, p =0.02, n=14). The heavier isotopic composition was mainly due to the increased residence time of soil water leached during base flow period. Indeed, the soil solution that interacts with the soil minerals is not same during both seasons which determine the type of mineral leached and the isotopic composition of upper estuaries during both seasons. In addition, the saturation indexes of upper estuaries indicate the potential dissolution of primary minerals (i.e., undersaturation of albite and K-feldspar) as well as clay mineral formation (i.e., over saturation of smectite and kaolinite) that is consistent with the Si isotopic signatures. However, we were not able to compare with major elements geochemistry due to the over estimation of atmospheric correction of major cations concentration.

1.1.2 Wet season

In wet season, a strong control of erosion was observed, especially in the northern estuaries. The amount of discharge seems to be the main relevant parameter to explain the particulate concentrations. In the middle wet estuaries, the lithogenic supply continues to dominate. However contrasted fate of this LSi was observed: in some estuaries (especially northwest), the continental supply increases dramatically in the estuaries while in other, sediment settling decreases the supply to the coast. Overall the lithogenic supply of materials within estuaries seems to be the primary control of Si variables in all Indian estuaries during wet period. The figure 1a summarise the processes that control the variability of ASi and LSi of Indian estuaries during both seasons.

The δ^{30}Si-DSi signatures of Indian estuaries varied with 1.3 ± 0.55 ‰ and were ~1‰ lighter than the dry period. We used the upper estuaries (salinity <2) as a representative of riverine end-ember and tried to understand the chemical weathering mechanisms. Our results once again evidenced the clay mineral formation (e.g., smectite and/or kaolinite) and consistent with the lighter Si isotopes being incorporated in the clay minerals, leaving a heavier signature in the solution. In addition, the relationship between the δ^{30}Si-DSi and clay mineral composition of the particle samples of upper estuaries clearly indicating the signature of smectite formation especially in the northern estuaries (note that there is no data for southeast estuaries). In southwest estuaries, the lighter δ^{30}Si-DSi could be due to the dissolution of

kaolinite in upper soil horizons when surface flow is high and undersaturation of rainwater (see below). Indeed, the saturation indexes of primary and secondary minerals of upper estuaries indicate the dissolution of primary minerals and concurrent clay mineral formation. In addition, the undersaturation of chlorite minerals (KBW, Kali and Netravathi) and positive relation with δ^{30}Si-DSi suggest congruent dissolution of chlorite minerals in the southwest estuaries. In addition, our data of oversaturation index of hydroxides minerals indicates the possible adsorption of DSi on hydroxides and this process fractionates lighter Si isotopes leaving a heavier isotopic signature in the solution. However, one needs to remember that the saturation indexes and the δ^{30}Si-DSi values are from sampling locations which are far from the clay mineral formation sites. Hence, our saturation indexes reflect estuarine conditions and not soil conditions. For instance, heavy rainfall during SW monsoon supply huge quantity of freshwater, undersaturated with respect to clay and primary minerals. In SW watershed, this meteoric water should lead to some dissolution of kaolinite (and supply of light Si isotopes) which is widespread in the upper saprolite. Indeed, the type of the minerals that interact with the soil water and their associated minerals leached along with Si varied between both the seasons i.e., heavy discharge favors the leaching of minerals from superficial soil (older highly weathered minerals) giving lighter isotopic signature in the solution and vice versa in the Indian estuaries. Therefore, this study confirms the predominant influence of weathering and clay formation on dissolved Si isotope signatures in the Indian estuaries.

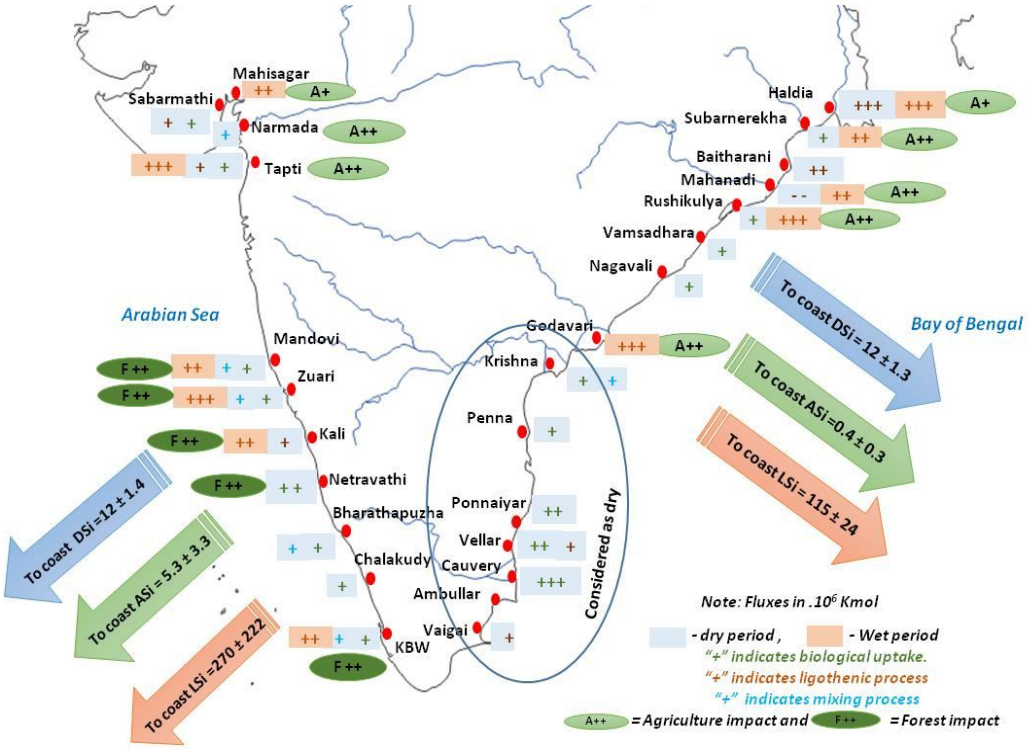

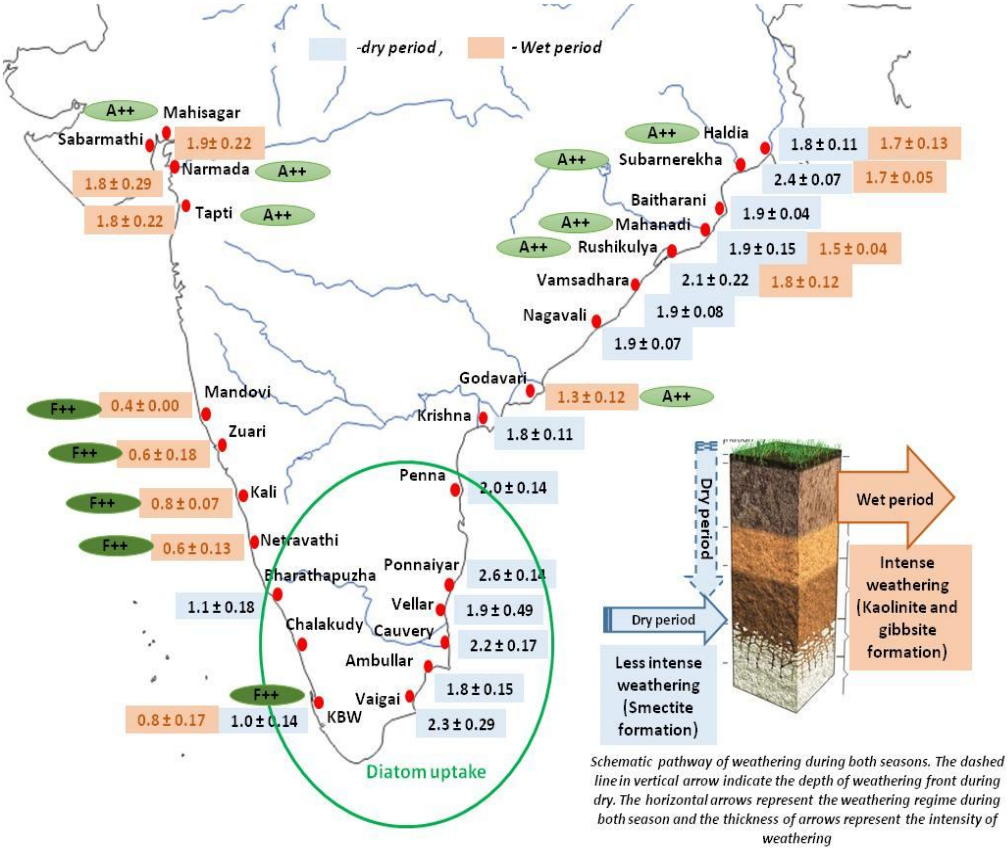

Schematic pathway of weathering during both seasons. The dashed line in vertical arrow indicate the depth of weathering front during dry. The horizontal arrows represent the weathering regime during both season and the thickness of arrows represent the intensity of weathering

Fig. 1 *(a) Variability of ASi and LSi and the controlling processes in the Indian estuaries during dry and wet periods respectively (b) δ^{30}Si-DSi variability of Indian estuaries during dry and wet period expressed in ‰ with 1SD. The encircled estuaries are southern estuaries indicating significant diatom uptake mechanism. Simplified cross sections of soil profile in (b) represent the weathering regime and the arrows indicating the intensity of weathering and possible type of secondary minerals leach during both seasons. The pale blue and brown filled small boxes in both (a) and (b) represent the sampling period i.e., dry and wet periods respectively. The green, brown and blue "+" symbols in (a) represent the biological, lithological (including anthropogenic effect for Tapti and Sabarmati) and mixing processes in the Indian estuaries respectively. The increasing number of "+"indicates the intensity of the respective process. The intensity was ranked based on the occurrence of same processes in the upper, middle and lower estuaries (e.g., diatom uptake in upper, middle and lower estuaries shown by "+++" with green font). In addition, the impacts of land use especially agriculture (A) and forest cover (F) of the watershed basin during wet period are indicated. The estuaries of Southeast are encircled in (a) because they were considered as dry period due to no discharge during wet period sampling. The fluxes of DSi, ASi and LSi to the Bay of Bengal and Arabian Sea during wet season respectively are shown in the figure (flux from the upper estuaries and flux to the coastal ocean are given). All the sampled estuaries are named and highlighted with red points. The "-"sign in (a) indicates that the estuaries are neither controlled by any of biological nor lithogenic process.*

We estimated the flux of ASi, LSi and DSi to the northern Indian ocean by correcting the upper wet fluxes for the non-conservativity during wet period. The results we obtained after the correction were reverse from the one estimated for upper estuarine flux (53% of DSi, 96% of ASi and 96% of LSi is supplied to the Bay of Bengal and the rest to the Arabian Sea). This corrected fluxes lead to the higher supply to the Arabian Sea with 12 ± 1.4, 5.3 ± 3.3 and 270 ± 222 x 10^6 kmol of DSi, ASi and LSi respectively than the Bay of Bengal with 12 ±1.3, 0.4 ± 0.3 and 115 x 10^6 ± 24 kmol of DSi, ASi and LSi respectively. These counterintuitive results were mainly due to the oversampling of Arabian Sea (i.e., 17.3% from total annual discharge) than the Bay of Bengal (7% from the total annual discharge) during wet period.

1.2 Impact of land use on Si cycle

A major highlight of our study is the strong land use impact on Si variability. Increasing agriculture activities played a major role in the Si biogeochemical cycle, increasing all Si fluxes in the eastern estuaries whose watersheds have higher agriculture cover. In contrast, relatively more forest cover prevents soil erosion and reduces the supply of ASi and LSi in the southwestern estuaries. In those estuaries, highest rainfall dilute DSi. This suggests that the silicon cycle is largely impacted by the anthropogenic activities over the Indian subcontinent and that they modify the Si supply to the coast. Interestingly, the impact of land use is also clearly evidenced on δ^{30}Si-DSi variability of Indian estuaries during wet period. The increasing agricultural activities in the eastern and northwestern regions (> 60%) likely alter the δ^{30}Si-DSi by incorporating lighter Si isotopes in their plant body. On contrary, the reduced agriculture in the southwestern estuaries and more forest cover enhances the clay dissolution because of high organic matter and low pH in the forest soils as noticed in other tropical (e.g., Congo, Amazon) and European estuaries (e.g., Scheldt). However, our results confirm that all the estuaries are not controlled solely by the natural processes (weathering or biological uptake) but also significantly by the anthropogenic impact (e.g., land use) that alters the Si cycle.

1.3 Groundwater

We also measured the δ^{30}Si-DSi of 13 groundwater samples around upper estuaries which are consistent with the δ^{30}Si-DSi of the Ganges shallow ground water (Georg et al. 2009). The ground waters are lighter in δ^{30}Si-DSi and higher in DSi concentration than the surface water likely indicating dissolution of primary and secondary minerals but no clear evidence about the type of mineral dissolved was identified using saturation indices. The shifts in the saturation of clay minerals indicate the dissolution of clay coatings and that could be responsible for the supply of lighter Si isotopes in the groundwater and can explain the enrichment of DSi. In addition, when comparing all the groundwater samples, weathering associated with clay mineral formation signature was noticed. However, we need further clear studies on each groundwater basin to trace the source of DSi and the associated processes like dissolution or adsorption/desorption.

2. Weathering: a first order control over biological uptake

Since the data of the present study was widely diversified, it is difficult to firmly conclude about the mechanisms that control the Si isotopic variability for each estuary. In order to have a more focused look, we have chosen two contrasted river basins from southern regions. From our above results, southern estuaries (SE and SW) estuaries seem to have a wide difference in their DSi concentration and δ^{30}Si-DSi composition. Therefore, we have chosen two river basins namely: Cauvery that runs eastward and draining in to Bay of Bengal and, Netravathi that flows westward and draining in to Arabian Sea. Moreover, these two basins have contrasted characteristics with respect to their size, lithology, climate, water flow, rainfall and land use (**Chapter 5**). The schematic representation concerning the process that gearstick the variability of δ^{30}Si-DSi of Cauvery and Netravathi basins are provided in the figure 2.

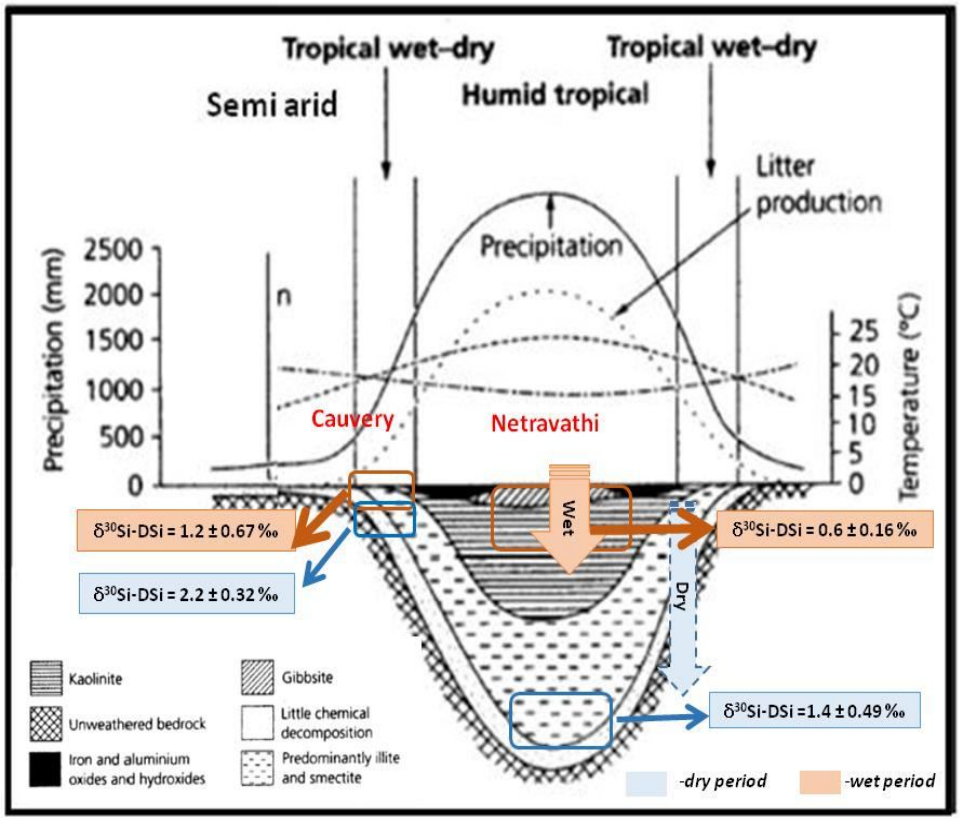

Fig. 2 *schematic relationship between weathering zones and the climatic zones adapted from Allen 1997. The δ^{30}Si-DSi of both basins are provided in the boxes for dry (pale blue) and wet (brown) periods respectively with 1SD. The thick arrows in blue and brown represent the weathering intensity and depth of the weathering regime. Deeper the arrow (dashed arrow) indicates the interaction of older soil water to near bed rock with smectite formation sites. Likewise, shorter the arrows indicating the interaction of*

younger soil water (e., rainwater) to the older and heavily weathered superficial soil with kaolinite and gibbsite formation sites. In addition, the thicknesses of arrows represent the intensity of weathering.

The main highlights of this study are: weathering is the dominant process that controls the variability of δ^{30}Si-DSi in both the basins in spatial as well as seasonal scales (Fig. 2). Both the basins were seasonally well contrasted and the Cauvery River is ~1 ‰ heavier than the Netravathi River. Accordingly, the weighed δ^{30}Si of DSi exported to the estuary is heavier in Cauvery (1.3‰) than in Netravathi (0.6‰). In Cauvery, diatoms uptake does not significantly impact Si isotopes in the mainstream and tributaries. Indeed, noticeable uptake in the Cauvery was noticed only in one reservoir during dry period. No ASi data on Netravathi basin to explain diatom uptake and unlikely occurring due to absence of reservoirs and lighter Si isotopes. However, the increased soil-water residence time and the interaction of base flow waters with the bed rock favors the secondary mineral formation by incorporating lighter isotopes in the clay minerals. This was particularly consistent with other weathering proxies, the Re index and DSi/(Na+K)* of dry period. In contrast, heavy runoff during wet period, intensifying the weathering process decreasing the fraction of silicon incorporated into secondary mineral and, leaving the solution with lighter Si isotopic signature.

Contrary to Cauvery, the Re index of Netravathi basin indicates relatively more intense weathering than Cauvery with the release of DSi characteristically from smectite-kaolinite formation during dry while DSi release during wet is from solution in which kaolinite-gibbsite formation has been favored. The intense weathering and lighter isotopic compositions of Netravathi basin were mainly due to the humid climate with heavy precipitation that should dissolve the superficial clay minerals. These results were confirmed by our clay mineralogy compositions on the upper estuaries with high proportion of kaolinite – gibbsite (in the Netravathi) and smectite (in the Cauvery) in the particles. Interestingly, these two basins exactly follow the degree of weathering noticed in the world largest Amazon basin (Hughes et al., 2013). Therefore, the Si isotopes are controlled mainly by the intensity of weathering associated with climate rather than the size of the basin.

This study also highlights that the watersheds in the southwest regions are very special in terms of weathering when compared to the other watersheds. In addition, our study emphasis that, the land use also contributes to the Si isotopes variability in the eastern and northwestern watershed areas. The other estuaries studied so far, indicate mainly the conservative nature of Si isotopes: in Tana estuary

(Hughes et al., 2012) and San Fransisco Bay estuary (De La Rocha et al., 2011). Biological net removal (during summer, otherwise conservative) in the Scheldt (Delvaux et al., 2013) and Elbe (Weiss et al., 2015) was also observed. On contrary, the overall present study tropical Indian estuaries are controlled by two other major processes namely; 1. Weathering associated with climate and lithology and 2. The impact of land use with high agricultural activities modifies the Si isotopic composition rather than the diatom uptake and mixing of seawater. Note that it is difficult to separate land-use from weathering since both are obviously interrelated.

3. Perspectives

Our present study on Indian estuaries is a pioneer and the wide variable nature of Si isotopic composition of each different basin at spatial and seasonal scale was observed and studied. Yet several gaps and unknown mechanisms are still lingering and few are listed below for future attention.

1. The processes associated with weathering, for example, fractionation factor during clay mineral formation because this is the major processes influencing the Si isotopic composition of rivers. By knowing the fractionation factor during the clay mineral formation then the δ^{30}Si ratio can be used as a proxy for clay mineral formation rate.
2. The present study provided the overall view on the Indian estuaries and on the seasonal effect. Nevertheless, we need closer resolution i.e., concentrating on few contrasted basins. This will give a better idea to predict the processes more precisely in terms of climate, lithology, land use etc. In addition, each basin should be studied from the head water to the coastal system to understand the fate of Si.
3. Despite the heavy agricultural and forest cover areas of the Indian subcontinent, the Lack of phytoliths study (both composition and isotopes) lingering a big gap to trace their contribution. In addition studies of Ge/Si would be interesting to trace Si cycling in plants and provide a better constraint on continental Si cycle.
4. In terms of methodology, the oxidation of the riverine samples can be recommended to devoid the DOC matrix interference completely on δ^{30}Si measurements. In addition, the ASi concentrations of Geotraces exercise are variable due to the different protocols used and one need more focus on the method constrains to measure the ASi preciously.

5. The combination of other isotopes of biogeochemical parameters apart from concentrations, i.e., nitrogen isotopes along the salinity gradient to study the impact of eutrophication potential in the densely populated coastal waters of India.

Hence, the present silicon biogeochemical cycle of Indian estuaries: a land-ocean continuum

IS JUST A BEGINNING!

4. References

De La Rocha, C. L., Bescont, P., Croguennoc, A. & Ponzevera, E. The silicon isotopic composition of surface waters in the Atlantic and Indian sectors of the Southern Ocean. *Geochim. Cosmochim. Acta* **75,** 5283–5295 (2011).

Delvaux, C. D. Cardinal., V. Carbonnel., L. Chou., H.J. Hughes., L. André. Controls on riverine δ30Si signatures in a temperate watershed under high anthropogenic pressure (Scheldt — Belgium). *J. Mar. Syst.* 1–12 (2013).

Hughes, H. J., Bouillon, S., André, L. & Cardinal, D. The effects of weathering variability and anthropogenic pressures upon silicon cycling in an intertropical watershed (Tana River, Kenya). *Chem. Geol.* **308–309,** 18–25 (2012).

Hughes, H. J., Sondag, F., Santos, R. V., André, L. & Cardinal, D. The riverine silicon isotope composition of the Amazon Basin. *Geochim. Cosmochim. Acta* **121,** 637–651 (2013).

Weiss, A., De La Rocha, C., Amann, T. & Hartmann, J. Silicon isotope composition of dissolved silica in surface waters of the Elbe Estuary and its tidal marshes. *Biogeochemistry,* doi:10.1007/s10533-015-0081-8, (2015).

Appendix of Chapter 3

APPENDIXES

Appendix A

Agreement with Ganges ASi data

The ASi values obtained in this study are compared with Frings et al. (2014) on Ganges basin (one of the largest river in India). The suspended matter (50 mg/L to several g/l^{-1}) and ASi concentrations (going from below detection limit up to to 300 μM) in Ganges are several folds higher compared to our data from other Indian estuaries (e.g. average for wet upper estuaries: 11 ± 15 μM for ASi and 123 ± 200 mg/l for TSM, cf. Table 1). The comparison between these two studies is not straightforward for three potential reasons. (i) The Frings et al. (2014) study was carried out in one of the largest river basin, Ganges, in India while the present study is performed on several estuaries of wide range of sizes. (ii) Unlike other rivers in India (monsoonal rivers), Ganges basin is a perennial river with relatively low seasonal variability on its discharge and is characterized by particularly high TSM due to high erosion of the Himalaya Mountains. (iii) There might a methodological issue on ASi measurement since Frings et al. (2014) used a 1% Na_2CO_3 leaching (Clymans et al., 2011) while we used 0.2 M NaOH (Ragueneau et al. 2005). This Na_2CO_3 method has been discussed and potentially overestimates ASi while the use of the strong NaOH base that underestimates ASi (Barao et al., 2015). In our study, we compared Haldia upstream samples (tributary of river Hooghly distributed from Ganges) to trace back the signature of lithogenic process in the system and the average TSM and ASi in the upstream estuaries during dry (278 mg/l and no ASi value because of too high lithogenic correction) and wet (617 ± 308 mg/l, 5.94 ± 3.05 μM respectively). Though the ASi values of present study are lower by several folds than the mean ASi (68 μM) of Ganges, the relationship between TSM and ASi following the similar logarithmic trend explained by Frings et al., 2014 for surface waters (Fig. A1). Indeed our upper wet estuaries TSM and ASi variability are consistent with the trend of Frings et al. (2014) since our average TSM is 123 mg/l. According to Ganges TSM – ASi relationship this should correspond to 20 μM ASi and we find 11 μM. So, even if there might be underestimation in ours and/or overestimation in Frings et al. (2014), the order of magnitude of both studies are consistent and the relatively lower TSM we have in our Indian estuaries explain why we have lower ASi compared to those from Ganges (Fig. A1).

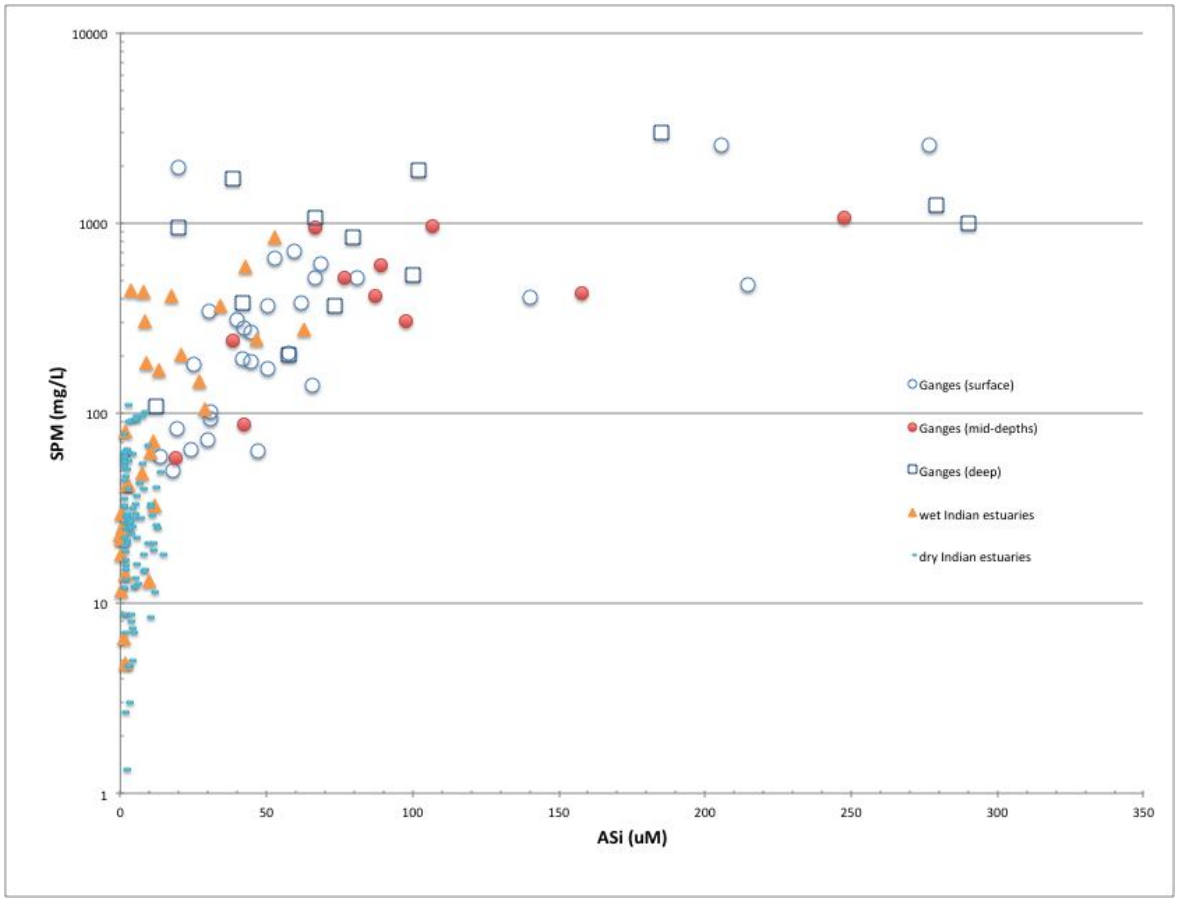

Fig. A1. *Comparison of TSM vs. ASi in Ganges river (circles and squares, data from Frings et al., 2014) and Indian estuaries (triangles and hyphens; this study).*

References

Barão, L. *et al.* Alkaline-extractable silicon from land to ocean: A challenge for biogenic silicon determination. *Limnol. Oceanogr. Methods* **13,** 329–344 (2015).

Clymans, W., Govers, G., Van Wesemael, B., Meire, P. & Struyf, E. Amorphous silica analysis in terrestrial runoff samples. *Geoderma* **167–168**, 228-235 (2011).

Frings, P. J., Clymans, W. & Conley, D. J. Amorphous Silica Transport in the Ganges Basin: Implications for Si Delivery to the Oceans. *Procedia Earth Planet. Sci.* **10,** 271–274 (2014).

Ragueneau, O. *et al.* A new method for the measurement of biogenic silica in suspended matter of coastal waters: using Si:Al ratios to correct for the mineral interference. *Cont. Shelf Res.* **25,** 697–710 (2005).

Appendix B

Individual samples data

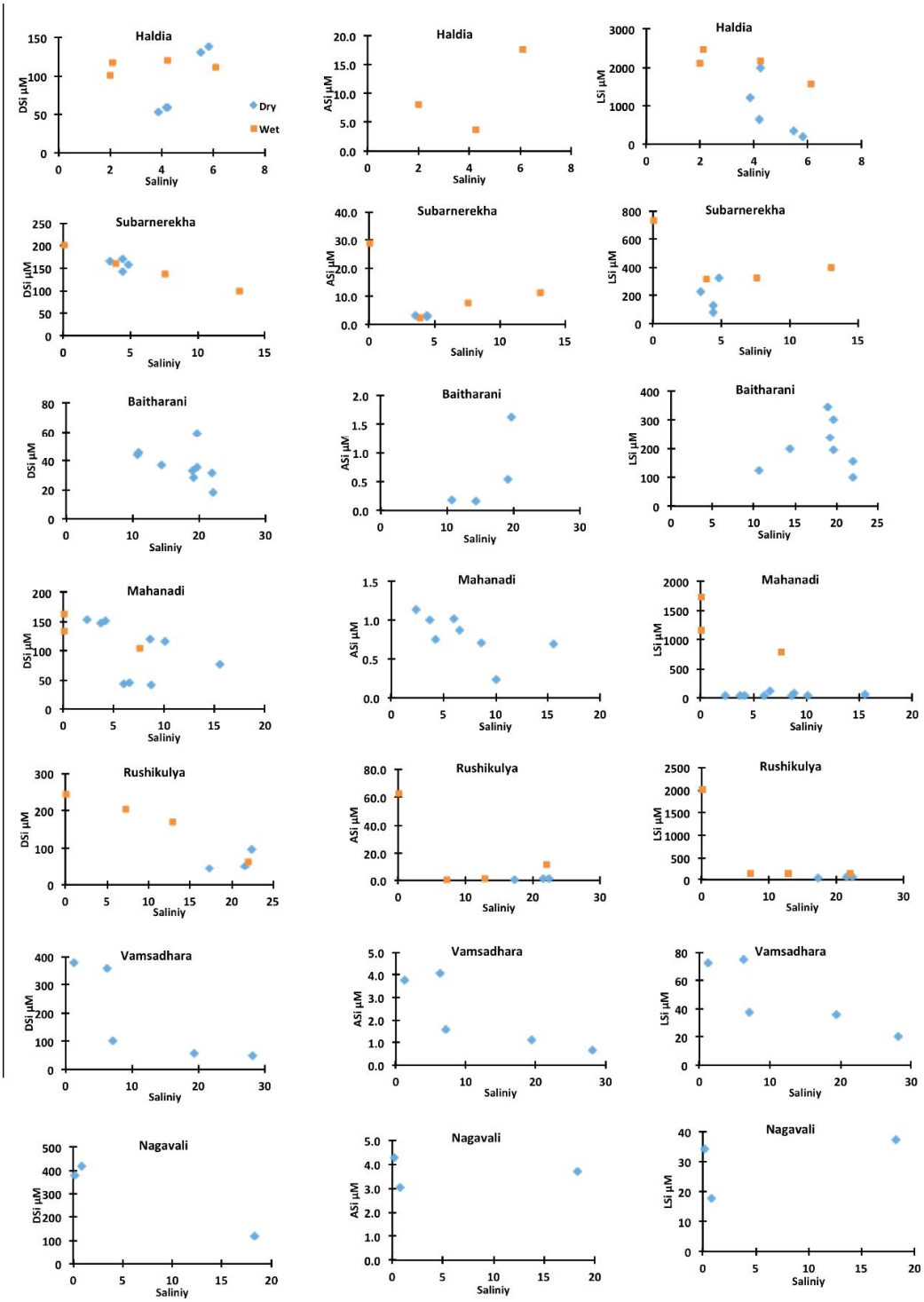

Fig. B1 *DSi, ASi and LSi vs. salinity for northeast estuaries (wet season: orange squares, dry season: blue diamonds).*

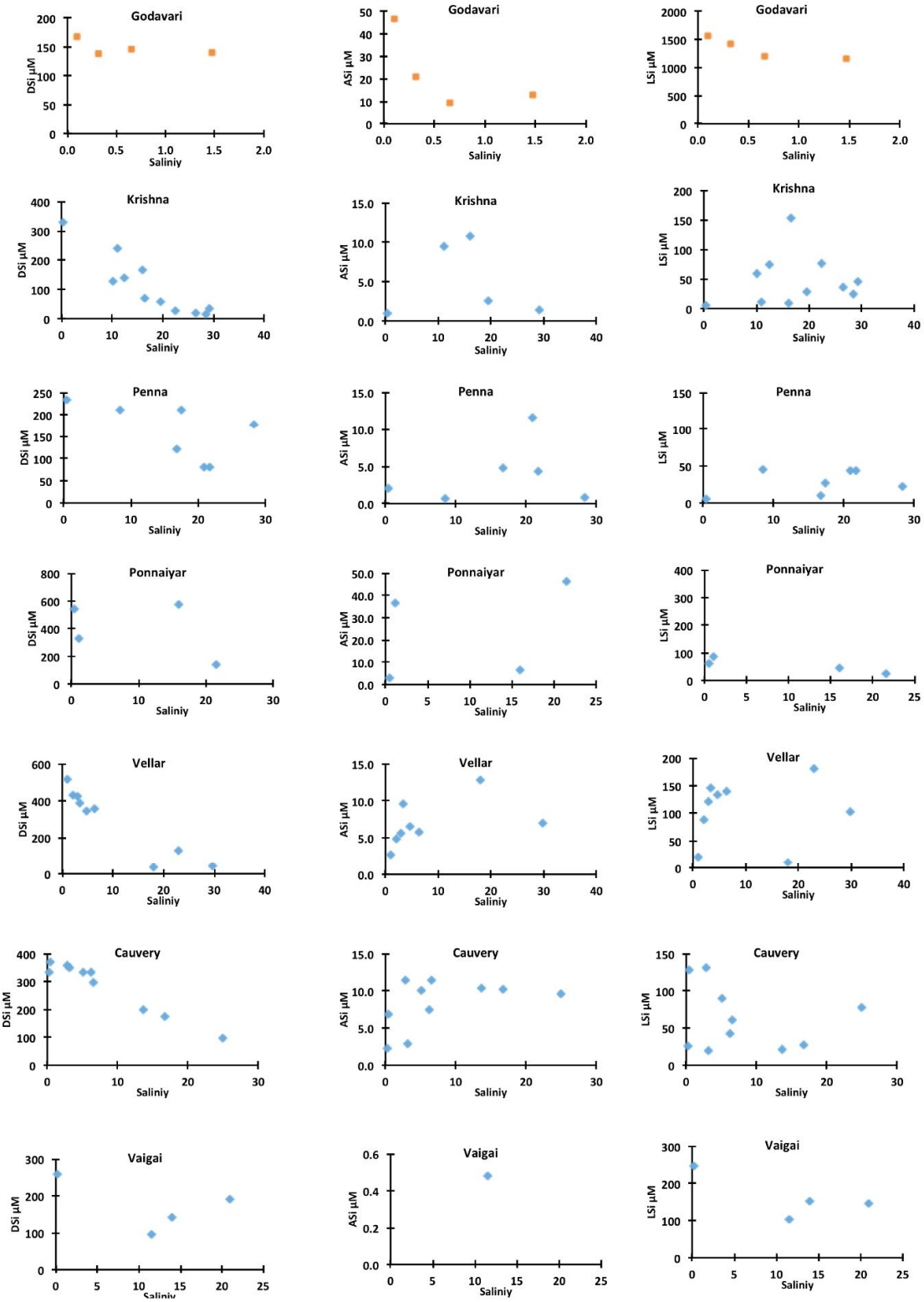

Fig. B2 *DSi, ASi and LSi vs. salinity for southeast estuaries (wet season: orange squares, dry season: blue diamonds).*

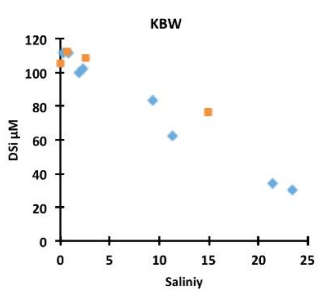
KBW
DSi µM
Saliniy

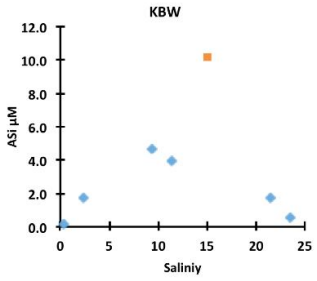
KBW
ASi µM
Saliniy

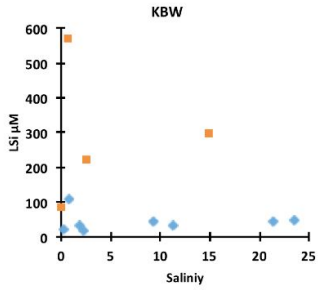
KBW
LSi µM
Saliniy

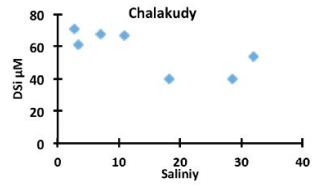
Chalakudy
DSi µM
Saliniy

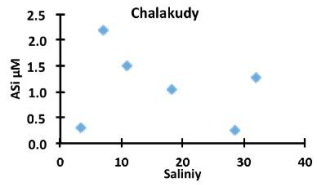
Chalakudy
ASi µM
Saliniy

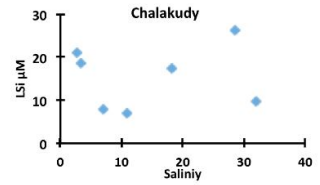
Chalakudy
LSi µM
Saliniy

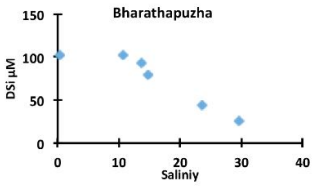
Bharathapuzha
DSi µM
Saliniy

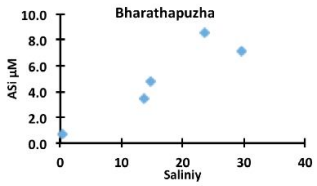
Bharathapuzha
ASi µM
Saliniy

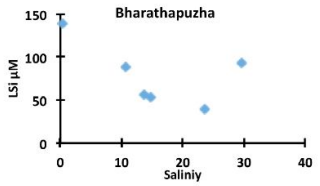
Bharathapuzha
LSi µM
Saliniy

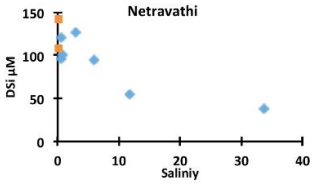
Netravathi
DSi µM
Saliniy

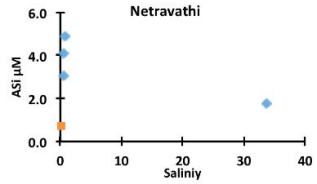
Netravathi
ASi µM
Saliniy

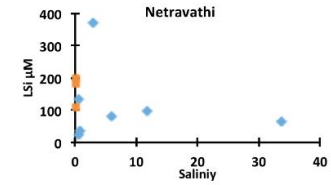
Netravathi
LSi µM
Saliniy

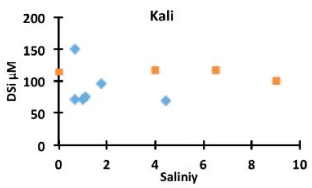
Kali
DSi µM
Saliniy

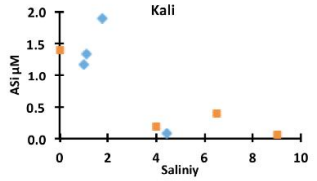
Kali
ASi µM
Saliniy

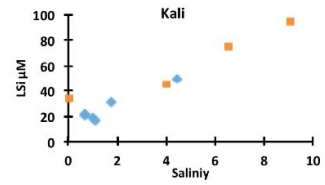
Kali
LSi µM
Saliniy

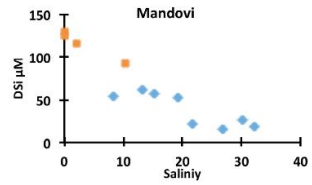
Mandovi
DSi µM
Saliniy

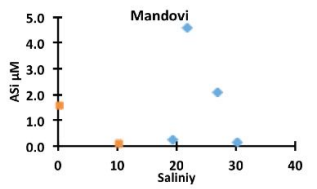
Mandovi
ASi µM
Saliniy

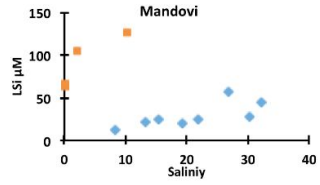
Mandovi
LSi µM
Saliniy

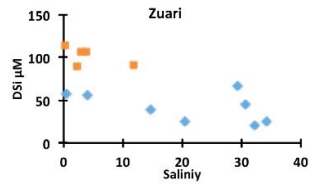
Zuari
DSi µM
Saliniy

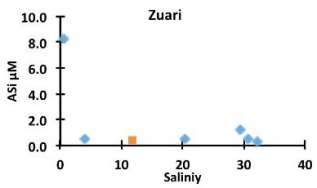
Zuari
ASi µM
Saliniy

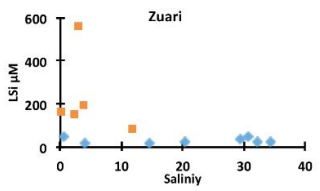
Zuari
LSi µM
Saliniy

Fig. B3 *DSi, ASi and LSi vs. salinity for southwest estuaries (wet season: orange squares, dry season: blue diamonds).*

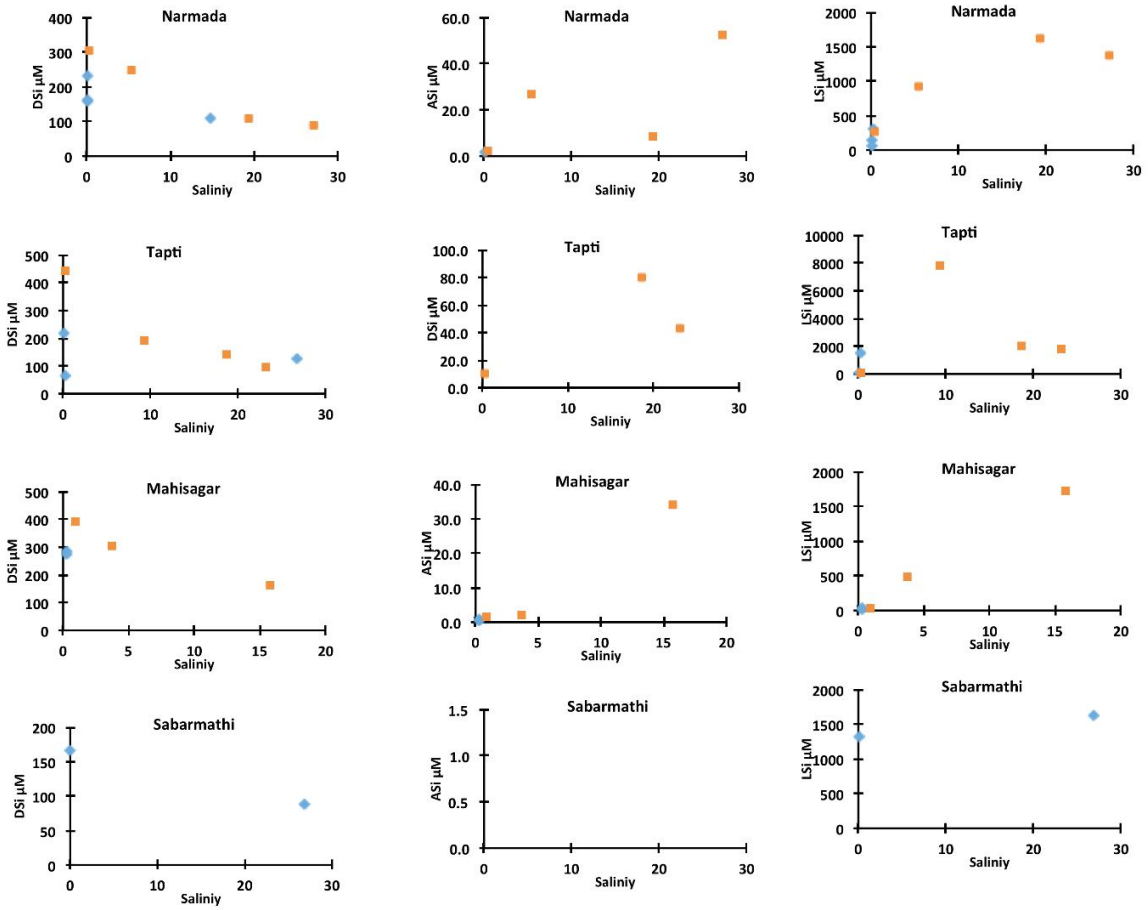

Fig. B4 *DSi, ASi and LSi vs. salinity for northwest estuaries (wet season: orange squares, dry season: blue diamonds).*

Appendix C

Additional PCA and clustering figures and tables

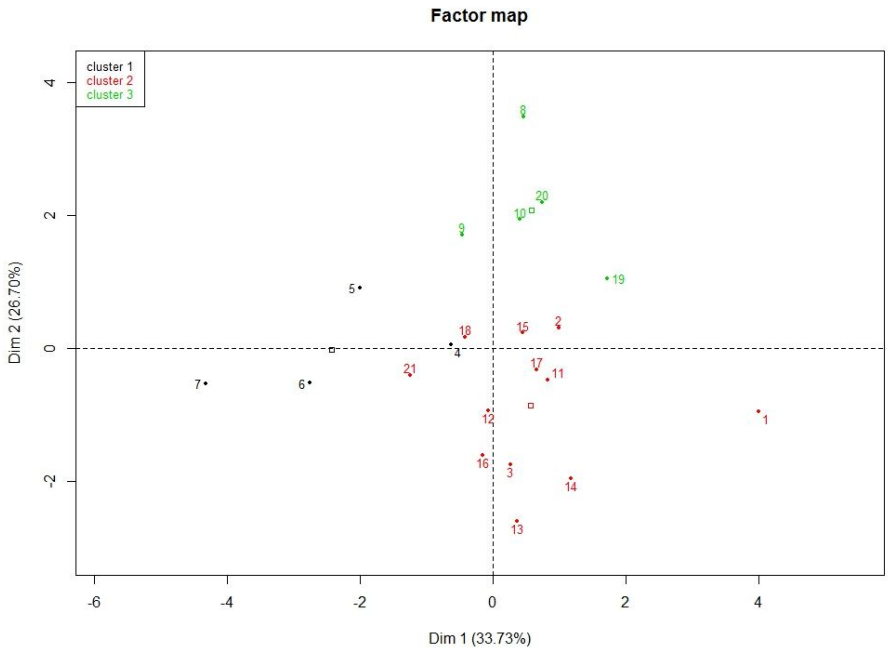

Fig. C1: PCA analysis on upper estuaries during dry period.

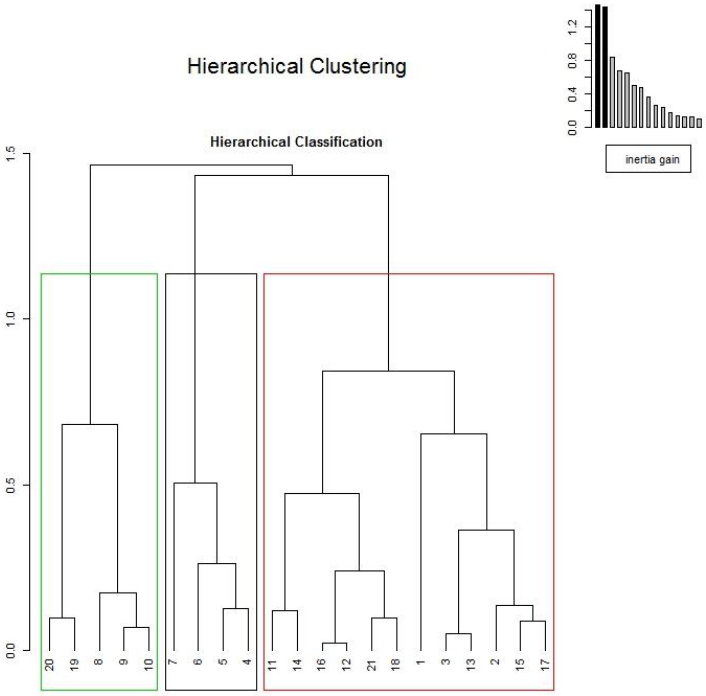

Fig. C2 Hierarchial clustering of PCA results on upper estuaries during dry period.

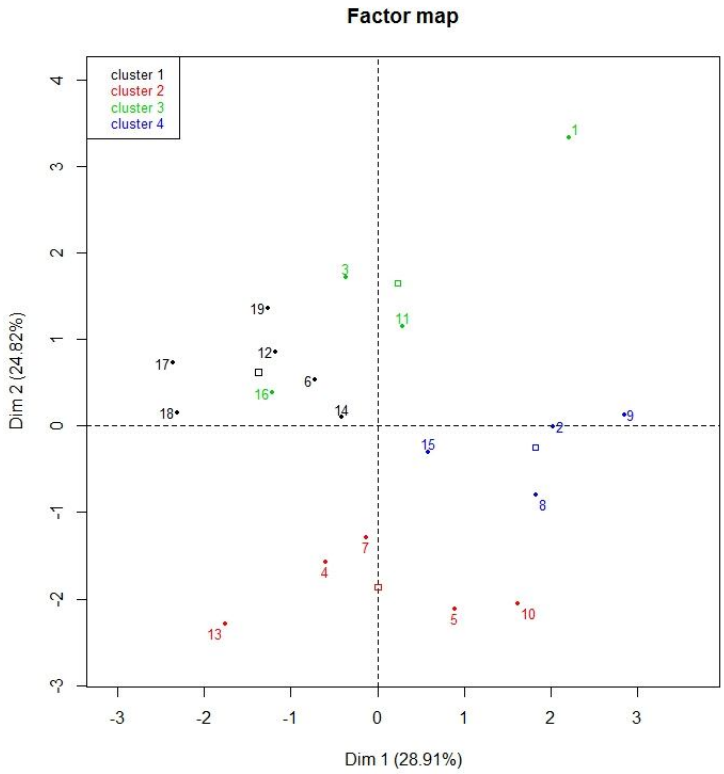

Fig. C3: PCA analysis on middle estuaries during dry period.

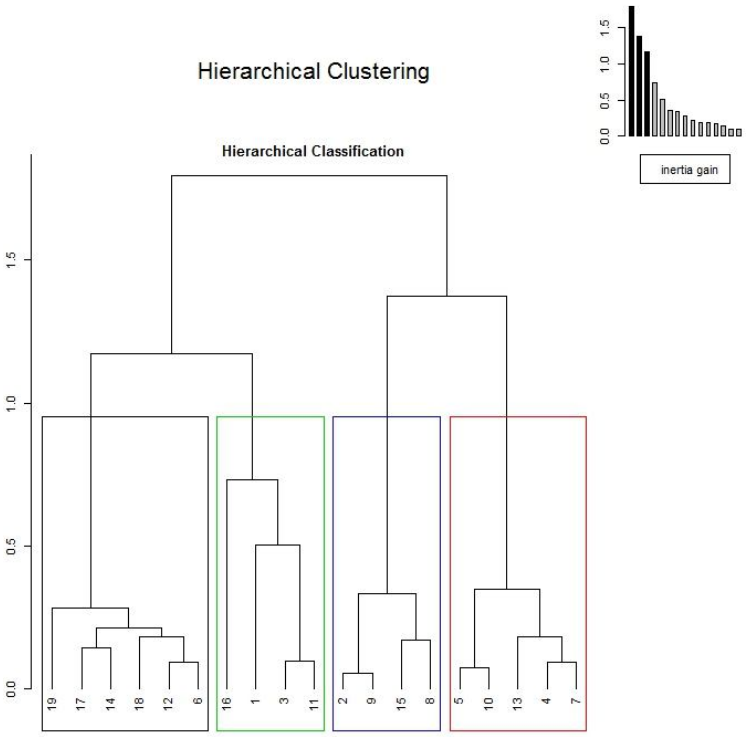

Fig. C4: Hierarchial clustering of PCA results on middle estuaries during dry period.

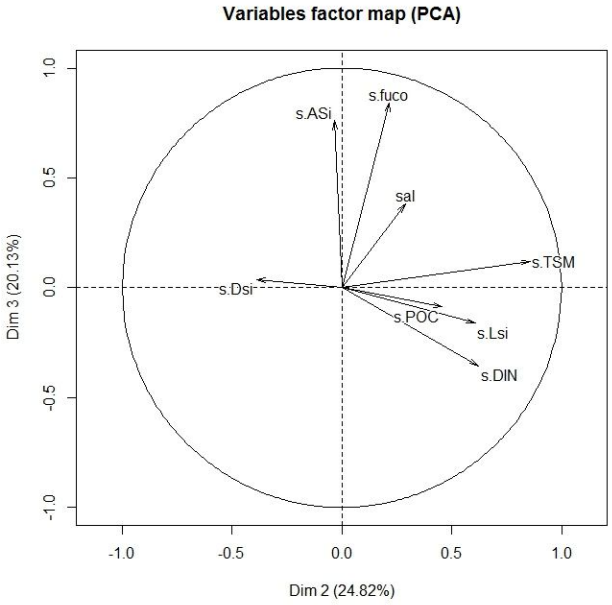

Fig. C5: PCA analysis on variables (PC 2 and PC3) in the middle estuaries during dry period

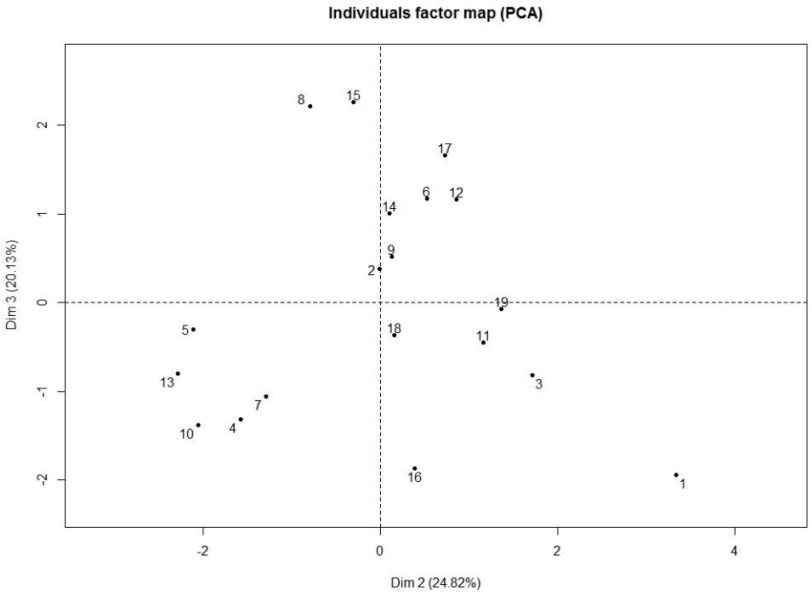

Fig. C6: PCA analysis on individuals (PC 2 and PC3) in the middle estuaries during dry period

Lower-dry

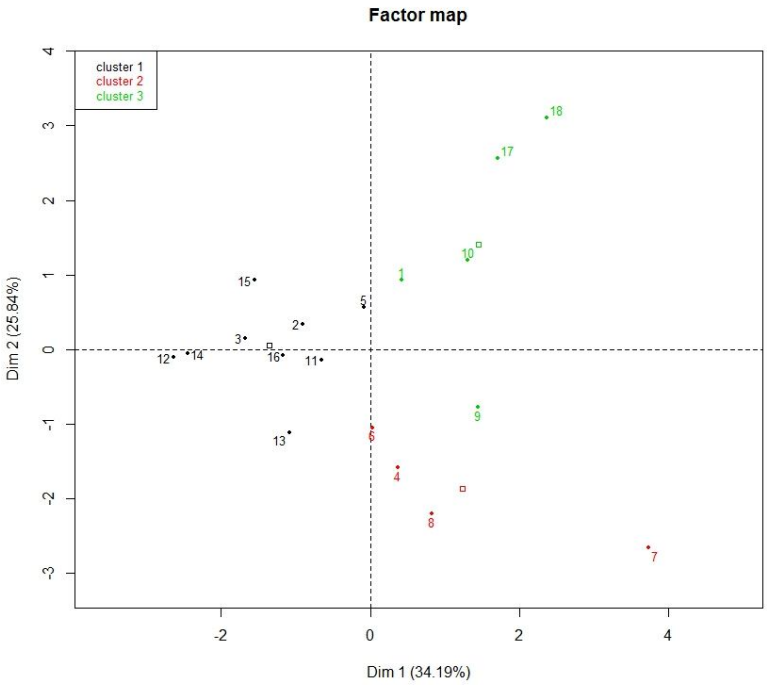

Fig. C7: PCA analysis on lower estuaries during dry period.

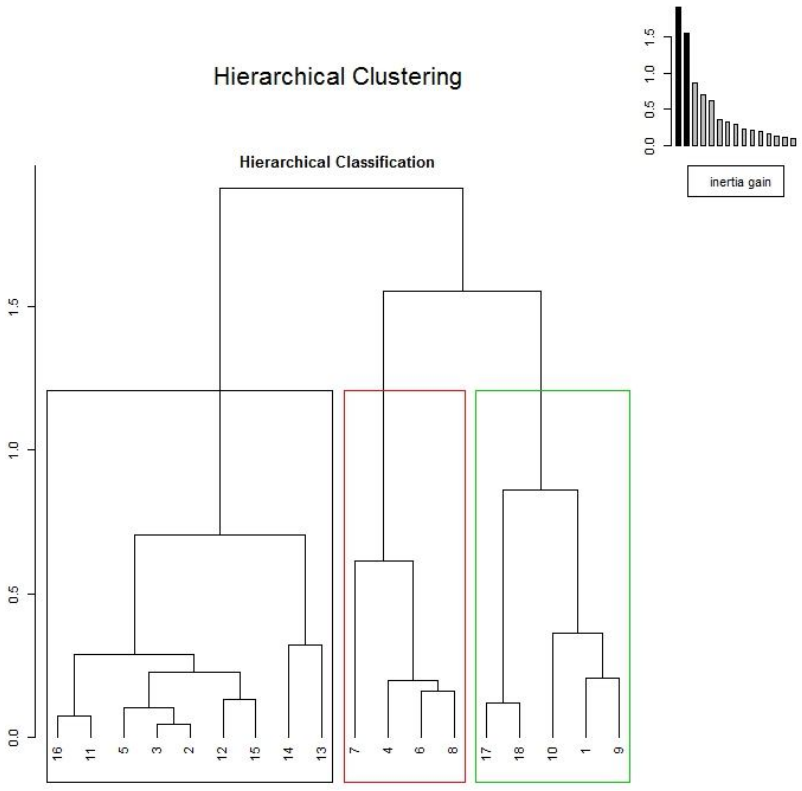

Fig. C8: Hierarchial clustering of PCA results on lower estuaries during dry period.

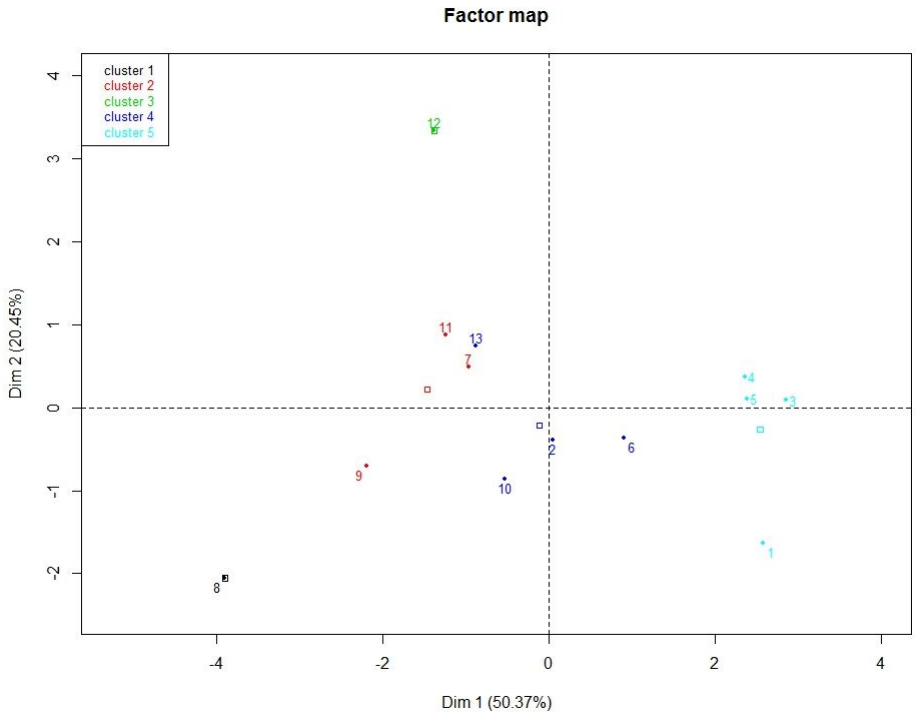

Fig C9: PCA analysis on upper estuaries during wet period.

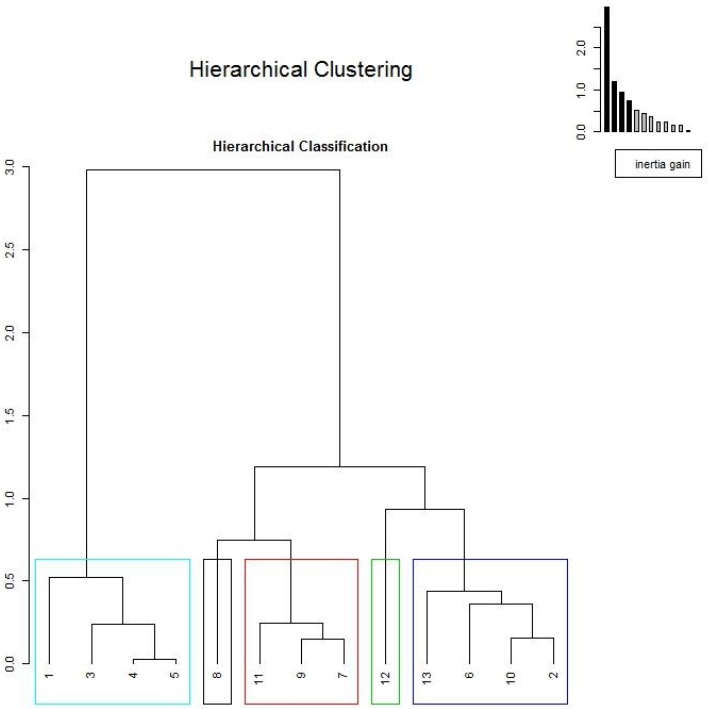

Fig. C10: Hierarchical clustering of PCA results on upper estuaries during wet period.

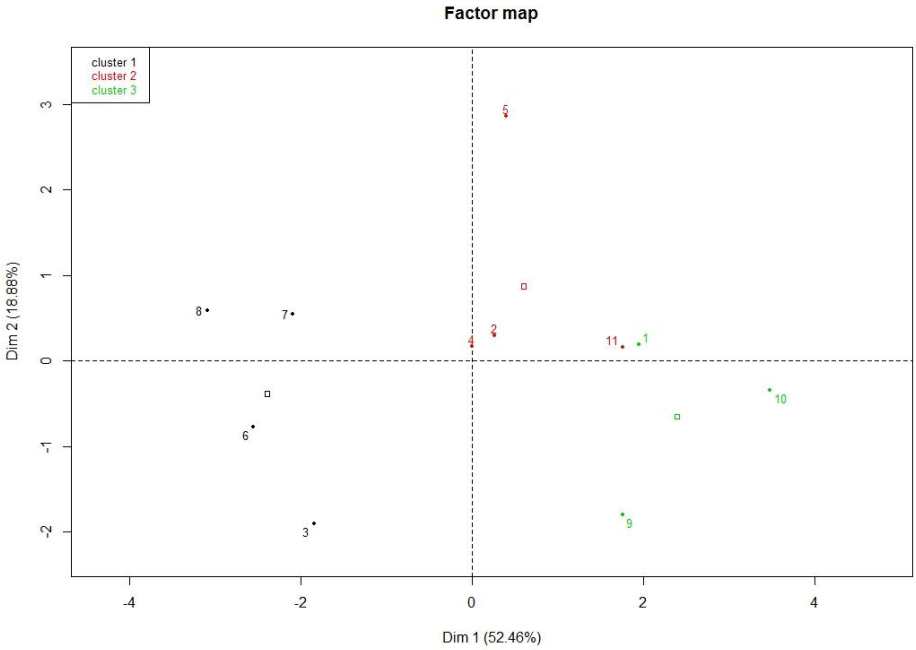

Fig. C11: PCA analysis on middle estuaries during wet period

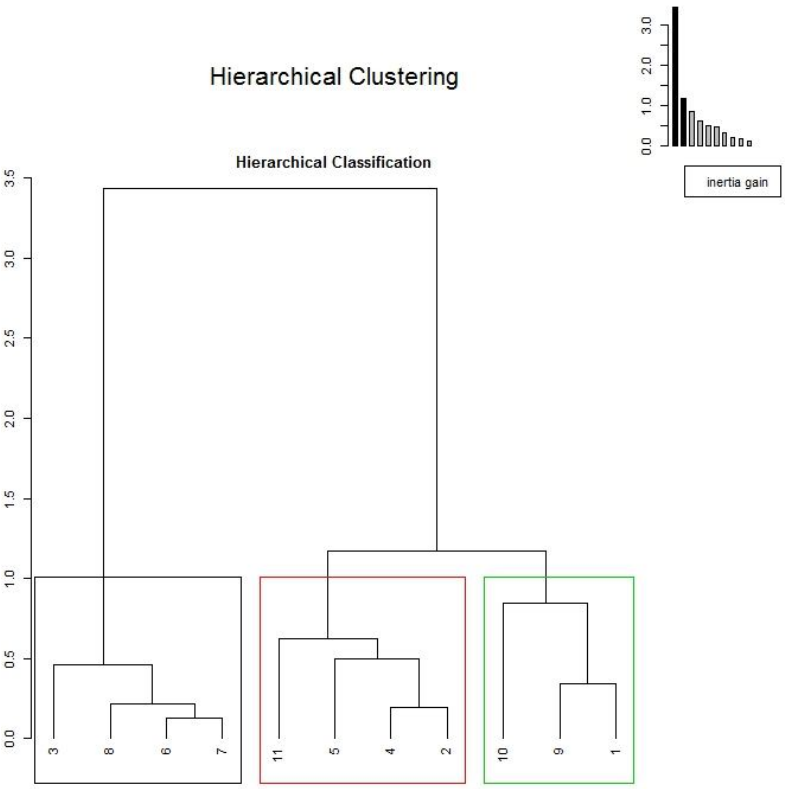

Fig. C12: Hierarchical clustering of PCA results on middle estuaries during wet period.

Data used for PCA and clustering

Ind.no	Estuary	Sal	DSi (µM)	TSM (mg/l)	POC (µM)	DIN (µM)	ASi (µM)	Fuco (µg/l)	LSi (µM)
1	Haldia- Hal	3.88	53	278	322	23	1.96	0.30	1213
2	Subernereka-Sub	3.51	164	32	93	10	3.37	1.92	225
3	Mahanadi-Mah	3.02	150	22	82	5	1.06	0.34	37
4	Vamsadhara- Vam	1.20	378	12	67	4	3.76	0.35	72
5	Nagavali-Nag	0.52	399	9	47	13	3.66	2.25	26
6	Penna-Pen	0.42	233	3	61	12	0.93	3.05	5
7	Krishna-Kris	0.40	327	3	10	75	2.01		6
8	Ponnaiyar-Pon	0.80	435	55	221	6	19.62	10.55	73
9	Cauvery-Cau	1.64	352	19	88	9	5.86	4.85	76
10	Vellar-Vel	2.35	442	44	183	20	5.69	3.57	94
11	Vaigai-Vai	0.17	258	85	124	10	1.80	0.13	246
12	Kochi backwater-KBW	1.31	106	66	51	18	1.62	0.76	45
13	Chalakudi-Cha	3.02	66	31	56	6	1.10	0.23	20
14	Bharathapula-Bha	0.39	103	63	132	3	0.72	0.14	140
15	Nethravathi-Net	1.22	110	30	74	5	3.94	1.61	141
16	Khali-kali	1.04	93	63	56	22	1.64	0.23	22
17	Zuari-Zua	2.25	56	63	65	11	4.38	2.02	34
18	Narmada-Nar	0.12	183	22	NA	34	2.26	0.73	171
19	Tapti-Tap	0.21	142	602	NA	23	4.15	1.34	772
20	Sabarmathi-Sab	0.04	166	84	NA	39	6.45	5.15	1330
21	Mahisagar-Mahi	0.25	278	39	NA	82	0.72	1.05	31

Table C1: upper estuaries- dry period.

Ind.no	Estuary	Sal	DSi (µM)	TSM (mg/l)	POC (µM)	DIN (µM)	ASi (µM)	Fuco (µg/l)	LSi (µM)
1	Haldia- Hal	4.93	97	109	209	30	2.02	0.36	791
2	Subernereka-Sub	4.53	157	29	107	8	8.18	1.39	177
3	Baitharani-Bai	12.00	42	40	138	13	0.81	0.82	160
4	Mahanadi-Maha	8.56	85	15	54	6	0.89	0.31	58
5	Vamsadhara- Vam	6.69	229	20	59	4	2.82	0.43	56
6	Krishna-Kris	11.21	170	53	49	21	5.53	2.44	48
7	Penna-Pen	8.45	211	17	63	11	0.60	0.77	45
8	Cauvery-Cau	7.88	290	26	114	5	9.82	6.13	54
9	Vellar-Vel	5.56	352	41	165	7	6.20	1.49	137
10	Ambalyar-Amb	4.20	317	17	95	7	2.51	0.21	40
11	Vaigai-Vai	12.70	118	58	124	8	1.13	0.59	128
12	Kochi backwater-KBW	10.32	73	95	51	11	4.31	1.98	37
13	Chalakudi-Cha	8.91	67	13	53	9	1.84	0.31	7
14	Bharathapula-Bha	13.05	91	32	79	7	3.44	1.63	66
15	Nethravathi-Net	8.82	75	38	77	2	6.64	5.35	89
16	Khali-kali	4.46	70	63	51	13	0.09	1.53	49
17	Zuari-Zua	14.62	39	51	58	12	4.25	2.77	20
18	Mandovi-Man	10.77	58	64	42	16	1.80	0.50	17
19	Narmada-Nar	14.74	108	NA	NA	46	2.48	NA	NA

Table C2: Middle estuaries- dry period

Ind.no	Estuary	Sal	Dsi (µM)	TSM (mg/l)	POC (µM)	DIN (µM)	ASi (µM)	Fuco (µg/l)	LSi (µM)
1	Baitharani-Bai	20.25	34	62	134	9	1.79	0.64	223
2	Rushikulya-Rus	20.42	63	27	57	7	1.36	0.43	54
3	Vamsadhara- Vam	23.76	53	28	57	5	0.90	0.69	28
4	Nagavalli-Nag	18.25	118	7	97	10	3.71	1.75	37
5	Krishna-Kris	23.39	66	57	53	13	3.32	0.70	57
6	Penna-Pen	21.03	134	16	39	14	5.33	1.97	29
7	Ponnaiyar-Pon	18.75	358	76	164	13	26.38	9.15	36
8	Cauvery-Cau	23.07	190	24	70	4	11.18	4.45	46
9	Vellar-Vel	23.58	71	74	159	7	7.55	2.80	98
10	Vaigai-Vai	20.94	191	65	124	14	1.84	0.18	145
11	Kochi backwater-KBW	22.45	32	77	NA	5	1.16	3.53	46
12	Chalakudi-Cha	26.26	44	10	45	5	0.85	0.82	18
13	Bharathapula-Bha	26.61	34	18	109	2	7.84	0.76	66
14	Nethravathi-Net	33.67	38	5	71	5	1.75	1.69	66
15	Zuari-Zua	29.37	36	45	68	9	0.93	1.17	31
16	Mandovi-Man	24.27	32	34	46	10	1.89	3.09	33
17	Tapti-Tap	26.69	125	49	NA	42	2.53	0.92	2635
18	Sabarmati-Sab	26.87	89	334	NA	60	NA	NA	1633

Table C3: Lower estuaries- dry period.

Ind.no	Estuaries	Sal	ASi (µM)	LSi (µM)	Dsi (µM)	DIN (µM)	TSM (mg/l)	POC (µM)	Fuco (µg/l)
1	Haldia- Hal	2.05	8.09	2284	109	27	706	141	NA
2	Subernereka-Sub	1.99	15.65	526	181	11	74	51	0.39
3	Rushikulya-Rus	0.13	62.78	2001	242	35	278	91	0.11
4	Mahanadi-Maha	0.08	32.56	1442	149	40	209	68	NA
5	Godavari-God	0.64	22.33	1338	147	54	200	76	NA
6	Kochi backwater-KBW	1.10	5.54	293	109	45	46	105	0.39
7	Nethravathi-Net	0.07	2.62	164	130	24	30	29	0.46
8	Khali-kali	2.02	0.80	39	116	5	9	17	0.10
9	Mandovi-Man	0.73	1.20	78	123	18	17	21	0.17
10	Zuari-Zua	2.28	5.42	270	104	21	46	38	0.54
11	Narmada-Nar	0.35	2.52	266	305	13	42	27	0.29
12	Tapti-Tap	0.25	9.82	57	443	18	13	36	1.68
13	Mahisagar-Mahi	2.29	1.75	262	347	32	42	34	0.54

Table C4:Upper estuaries- wet period.

Ind.no	Estuaries	Sal	ASi (µM)	LSi (µM)	Dsi (µM)	DIN (µM)	TSM (mg/l)	POC (µM)	Fuco (µg/l)
1	Haldia- Hal	5.17	10.71	1869	116	31	427	111	0.47
2	Subernereka-Sub	10.33	9.49	360	119	26	60	31	0.93
3	Rushikulya-Rus	10.05	0.95	135	187	11	25	16	0.20
4	Mahanadi-Maha	7.60	9.92	796	105	5	137	NA	NA
5	Kochi backwater-KBW	14.94	10.14	297	77	16	62	84	1.35
6	Khali-kali	7.79	0.23	85	109	7	21	25	0.23
7	Mandovi-Man	10.31	0.09	127	92	7	29	34	
8	Zuari-Zua	11.76	0.45	85	91	1	22	31	0.26
9	Narmada-Nar	5.41	27.01	914	249	39	147	51	0.46
10	Tapti-Tap	9.25		7797	195	50	4236	NA	2.26
11	Mahisagar-Mahi	15.75	33.98	1737	162	53	368	NA	0.44

Table C5: middle estuaries- wet period.

Appendix D

Details of Flux calculation

In the following, we estimate the fluxes of ASi, LSi and DSi to the coastal Arabian Sea and Bay of Bengal. The Indian estuaries are mostly monsoonal estuaries and receive maximum runoff during the southwest monsoon period and the extreme supply of materials via rivers also occurs mostly during that period (Subramaniyan et al., 2006). We estimated the fluxes of ASi, LSi and DSi for dry and wet periods of the estuaries where we have monthly discharge for full annual scale (Mahanadi, Kochi backwater, Netravathi, Narmada and Mahisagar, Fig. D1, data from http://www.india-wris.nrsc.gov.in/). We assume that the DSi, ASi and LSi concentrations measured in our dry season samples are representative of all low discharge months and similarly for our wet season samples being representative of all high discharge months. We extrapolate our data depending on the length of seasonal (3 to 4 months for wet and 8 to 9 months for dry depending on monthly discharge for each river) to compare seasonal flux using monthly discharge. The wet water discharge represents ~70-99% of annual discharge for the five rivers (Table D1). Weighted by silicon concentration, we find that, around 70 to 99% of DSi, 93-99% of ASi (except Mahisagar which is 47%) 93 to 99% of LSi and 95-99% of TSM (except KBW which is 61%) fluxes are supplied only during the wet period (Sup. table: 5b).

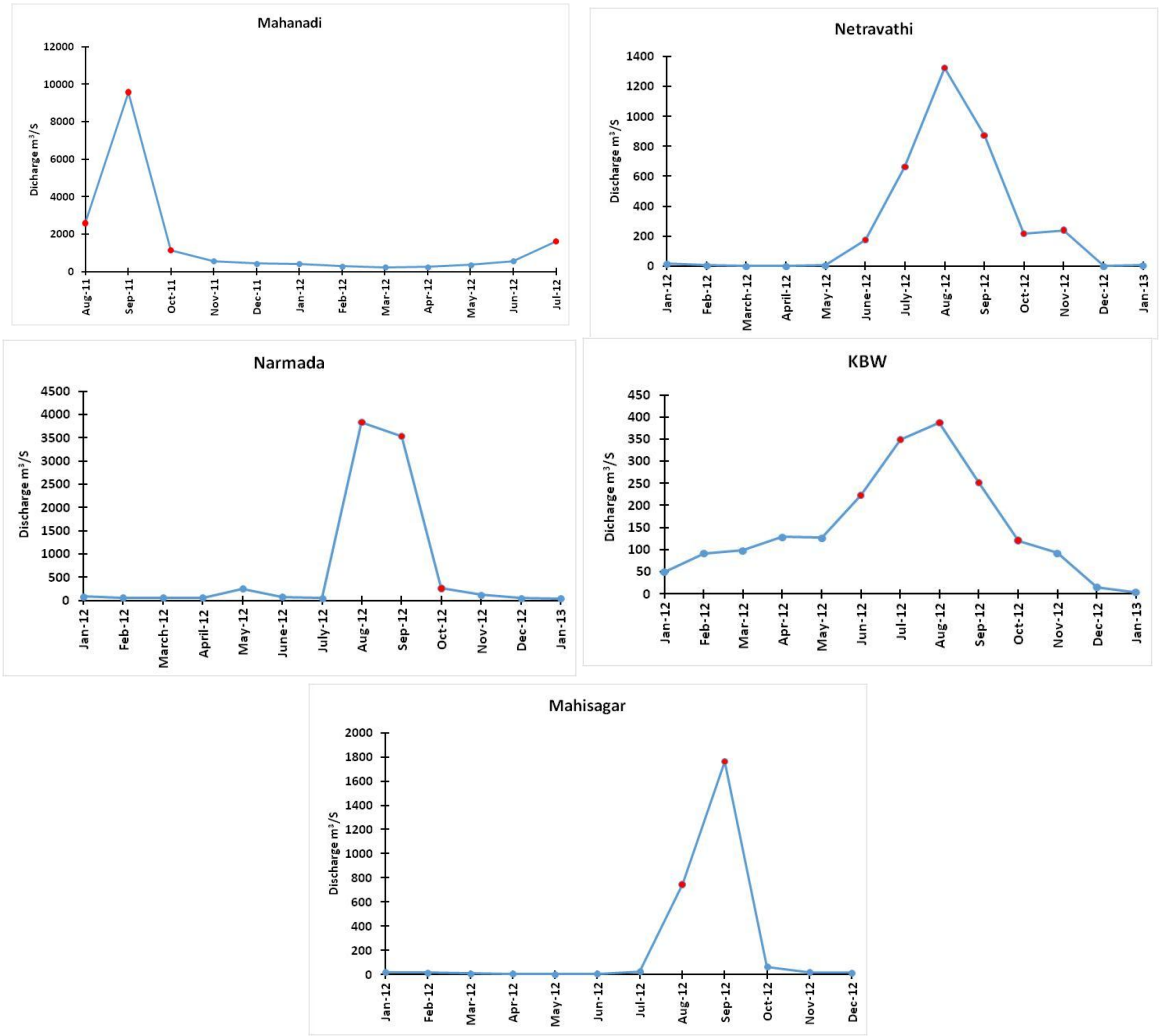

Fig. D1. *Monthly discharge of upper estuaries. The months considered as wet season are highlighted in red.*

Only annual mean discharges of Haldia, Subarnarekha and Kali estuaries are available however there is no seasonal variation of the discharge for these rivers. Therefore, we assume that these estuaries are having the similar seasonal behavior to their adjacent estuaries namely, Hooghly, Mahanadi and Netravathi respectively, and we use the later fraction of wet vs. dry water discharge to calculate the wet period contribution of DSi, LSi and ASi of Haldia, Subarnareka and Kali estuaries respectively. For example, in the estuary Netravathi 98% of total annual discharge is contributed during wet period. Since Netravathi, is adjacent to Kali, we apply the 98% wet contribution to Kali Si concentrations to compute their wet period contribution. Likewise, Hooghly (tributary of Ganges) has 75% of annual discharge

during wet period and is used for Haldia (distributed from Hooghly) and finally, Mahanadi has 83% of annual discharge during wet period is used for Subarnereka to compute their total wet period discharge.

Estuaries	% of Discharge wet season	DSi flux		% flux wet season	ASi flux		% flux wet season	LSi flux		% flux wet season	TSM flux		% flux wet season
		Kmol/yr	Kmol/wet season		Kmol/yr	Kmol/wet season		Kmol/yr	Kmol/wet season		kg/yr	kg/wet season	
Mahanadi	83	6952155	5723023	82	1264570	1256745	99	56067273	55760805	99	8268470	8097304	98
KBW	69	542159	375301	69	21369	19891	93	1079908	1009666	93	262805	159943	61
Netravathi	99	1192000	1180058	99	6822	6389	94	1501322	1486057	99	279362	276119	99
Narmada	90	6431194	6030331	94	53306	49790	93	5641360	5265967	93	886820	838654	95
Mahisagar	93	2381954	2253557	95	24073	11373	47	1721386	1701795	99	286748	274048	96

Table D1. *Contribution of DSi, ASi, LSi and TSM flux during wet season*.

The fluxes have been calculated for wet period for each upper estuary (Table 11). Since variables are not necessarily conservative (Appendix B), we corrected the upper wet fluxes from this non-conservativity. This led to increase or to decrease the fluxes (Table 11).

Appendix-E

SEM pictures

Source: **S. Caquineau**

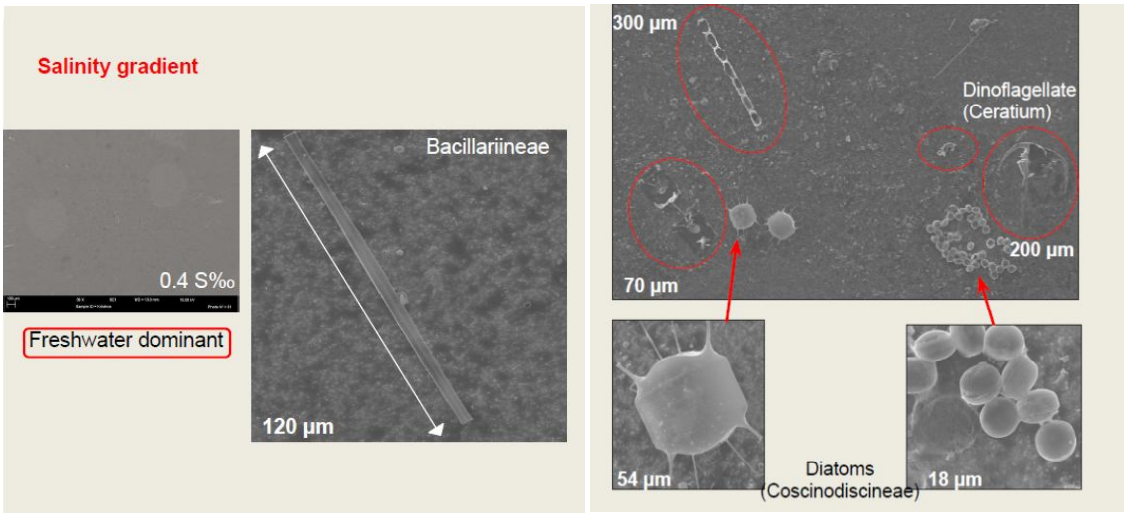

Fig: *SEM pictures of estuary Krishna- dry period. Note the large size and good shape of diatom silica frustules.*

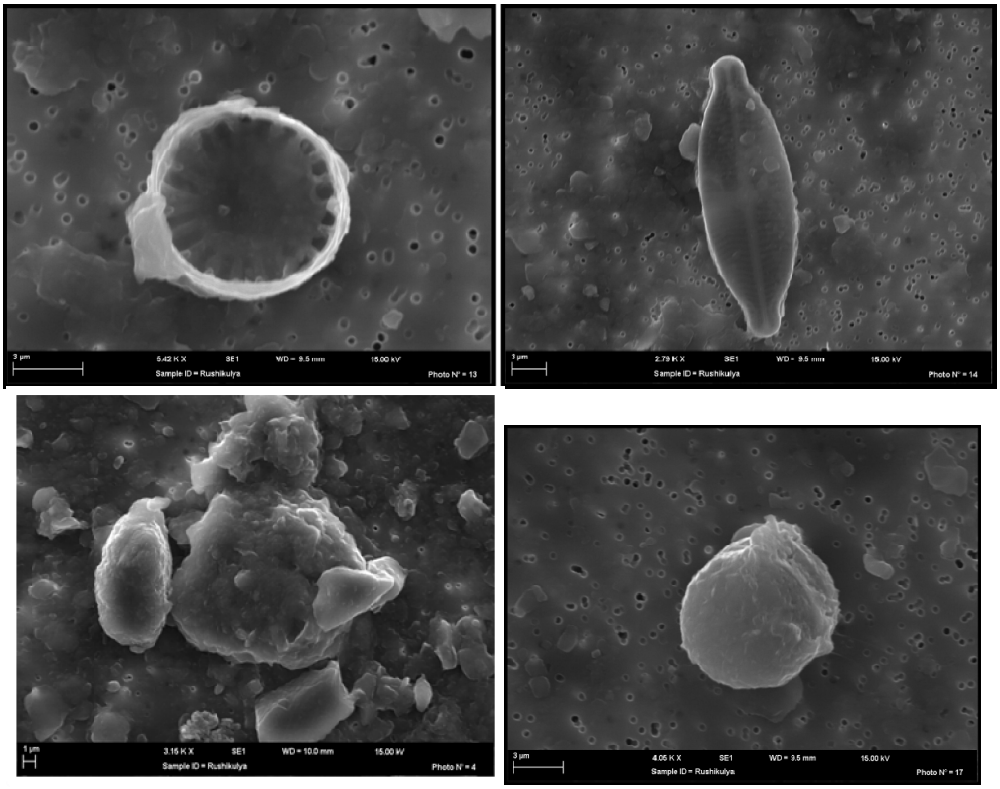

Fig: *SEM pictures of estuary Rushikulya- during wet period. Note the broken and partly dissolved silica frustules.*

Appendix-F

Lithogenic contribution

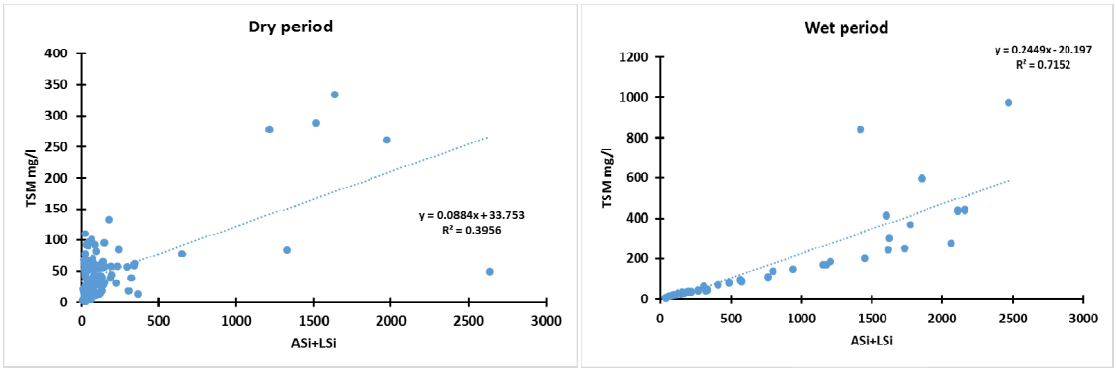

Fig: *Relationship of TSM with total particle Si pool (ASi+LSi) during dry and wet period indicating more influence of lithogenic supply during wet period when compared to dry.*

Appendix-G

Influence of Nitrogen in land use

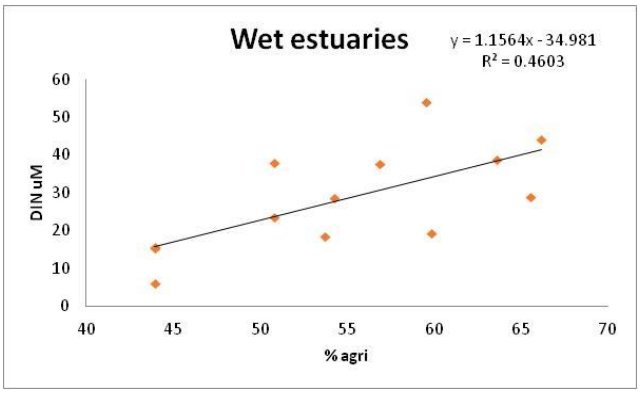

Fig: Impact of land use especially with % of agriculture is evidenced by DIN concentration during wet period.

Appendix of Chapter 4

Annex-A

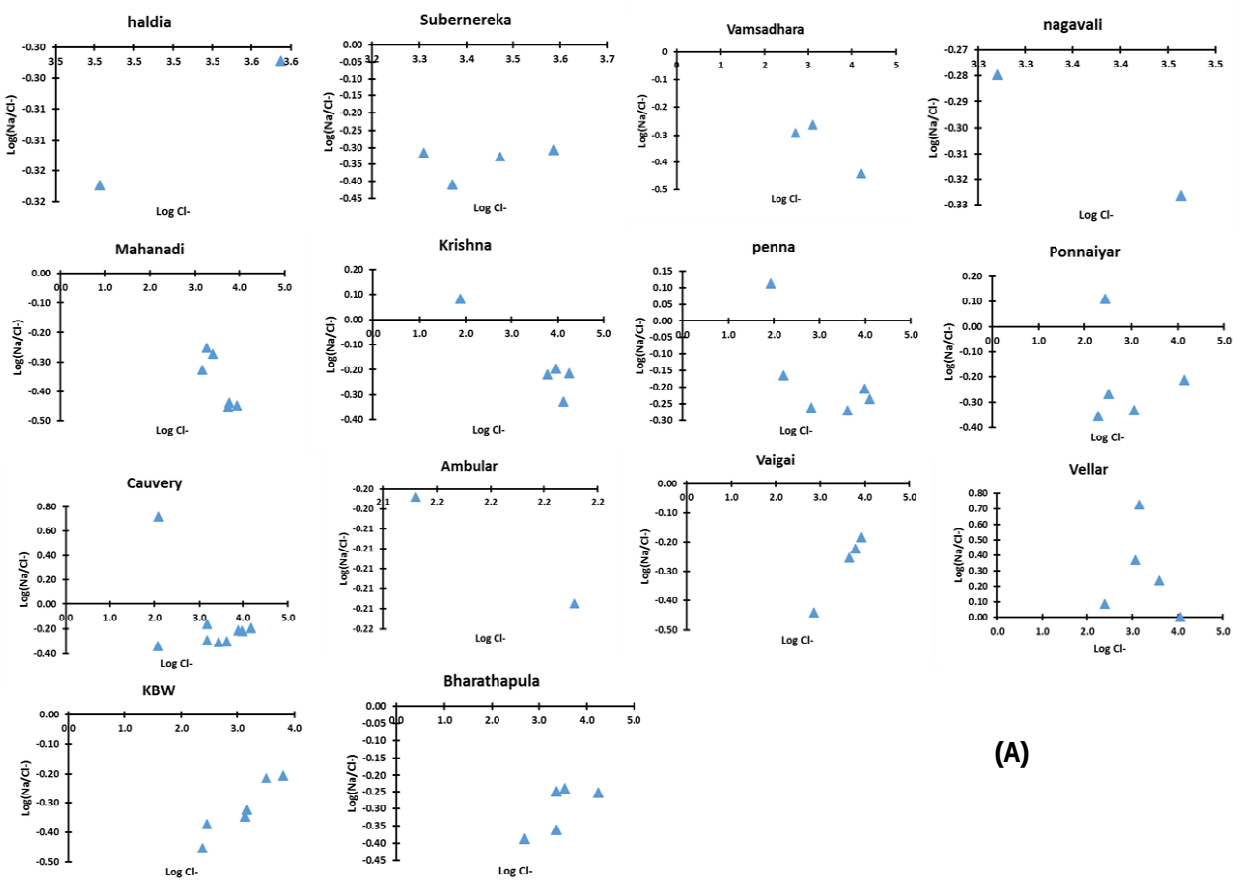
haldia
Subernereka
Vamsadhara
nagavali
Mahanadi
Krishna
penna
Ponnaiyar
Cauvery
Ambular
Vaigai
Vellar
KBW
Bharathapula
Log(Na/Cl-)
Log Cl-

(A)

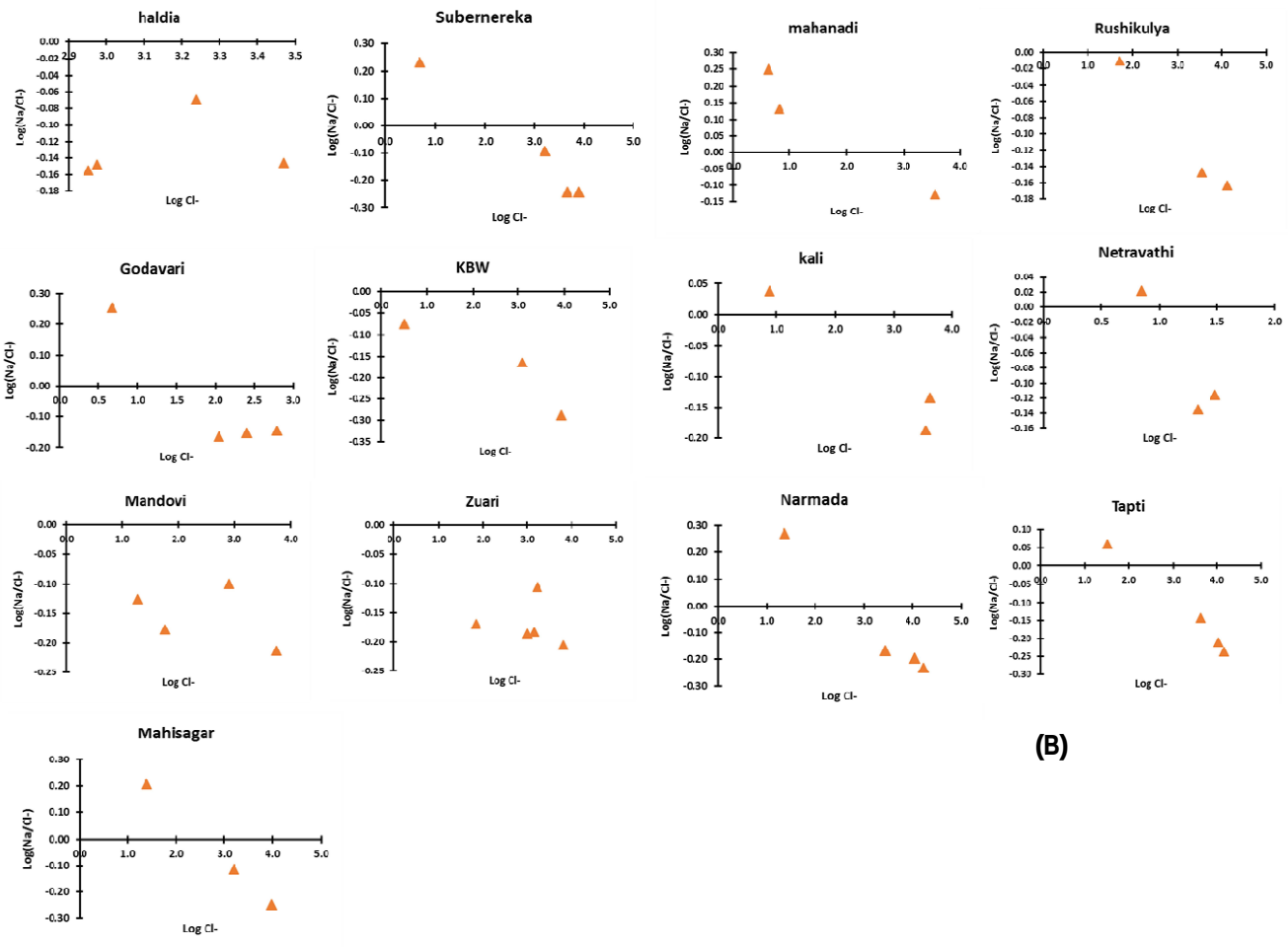

Fig. 1 *The influence of Cl containing fertilizer (MOP-Muriate of potassium) on the Cl concentration measured in the Indian estuaries during dry (A) and (B) wet period. The impact of artificial supply is well evidenced during dry period rather than the wet period. The seawater log (Na/Cl) and log (Cl) is found to be -0.25 and considered as threshold limit. The values lower than this indicate the impact of fertilizer. Note the log scale representation on both the axes. This is responsible for the negative values of atmospheric corrected cation concentration during dry period.*

Total cations

The major cations concentrations of estuaries were corrected for the atmospheric input assuming that sea salt is the major contributors and corrected using marine element ratio (Cardinal et al., 2001). The atmospheric correction was carried out using the Equation (1),

$$X^* = X_{river} - Cl_{river} * (X_{Seawater} / Cl_{Seawater}). \quad \text{(Eq. 1)}$$

The X_{river} and Cl_{river} are the concentrations of X and Cl in the river water respectively and $X_{seawater}$ and $Cl_{Seawater}$ are the concentrations of X and Cl in the sea salt brought by atmospheric inputs. Surprisingly, we found negative values of major elements after the atmospheric correction (mainly for Na), especially noticed during dry period. This indicates the overestimation of atmospheric correction of the estuarine samples. It is noteworthy that, high fertilizer consumption in India (ranks 2nd in the world, as discussed in chapter 3) for the agricultural purpose particularly potash (Potassium chloride, Kinekar and Nagar, 2011) for high yield, might introduce the excess chloride from agricultural land. Therefore assuming solely atmospheric input for Cl might overestimate the correction and explain such negative values. Moreover, the impact of Cl^- containing fertilizer was noticed in most of the estuaries during the dry period when compared to the wet period (Fig. 1a and b). The impact of fertilizers was noticed based on the threshold log (Na/Cl) of seawater (-0.25). The values below the threshold limit indicate the impact of Cl containing fertilizers. During dry period, the impact of fertilizers is more evidenced in all the estuaries (≤ -0.25) but is negligible during wet period (Fig. 1b). Therefore, the negative values after atmospheric correction mainly due to the fertilizer impact and hence we did not use the corrected major cation concentration.

Major element ratios are commonly used as indicative of weathering processes. For instance, the elemental ratios of DSi/ (Na+K)* has been used as a tracer of the type of weathering (Hughes et al., 2013) in the Amazon basin. Na* solely is an indicator for the weathering of primary minerals since it is not generally incorporated into the clay minerals while K can be incorporated in the secondary minerals (e.g. illite) and is also involved in soil-plant macronutrient cycle (Hughes et al., 2013; Meunier et al., 2015). Therefore, DSi/Na* can be an excellent proxy to determine the primary weathering degree. The * indicate that Na and K concentrations are corrected from atmospheric inputs. A study on the Amazon basin used the DSi/ (Na*+K*) ratio to determine the proportion of Si remaining immobilized in the secondary minerals (Hughes et al., 2013). Thus, a lower ratio in solution indicates a higher proportion of Si remaining immobilized in secondary clay minerals. A ratio lower than 2 indicates the smectites formation (bisiallitization with formation of 2:1 clays), ratio from 2 to 3.5 indicates the kaolinite formation (monosiallitization with formation of 1:1 clays) and ratio greater than 3.5 indicates that all silicon is leached and results in gibbsite formation (allitization process) (Hughes et al., 2013).

On contrary to what we see on δ^{30}Si-DSi vs. Si/(Na*+K*)in two Indian rivers (e.g., Chapter 5), there is no clear relationship between the δ^{30}Si-DSi and Si/(Na*+K*) in Indian estuaries to explain the type of chemical weathering. All the upper estuaries of DSi/(Na*+K*) values are < 1 (fig. 2), indicating smectite type secondary mineral leaching (Hughes et al., 2013). This is not possible because the variability of Si isotopes between north and south (0.2 to 0.7 ‰) is higher and cannot associated with single type of smectite clay formation process to answer the variability of Si isotopes. Therefore, this proxy does not give clear information regarding the type of weathering and reasons remain unclear.

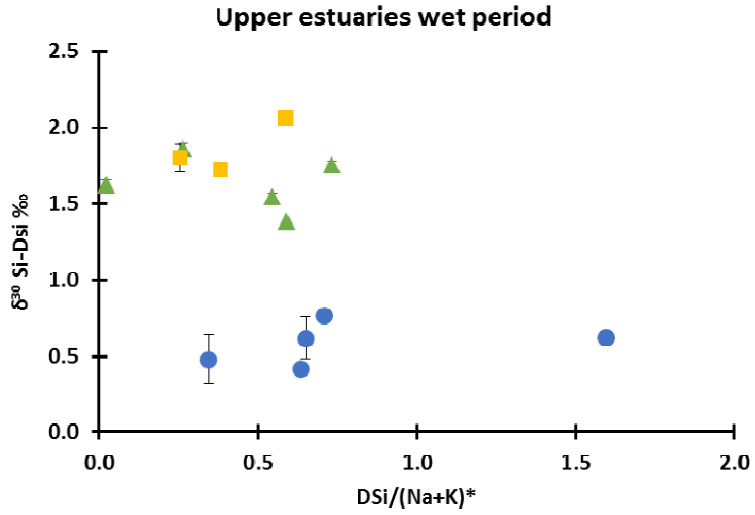

Fig. 2 *Relationship between δ^{30}Si-DSi and DSi/ (Na+K)* to determine the type of clay mineral formation during weathering in the upper wet estuaries.*

Annex-B

Conservativity of DSi and δ^{30}Si-DSi in individual estuaries

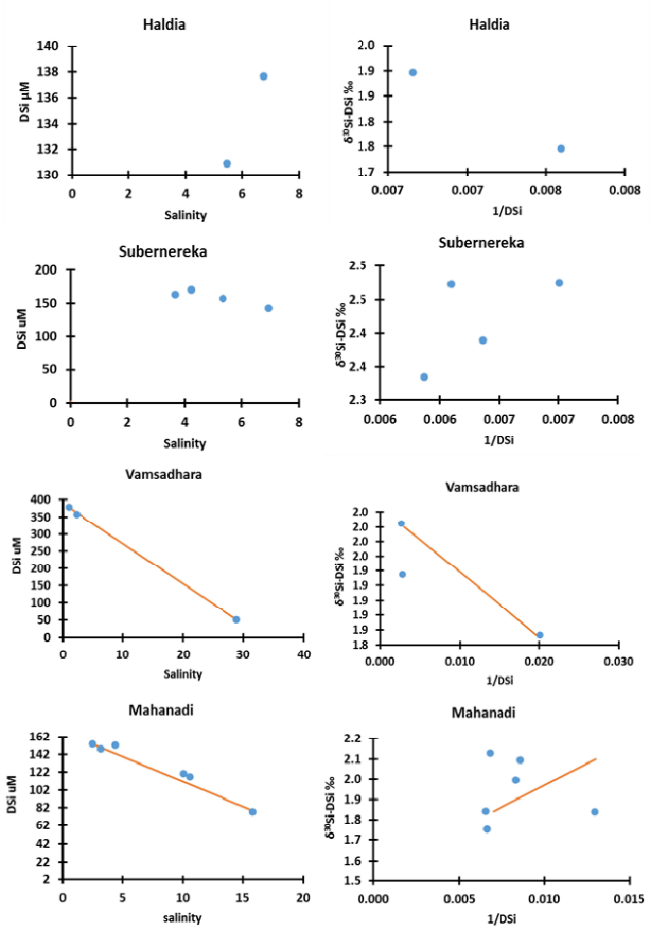

Continued…

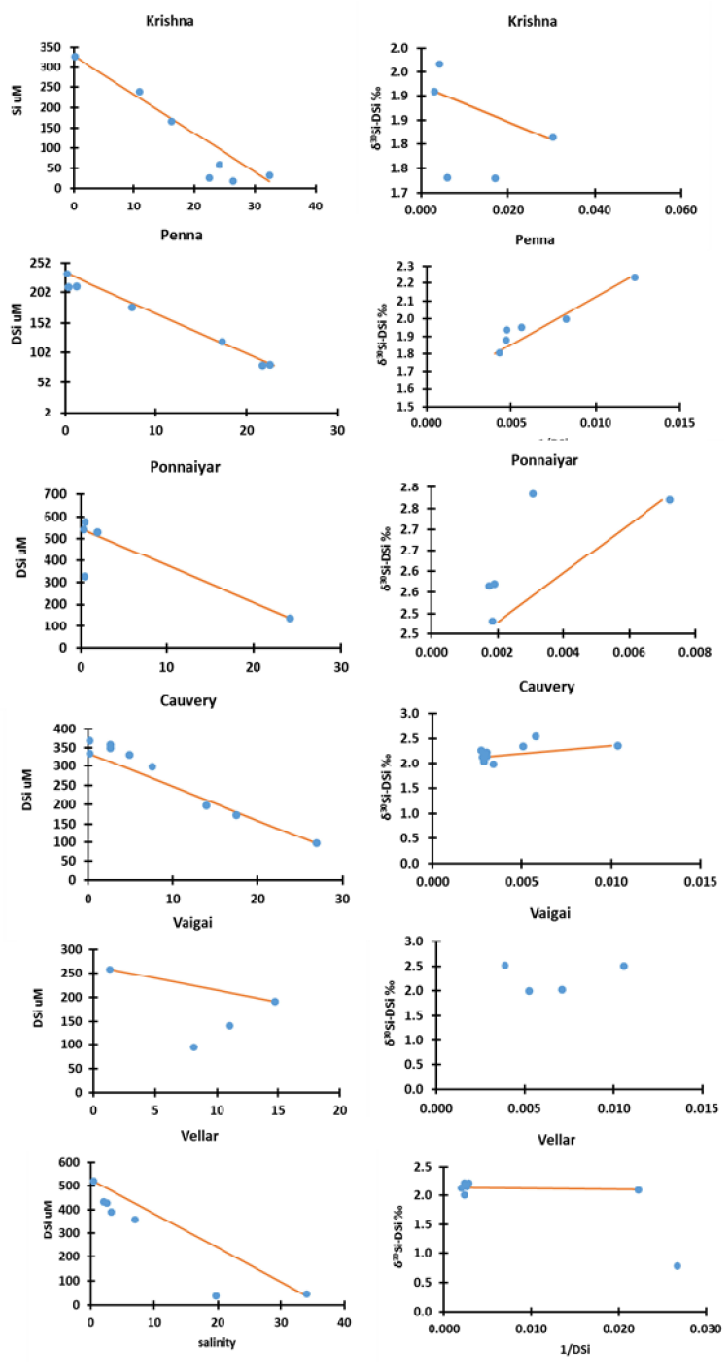
Krishna
Si uM
Krishna
δ30Si-DSi ‰
Penna
DSi uM
Penna
δ30Si-DSi ‰
Ponnaiyar
DSi uM
Ponnaiyar
δ30Si-DSi ‰
Cauvery
DSi uM
Cauvery
δ30Si-DSi ‰
Vaigai
DSi uM
Vaigai
δ30Si-DSi ‰
Vellar
DSi uM
salinity
Vellar
δ30Si-DSi ‰
1/DSi

Continued...

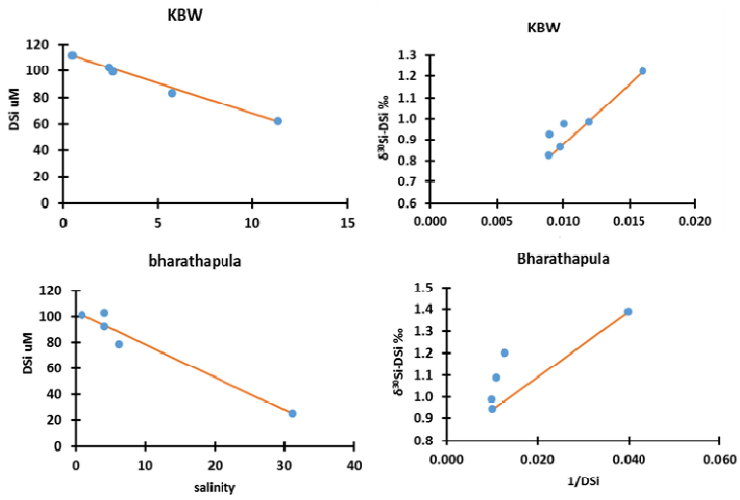

Fig. 3 *Conservativity and non conservativity behavior of DSi and δ^{30}Si-DSi of individual estuaries during dry period.*

Annex-C

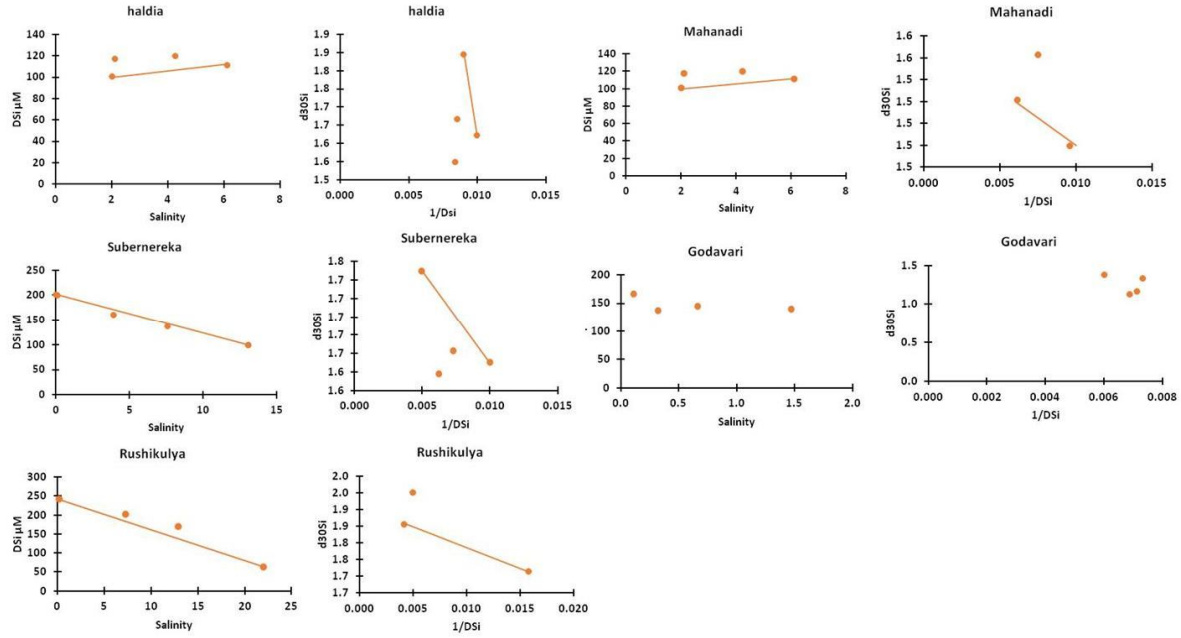

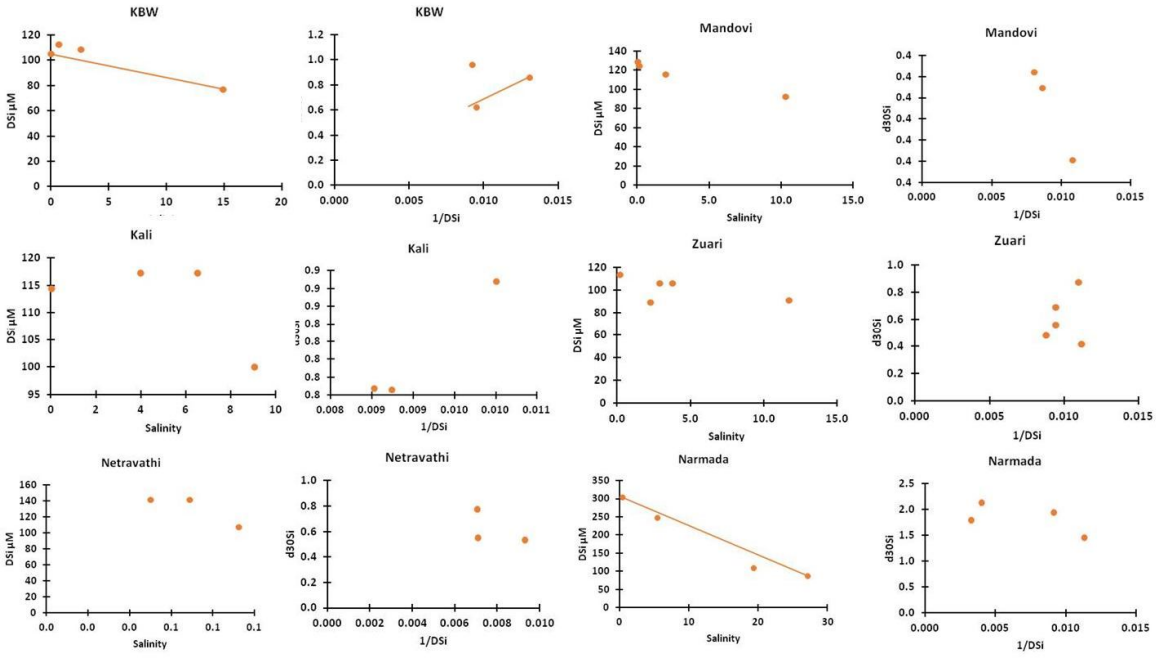

Figure continued..

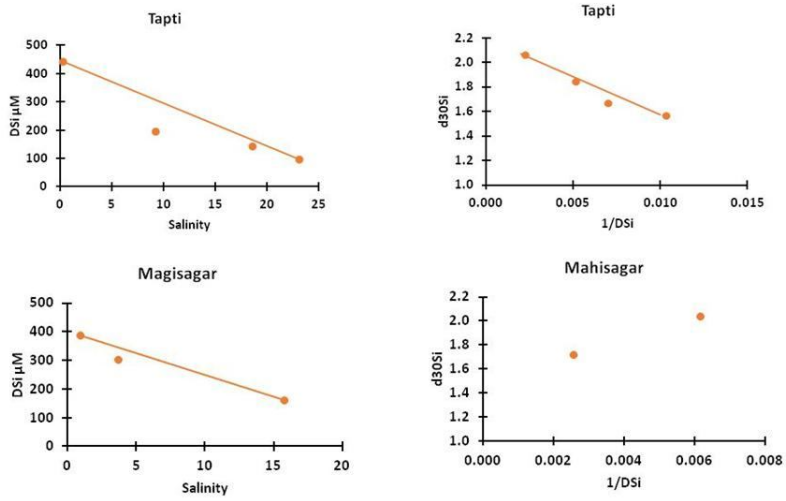

Fig. 4 *Conservativity and non conservativity behavior of DSi and δ^{30}Si-DSi of individual estuaries during wet period.*

Sampling pictures from wet season

Continued...


Godavari # 1


Godavari # 2


Godavari # 3


Godavari # 4


Krishna # 1


Krishna # 2


Krishna # 3


Krishna # 4


Vellar # 1


Vellar # 2


Vellar # 3


Vellar # 4


Ponnaiyar # 1


Ponnaiyar # 4

Continued...


Penna # 1


Penna # 2


Penna #3 & 4


Cauvery # 1


Cauvery # 2


Cauvery # 3


Cauvery # 4


KBW # 1


KBW # 2


KBW # 3


KBW # 4


Netravathi # 1


Netravathi # 2


Netravathi # 4

Continued...

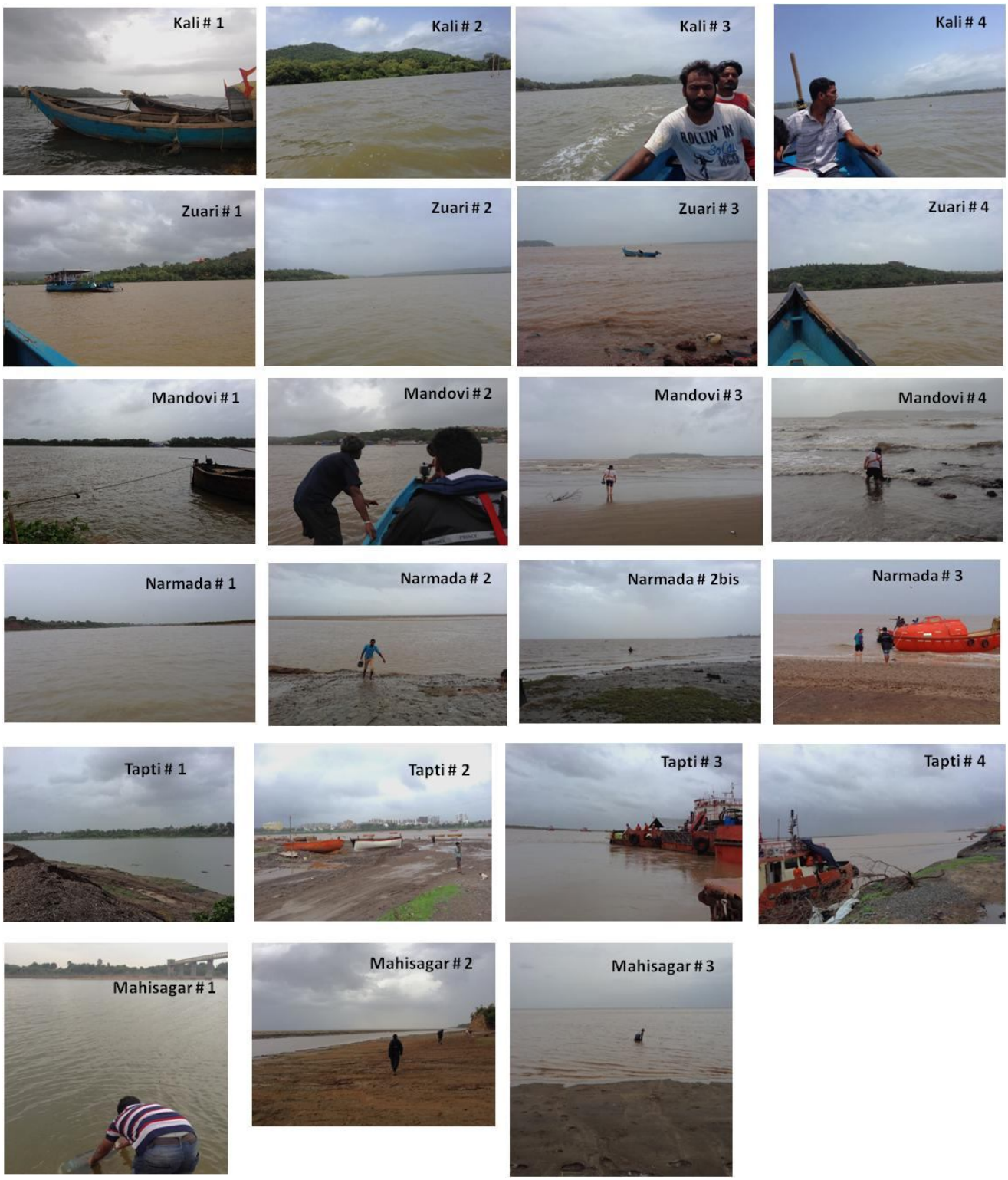

Fig. 5 *The list of estuaries sampled during wet period (July-August 2014) and the number preceding the name of the estuaries are the station number of each estuary.*

References

Cardinal, D., Dehairs, F., Cattaldo, T. & André, L. Geochemistry of suspended particles in the Subantarctic and Polar Frontal zones south of Australia: Constraints on export and advection processes. *J. Geophys. Res.* **106,** 31637, 2001.

Hughes, H. J., Sondag, F., Santos, R. V., André, L. and Cardinal, D.: The riverine silicon isotope composition of the Amazon Basin, Geochim. Cosmochim. Acta, 121, 637–651, doi:10.1016/j.gca.2013.07.040, 2013.

Kinekar, B. K. & Nagar, Z. Potassium fertilizer situation in India : Current use and perspectives. **24,** 2011.

Meunier, J. D., Riotte, J., Braun, J. J., Sekhar, M., Chalié, F., Barboni, D. and Saccone, L.: Controls of DSi in streams and reservoirs along the Kaveri River, South India, Sci. Total Environ., 502, 103–113, doi:10.1016/j.scitotenv.2014.07.107, 2015.